An investigation into the role of TbZC3H20: a zinc finger protein that acts as a post-transcriptional regulator of gene expression in *Trypanosoma brucei*

Alexandra Susan Ling

A thesis submitted for the degree of Doctor of Philosophy

Division of Cell and Molecular Biology

Imperial College London

DECLARATION

I, Alexandra Susan Ling, confirm that the work presented in this thesis is my own. Where information and data has been derived from other sources, I confirm that this has been indicated in the thesis.

PAPERS PUBLISHED FROM THIS THESIS

Ling AS, Trotter JR, Hendriks EF (2011) A zinc finger protein, TbZC3H20, stabilises two developmentally regulated mRNAs in Trypanosomes. *J. Biol Chem*, Apr 5. [Epub ahead of print]

ABSTRACT

Trypanosomes rely on post-transcriptional mechanisms to regulate gene expression, thus RNA-binding proteins are of particular significance in these parasites. This project focuses on a CCCH zinc finger protein TbZC3H20, which is hypothesised to regulate gene expression via mRNA stability, and consequently control normal cell functions. Using reverse genetics such as RNAi down-regulation and ectopic over-expression, the role of TbZC3H20 in insect procyclic form and mammalian bloodstream form *Trypanosoma brucei* has been investigated. Phenotypes resulting from perturbing the expression of TbZC3H20 in both life forms were examined and characterised, and these provided clues about the mRNA species that might be regulated by this protein. In combination with microarray analysis, specific mRNA targets were selected for further investigation: to verify that TbZC3H20 regulates transcripts via mRNA stability and turnover, to demonstrate their direct interaction with TbZC3H20, and to show that the 3' UTR is responsible for regulation by TbZC3H20. This analysis also addressed the possibility of creating TbZC3H20 null mutants in bloodstream forms and procyclic forms, which indicated the essential nature of TbZC3H20 itself in either life form, as well as providing a useful tool in characterising its role within the cell. In conclusion, this project reveals a novel RNA-binding protein that is able to regulate mRNAs involved in the highly coordinated process of differentiation from one life form to another, as well as regulating life cycle stage enriched transcripts essential for trypanosome cell survival.

ACKNOWLEGEMENTS

I would firstly like to thank my PhD supervisor, Dr Ed Hendriks, who has been an invaluable teacher and inspirational mentor throughout my studies. He has brought out the best of my capabilities as a scientist, for which I am truly grateful.

I would also like to express thanks to my other PhD supervisor, Professor Erhard Hohenester, who has provided me with the opportunity for this PhD project with Ed.

Within the Hendriks' group I would like to show my appreciation to Dr. James Trotter for his guidance and support, in addition to his technical assistance during the first half of my PhD. My acknowledgement goes to Lauren Hagedorn and Adrian Buckroyd for their technical assistance with my project, and to Kevin Crawford for his practical support in the lab. I am appreciative for the assistance provided by Dr. Raffaella Carzaniga for the electron microscopy work in this thesis.

I would like to make a special mention all my close friends at Imperial College: Ana Cehovin, Cate Reynolds, Kieran McGourty, Henry Evans, Graham Joyce, Andrej Trauner and Dan Brown. They have, in addition to providing support with my project, made my PhD studies and time at Imperial a fantastic and unforgettable experience. My thanks also go to Alexandra Anderson, Nell Rossiter and Cate Reynolds for being awesome flatmates during my studies.

I would like to thank my family for their support; my mum Sue, my step-dad Vic, and my two sisters Toni and Jess, and a special mention to my mum for providing strength and belief.

Finally, I would like to acknowledge Rich. He has had amazing patience during the busy, tough times, and I thank him for his consistent encouragement, interest and support through my PhD.

TABLE OF CONTENTS

DECLARATION 2

PAPERS PUBLISHED FROM THIS THESIS 3

ACKNOWLEGEMENTS 5

TABLE OF CONTENTS 6

LIST OF TABLES 12

ABBREVIATIONS 13

CHAPTER 1. INTRODUCTION 14

1.1 T*rypanosoma brucei* as the cause of an infectious disease 15

1.2 The *Trypanosoma brucei* lifecycle 16
1.2.1 Adaptation in mammal and fly 18
1.2.2 Cellular and molecular mechanisms of *T. brucei* differentiation 21

1.3 Nuclear gene expression in *T. brucei* 24
1.3.1 Polycistronic Transcription and pre-mRNA processing 25
1.3.2 RNA degradation and translation 26

1.4 Regulatory mechanisms of gene expression in *T. brucei* 29
1.4.1 Developmental regulation at the transcriptional level 29
1.4.2 Developmental regulation at the post-transcriptional level 32
1.4.3. Developmental regulation at the post-translational level 39

1.5 Regulation of gene expression by RNA-binding proteins 41
1.5.1 CCCH zinc finger proteins 42

CHAPTER 2. MATERIALS AND METHODS 48

2.1 Plasmid constructs and cloning 49
2.1.1 PCR 49
2.1.2 DNA gel electrophoresis, PCR purification and ligations 51
2.1.3 Small and large scale plasmid DNA preparations from *E. coli*, and restriction enzyme digests 51

2.2 Trypanosome culture maintenance and transfections 52

2.3 Heterologous Expression in *E. coli* and Homopolymer RNA binding Assays 53

2.4 Immunofluorescence assays 54

2.5 Endocytosis assay 55

2.6 Transmission electron microscopy 56

2.7 *T. brucei* genomic DNA extraction and PCR of null mutants 56

2.8 Protein extraction from *T. brucei*, SDS-PAGE and western analysis 57

2.9 RNA isolation and Northern analysis; transcriptional and translational inhibition 58

2.10 RNA Riboprobe preparation 59

2.11 RNA Electrophoretic Mobility Shift Assays (EMSA) 60

2.12 Reverse transcriptase PCR (RT-PCR) and Quantitative Real-Time PCR (qPCR) 60

2.13 Purifying TAP-tagged TbZC3H20 mRNA complexes 61

2.14 Microarray analysis 62

2.15 Computing, Statistics and Bioinformatics 63

2.16 Reagents and Buffers **63**

CHAPTER 3. ZC3H20 REGULATES LIFE CYCLE ENRICHED GENES VIA MRNA STABILITY IN PROCYCLIC FORM *T. BRUCEI* **75**

3.1 Introduction **76**
3.1.1 TbZC3H20 is a CCCH zinc finger protein specific to Trypanosomes 76
3.1.2 TbZC3H20 can bind RNA *in vitro* 76
3.1.3 Expression of Z3H20 between the life cycle stages 78

3.2 Investigation if ZC3H20 and ZC3H21 are essential for growth in procyclic form *T. brucei* **79**
3.2.1 Down-regulation of ZC3H20 or 21 by RNA interference (RNAi) causes a growth defect in PF *T. brucei* 80
3.2.2 ZC3H20 and ZC3H21 are essential genes in PF *T. brucei* 82

3.3 Investigation of the mRNA targets of ZC3H20 in PF *T. brucei* **84**
3.3.1 Microarray analysis identifies a small number of genes with an altered mRNA abundance when ZC3H20 is depleted in PF *T. brucei* 84
3.3.2 Inhibition of protein synthesis determines if an mRNA species is stabilised or destabilised in PF *T. brucei* 86
3.3.3 ZC3H20 is capable of binding TS-like E, MCP12 and PHAP mRNA *in vivo* 89
3.3.4 Down-regulation of ZC3H20 causes an increased decay rate of the developmentally regulated TS-like E and MCP12 mRNA transcripts 91

3.4 Regulation of MCP12 and TS-like E mRNA via their 3' UTR **94**
3.4.1 ZC3H20 can directly bind the 3'UTR of MCP12 and TS-like E mRNA *in vitro* 94
3.4.2 The 3'UTR of MCP12 and TS-like E is sufficient to regulate a reporter gene in a ZC3H20 dependent manner 95

3.5 Discussion of Chapter 3 ..... **97**

CHAPTER 4. BLOODSTREAM FORM ENRICHED ENDOCYTIC MOLECULES ARE DOWN-REGULATED BY ZC3H20 IN PROCYCLIC FORM *T. BRUCEI* **103**

4.1 Introduction **104**

4.2 Investigation of the phenotypic effect of over-expression of TbZC3H20 and TbZC3H21 in procyclic form *T. brucei* **105**
4.2.1 Over-expression of TbZC3H20 and TbZC3H21 in procyclic form *T. brucei* causes a growth and morphological defect 105
4.2.2 Over-expression of ZC3H20/21 in PF *T. brucei* correlates to the phenotype observed 109
4.2.3 Both CCCH zinc finger motifs of ZC3H20 are necessary to cause the BigEye phenotype from ZC3H20 over-expression in PF *T. brucei* 111
4.2.4 Over-expression of TbZC3H20 causes an enlargement of the flagellar pocket 113
4.2.2 TbZC3H20 over-expression causes an endocytic defect in procyclic form *T. brucei* 116

4.3 Investigation into the cause of flagellar pocket enlargement by ZC3H20 over-expression in PF *T. brucei* **118**
4.3.1 TbZC3H20 has no involvement with mitochondrial maintenance in PF *T. brucei* 120
4.3.2 Investigation of TbZC3H20 involvement with clathrin-mediated endocytosis in PF *T. brucei* 122

4.4 Investigation into the regulation of mRNA targets that cause the ZC3H20 over-expression phenotype **130**
4.4.1 The endocytosis-associated mRNAs are destabilised by protein factors and are capable of being bound by ZC3H20 in PF *T. brucei* 130
4.4.2 Over-expression of ZC3H20 causes an increased turnover of the PDI-BS2 mRNA transcript 132
4.4.3 Down-regulation of PDI-BS2 in PF *T. brucei* does not cause the BigEye phenotype 136

4.5 Discussion of Chapter 4 ..... **137**

CHAPTER 5. ZC3H20 ACTS AS A MOLECULAR TRIGGER OF DIFFERENTIATION IN BLOODSTREAM FORM *T. BRUCEI* **145**

5.1 Introduction **146**

5.2 Investigation into the requirement of ZC3H20 in BF *T. brucei* **147**
5.2.1 Down-regulation of ZC3H20 or ZC3H21 by RNAi does not affect growth in BF *T. brucei* 147
5.2.2 Down-regulation of ZC3H20 or ZC3H21 compromises the ability of BF *T. brucei* to differentiate 149
5.2.3 ZC3H20 is not an essential gene in BF *T. brucei* 150
5.2.4 Triggering differentiation in the absence of ZC3H20 151
5.2.5 Discussion of section 5.2 154

5.3 Cellular effects of TbZC3H20 over-expression in BF *T. brucei* **155**
5.3.1 Over-expression of ZC3H20 in BF *T. brucei* causes a growth defect 155
5.3.2 ZC3H20 over-expression in BF *T. brucei* causes surface expression of procyclin and kinetoplast repositioning 156
5.3.3 BF cells triggered to differentiate from ZC3H20 over-expression may be able to re-enter the cell cycle 159
5.3.4 Both CCCH zinc finger motifs of ZC3H20 are necessary for the function of ZC3H20 in BF *T. brucei* 160
5.3.5 Over-expression of the similar ZC3H protein, TbZC3H21 also triggers BF *T. brucei* to differentiate 162
5.3.6 Discussion of section 5.3 163

5.4 ZC3H20 as a molecular trigger for differentiation compared to chemical induction and temperature shift *in vitro* **165**
5.4.1 Triggering differentiation in monomorphic BF SMB cells 165
5.4.2 ZC3H20 over-expression in combination with a temperature drop to 27°C triggers a greater proportion of BF cells to differentiate than ZC3H20 alone 168
5.4.3 Discussion of section 5.4 170

5.5 Capacity of BF monomorphic cell lines to differentiate **172**
5.5.1 Monomorphic BF cells do not require a position in the cell cycle to receive the signal from ZC3H20 to differentiate 173
5.5.2 Cell density does not affect the ability of monomorphic BF cells to differentiate when triggered by ZC3H20 over-expression 175
5.5.3 Inducing stumpy characteristics increases the ability of monomorphic BF cells to differentiate when triggered by ZC3H20 over-expression 177
5.5.4 Discussion of section 5.5 180

5.6 Investigation of the mRNA targets regulated by ZC3H20 as a molecular trigger of differentiation **182**
5.6.1 Microarray analysis identifies genes involved in differentiation up-regulated when ZC3H20 is over-expressed in BF *T. brucei* 182
5.6.2 ZC3H20 is capable of binding to the upregulated mRNA targets from over-expression in BF *T. brucei* 187
5.6.3 The mRNA targets upregulated during ZC3H20 over-expression are also stabilised when ZC3H20 is over-expressed 188
5.6.4 ZC3H20 over-expression increases the abundance of mRNAs that are upregulated in stumpy cells and upon differentiation triggered by cold shock or *cis*-aconitate 192
5.6.6 Discussion of Section 5.6 194
5.6.7 Chapter 5 conclusions 197

CHAPTER 6. FINAL CONCLUSIONS **203**

6.1 Discussion and conclusion of thesis **204**

6.2 Potential further work on TbZC3H20/21 ..... **210**

REFERENCES **212**

LIST OF FIGURES

Figure 1.1 Life cycle of *Trypanosoma brucei*. **17**
Figure 1.2. Schematic drawing of *T.brucei* ultrastructure. **18**
Figure 1.3 Major events of differentiation. **23**
Figure 1.4. Schematic representation of the DNA cell cycle events in *T. brucei*. **23**
Figure 1.5. A model of the mRNA fates in Trypanosomes. **28**
Figure 1.6. VSG genes and their genomic location in *T. brucei*. **30**
Figure 1.7. Predicted secondary structure of the 3'UTR of EP procyclin mRNA. **35**
Figure 2.1 Plasmid maps of constructs used in this study **70**
Figure 3.1. ZC3H20 and ZC3H21 as *T. brucei* RNA-binding ZC3H proteins **77**
Figure 3.2. Expression of ZC3H20 in BF and PF T. brucei, and generation of an antiZC3H20 antibody **79**
Figure 3.3. RNAi down-regulation of ZC3H20 and ZC3H21 in PF *T. brucei* **81**
Figure 3.4. Creating ZC3H20 and ZC3H21 null mutants in PF *T. brucei* **83**
Figure 3.5. Effect of a translational inhibitor to mRNA abundance of genes from PF ZC3H20 RNAi microarray **88**
Figure 3.6. ZC3H20 TAP-tag analysis in PF *T. brucei* and RT-PCR of bound mRNA targets **90**
Figure 3.7. RNA abundance after treatment of PF *T. brucei* with a transcriptional inhibitor and induced for ZC3H20 RNAi down-regulation **92**
Figure 3.8. Densitometry analysis to determine RNA decay rate after ZC3H20 RNAi down-regulation in PF *T. brucei* **93**
Figure 3.9. RNA EMSA to show direct binding of recombinant GST-ZC3H20 to TbMCP12 and TS-like E 3' UTR RNA **95**
Figure 3.10. Luciferase reporter assay to show regulation of TbMCP12 and TS-like E mRNA via the 3'UTR **96**
Figure 3.11. 3' UTR regions of TbTS-like E and TbMCP12 mRNA **100**
Figure 4.1. Effect on growth from over-expression of ZC3H20 and ZC3H21 in PF *T. brucei* **106**
Figure 4.2. Phentoypes caused by over-expression of ZC3H20 or ZC3H21 in PF *T. brucei* **108**
Figure 4.3. GFP-tagged over-expression of ZC3H20 and ZC3H21 in PF *T. brucei* **110**
Figure 4.4. Schematic of the ZC3H20 deletion and point mutants **111**
Figure 4.5. Expression of ZC3H20 deletion and point mutants in PF *T. brucei* **112**
Figure 4.6. Immunofluorescence and electron microscopy to identify the flagellar pocket upon ZC3H20 over-expression in PF *T. brucei* **114**
Figure 4.8. Immunofluorescence microscopy of the mitochondrial structure upon ZC3H20 over-expression in PF *T. brucei* **121**
Figure 4.9. Immunofluorescence microscopy to probe the ER and lysosome structure upon ZC3H20 over-expression in PF *T. brucei* **123**
Figure 4.10. Quantitative real-time PCR of mRNA from PF *T. brucei* after ZC3H20 over-expression. **128**

Figure 4.11. Northern analysis of genes down-regulated in microarray when ZC3H20 is over-expressed in PF *T. brucei* **129**
Figure 4.12. Translational inhibitor assay and ZC3H20 TAP-tag RT-PCR for candidate genes from PF ZC3H20 over-expression microarray **131**
Figure 4.13. RNA abundance after treatment of PF *T. brucei* with a transcriptional inhibitor and induced for ZC3H20 over-expression **133**
Figure 4.14. Densitometry analysis to show turnover of CAP15, PHAP and clathrin RNA in PF ZC3H20 OeX *T. brucei* **134**
Figure 4.15. Densitometry analysis to show turnover of PDI-BS2 RNA in PF ZC3H20 OeX *T. brucei* **135**
Figure 4.16. RNAi down-regulation of PDI-BS2 in PF *T. brucei* **137**
Figure 4.17. 3' UTR regions of PDI-BS2 mRNA **141**
Figure 5.1. RNAi down-regulation of ZC3H20 or ZC3H21 in BF *T. brucei* **148**
Figure 5.2. Differentiation ability of BF *T. brucei* induced for ZC3H20 or ZC3H21 RNAi down-regulation **149**
Figure 5.3. Generation of ZC3H20 null mutants in BF *T. brucei* **151**
Figure 5.4. Ability of *T. brucei* BF ZC3H20 null mutants to differentiate to PF **153**
Figure 5.5. Ectopic over-expression of ZC3H20 in BF *T. brucei* **156**
Figure 5.6. Morphological effect of ZC3H20 over-expression in BF *T. brucei* **158**
Figure 5.7. Karyotype analysis of EP positive cells after ZC3H20 over-expression in BF *T. brucei* **159**
Figure 5.8. Expression of ZC3H20 deletion and point mutants in BF *T. brucei* **161**
Figure 5.9. Ectopic over-expression of ZC3H21 in BF *T. brucei* **163**
Figure 5.10. Treatment of BF *T. brucei* with *cis*-aconitate and a temperature drop to trigger differentiation to PF **166**
Figure 5.11. Treatment of BF *T. brucei* with TbPT1B inhibitor to trigger differentiation to PF **168**
Figure 5.12. Effect of temperature drop in combination with ZC3H20 over-expression of BF *T. brucei* to trigger differentiation **169**
Figure 5.13. Effect of cell cycle synchronisation on the differentiation kinetics of BF *T. brucei* induced for ZC3H20 over-expression **174**
Figure 5.14. Effect of cell density on the differentiation ability of BF *T. brucei* induced for ZC3H20 over-expression **176**
Figure 5.15. Effect of cAMP treatment on the differentiation ability of BF *T. brucei* induced for ZC3H20 over-expression **179**
Figure 5.16. Northern analysis to show mRNA abundance when ZC3H20 is over-expressed in BF *T. brucei.* **186**
Figure 5.17. RT-PCR of bound mRNA targets from ZC3H20 TAP-tag analysis **188**
Figure 5.18. RNA abundance after treatment of BF *T. brucei* with a transcriptional inhibitor and induced for ZC3H20 over-expression **189**
Figure 5.19. Densitometry analysis to show turnover of Actin, PAD2, Procyclin and META RNA in BF ZC3H20 OeX *T. brucei* **190**

Figure 5.20. Densitometry analysis to show turnover of SCAS, Tb927.5.4020 and PDI-BS2 RNA in BF ZC3H20 OeX *T. brucei* 191
Figure 5.21. Northern analysis of RNA isolated from BF SMB and 20 OeX cells exposed to different conditions. 194
Figure 5.22. Model for involvement of ZC3H20 in regulating *T. brucei* differentiation from BF to PF pathway 199

LIST OF TABLES

Table 2.1. Oligonucleotides used in this study **68**
Table 2.2 List of plasmids used in this study **74**
Table 3.1. Summary of the microarray analysis from PF TbZC3H20 RNAi cells **85**
Table 4.1 Summary of the PF ZC3H20 over-expression microarray analysis to show genes with up-regulated levels of RNA **125**
Table 4.2. Summary of the PF ZC3H20 over-expression microarray analysis to show genes with down-regulated levels of RNA **126**
Table 4.3. Summary of the PF ZC3H20 over-expression microarray analysis to show change in RNA level of genes that encode molecules of the endocytic pathway **127**
Table 5.1 Summary of the BF ZC3H20 over-expression microarray analysis to show genes with down-regulated levels of RNA **183**
Table 5.2. Summary of the BF ZC3H20 over-expression microarray analysis to show genes with up-regulated levels of RNA **184**

ABBREVIATIONS

ARE – AU-rich element

BF – bloodstream form

BSA – bovine serum albumin

DAPI – 4,6-diamidine-2,phenylindole

dNTPs – deoxynucleotide phosphates

dATP – deoxyadenosine phosphate

dGTP – deoxyguanine phosphate

dTTP – deoxythymidine phosphate

dCTP – deoxycytosine phosphate

EDTA – ethylenediaminetetraacetic acid

EGTA – ethylene glycol tetraacetic acid

EMSA – electrophoretic mobility shift assay

FBS – foetal bovine serum

FITC – Fluorescein Isothiocyanate

GFP – Green fluorescent protein

GST – Glutathione-S-transferase

GRE – GU-rich element

KO – knock out

IPTG – Isopropyl β-D-1-thiogalactopyranoside

LB – lysogeny broth

OeX – over-expression

PBS – phosphate buffered solution

PCR – polymerase chain reaction

PF – procyclic form

RBP – RNA binding protein

RNAi – RNA interference

RNase – ribonuclease

sdH_2O – sterile deionised water

SDS – sodium dodecyl sulphate

SDS-PAGE – SDS polyacrylamide gel electrophoresis

TAP – tandem affinity purification

Tet – tetracycline

VPBS – Voorheis' modified PBS

WT – wild-type

ZC3H – CCCH zinc finger (protein)

CHAPTER 1. Introduction

1.1 T*rypanosoma brucei* as the cause of an infectious disease

Trypanosomes are flagellated protozoan parasites belonging to the family of *Kinetoplastida*. *Trypanosoma brucei* is the causative agent of the fatal disease, Human African Trypanosomiasis (HAT), also known as sleeping sickness in humans and nagana in domestic livestock. Currently, the estimated number of cases is around 50,000 – 70,000 (about 10,000 reported new cases in 2008) resulting in a significant impact on human health and contributing to economic burden in 36 countries of Sub- Saharan Africa [1, 2]. The disease tends to occur in remote rural areas, and the geographical focal nature of the disease, along with poor surveillance, means that the current status is difficult to determine [3]. The trypanosome is transmitted to its mammalian hosts via the tsetse fly, *Glossina* spp.. The disease only occurs in areas populated by the tsetse fly, and presents itself as two types dependent on geography and parasite species: *Trypanosoma brucei gambiense* causes chronic disease in central and western regions of sub-Saharan Africa, and *Trypanosoma brucei rhodesiense* causes more acute disease in the eastern and southern regions [4]. After the tsetse fly has a blood meal from an infected host, the parasite establishes itself in the midgut, and then migrates to the salivary glands ready for transmission to a new host. In mammals, the parasite resides first in the bloodstream, lymphatic system and interstitial spaces, causing fever, headache, joint pain and enlarged lymph nodes. In the latter stages of infection, the parasite invades the central nervous system leading to mental, sensory and sleep-anomalies [4]. Without treatment, sleeping sickness will lead to death. Administration and success of drug treatment is stage specific; for treatment of the first stage, the drugs are less toxic, easier to administer and more effective than treatment for the second stage, which requires drugs to cross the blood-brain-barrier [1]. Severe side effects are often reported for later stage treatment, such as renal failure, anaphylactic shocks and neurotoxic signs, and new developments from these old drugs are urgently required [5].

Other members of the kinetoplastid group also cause human diseases found in tropical and sub-tropical parts of the world, such as Chagas disease caused by *Trypanosoma cruzi*, and various forms of leishmaniasis caused by different species of *Leishmania*. With over half a billion people at risk from contracting these kinetoplastid diseases, 20 million people infected, and an estimated 100,000

deaths a year [4], this group of parasites represent major neglected tropical diseases. Over recent years, many reports to identify a “breakthrough in sleeping sickness” and treat this “killer disease” emphasise the impact of this disease, and the many efforts to tackle the “The deadliest disease in the heart of Africa” [6, 7].

1.2 The *Trypanosoma brucei* lifecycle

Trypanosomes are eukaryotic organisms that survive in both a mammalian host (as a bloodstream form) and an insect vector (as a procyclic form) to complete their lifecycle (Fig. 1.1) [8]. *T. brucei* proliferate in the mammalian bloodstream as the morphological slender form, and are able to evade the immune response through antigenic variation by periodic shifts in expression of variable surface glycoproteins (VSG) (Fig. 1.1). At the peak of parasitaemia, they transform to the non-proliferative stumpy form [9]. This may allow the immune response to clear the major variant of VSG expressed by slender and stumpy cells, but a very small number of dividing slender forms with a new VSG variant are able to repopulate causing a relapsing infection, and a new cycle of fever by the host. If they are not cleared, the division-arrested stumpy parasites are then transmitted to the tsetse fly triggering differentiation to the procyclic form. Morphologically, the trypanosome undergoes surface antigen exchange where the VSG coat is replaced with a less dense coat of EP and GPEET procyclins (Fig. 1.1), and then the kinetoplast (mitochondrial DNA) is repositioned from the posterior end of the cell to halfway between the posterior and nucleus (Fig. 1.1). These morphological changes are synchronously co-ordinated with cell-cycle re-entry by establishing the appropriate cell architecture for division of the differentiated parasite [9]. After multiplication in the fly's midgut, the procyclic organisms migrate to the salivary glands, where they differentiate to the epimastigote form. This transformation is achieved through an asymmetric division that produces one long and one short daughter epimastigote; the long epimastigote daughter appears to die [10]. Due to the differentiation process, the surviving epimastigote is two-thirds smaller than the proliferative midgut procyclic cell, and displays a reversal of positions of the kinetoplast and nucleus (nucleus is closer to the posterior pole than the kinetoplast) [10]. The differentiation of epimastigotes to the division-arrested (infective) metacyclic form occurs while the cells are attached to the salivary gland epithelium, but this is not well characterised [10]. The procyclin coat is replaced with a single VSG coat upon

differentiation to the metacyclic form, and the positions of the kinetoplast and nucleus are reversed back so the kinetoplast is at the posterior end of the cell. Fully differentiated metacyclics are then transmitted to the mammalian bloodstream upon a blood meal to complete the life cycle.

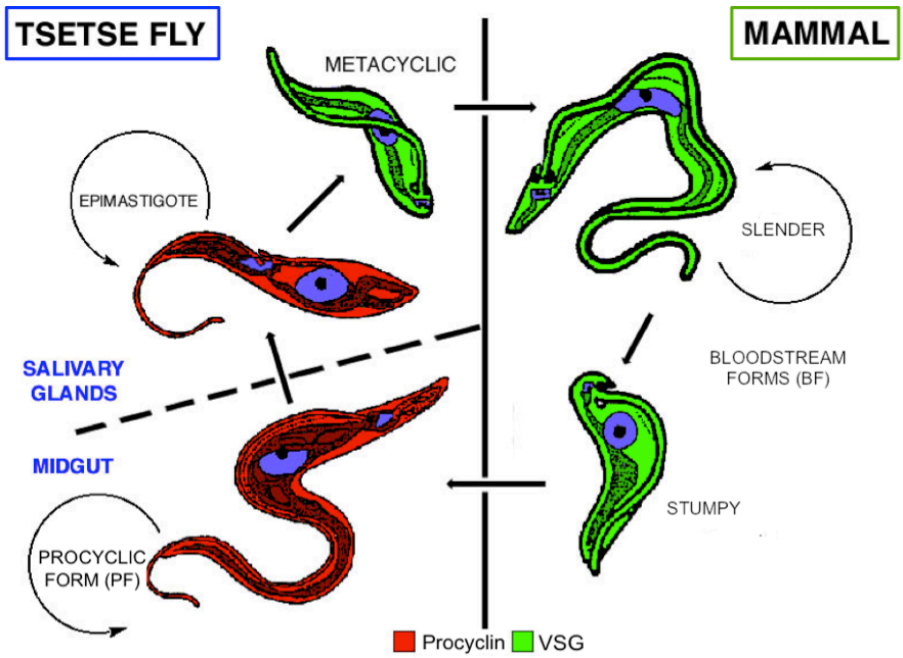


Figure 1.1 Life cycle of *Trypanosoma brucei*.

Adapted from [11]. Trypanosomes replicate in the bloodstream of the mammal host as the slender form, and then differentiate to the non-replicative stumpy form. These are ingested by the tsetse fly during a blood meal, and immediately differentiate to the dividing procyclic form. These then migrate to the salivary glands and divide as epimastigotes, finally differentiating to the non-dividing metacyclic, ready for transmission to the mammalian host, thus completing its life cycle. The bloodstream form cells have a surface coat composed of the variable surface glycoprotein (VSG, green), and the procyclic form cells posses a coat of EP and GPEET procyclins (red). The kinetoplast and nucleus are indicated in blue. The kinetoplast is at the posterior end in metacyclics and bloodstream forms, halfway between the nucleus and posterior in procyclic form, and on the anterior side of the nucleus in the epimastigote).

The differentiation from a slender to a stumpy to a procyclic form, results in identifiable morphological changes. The slender form has a long free flagellum, an elongated centrally located nucleus and a tightly attached undulating membrane, whereas stumpy forms are characterized by the virtual absence of a free flagellum, the presence of a highly developed undulating membrane, a posterior rounded nucleus and a large increase in the cellular volume [12]. During differentiation from bloodstream to procyclic form, the kinetoplast is repositioned by microtubule

outgrowth at the posterior end of the cell [13], which also causes an increased body length by the differentiated procyclic from. Between the two life cycle stages, the bloodstream form has a simple, linear mitochondrion, whereas the procyclic form has a more complex, branched mitochondrion – emphasising the differential need of this organelle [14]. The procyclic form displays many diverse features compared to the bloodstream form, as the midgut of an insect is a different environment to that of the mammalian bloodstream. Accordingly, these organisms demonstrate distinct morphological and metabolic characteristics throughout their life cycle to enable adaptation and survival within two challenging environments.

1.2.1 Adaptation in mammal and fly

T. brucei resides in the mammalian bloodstream, which is at 37°C and glucose-rich, but then adapt to the 27°C and glucose-deprived environment of the tsetse fly midgut. The abundance of glucose and nutrients available to the parasite in the bloodstream coincides with its basic metabolism. ATP is generated by the degradation of glucose to pyruvate by glycolysis, where glucose is degraded in the glycosomes and an intermediate from this reaction is then converted to pyruvate in the cytosol [15]. Mitochondrial activity is repressed, except for a glycerol-3-phosphate shuttle and an alternative oxidase, which maintain the redox balance in glycosomes [15]. Upon differentiation to the procyclic form, the mitochondrion (Fig. 1.2) is activated and there are extreme changes in energy metabolism and enzyme activity [16]. The major carbon source for procyclic *T. brucei* is proline, that is highly abundant in the insect midgut, and is used for ATP production via oxidative phosphorylation [17].

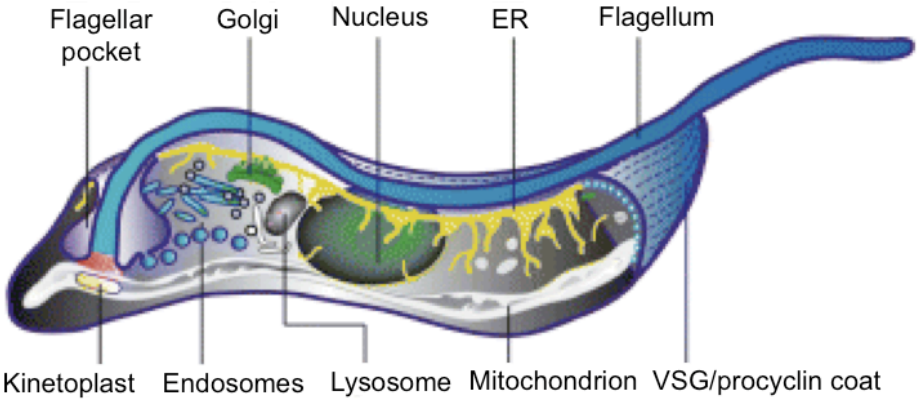


Figure 1.2. Schematic drawing of *T.brucei* ultrastructure.
Adapted from [18]

The surface of the procyclic form *T. brucei* consists of a coat of GPI-anchored invariant glycoproteins as two forms called EP procyclin and GPEET procyclin (Fig. 1.2). Expression of these molecules is important for survival in the tsetse fly [19], and may provide protection from proteolytic enzymes in the midgut [20]. However, procyclin expression is not essential to complete the lifecycle in the insect to generate infective metacyclic cells [21]. The mammalian bloodstream poses a challenge to *T. brucei* to constantly evade the immune system, and the parasite has responded by developing a mechanism of antigenic variation. The surface of bloodstream form parasites is covered with a dense homogenous coat of GPI-anchored VSG (Fig. 1.2). The VSG is repeatedly changed in a small sub-population of cells, thus avoiding antibody-mediated killing, repopulating the host and subsequently causing a long-lasting chronic infection [22]. More specifically, antigenic variation occurs via transcriptional switching thus activating different VSG expression sites (see Section 1.4.1) or by VSG homologous recombination within the active VSG expression site [22]. The trypanosome can then switch the VSG on its surface for a new variant thus escaping the antibody response against the old one. In the early stages of an anti-trypanosome immune response, the parasite utilises another mechanism to remove bound antibody-VSG complexes. Bloodstream form *T. brucei* have an extremely fast rate of endocytosis where the entire VSG coat is recycled through the endocytic system every 12min [23]. This allows rapid clearing of VSG-bound antibody complexes and thus extends parasite survival by preventing complement-mediated lysis [24]. Interestingly, the mechanism of antibody clearance was reported to require hydrodynamic forces that are generated from swimming trypanosomes, creating a current that sweeps the surface bound antibodies to the posterior for internalisation [25].

The mechanisms employed by *T. brucei* to evade the immune system require a highly efficient protein trafficking system for surface coat exchange. It is widely accepted that the endocytic system is a means for survival, specifically for bloodstream form parasites. In the insect midgut, such an elaborate clearance system is not required and the procyclic form has an endocytic rate approximately 10-fold slower than the bloodstream form [26]. Nonetheless, both forms are dependent on their basal endocytic system for uptake of nutrients from their external environment for growth and development. The flagellar pocket is an

invagination of the plasma membrane at the base of the flagellum [27] (Fig. 1.2) and is the sole site for all endocytosis and secretion in *T. brucei*. The flagellar pocket membrane, pellicular plasma membrane and flagellar membrane are physically contiguous but have highly differentiated biological functions with distinct proteins localised to each of these surfaces [28]. A flagellar pocket cytoskeletal protein, BILBO1 has been characterised as essential for flagellar pocket biogenesis and demonstrates a link between the cytoskeleton and endo/exocytic systems [29].

Both procyclin and VSG surface coat proteins are trafficked and recycled from the cytoplasm via the flagellar pocket to the cell surface, while receptors for the uptake of macromolecules are retained at the flagellar pocket. From the flagellar pocket, endocytic vesicles pinch off and deliver cargo to the early endosome (Fig. 1.2). After sorting, material is delivered either to recycling endosomes or to lysosomes (Fig. 1.2).

In eukaryotic cells, a major classification of endocytic pathways studied is defined by the dependence or independence on the membrane protein clathrin [30]. Clathrin contains a heavy chain (CLH) and a light chain (CLL), and the CLH of *T. brucei* (TbCLH) is structurally almost indistinguishable from mammalian clathrin [31]. The absence of a caveolin homologue in *T. brucei* suggests clathrin-independent mechanisms are not used by trypanosomes i.e. endocytosis is clathrin-dependent [32]. Clathrin-mediated trafficking involves transporting cargo such as proteins and lipids that are packaged into vesicles surrounded by a coat made of clathrin and adaptor protein complexes [33]. Clathrin-coated vesicles mediate endocytosis from the plasma membrane to transport cargo to endosomes, from the *trans*-Golgi (Fig. 1.2) to endosomes [34] and transport newly synthesised enzymes from the *trans*-Golgi network to the lysosome [35]. TbCLH expression is essential in trypanosomes [36], and the level of expression correlates with endocytic activity i.e. TbCLH is markedly upregulated in bloodstream form cells compared to procyclics [37]. However, clathrin is still necessary in the trafficking system in procyclic cells, as the transport and localisation of a lipoprotein receptor, the cysteine acidic repetitive transmembrane protein (CRAM) from the ER (Fig. 1.2), to the flagellar pocket of procyclic *T. brucei*, is dependent on TbCLH expression [38]. Down-regulation of TbCLH in procyclic cells also reduces the

endocytosis efficiency, suggesting that clathrin still plays a role in receptor-mediated endocytosis in procyclic cells [38].

Changes in energy metabolism and cell surface protein expression between bloodstream and procyclic form cells are crucial for growth and survival within their environment. In addition, the requirement of the trypanosome trafficking system, also developmentally regulated, is linked to these changes. An elaborate endocytic system is vital to replace the VSG coat of bloodstream form parasites in a rapid fashion, but there could be a requirement for the specific trafficking of certain enzymes, transporters and metabolites between the life cycle stages to meet the different metabolic needs. This demonstrates the vital role of intracellular trafficking in life cycle progression to assist with the major morphological and metabolic elements critical for trypanosome differentiation and cell development. Indeed, during differentiation the trypanosome trafficking system transcriptome is remodelled [39], and this emphasises the complex and coordinated changes that occur to enable the *T. brucei* parasite to adapt between mammalian bloodstream and tsetse fly.

1.2.2 Cellular and molecular mechanisms of *T. brucei* differentiation

The differentiation of a bloodstream form into an insect form is a major change for the parasite, and consequently it goes through some progressive, as well as rapid, changes to ensure survival and adaptation in the exposed environment. In isolates from field infections, bloodstream parasites exist as either proliferative slender forms or non-permissive, transmissible stumpy forms [14]. Early in a wave of parasitaemia, the slender cells continue to proliferate until late in parasitaemia, they differentiate to the division-arrested stumpy form. This controls the parasitic load within the host to prevent host death whilst at the same time prolonging trypanosome survival for tsetse uptake and transmission [40]. Despite some disagreement [41], the stumpy form is considered to express pre-adaptive qualities for survival in the fly midgut and only they are able to efficiently differentiate and establish as the procyclic form [42, 43]. In stumpy forms (and an intermediate form between slender and stumpy), the mitochondrion is more developed and associated enzymes are partially activated compared to the slender form [44], suggesting pre-adaption for survival in the glucose-deprived insect midgut. Stumpy forms have also been shown to adapt to acidic and proteolytic

stress more effectively than slender forms, comparable to the immediate and harsh environment posed to the parasite upon ingestion by the tsetse fly [45]. Finally, stumpy forms are cell-cycle arrested within the G1/G0 phase (they have entered the G0 “resting” phase from the G1 phase) resulting in rapid and synchronous differentiation when triggered, and it is suggested that bloodstream forms can only differentiate when they reach this point in the cell cycle [9, 46]

Exposure of stumpy form cells *in vitro* to citrate or *cis*-aconitate, and a drop in temperature to 27°C induces synchronous transformation to the procyclic form and co-ordinated cell cycle progression [47]. The significance of this trigger *in vivo* has been in doubt for some time, as the concentrations used *in vitro* are exceedingly high compared to the levels present in the tsetse blood meal [48]. However, more recent studies have found that a drop in temperature to 20°C (compatible with the temperature of feeding flies at dusk) increases the sensitivity of stumpy cells to *cis*-aconitate at more physiologically relevant levels [49]. The molecular basis of this was discovered to involve surface carboxylate transporters known as PAD proteins, which were only expressed by stumpy forms and redistributed to the cell surface from the flagellar pocket upon cold shock at 20°C, thus acting as a thermo-regulated transducer of the differentiation signal [50].

Upon receiving the differentiation signal, the parasite goes through a regulated programme of events (Fig. 1.3). Firstly, the VSG coat is shed by a combination of the glycosylphosphatidylinositol-specific phospholipase C (GPI-PLC) that hydrolyses the GPI anchor on VSG, and a surface-localised zinc metalloprotease that causes endoproteolysis and removal of the VSG [51]. Coincidental with VSG release, EP and GPEET procylins are induced, with GPEET as the major procyclin expressed on the surface, and then GPEET expression is repressed after 7 days, with glycosylated EP procyclin expression continues in the late procyclic cells [52]. This GPEET repression coincides with the migration of the parasites to a different region of the fly midgut [52].

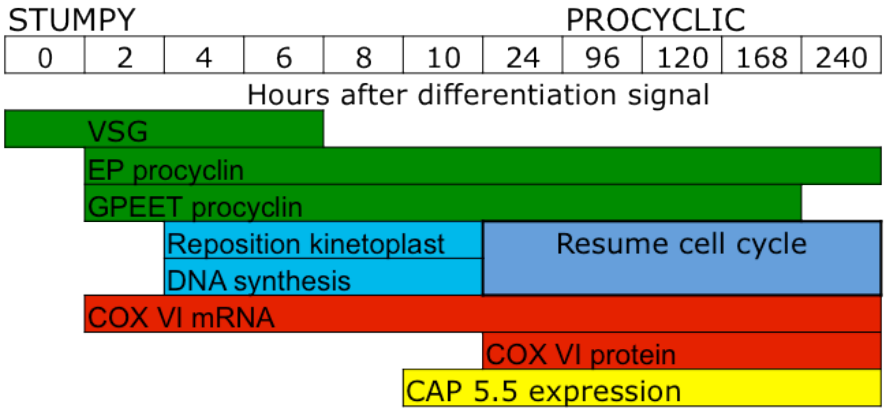


Figure 1.3 Major events of differentiation.

Adapted from [53]. Chart to show the expression of genes or events that occur during the time frame of differentiation from stumpy to procyclic form.

Not long after initiation of EP and GPEET gain, the kinetoplast is repositioned from the posterior location (distinct in bloodstream forms) to midway between the nucleus and posterior as seen in procyclic cells (as described above, section 1.2). This repositioning event occurs simultaneously with the first DNA replication phase of the cell cycle, thus causing cells to re-enter the cell cycle and resume proliferation [13]. The cell cycle of trypanosomes shows the same nuclear events of that in a normal eukaryotic cells cycle i.e. G1, S, G2 and M phases, and a series of event markers define particular stages through the *T. brucei* cell cycle such as elongation of the flagellum, division and separation of the kinetoplast, mitotic division of the nucleus, and finally cytokinesis [54]. Important to note however, is that the kinetoplast and nucleus have a distinct S phase, and the segregation of the kinetoplast occurs before nuclear mitosis (Fig. 1.4) [55]. The order and timing of cell cycle events thus allows the identification of the cell cycle position of an individual trypanosome [55].

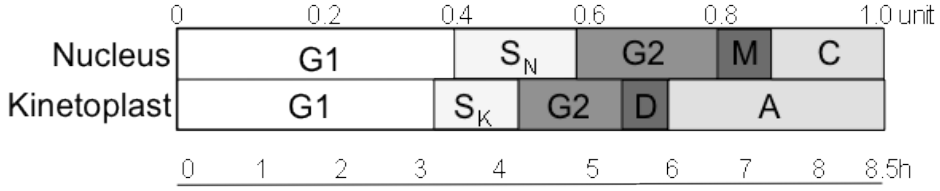


Figure 1.4. Schematic representation of the DNA cell cycle events in *T. brucei*.

Adapted from [56]. S_K, kinetoplast S phase; D, kinetoplast division; A, kinetoplast segregation; S_N, nuclear S phase; M, mitosis; C, cytokinesis

After 24h from initiation of differentiation, elaboration of the mitochondrion is identified by expression of the cytochrome oxidase (COX) subunit VI, and cytoskeletal restructuring is detected by expression of the procyclic-specific cytoskeleton-associated protein CAP5.5 (Fig. 1.3). Finally, studies have shown that stumpy forms must receive both a temperature drop and *cis*-aconitate to fully commit to differentiation, as exposing stumpy cells to just a cold shock can induce reversible expression of EP procyclin on the cell surface [49].

Recent studies have used microarrays to study changes in mRNA levels across the whole *T. brucei* genome during the transition from slender stage to stumpy, and from stumpy to procyclic stage [57-59]. These identified clusters of genes that were down or up-regulated in a co-regulated fashion, consistent with the biology of the differentiating parasite. Overall, these studies provide information regarding the dramatic reprogramming of gene expression that occurs during differentiation of the parasite, and it is unsurprising therefore that tight regulation of differential gene expression is required by trypanosomes.

1.3 Nuclear gene expression in *T. brucei*

The *T. brucei* nuclear genome is 26 megabases of DNA arranged into 11 large chromosomes [60]. The completed sequence genome data shows that the majority of open reading frames are arranged in long polycistronic arrays that may contain 100 genes or more [60]. This is unusual considering that most eukaryotic genes are arranged in monocistronic arrays to produce individual transcripts, and instead trypanosomes have organised their protein-coding genes sequentially on the same DNA strand, a feature commonly found in prokaryotic genomes. In contrast to eukaryotic genes, the majority of trypanosome protein coding genes lack introns with just two instances of *cis*-splicing reported for the poly (A) polymerase gene [61] and for a putative RNA helicase [62]. Importantly, transcription of trypanosome gene arrays produces polycistronic RNA precursors that are then processed into individual mature mRNAs by *trans*-splicing and polyadenylation [63, 64]. Additionally, genes transcribed from the same polycistron do not usually encode proteins of related function as would be seen in bacterial and nematode operons [65].

1.3.1 Polycistronic Transcription and pre-mRNA processing

Despite the unusual gene organisation, the RNA polymerases of trypanosomes largely resemble their eukaryotic counterparts in activity and structure; RNA polymerase I (RNAPI) which transcribes the pre-rRNA (18S, 5.8S and 28S) gene cluster, RNA polymerase II (RNAP II) which transcribes all (but two) mRNAs, and RNA polymerase III (RNAP III) which transcribes tRNAs, 5S RNA and U-rich snRNAs [66]. The activities of these RNAPs are as expected for a eukaryotic organism, with the exception that RNAP I additionally transcribes two mRNAs; the life cycle stage specific surface coat mRNAs of the VSG and procyclins (see above, section 1.2). *T. brucei* is the only member of the kinetoplastids that uses RNAP I for mRNA transcription. The reason for this unique feature is suggested to be the important role of VSG as a host defence mechanism and, with procyclins, the requirement of adapting quickly to different environments during the parasite's life cycle [66]. Promoter regions of genes transcribed by RNAP I and III, including VSG and procyclin promoter, have all been identified and characterised to some degree [67]. The identification of RNAP II promoter regions has remained elusive for all protein-coding genes and only a few general transcription factors have been identified in the genome [67]. Studies in *Leishmania major* have shown that RNAP II transcription initiates in the strand-switch region between two divergent polycistronic units [68]. There has however been one promoter for RNAP II transcription identified and characterised, which is that of the spliced leader (SL) RNA [69]. Like VSG, this is an extremely important gene required for *trans*-splicing and is transcribed from a tandem array of a few hundred SL genes [70].

Mature nuclear mRNAs are generated from primary transcripts by a trans-splicing reaction, which adds a capped 39nt RNA (the SL RNA) to the 5'end of mRNA, and polyadenylation at the 3' end [71]. Similar to *cis*-splicing, *trans*-splicing proceeds through a two-step *trans*-esterification reaction, but forms a Y-structure instead of a lariat intermediate [64]. The 5' donor splice site is a GU dinucleotide from the SL RNA and the splice acceptor site is an AG dinucleotide that is preceded by a polypyrimidine-rich motif [64, 72]. Polyadenylation sites generally occur 80-140nt from the downstream polypyrimidine tract [73], thus polyadenylation is spatially coupled and dependent on *trans*-splicing of the downstream gene [74]. The SL RNA not only provides a cap structure (a cap4 structure where the first 4 nucleotides after the m^7G cap are modified) [75] to the

5'end of mRNA that is critical for mRNA translation to protein and protection from degradation, but also functions with polyadenylation to cleave individual mRNAs from the polycistronic precursor [64].

1.3.2 RNA degradation and translation

After export from the nucleus the mature mRNA has two basic fates, either stabilised and bound by the translational apparatus for protein synthesis, or it is degraded. The degradation of yeast and mammalian mRNA is considered to occur via two general pathways, both of which require removal of the poly (A) tail as the first step [76]. In one pathway, the mRNA is then degraded in a 3' to 5' direction by a complex of 3' exonucleases, the exosome, before the cap structure is hydrolysed [76]. In the other pathway, the cap is hydrolysed after deadenylation, followed by degradation in a 5' to 3' direction by the 5' exonuclease XRN1 [76]. Several eukaryotic deadenylases have been identified. In yeast, these are the Pan2/Pan3 and Ccr4/Caf1/Not complexes [77], and the DAN/PARN enzyme is present in mammalian cells [78]. Homologues of the PAN2/PAN3 complex, a CAF1/NOT complex and 3 possible homologues of PARN have been identified in trypanosomes [79]. PAN2 and CAF1 activity has been demonstrated in *T. brucei*, and CAF1 is considered to be the major deadenylase for most trypanosome mRNAs [80, 81].

In yeast, the exosome has been recognised as a complex of exoribonucleases that degrade mRNA in a 3' to 5' direction [82]. The exosome, consisting of 11 subunits, has to be recruited by RNA binding proteins that recognise AU rich elements in the 3' untranslated region (UTR) of unstable mRNAs, thereby promoting mRNA degradation [83]. The trypanosome exosome homologue has only 8 subunits compared to yeast [84] and its role within the trypanosome cell has been proposed to be required for the rapid degradation of unstable mRNAs [85].

For 5' to 3' mRNA decay, after deadenylation, the cap structure has to be removed. The enzymes responsible for decapping activity in yeast are identified as Dcp1 and Dcp2 [86, 87], although Dcp2 has been demonstrated to show decapping activity in the absence of Dcp1 in other eukaryotes such as human cells and *Caenorhabditis elegans* [88]. The enzymes release m^7GDP from the 5' m^7GpppN end of the transcript, thus making the mRNA sensitive to 5' to 3'

exonucleolytic degradation by Xrn1 [89, 90]. Several factors that enhance decapping have also been identified, such as the helicase Dhh1 and Edc proteins [88]. Decapping activity has been shown in trypanosomes [91], but the enzymes themselves have not been identified, with the exception of a DHH1 homologue [92]. Additionally an XRN1 homologue, XRNA has been localised in the nucleus and cytoplasm in *T. brucei*, and demonstrated 5' to 3' exonucleolytic activity to degrade unstable mRNAs [93].

As well as protection from 5' to 3' degradation, the mRNA cap forms a tight complex with the eukaryotic initiation factor eIF4F thus stabilising the transcript and activating translation [88]. Consequently, decapping requires displacing the eIF4F-cap complex along with other translational complex factors like poly (A) binding protein, thus inhibiting translation and allowing decapping to continue [94]. More recent studies have shown that the enzymes associated with decapping and 5' to 3' mRNA decay in addition to mRNA (non-translated) are concentrated into cytoplasmic ribonucleoprotein processing bodies (P-bodies) [95]. The yeast decapping activators, Dhh1 and Pat1p have been demonstrated to function as translational repressors and facilitators of P-body formation [96], and mRNA localised to the P-bodies can either be degraded or stored (when growth is inhibited) and returned to translation [97].

P-body-like granules have been visualised in trypanosomes with the identification of Dhh1, the RNA-binding protein SCD6 and the exonuclease XRNA [92]. These granules are formed by the recruitment of mRNAs and proteins when the trypanosome is deprived of a carbon source, and protect the mRNAs from degradation [98]. A recent study of Dhh1 in *T. brucei* has suggested how this protein may be involved in the regulation of a subset of developmental mRNAs through translational repression [99].

The translation mechanisms used in trypanosomes are not well known at present. In higher eukaryotes and yeast, the mRNA cap is bound by the nuclear cap binding complex (CBC) before export from the nucleus, and once in the cytoplasm directs a "pioneer" round of translation (as a form of mRNA quality control) [100]. Then the cap is bound by eIF4E from the eIF4F complex (which contains a helicase (eIF4A), a molecular chaperone (eIF4G) and an initiation factor (eIF3) to bind to the ribosome) and after recognition of the AUG start codon in the

5' UTR, the large ribosomal subunit joins, and translation begins [101]. Importantly, the chaperone of the eIF4f complex, eIF4G, interacts with the poly (A) binding protein, which is bound to the poly (A) tail, thus resulting in the circularisation of the RNA by bringing the 5'UTR and 3'UTR together [101]. As well as functioning in the initiation of translation and regulation of mRNA decay, this "closed loop" structure protects mRNAs from degradation [102]. Four potential homologues of eIF4E have been identified in the trypanosome genome, but further characterisation is needed to determine which one is active in translation initiation, and two isoforms of the eIF4A helicase have been identified [103]. Additionally, a homologue of the poly (A) binding protein, PABP1 has been shown to stabilise mRNA in trypanosome cell extracts by protecting transcripts from deadenylation, thus demonstrating involvement in the mRNA turnover pathway in trypanosomes [104]. A summary of the mRNA fates in trypanosomes is shown in Fig. 1.5 to demonstrate the current understanding of mRNA translation and degradation.

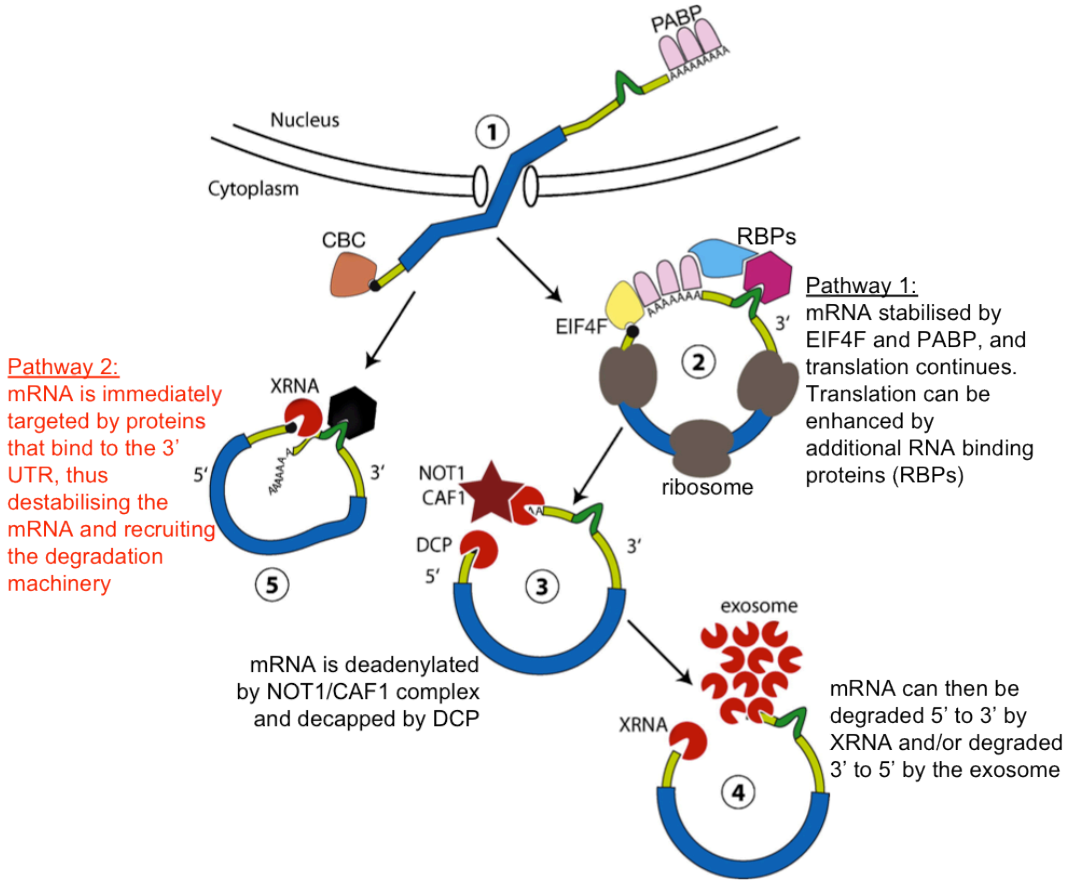


Figure 1.5. A model of the mRNA fates in Trypanosomes.

Adapted from [103]. After export from the nucleus when the mRNA is bound by PABP and the nuclear cap-binding complex (CBC), the mRNA can follow Pathway 1 to be stabilised and translated then degraded, or follow Pathway 2 to be immediately destabilised and degraded.

In conclusion, *T. brucei* presents many differences in terms of gene arrangement, transcription and mRNA processing compared to other eukaryotes. However, the mechanisms involved in mRNA turnover and translation remain generally similar to those studied in eukaryotes, with many *T. brucei* homologues identified for molecules involved in these pathways. The differences could suggest that the trypanosome utilises these modifications to achieve the distinctive features of parasite biology. However in the same context, the similarities in mRNA turnover and translation are just as relevant, as they imply that conserved mechanisms could be exploited in a different and specific manner within a unique organism. This leads to the question of how and why these key processes of transcription through to translation are employed by *T. brucei* to allow the dramatic changes in gene expression necessary for cell development, growth and survival. Consequently, this reveals how eukaryotic gene expression can be controlled and regulated, even within an organism that requires an extreme degree of tight differential gene regulation and expression.

1.4 Regulatory mechanisms of gene expression in *T. brucei*

Regulation of gene expression is a constitutive and fundamental process that is necessary for a range of universal biological processes involved in general cell growth and survival. This is of course applicable to *T. brucei*, but due to the on-going environmental changes that occur during its life cycle, controlling the expression of developmental genes is a crucial role for the parasite's regulatory machinery. Thus, in light of the systems and molecules identified for *T. brucei* gene expression, and their unique or conserved nature as described above (Section 1.3), various mechanisms of regulation are employed by trypanosomes to ensure the correct expression of developmental genes.

1.4.1 Developmental regulation at the transcriptional level

Transcription initiation is the major control point for regulation of gene expression for most organisms. This can be mediated by transcriptional factors, repressors and activators, which influence how efficiently the RNA polymerase binds to the template and carries out transcription. In trypanosomes, due to the nature of polycistronic transcription, all genes that are part of the same array are

transcribed at the same level. With the lack of identified promoters and few transcription factors for RNAPII transcription, the regulation of developmental genes to cause their differential abundance is most likely not to occur at the level of transcription, but at the post-transcriptional level. The exception to this is the regulation of the VSG and procyclin genes, which encode the major surface proteins of the bloodstream and procyclic insect forms, respectively, of *T. brucei*. These are transcribed by RNAPI, and undergo distinct transcriptional activation or repression during developmental differentiation.

The VSG coat of bloodstream parasites provides protection from host immune attack by complement-mediated lysis, and switching the VSG coat by antigenic variation allows the trypanosome to constantly evade antibody responses thus prolonging a chronic infection in the host [105]. There are over 1000 different VSG genes, pseudogenes and fragments located within chromosomes, but only one VSG is expressed at any one time [106] (Fig. 1.6).

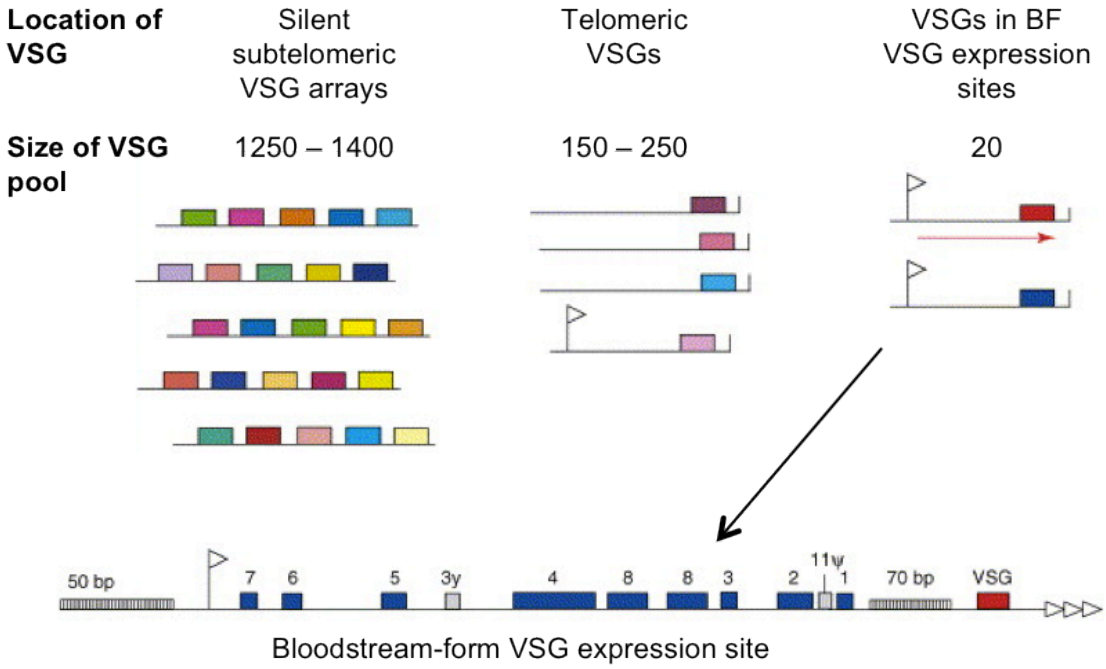


Figure 1.6. VSG genes and their genomic location in *T. brucei.*

Adapted from [107]. VSG genes are located in subtelomeric VSG arrays, telomeres or in one of the VSG expression sites. VSG expression sites are shown with flags indicating the promoters, and the red arrow indicates transcription from an active site. An approximate of the number of VSGs at each genomic location is also indicated. The arrow demonstrates a more detailed view of the VSG expression site showing the promoter (flag), ESAGs (numbered blue boxes), pseudogenes (ψ), intact VSG (red box), telomere repeats (horizontal triangles), and characteristic repeat arrays upstream of the *VSG* expression site (50-bp repeats) or upstream of the *VSG* gene (70-bp repeats).

The VSG is expressed from one of around 20 telomeric expression site transcription units, which are transcribed as polycistronic transcription units and consist of an RNAPI promoter, 12 different families of expression site-associated genes (ESAGs) as well as the telomeric VSG [105] (Fig. 1.6).

On the other hand, procyclin is transcribed from a polycistronic unit that starts with two or three procyclin genes followed by one or two procyclin-associated genes (PAGs) [108]. Transcription occurs from the promoter regions of both transcription units constitutively in bloodstream and procyclic form cells, thus suggesting that control of the stage-specific expression of VSG and procyclin genes is not at the level of transcription initiation [109]. Instead, down-regulation of procyclin transcription in the bloodstream stage, and vice versa for decreased transcription of VSG units in procyclic stage, appears to due to a progressive arrest of RNA elongation [110].

Constitutive transcription at a low-level activity of the 'inactive' VSG expression sites has led to the suggestion that strong activation of one expressor site provides regulation of expression [111]. Interestingly, the inactive VSG transcription units showed defective RNA elongation and processing, thus suggesting that transcription of the active VSG transcription units also requires selective recruitment of the RNA elongation/processing machinery [112]. The mechanisms of monoallelic VSG expression obviously only occur in the bloodstream form (as all VSGs are down-regulated in procyclic forms), which presents an extra complexity to gene expression, and a range of other hypotheses regarding these mechanisms has been proposed. One study shows that recruitment of just one VSG expression unit to a RNAPI containing-extranucleolar body (ES body) permits active monoallelic expression of the locus [113] and a similar nucleolar repositioning mechanism of the VSG promoter site is employed for developmental regulation during differentiation to the procyclic stage parasite [114]. Other studies report that chromatin remodelling regulates the silencing of VSG expression sites via the chromatin remodelling factor ISWI [115] or the histone H3 methyltransferase, DOT1B [116], as down-regulation or deletion of either molecule results in derepression of the silent VSG expression sites. Lastly, telomere integrity has been suggested to play a role in VSG regulation, as this is the position on the chromosome from which the VSG sites are expressed, and downregulation of the telomeric protein TbRAP1 leads to specific derepression of silent VSG units [117].

The developmental expression of procyclin is highly regulated and suggested to be down-regulated 1000-fold in bloodstream forms compared to expression in procyclin forms, which is controlled at the level of transcription initiation and elongation, mRNA stability and translation [118]. Thus, even with the presence of a procyclic promoter and transcription by RNAPI, regulated expression of this critical gene does not stop at the transcriptional level. VSG and procyclin are therefore unique examples of genes in *T. brucei* that are developmentally regulated at the transcriptional and post-transcriptional level, and regulated in an additional complex manner within a life cycle stage at the level of transcription.

1.4.2 Developmental regulation at the post-transcriptional level

With the lack of control of gene expression at the transcriptional level for protein-coding genes transcribed by RNAPII in trypanosomes, there are alternative approaches used by the parasite to increase or decrease RNA abundance. In *T. brucei* important house-keeping genes, required constitutively in all life cycle stages, such as tubulin (13-17 copies of alternating α and β) [119] and the SL RNA (around 200 copies) [120], are duplicated many times in the genome. This produces a greater number of RNA molecules of these genes to cope with the demand within the cell by. For other protein-coding genes, regulation at the post-transcriptional level provides an alternative mechanism, and is of great importance for developmentally regulated genes. This can involve control of splicing, polyadenylation, export from the nucleus, mRNA stability, RNA compartmentalisation or translational efficiency. Recent microarray analysis of total mRNA expression in several stages of parasite development reported that the transcript abundance of over 25% of genes changed by at least 2-fold during the transition of the parasite between a dividing slender bloodstream, to a non-diving stumpy form, and a dividing insect procyclic form [58]. This suggests that the post-transcriptional mechanisms to regulate RNA abundance and gene expression are responsible for the parasite's ability to transform between different life cycle and growth stages.

Given the nature of the coupled *trans*-splicing and polyadenylation mechanism to produce mature mRNAs from polycistronic primary transcripts (see section 1.2.1), and that genes of the same polycistron are not necessarily of related function, it is unlikely that regulation of gene expression occurs at the level of

mRNA processing. There has been one report however, of a two-step *trans*-splicing mechanism in *T.cruzi* where 'splice site-skipping' produces a non-translatable intermediate RNA, which can be subsequently processed into a mature RNA, thus providing a mechanism for gene regulation [121]. Two examples of the intermediate RNA were demonstrated; a TcUBP dicistron that encodes two functionally related RRM RNA-binding proteins (TcUBP1 and TcUBP2), and a *trans*-sialidase (TS) transcript that is *trans*-spliced in the 3'UTR after RNA processing. Interestingly, both these transcripts are developmentally regulated, and this report suggests that the regulation of *trans*-splicing of intermediate mRNAs is necessary to generate mature mRNA transcripts for translation, possibly in a developmental manner [121].

Post-transcriptional regulation via translational efficiency and mRNA stability and the degradation machinery has been studied extensively in these parasites, and these mechanisms require sequences within the 3' UTR of regulated mRNAs to determine their abundance [79]. The 3' UTR of the procyclins EP and GPEET have been extensively characterised for regulatory motifs. As vital and developmentally highly regulated genes, enriched in the procyclic life cycle stage, the procyclins are also one of the major transcripts to be upregulated upon initiation of differentiation from bloodstream to procyclic form.

As discussed in Section 1.2.1, *T. brucei* receives an environmental "shock" upon moving from a 37°C glucose-enriched surrounding to a 27°C nutrient-poor one. GPEET has an element in its 3'UTR that confers regulation in response to glycerol and hypoxia [52]. The significance of this regulation can be explained by GPEET expression for the first few days after differentiation into a procyclic form parasite, and then repression of expression coinciding with the parasite migrating to a new part of the insect midgut, thus showing the importance of post-transcriptional regulation in host-parasite interactions [52]. A similar environmental responsive element is found in the 3'UTR of EP, where deletion analysis showed that a cold shock element is present between positions 173 and 297 (the last 124nt) of the 3'UTR [49]. Bloodstream trypanosomes exposed to a cold shock (20°C) induces the expression of EP, a natural phenomenon that could occur when bloodstream parasites are triggered to differentiate upon ingestion by the tsetse fly [49]. This difference in temperature could affect RNA conformation that may change how the RNA is recognised by the regulatory machinery and thus how EP

is expressed at 20°C compared to 37°C [103]. These elements in the 3'UTR demonstrate their influence upon expression of the procyclins during differentiation in an environment-dependent manner, in addition to showing a specific developmental regulatory mechanism.

For parasite survival, as discussed in Section 1.2.1, procyclin must be tightly down-regulated in the bloodstream form (expression of the invariant procyclin would compromise host immune evasion) and upregulated in the procyclic form (protection in the insect midgut). Several elements within the 3'UTR of EP procyclin have been identified which are responsible for the RNA and protein abundance between life cycle stages. A 16ntd region forms part of a stem-loop structure in the 3' UTR of EP mRNAs, referred to as Loop III (Fig. 1.7), and its sequence and secondary structure have been shown to enhance translation of a reporter gene in procyclic form *T. brucei* [122]. This 16-mer was later found to exert a positive influence on procyclin expression in procyclic forms in the context of the entire 3'UTR [123]. The same study identified a second positive element in the 3'UTR, the first 40ntds after the stop codon referred to as Loop I (Fig. 1.7). Deletion of Loop I caused a substantial decrease in protein expression (8-fold) of a reporter gene, as did deletion of Loop III (decrease 25-fold) [123]. Both these deletions however only had a modest effect on mRNA levels (decrease of 2-fold), suggesting that translational repression was the main mechanism for down-regulation. Further analysis identified a 26ntd region in the 3'UTR that acted as a negative element, referred to as Loop II (Fig.1.7) where deletion of the loop structure caused an increase in reporter gene expression in procyclic cells [123]. In contrast to the positive elements, the Loop II deletion caused an increase an mRNA levels, suggesting regulation is via mRNA stability.

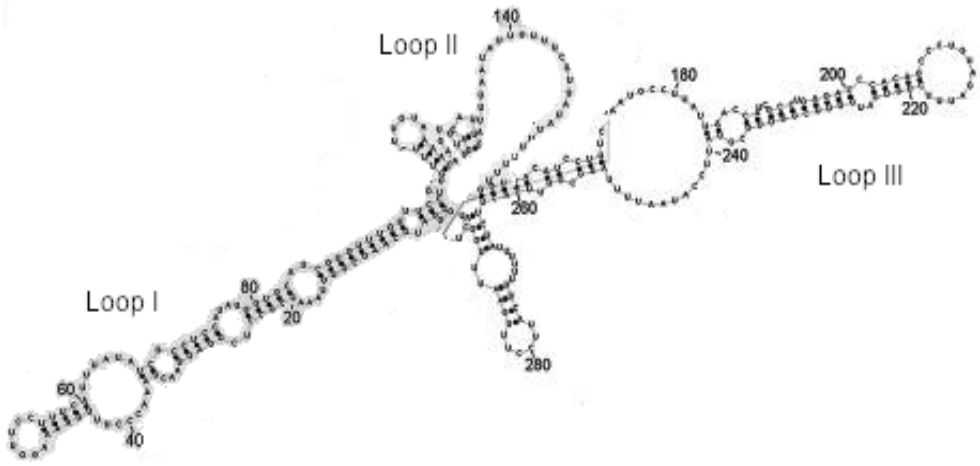


Figure 1.7. Predicted secondary structure of the 3'UTR of EP procyclin mRNA. Adapted from [49].

A model for post-transcriptional regulation of EP suggests that the positive elements (Loop I and III) offset the effect of the negative element (Loop II), which causes mRNA instability and inhibits translation [123]. In bloodstream form cells, deletion of each element has been demonstrated to cause up or down-regulation of a reporter gene in the same manner as in procyclic cells. However, deletion of the 26-mer negative element caused a greater increase of reporter gene expression in bloodstream cells (30 fold increase) compared to that seen in procyclic cells (7-fold increase) [124]. Both these studies suggest an interesting hypothesis that these elements in the 3'UTR do not confer stage-specific regulation, but instead the mRNA exists in two conformations, a stable and unstable one, present in both life forms. The stable conformation would exist predominantly in the procyclic form where the negative element is masked by factors that bind to the positive elements. The unstable conformation would be present mostly in the bloodstream form where the negative element is exposed to a nuclease or binds a translational repressor [123, 124]. Hotz and Clayton [125] suggest an alternative theory that the 26-mer negative element is regarded as the instability element in bloodstream forms. They show that deletion of the negative element in a reporter assay caused turnover rates similar to that of non-developmentally regulated genes, whereas the presence of the negative element caused a greater turnover rate and rapid degradation, thus conferring stage-specific regulation. This study also showed that a point mutation in the 26-mer sequence abolished translational repression without

affecting the level of mRNA in bloodstream cells, which is in agreement with the Schurch et al. hypothesis of a *trans*-acting translational repressor [124, 125].

In addition to defining elements within the 3'UTR of EP that affect its up and down-regulation within a life cycle stage, the presence of these elements can also influence the mechanisms of mRNA turnover and degradation. The presence of the 26-mer negative element has been shown to cause quick degradation of a reporter gene compared to reporters which have the constitutive actin 3' UTR or an EP 3'UTR lacking the 26-mer element. It was shown that reporters with constitutive UTRs were deadenylated and then degraded in a 5' to 3' and 3' to 5' direction by exonucleases when transcription was inhibited in bloodstream forms. However, the reporter bearing the full EP 3'UTR with the 26-mer instability element disappeared very quickly, suggesting either rapid deadenylation or endonuclease activity on the 26mer element [126]. The decay kinetics of the developmentally regulated EP procyclin has been investigated further by studies that suggest two different mRNA degradation pathways exist in trypanosomes depending on the stability of target mRNAs [81, 93]. Transcripts that are not developmentally regulated or stable mRNAs such as actin can be degraded in the 5' to 3' and 3' to 5' direction, but the degradation rate is not limited by the exosome or the exonuclease XRNA when either are depleted [93]. Instead, it appears that the degradation of constitutively expressed and stable mRNAs is dependent and controlled by the rate of deadenylation by the deadenylase CAF1 [81]. Transcripts that are developmentally regulated and unstable mRNAs are rapidly degraded by a second mechanism dependent on the exosome and XRNA [93]. It is also suggested that the rapid degradation pathway, which is XRNA-dependent and deadenylation-independent, targets the majority of EP mRNA, but there is still a slower CAF1 dependent pathway responsible for the degradation of a small subset of EP mRNAs [81]. A possible explanation for the choice of mRNA degradation pathway and the complicated decay kinetics of EP, is dictated by the binding of regulatory RNA binding proteins that may recruit either XRNA or a deadenylase [81]. The role of regulatory RNA binding proteins and their influence on gene expression will be discussed in Section 1.5.

The post-transcriptional regulation of other *T. brucei* developmentally regulated genes is not as extensively characterised as for the procyclin genes, but studies have discovered various elements within the 3' UTR responsible for the enrichment

of a transcript in a particular life cycle stage. The phosphoglycerate kinase (PGK) genes display strong developmental regulation, required to meet the opposing energy metabolism needs between bloodstream form and procyclic form cells. The *T. brucei* PGK-B gene encodes a cytoplasmic enzyme predominant in procyclic forms and PGK-C encodes the major glycosomal enzyme in bloodstream forms [127]. PGK-C mRNA is 20-fold more abundant in bloodstream forms than procyclic, and PGK-B is 10-fold regulated [128], and reporter assays verified that the 3'UTR of each enzyme is responsible for their stage-specific expression [129]. The regulatory region in the 3'UTR of PGK-C mRNA responsible for its bloodstream specific expression has been identified, but a particular sequence element has not been characterised [128]. However, the PGK-B mRNA contains a regulatory AU-rich element (ARE) in the 3' UTR that is responsible for its destabilisation in bloodstream form and similar to the EP procyclin element [130]. The AU rich motif, AUUUA, found in the UTR of PGK-B, is a pentamer sequence often found within U-rich regions of the 3'UTR of transiently expressed lymphokines and cytokines in mammalian cells [130, 131]. An ARE-mRNA database (ARED), using computational analysis, has identified that ARE-containing mRNAs represent 5-8% of human genes, and that they encode functionally diverse proteins important in many transient biological processes such as cell growth and differentiation, metabolism, apoptosis and nutrient transport [132, 133]. The presence of an AU-rich region within the mRNA 3'UTR is classically regarded as a destabilisation element required to regulate degradation of the target mRNA, however, there are plenty of examples of an ARE conferring stabilisation of an mRNA [134]. There are 3 classes of AREs: Class I is defined by several dispersed copies of AUUUA motif within U-rich regions; Class II possesses at least 2 overlapping UUAUUUA (U/A)(U/A) nonamers; and Class III which are U-rich regions but contain no AUUUA motif [134]. The mRNAs that possesses a particular class of ARE tend to encode similar functionally related proteins, and although the classification of ARE was not based on biological function, it is suggested that they may group together mRNAs controlled by similar pathways [134].

The concept that a similar or consensus sequence within the 3'UTR of a group mRNAs that influences their RNA abundance, is receiving much attention, particularly for developmentally regulated genes. Nuclear components of the cytochrome oxidase (COX) complex are developmentally regulated, as they are

not expressed in the bloodstream stage, but are induced upon differentiation to the procyclic form when the mitochondrion is activated [135, 136]. Seven of the COX components are specifically destabilised in bloodstream forms at the mRNA level, and regulation of two of these components, COX V and COX VI are shown to operate principally at the translational level [136]. Reporter assays were used to identify sequence elements responsible for down-regulating COX expression, and in particular, the major regulatory element in the COX V 3'UTR is structurally and functionally similar to the 26mer negative element in the EP procyclic 3'UTR [136]. Further analysis showed that the core element of the 26mer sequence (UAUUUUUU) was present in the 3'UTR of one-third of procyclic form enriched transcripts compared to just 9.6% of all UTRs and 8% of bloodstream form enriched transcripts. This suggests a genome-wide conservation of regulatory sequences across a range of procyclic enriched transcripts [136].

On a more specific scale, subsets of mRNAs that contain the same/similar sequence elements in their 3' UTR and are regulated in a coordinated fashion, is becoming a well recognised phenomenon in several eukaryotes [137], and is likely to exist in *T. brucei* [138]. This concept is referred to as a post-transcriptional operon, where *trans*-acting factors act to regulate a group of functionally related mRNAs at several post-transcriptional levels in order to respond to a cell's need with great efficiency and flexibility [137]. In *T. brucei*, the RNA-binding protein TbPUF9 regulates a subset of mRNAs that encode proteins involved in replicative processes of the cell cycle [139]. Analysis of the mRNA 3'UTRs showed an over-represented 6-mer sequence that when mutated, abolished PUF9 mediated stabilisation of a reporter gene carrying an mRNA target 3'UTR, suggesting these PUF9 targets constitute a post-transcriptional regulon [139]. In the absence of identified *trans*-acting factors that regulate subsets of mRNAs, consensus 3'UTR sequences shared by groups of functionally related mRNAs also suggest co-ordinated post-transcriptional regulation. Analysis of the *T. brucei* COX 3'UTRs and a subset of mRNAs that encode mitochondrial components identified an overrepresented consensus sequence amongst them, suggesting an example of a post-transcriptional operon [136]. Microarray analyses have identified clusters of differentially expressed mRNAs that are regulated in a co-ordinated fashion during differentiation from bloodstream to procyclic form [138]. These examples demonstrate the potential of post-transcriptional regulons operating for

developmentally regulated genes during differentiation as well as within a life cycle stage.

Importantly, as mentioned above, apart from the sequences and elements within the 3'UTR of mRNAs themselves that determine post-transcriptional regulation, the *trans*-acting factors that recognise and bind them are ultimately responsible for regulating the fate of the mRNA whether it be stored, degraded or translated. Additionally, clusters of co-regulated genes identified from microarray analysis contained mRNAs that encode for RNA-binding proteins that could be responsible for regulating subsets of genes in a co-ordinated manner during differentiation and development [59]. The role of these *trans*-acting factors and their importance in post-transcriptional regulation will be discussed in Section 1.5 below.

1.4.3. Developmental regulation at the post-translational level

Very little is known about the role of post-translational regulation of genes in *T. brucei*, particularly when considering developmental gene regulation. A couple of examples have been reported for mitochondrial proteins, which are down-regulated or re-localised to meet the metabolic needs of the bloodstream form parasite. The level of cytochome c mRNA is at similar levels between bloodstream and procyclic form cells, but the level of protein is greatly decreased in bloodstream forms, suggesting that the developmental regulation of cytochrome c is at the post-translational level due to rapid protein turnover in bloodstream form *T. brucei* [140]. The mitochondrial carrier protein MCP6 is developmentally regulated via subcellular localisation; in bloodstream forms it is localised in the glycosome (for glycolysis), and in procyclic forms it is localised to the mitochondrion [141].

Of course the role of protein processing, modification, transport and degradation would be predicted to play an important part, not just for the expression of stage-specific genes, but also for the regulation of RNA-binding proteins that are required to regulate mRNAs at the post-transcriptional level. A large-scale proteomic analysis in procyclic form *T. brucei* has been undertaken that identified over 700 distinct proteins that exist as multiple isoforms suggestive of post-translational modifications, or of protein degradative products [142]. Post-translational

modifications of proteins, such as phosphorylation, myristoylation, farnesylation, cysteine oxidation, ubiquitination, acetylation or methylation, can regulate protein function, by causing changes in protein activity, cellular localisation and dynamic interactions with other proteins [143]. Protein modifications are central to numerous signalling cascades, and recently, a phosphatase cascade has been demonstrated to regulate trypanosome development by transducing an environmental signal to trigger the cell to differentiate [144]. As mentioned above (Section 1.4.2), the role of *trans*-acting factors in co-ordinating the regulation of subsets of genes during differentiation and within specific life cycle stages demonstrates great importance. Therefore, these *trans*-acting factors require their own regulation, and post-translational modification of RNA binding proteins represent a central means of regulating their function within the cell. Phosphorylation of the RNA-binding protein TTP is reported to affect its activity, localisation and stability, thus regulating the expression of the ARE-containing cytokine mRNAs targeted by TTP in a co-ordinated manner [145]. Ubiquitination is also suggested to play a role in the regulation of RNA binding proteins, such as the *C. elegans* germline specific CCCH RNA-binding proteins (PIE-1, POS-1, MEX-1, MEX-5, MEX06) which are degraded upon binding by ZIF-1 that then recruits E3 ubiquitin ligase [146].

Post-translational regulation potentially plays a crucial role in regulating developmental gene expression in trypanosomes. It has been shown to be involved in signalling the differentiation pathway and may be required to regulate *trans*-acting factors required for post-transcriptional mechanisms.

In conclusion, after consideration of the gene arrangement and expression machinery identified in *T. brucei*, the regulatory mechanisms described in this section (1.4) complement the unique nature of gene expression displayed by this parasite. With the lack of RNA polymerase II promoters (and consequently transcriptional control), the ever-increasing evidence of post-transcriptional regulation emphasises its importance as the main point of gene expression control in trypanosomes. This is particularly apparent for the control of key developmentally regulated genes that require tight regulation within different life cycle stages of the parasite to ensure cell survival. *T. brucei* has also taken advantage of using RNA polymerase I to transcribe two vital developmental genes, VSG and procyclin, both necessary to evade the host immune system and protect from the insect midgut. It is commonly believed that the reason for using RNA

polymerase I is that it allows for a faster rate of mRNA synthesis, separating VSG and procyclin from the transcriptional machinery for other protein-coding genes, and ensuring expression of these crucial genes to meet the needs of the parasite's unique life cycle [66]. In contrast, the reliance on mRNA stability and translation to control the dramatic changes in gene expression both during differentiation and within life cycle stages, are of great significance when considering eukaryotic regulation of gene expression as a whole. As this section has explained, as well as the genes themselves that are developmentally regulated, the *trans*-acting factors that bind and control the RNA abundance of these life cycle stage-enriched transcripts are of vital importance to ensure cell survival.

1.5 Regulation of gene expression by RNA-binding proteins

As discussed so far, RNA binding proteins (RBPs) are the key regulators of post-transcriptional events [147], and considering that trypanosomes almost completely lack transcriptional control of gene expression, the role of RBPs to modulate mRNA stability and translational efficiency is of greatest importance in these parasites to survive and transform between mammalian and fly environments. RBPs bind to *cis*-motifs, often located in the 3' UTRs of mRNA, forming ribonucleoprotein complexes which determine the fate of the mRNA, be it translated, degraded, stored or another processing event [148]. They can be classified by the functional motifs they contain, which include the RNA recognition motif (RRM), K-homology (KH) domain, RGG (Arg-Gly-Gly) box, RNA helicase DEAD box domain, zinc finger (CCCH, C2H2, CCCC, CCHC), Pumilio (PUF) domain, double stranded RNA binding domain (dsRBD), and Sm domain [149].

Many RBPs have been identified in *T. brucei* that are involved in a regulating a range of post-transcriptional mechanisms such as the RRM-containing protein, La for SL RNA processing [150], TSR1 is implicated in *trans*-splicing [151], TbPUF9 shown to stabilise mRNA targets [139], and Poly (A) binding protein, PABP1 involved in translational efficiency [104]. In *T. cruzi,* TcPuf6 has been shown to promote degradation of target mRNAs [152]. Despite the identification of numerous developmentally regulated genes in trypanosomes that are controlled by post-transcriptional mechanisms via sequences in the 3' UTR, the *trans*-acting factors that bind and regulate them have remained comparatively elusive. Two small RRM

proteins, TcUBP1 and TcUBP2 in *T. cruzi* are good examples of RBPs that demonstrate a role in developmental gene regulation in trypanosomes. These have been shown to bind an ARE in the 3'UTR of mucin (SMUG) mRNAs and cause instability of the mRNA in a specific life stage of the parasite, allowing developmental regulation of mRNA degradation [153, 154]. In this example, given that RBP and mRNA target have been identified, the mechanism of stabilisation and destabilisation of the developmentally regulated mRNA requires characterisation.

It would be naïve to assume that there is just one RBP for one RNA target, and with the increasing evidence of post-transcriptional regulons in a range of eukaryotic systems, including trypanosomes [136, 139] (see section 1.4.2), the concept of an RBP regulating a specific subset of coordinated genes is a likely scenario. Transcriptome analysis of trypanosomes at different stages in the differentiation process show that sets of mRNAs that function in particular pathways are often co-regulated and show almost identical patterns of regulation, such as those which encode surface coat proteins, or involved in specific metabolic pathways [59].

1.5.1 CCCH zinc finger proteins

One method to identify regulatory proteins is to analyse genes that encode a functional motif. Zinc finger proteins, bearing the C2H2 zinc finger motif, are classically thought of as DNA-binding transcription factors [155]. On the other hand, zinc finger proteins that have variations of the motif such as CCHC, CCCC, as well as the CCCH motif, are widely recognised as RBPs [156]. CCCH zinc finger (ZC3H) proteins have been studied in a range of eukaryotic systems such as yeast [157], Xenopus [158], *Arabidopsis thaliana* [159], *Caenorhabditis elegans* [160] and mammals [161]. Many of these ZC3Hs are required to regulate the expression of developmental genes, such as MOE1/2/3 in *C. elegans* oocyte maturation [162], HUA-1 in *Arabidopsis thaliana* that governs flower development [163], and *Muscleblind* in *Drosophila* required for photoreceptor differentiation [164]. They are involved in many different types of post-transcriptional control such as PIE-1 in *C. elegans* that regulates mRNA transcription and translational activation [165], and Yth1 in yeast that controls 3' end processing [166]. Of particular relevance, the mammalian tristetraproline (TTP) family of proteins, which

contain tandem CCCH zinc fingers of the type $CX_8CX_5CX_3H$, bind AREs in the 3'UTR of TNF-α and GM-CSF mRNAs, causing their deadenylation and decay [167]. There is further evidence to suggest that TTP and other ARE binding proteins that promote unstable mRNA decay, recruit and interact with the exosome (which does not recognise AREs by itself) to initiate degradation after deadenylation has completed [83]. A more recent model for ARE-mediated degradation suggests that TTP possesses two activation domains, one that recruits decay enzymes and one that employs distinct *trans*-acting factors, maybe required to render the mRNP complex accessible to enzymes for RNA decay [168]. Additionally, TTP has been shown to interact with decapping enzymes and enhance decapping of RNA *in vitro* [169]. Another ZC3H protein (with four motifs), zinc finger anti-viral protein ZAP mediates destabilisation of Moloney murine leukaemia virus and Sindbis virus RNA and prevents their accumulation in host cells [170, 171]. ZAP has also been found to interact with the exosome suggesting a similar mechanism of mRNA decay as TTP [172]. Controversially, ZAP does not target ARE-containing mRNAs, although a common motif in the viral RNAs has not been defined [173].

As discussed in section 1.4.2 above, AREs in the 3' UTR of *T. brucei* procyclic-form specific EP/GPEET and PGKB mRNAs have been identified to promote degradation in bloodstream trypanosomes [125, 130]. Several RRM proteins in *T. brucei* that regulate mRNA stability have been identified, but the protein-mRNA complexes are not yet fully characterised. TbUBP1/2 is shown to stabilise a set of transmembrane proteins in bloodstream forms, and the TbPTP1/TbDRDB3 causes mRNA stabilisation and destabilisation, and affects *trans*-splicing, thus demonstrating the multiple regulatory roles that these proteins can employ [174-176]. Thus, RRM-containing RBPs have been identified that regulate mRNA stability in trypanosomes, but to date, no ZC3H proteins have been shown to do so.

In Trypanosomes, genes that encode ZC3H proteins have been recognised as factors that potentially play a vital role in regulating gene expression of target mRNAs through stability and/or translational efficiency. A total of 50 putative ZC3H proteins have been identified in the completed *T. brucei* genome [177]. Most of the ZC3Hs identified in trypanosomes contain the "conventional" motif classified as C-X_{7-8}-C-X_5-C-X_3-H, where X is any amino acid [177]. However, the spacing after the

first cysteine residue is quite variable (from 4 to 15) as seen in many organisms and there are 14 of the ZC3H proteins in *T. brucei* that contain one of these "non-conventional" CCCH motifs [177]. A study which screened lower eukaryote genomes for ZC3H motifs, showed that there is a higher number of conventional ZC3H motifs in the *T. brucei* genome (59) compared to yeast (12-17), or other protozoa such as *Plasmodium falciparum* (26), although the protozoa *Toxoplasma gondii* also has a high number of motifs (49) [177]. This study suggests that the number of ZC3H proteins in *T. brucei* is only slightly higher than in some other protozoa, but importantly, the majority of these ZC3H proteins identified are unique to kinetoplastids [177]. It may be that distinct ZC3H proteins play roles to regulate specific biological processes to meet the needs of a particular organism, and in the case of trypanosomatids, a considerable requirement for regulating developmental genes in a post-transcriptional manner.

Of the identified genes that encode CCCH ZFPs in *T. brucei*, only 4 of them could be assigned predicted functions based upon homologues in other eukaryotes. The splicing factor U2AF35 [178], a FIP-1 like polyadenylation factor [179], the cleavage and polyadenylation specificity factor TbCPSF30 [180] demonstrate the role of trypanosome ZC3Hs in RNA processing. The budding yeast mRNA export factor Mex67 (or mammalian NXF1) does not contain a ZC3H motif, but homology searches identified a *T. brucei* ZC3H protein TbMex67 with characteristic domains of MXF1-related proteins [177]. However, the role of the ZC3H motif in TbMex67 is unknown.

In contrast, studies of another three *T. brucei* ZC3Hs, TbZFP1/2/3, have shown their importance in regulating cellular morphology and differentiation [181-183]. TbZFP1 mRNA levels are shown to be transiently enriched during differentiation to the procyclic form and maintained in procyclic cells, and protein levels of ZFP1 were shown to mirror this stage-specific expression [183]. The generation of a ZFP1 null mutant in bloodstream parasites showed that it is non-essential in this life form. However when triggered to differentiate *in vitro*, the null mutants were compromised in their ability undergo kinetoplast repositioning via microtubule outgrowth at the posterior end of the cell [183]. Even though the kinetoplast repositioning event was disrupted, genetic ablation of ZFP1 did not affect VSG loss, EP procyclin gain or cell cycle progression, which are differentiation events before and after kinetoplast repositioning. This demonstrated that the programmed

events of trypanosome differentiation could be uncoupled at the molecular level [183]. In contrast, ZFP2 is constitutively expressed, but ablation by RNA interference in bloodstream form cells compromises differentiation to the procyclic form [182]. TbZFP3, like ZFP2, is constitutively expressed, and conversely, ectopic over-expression of ZFP3 in bloodstream forms induces enhanced differentiation (i.e. a 2 -fold higher proportion of EP procyclin expressing cells) when triggered *in vitro* [181]. Additionally, ectopic over-expression of ZFP2 or ZFP3 generates a procyclic stage-specific morphological "nozzle" phenotype involving polarised extension of microtubules at the posterior end [181, 182]. Both ZFP2 and ZFP3 possess a WW domain, which is present in members of the E3 ubiquitin ligase family, and in addition to the CCCH motif, are essential but not sufficient for inducing the nozzle phenotype [181, 182]. The WW domain was also shown to be essential for both proteins to bind directly to ZFP1, which possesses the complimentary target of a PPPPY motif, and co-immunoprecipitation studies provided evidence that these proteins can co-associate in the cell [181]. Recently, ZFP3 has been shown to regulate GPEET and EP procyclin isoform protein expression [184], and to co-associate with the translational apparatus specifically in procyclic forms [181]. TbZFP3 also showed sequence-specific association with the previously characterised Loop II (26-mer) negative element and the 16-mer (Loop III) positive element, which repressed or enhanced translation respectively (See section 1.4.2 above), indicating the role of ZFP3 in translational regulation [184]. This study used RNAi down-regulation of ZFP3 with deletion analysis of the EP 3'UTR to suggest that ZFP3 acted primarily as an anti-repressor that competes with a negative regulator for binding of Loop II, thus causing efficient or poor translation respectively [184].

T. brucei relies on post-transcriptional mechanisms to regulate differential gene expression and consequently, the putative role of RBPs within this parasite is of particular importance. ZC3Hs in a range of eukaryotic organisms, as well as TbZFP1/2/3 identified in *T. brucei,* have demonstrated their critical involvement in regulating cellular development and differentiation. Thus, this family of RBPs represent interesting and valuable targets of study to gain further insight into their potential role as post-transcriptional regulators of developmental gene expression.

1.6 HYPOTHESIS AND AIMS

The life cycle of *T. brucei* requires dramatic changes in gene expression to survive within the extreme environments of a mammalian host and insect vector. Given the skew in regulation of gene expression at the post-transcriptional level in trypanosomes, RBPs potentially play an essential role in the tight control and co-ordination of the cellular events required for cell survival.

Whilst other studies have provided information about *T. brucei* genes that are regulated at the level of RNA, the RBPs required to control their regulation have remained relatively elusive. We hypothesise that the ZC3H family of RBPs, which have been shown to play central roles in the regulation of cellular development in other eukaryotic organisms, may have significant roles in controlling the highly regulated biology of *T. brucei*. Three *T. brucei* ZC3H proteins have already shown their involvement in controlling biological processes crucial for trypanosome development.

The main aims of this PhD project are:

1. **To find out whether a ZC3H protein, TbZC3H20, is important for regulating specific cellular processes and development in *T. brucei***
2. **To identify gene(s) that are regulated by ZC3H20 and investigate the mechanisms of control**

The approaches used to address these aims are:

a) Use TbZC3H20 RNAi analysis and null mutants in bloodstream and procyclic form *T. brucei* to determine if the absence of ZC3H20 compromises cell survival.

b) Perform TbZC3H20 RNAi down-regulation or ectopic over-expression in bloodstream and procyclic form *T. brucei* to produce a mutant phenotype, which can be analysed via cell growth, cell cycle and extracellular and intracellular morphology, to suggest a cellular role of ZC3H20.

c) Use microarray analysis to survey the global effect on mRNA levels upon up-regulating or down-regulating TbZC3H20 in *T. brucei*, and in combination with phenotypic data, identify genes that may be regulated by TbZC3H20

d) Investigate the mechanism of post-transcriptional gene regulation by TbZC3H20 by determining i) the capability of RNA binding by TbZC3H20, ii) TbZC3H20-dependent RNA stabilisation or destabilisation, iii) the nature of target mRNA *cis*-elements (if these can be identified) that confer regulation by TbZC3H20.

CHAPTER 2. Materials and Methods

2.1 Plasmid constructs and cloning

2.1.1 PCR

Oligonucleotides used in this study are shown in Table 2.1 and plasmid maps used are shown in Figure 2.1.

The entire coding region of TbZC3H20 was PCR amplified from *T. brucei* genomic DNA (strain 427) using primers that incorporated restriction enzyme sites *Hin*dIII and *Bgl*II. The PCR products were cloned first into the pGEM–T Easy Vector (Promega) (to create pGEM ZC3H20/21) as by the manufacturer's recommended protocol. The ZC3H20/21 in pGEM was then cloned into p2T7i (creating p2T7i 20/21) for tetracycline (tet) inducible double-stranded RNA production (RNAi) [185], or into the tet inducible over-expression vector pHD451 [186] which was modified to express the epitope tag TY1 at the C-terminus of the cloned ZC3H20/21 [187]. The same strategy was used for cloning into the *E. coli* expression vector pGEX-2TK (GE healthcare), except that the primers used incorporated restriction sites for *Bgl*II and *Eco*RI (cloned by Dr. E. Hendriks). The above strategy was also used for cloning ZC3H20 into the pHD451 GFP vector (same as pHD451, but with GFP fused to N-terminus of coding region), but required the use of primers that incorporated *Xba*I and *Bgl*II restriction sites to clone ZC3H20 into the vector.

The pHD451 ZC3H20 construct was also used to introduce a point mutation from CCCH to CCAH for each zinc finger motif of TbZC3H20. The first CCCH zinc finger motif was mutated (C70A) using the Quikchange® II Site-Directed Mutagenesis Kit (Stratagene) with the TbZC3H20 CCCH ZFM1 F and TbZC3H20 CCCH ZFM1 R primers (Table 2.1) by the manufacturer's recommended protocol. The single site-directed mutant (ZFM1) was verified by sequencing, and then used in a subsequent round of mutagenesis using the same kit and protocol but with the TbZC3H20 CCCH ZFM2 F and TbZC3H20 CCCH ZFM2 R primers (Table 2.1) to introduce the mutation into the second zinc finger motif (C178A). This double site-directed mutant (ZFM 1+2) was verified by sequencing. A single site-directed mutant with just the second zinc finger motif (C178A) mutated (ZFM2) was carried out using the same protocol as above, and also verified by sequencing.

For deletion mutants of TbZC3H20 coding region, the same PCR and cloning strategy was used as for the full-length coding region except internal primers were used instead. These primers incorporated the same restriction enzyme sites for cloning into pHD451.

To create the knockout constructs (cloned by Dr. James Trotter), the 5´ and 3´ flanking regions of TbZC3H20 were amplified from genomic *T. brucei* DNA by PCR using oligonucleotides TbZC3H20 5' UTR F/R and TbZC3H20 3' UTR F/R for ZC3H20. The knockout strategy is described in Chapter 3 (Section 3.2.2), and the constructs used are as described by [188] (kindly donated by Kenneth Stuart, Seattle Biomedical Research Institute, University of Washington). These sequences were used to replace the targeting regions of pLEW13 using the unique restriction sites *Not*I, *Xho*I and *Stu*I, leading to the construct for the first replacement, TbZC3H20-KO1. The same sequences were also used to replace the targeting regions of pLEW90 using the restriction sites *Not*I, *Xho*I *(at 907), Xba*I and *Stu*I, leading to the construct for the second replacement, TbZC3H20-KO2 (cloning was carried out by Dr. James Trotter of the Hendriks' lab). Correct integration of the constructs after transfection of PF and BF *T. brucei* (Section 2.2) was tested by PCR, using oligonucleotides that amplified from a gene specific 5' or 3' UTR and from within the integrated construct, to show replacement of the allele (described in Chapters 3 and 5). The same strategy and corresponding primers were used to create knockout constructs for ZC3H21, and then transfected into PF cells.

The pLEW79 – TbZC3H20-TAP (-MH) construct was created as [189] (kindly donated by Ken Stuart, Seattle Biomedical Research Institute, University of Washington), except the coding sequence used was that of TbZC3H20 subcloned from pGEM-20, using the incorporated restriction sites *Hin*dIII and *Bgl*II.

For luciferase reporter assay constructs, the 3' UTR of TbMCP12 and TbTS-like E were PCR amplified from *T. brucei* genomic DNA using primers incorporating *Bam*HI and *Xho*I restriction enzyme sites. PCR products were cloned into pGEM T-easy then subcloned into pGR86 [190] (kindly provided by Antonio Estevez, Instituto de Parasitologia y Biomedicina Lopez-Neyra, Granada, Spain).

For all PCR and RT-PCR reactions, a 50µl reaction was set up with 10µl [5X] Go-Taq® buffer (1.2mM $MgCl_2$ final concentration) and 0.5µl Taq polymerase

(Promega), 2µl of 10µM Forward primer, 2µl of 10µM Reverse primer, 1.5µl of dNTPs (stock concentration of 10mM dATP, dTTP, dCTP, dGTP), 2µl *T. brucei* PF WT genomic DNA (stock concentration approx. 2µg/µl), and then made up to a 50µl reaction with water. PCR conditions were as follows: 1 cycle at 95°C for 5min; 40 cycles at 95°C for 15s, 55°C for 1min, 72°C for 1min per 1kb of target; 1 cycle at 72°C for 2min.

2.1.2 DNA gel electrophoresis, PCR purification and ligations

Electrophoresis of DNA was carried out using 1% agarose (unless stated otherwise) dissolved in TAE buffer and stained with SYBR Safe (Invitrogen). The gel was submersed in TAE buffer, then DNA loaded and electrophoresis was carried out at 100 volts for approximately 45min.

All PCR products used for subsequent cloning were purified using a Gel Extraction kit (Qiagen) and eluted with 30-50µl of water. These purified products were first ligated into pGEM-T easy vector (Promega) according to the manufacturer's instructions, and then 4µl of the ligation used for transformation into 50µl competent *E. coli* DH5α (Invitrogen) or *E. coli* BL21 for the pGEX-2T vector transformation. For ligation into vectors other than pGEM-T, the same T4 ligase and buffer supplied with the pGEM-T kit was used with the 3:1 ratio of insert to vector. The ligation and cells were incubated together on ice for 30min, then heat shocked at 42°C for 30s, then on ice for 2min. The cells were left to recover in SOC medium for 1h at 37°C before plated out onto LB-ampicillin (at 100µg ml^{-1}) agar plates and left to grow overnight at 37°C.

2.1.3 Small and large scale plasmid DNA preparations from *E. coli*, and restriction enzyme digests

For small scale plasmid preparation from *E. coli*, 5ml LB-ampicillin cultures were grown for 12-16h shaking at 37°C. For crude plasmid extraction, a modification of the alkaline lysis method described by Birnboim and Doly was used [191]. From the overnight cultures, 1.5ml was centrifuged for 2min at 13,000*g*, and the pellet resuspended in 100µl Solution I. Then 200µl Solution II was added, inverted to mix thoroughly, and left at room temperature for 3-5min. After cell lysis, 150µl ice-cold Solution III was added, mixed thoroughly by inversion, and spun at 13,000g for 10min at room temperature. To the removed supernatant, 2 volumes of absolute

ethanol was added, mixed by inversion, left on ice for 10min and then spun at 13,000*g* for 15min at room temperature. The pellet was washed in 500µl 70% ethanol, air-dried and resuspended in 50µl water or TE buffer (10mM Tris HCl pH8, 1mM EDTA). For plasmid extraction used subsequently for sequencing, a QuickLysis Mini Prep kit (Qiagen) was used according to the manufacturer's instructions and plasmid DNA eluted in 50µl buffer QLE. These preparations were then sent to an external company (Cogenics™, Essex) for sequencing with the relevant primers. For large scale plasmid preparation of *E. coli*, 50ml LB-ampicillin cultures were grown for 12-16h shaking at 37°C. For plasmid extraction, a Midi Prep kit (Qiagen) was used according to the manufacturer's instructions and plasmid DNA eluted in 100µl buffer EB supplied with the kit.

Restriction digests of plasmid DNA were carried out as follows: 1U of required restriction enzyme(s) (Roche) per 1µg DNA to be digested, 1µl of suitable [10X] Buffer (Roche) per 10µl total reaction, required amount of plasmid DNA, and sdH_20 to make up final volume. All reactions were left at 37°C for 1-2h, except for *Not*I digests for linearising plasmid DNA (15µg) for transfection into *T. brucei*, where the reaction was left overnight at 37°C. The *Not*I digests were then cleaned up with a Qiaquick PCR Purification Kit (Qiagen) according to manufacturer's instructions and plasmid DNA eluted in 50µl water.

2.2 Trypanosome culture maintenance and transfections

PF *T. brucei brucei* strain Lister 427 (WT), PF 29-13 and PF 449 cells were cultured in SDM-79 medium [192] (See 2.16 Reagents and Buffers) at 27^{o}C. BF *T. brucei brucei* strain Lister 427 clone 221 (WT) and BF SMB cells were cultured in HMI-9 medium [193] plus 10% foetal calf serum at 37°C in 5%CO_2.

PF 29-13 and BF SMB cells had been previously engineered to co-express T7 RNA polymerase and tet repressor [194]. PF 29-13 cells were grown in medium with G418 (15µg ml^{-1}) and Hygromycin (50µg ml^{-1}), and BF SMB cells with G418 (2µg ml^{-1}). PF449 cells had been previously engineered to express the tet repressor [188], and grown in medium with Phleomycin (5µg ml^{-1}). Cells counts were carried out using a Z1 Coulter Counter (Beckman Coulter), and PF cells were maintained between 2 x 10^6 - 2 x 10^7 cells ml^{-1} and BF cells between 1 x 10^5 - 2 x 10^6 cells ml^{-1}.

For each PF transfection, a 2ml culture at 1-2x10^7 cells ml^{-1} was harvested by centrifugation at 1300*g* at 4°C, washed in 10ml of cold Cytomix [195], and spun again at the same conditions. Cells were resuspended in 450µl cold Cytomix, transferred to a 0.4cm gap-width cuvette containing 15µg of *Not*I linearized plasmid DNA (on ice) and electroporated (BTX ECM830). Electroporation conditions were 1600 volts, 2 pulses each of 180µs, with a 500ms interval between pulses. Electroporated cells were transferred to a flask containing 10ml SDM-79 medium (without antibiotic selection) to allow recovery for 18h. The next day, flasks were made up to 18ml with fresh SDM-79 medium and the appropriate antibiotics added before transferring 3ml per well to the first row (6 wells) of a 24 well plate. Cells were then serially diluted across the second, third and fourth rows (6 wells each) of the 24 well plate with selective medium. Drug concentrations used for PF selection were as described in [180] and puromycin at 1µg ml^{-1}. Resistant clones were obtained after 14 - 20 days.

For each BF transfection, a 30ml culture at 4 x 10^5 – 1X10^6 cells ml^{-1} was harvested and prepared for electroporation as for the PF cells, except all steps were carried out at room temperature. Electroporation conditions for BF cells were 1600 volts, 3 pulses each of 100µs, with a 200ms interval between pulses. Electroporated cells were transferred to a flask containing 10ml HMI-9 medium (without antibiotic selection) to allow recovery for 18h. The next day, flasks were made up to 50ml with fresh HMI-9 media and the appropriate antibiotics added before transferring 2ml per well into a 24 well plate. Drug concentrations used for BF selection were as described in [180] and puromycin at 0.1µg ml^{-1}. Resistant clones were obtained after 7 - 14 days.

For each BF and PF transfection, a mock control was included in which plasmid DNA was replaced with sterile water. Stable transfectants were induced for RNAi (p2T7i), over-expression (pHD451), or TAP tag expression (pLEW79 TAP) with 1 µg ml^{-1} tetracycline.

2.3 Heterologous Expression in *E. coli* and Homopolymer RNA binding Assays

BL21 transformants (with pGEX2T ZC3H20/U2AF35 or GEX2T (GST alone) constructs) were expanded to a 50ml culture in LB plus 100µg ml^{-1} ampicillin at

37°C and grown to OD_{600} 0.4-0.6. They were then induced with 0.1mM IPTG and left at 17°C overnight shaking. After induction the cells were pelleted and resuspended in BugBuster (Novagen). After 20min rotating at room temperature, pelleted protein (insoluble) and supernatant (soluble) were separated, and the soluble fraction passed through a 0.45µm filter. The filtered lysate was then applied to a GSTrapFF column (GE Healthcare) that had been equilibrated with PBS. This was passed back through the column five times, then washed with PBS and eluted with 50mM Tris HCl and 10mM reduced glutathione pH8.0. Eluted protein fractions (0.5ml) were quantified using Bradford Assay Reagent (Sigma) as per the manufacturer's recommended protocol.

For the RNA homopolymer assay, 500nMoles of GST-purified recombinant TbZC3H20 was mixed with 50µl [20X] Binding Buffer and made up to 1ml volume with water. This was then added to 50µl of 'poly A/C/U/G' sepharose/agarose beads (Sigma), and then rotated for 1h at 4°C. The beads were then washed four times in 1ml wash buffer (100mM NaCl) with incubations for 10min at 4°C. The beads were then resuspended in [4X] laemelli buffer and analysed by SDS-PAGE and Coomassie staining (see below).

2.4 Immunofluorescence assays

To determine *T. brucei* cell cycle status, immunofluorescence analysis was performed on DAPI (4,6-diamidine-2,phenylindole) stained cells. 1 x 10^7 cells were spun at 1300*g* for 10min and 30-40µl of resuspended cells spread onto a slide and fixed in ice-cold methanol for >1h at -20°C. Cells were rehydrated with PBS after which cells were stained with DAPI (diluted 1:1000 in PBS) for 5min to detect nucleic material, washed twice in PBS for 5min and mounted in Mowiol. Slides were viewed with a Nikon Eclipse E600 microscope. Karotype analysis was determined by scoring the number of nuclei (N) and kinetoplasts (K) of over 200 cells. All images were acquired with ACT-1 software on a Nikon Eclipse E600 microscope, using a Nikon Digital Camera DXM1200, and processed with ImageJ software.

For EP procyclin staining, the slides were prepared as for DAPI staining, except after rehydration were probed with antibody to procyclin (1:500 in PBS; Cedar Lane Laboratories), washed twice, then probed with the secondary antibody Oregon

Green goat anti-mouse (1:100 in PBS; Molecular Probes). Slides were then stained with DAPI, mounted and viewed as above.

For the FITC-Tomato lectin assay, 1 x 10^7 cells were spun at 1844*g* for 3min, incubated with SDM-79/1%BSA for 20min at room temperature, incubated at 4°C for 1h in the dark with 100ug ml^{-1} of FITC-Tomato Lectin (Molecular Probes) in SDM-79/1%BSA, washed with SDM-79/1%BSA at 4°C for 30min, fixed with 3% paraformaldehdye (cells resuspended in 0.5ml VPBS, then 0.5ml 6% paraformaldehyde) for 1h at 4°C and washed twice in PBS. After which, 30-40µl of resuspended cells were spread onto a slide and fixed in ice-cold methanol for 20min. PBS was used to rehydrate the cells, after which cells were stained with DAPI, mounted and viewed as above.

For the MitoTracker assay, the assay was the same as for the FITC-Tomato lectin, except cells were incubated with 100nM MitoTracker™ CMXRos (Molcular Probes) for 15min at 27°C.

For BiP and p67 immunofluorescence assays, 1 x 10^7 cells were spun at 1844*g* for 3 min, washed in VPBS, incubated with 3% paraformaldehyde (as described above) for 15min on ice, washed twice with VPBS and spread into a microscope slide. Cells were permeabilised with 0.1% Triton-X100 for 10min, blocked with 3% BSA/PBS for 1h, incubated with primary antibody i.e. mouse anti-p67 (1:100) and rabbit anti-BiP (1:1500) (both antibodies generously donated by J. Bangs, University of Wisconsin-Madison Medical School) for 1h, and then with relevant secondary i.e. goat anti-mouse Oregon-Green (1:200) or goat anti-rabbit Texas Red (1:200; Molecular Probes) for 1h. Cells were then stained with DAPI, mounted and viewed as above.

2.5 Endocytosis assay

Microscopic analysis of FM4-64FX (fixable analogue of N-(3-triethylammoniumpropyl)-4-(6-(4-(diethylamino)phenyl)hexatrienyl)pyridinium dibromide) (Invitrogen) uptake was carried out by a modification to the protocol used by Bonhivers et al. [29]. A total of 1x10^7 cells of PF449 or induced PF449 20 OeX were harvested by centrifugation at 1844*g* for 3min, washed in PBS and resuspended in 1ml PBS, 0.1mM adenosine, 10mM glucose. FM4-64FX was added to give a final concentration of 2.5µg ml^{-1}, and then incubated at 27°C for

15min on a rotary shaker (25rpm). The cells were then immediately put on ice, centrifuged at 1844*g* for 3 min at 4°C, washed in ice-cold PBS and spun again at 1844*g* for 3 min at 4°C. They were then fixed in cold 4% paraformaldehyde (cells resuspended in 0.5 ml VPBS, then 0.5 ml 8% paraformaldehyde) and incubated at 4°C in the dark for 15min. The fixed cells were again spun at 1844*g* for 3min at 4°C, washed in ice-cold PBS and 30-40µl of resuspended cells spread onto a microscope slide. The slides were left to dry at 4°C in the dark. DAPI in PBS (as Section 2.4) was added to the dried slides and incubated for 5min at 4°C in the dark. Slides were washed twice in ice-cold PBS for 5min at 4°C in the dark, mounted with MOWIOL and allowed to set in the fridge. Images were acquired as above for immunofluorescence assays.

2.6 Transmission electron microscopy

A total of 1 x 10^7 cells of PF449 or induced PF449 20 OeX were harvested by centrifugation at 1300*g* for 10min. Samples were prepared as described by [36], except a Transmission Electron Microscope Tecnai 12 (FEI, Eindhoven, Holland) was used for observation and a CCD camera for the image acquisition. This was performed in collaboration with Dr. Raffaella Carzaniga (Electron Microscopy Centre, Imperial College London).

2.7 *T. brucei* genomic DNA extraction and PCR of null mutants

Genomic DNA extraction from PF and BF ZC3H20/1 single and double knockout mutants was carried out as described by [196] but with some modifications. Cells (2 - 2.5x10^8) were spun at 2000*g* for 10min at room temperature. Culture medium was removed and cells resuspended in 1ml lysis buffer plus 100µg Proteinase K. The cells were incubated at 37°C for 1h with gentle agitation, then to 65°C for 15min. Two volumes of absolute ethanol were added and the sample spun at 10,000*g* for 30min at 4°C. Supernatants were discarded and pellets allowed to air-dry prior to resuspension in 60µl water. For each PCR reaction, approximately 200-300ng of genomic DNA and 1ng of plasmid DNA was used. Primers sequences for verifying knockout construct integration are shown in Table 2.1. PCR conditions as follows: 95°C for 5min x 1 cycle; 95°C for 15s, 60°C for 1min, 72°C for 1min 30s x 40 cycles; 72°C for 2min x 1 cycle.

2.8 Protein extraction from *T. brucei*, SDS-PAGE and western analysis

For protein isolation from BF and PF cells, $2x10^7$ cells were harvested by centrifugation at 1300*g* for 10min and washed in 1ml of PBS. The cell pellet was then re-suspended in 75µl of PBS and 25µl of [4X] laemelli buffer. The sample was then boiled at 100°C for 5-10min before loading 10µl ($2x10^6$ cells) per well of an SDS-PAGE gel.

SDS-PAGE gels made for separation of protein samples were 10% polyacrylamide (37.5 acrylamide:1 bis-acrylamide) for the lower separating gel and 7.5% for the upper stacking gel. The gel was submersed with running buffer in an electrophoresis tank and after loading of boiled, denatured protein samples and unstained recombinant protein ladder (M0671, Sigma), was subjected to 120V for approximately 80min.

The electrophoresed gels were then either Coomassie stained, Sypro Ruby stained or used for transfer of proteins to a nitrocellulose membrane. Gels were submersed and agitated in Coomassie stain for 30 min at room temperature, then destained (40% methanol, 10% acetic acid) for 30min 2-3 times. The gel was imaged using a photo scanner (Epson V700 Photo) and imaging software (Lasersoft Imaging Silverfast Epson software). Gels were submersed and agitated in Sypro Ruby overnight at room temperature, then destained (10% methanol, 7% acetic acid) for 1-2h with two washes with distilled water for 10s. The gel was imaged with a UV transilluminator.

For transfer of proteins to a nitrocellulose membrane, a semi-dry blotting apparatus was used. Transfer buffer with 20% methanol was used to activate the nitrocellulose membrane and wet the blotting pads. The transfer was carried out at 15V for 30-45min.

The nitrocellulose membrane was then stained with Ponceau stain for 3min and destained with distilled water, to check transfer of proteins and mark the protein ladder.

The membrane was blocked in 5% milk with PBS overnight at 4°C, washed in PBS for 5min, then incubated with mouse BB2 (anti-Ty) antibody (generously donated by Keith Gull, University of Oxford) at 1:20 dilution in 5% milk/PBS for 2h at 4°C. The membrane was washed three times for 10min in PBS, then incubated with rabbit anti-mouse antibody conjugated to HRP (DakoCytomation) at 1:2000 dilution in PBS – Tween (0.1% $Tween^{20}$) for 1h at 4°C. The membrane was

washed three times in PBS-Tween for 15min and once in PBS for 5min. The chemilluminescence signal was detected with Pierce® ECL Western Blotting Substrate (Thermo Scientific) to identify TY1 tagged ectopic ZC3H20 overexpression in PF449 cells, and detected with Pierce® ECL West Femto Substrate (Thermo Scientific) to identify ectopic over-expressed ZC3H20 in BF SMB cells. The Western blot signals were captured using a LAS-3000 Fuji imager (Fujifilm).

For western blots to be probed with anti – TbZC3H20 antibody, the membrane was blocked overnight as above, and then incubated with purified rabbit anti-TbZC3H20 peptide antibody (1:10) in 1% BSA/PBS for >3h at 4°C. The membrane was washed as above, then incubated with swine anti-rabbit antibody conjugated to HRP (DakoCytomation) at 1:2000 dilution in PBS-Tween (0.1% Tween^{20}) for 1h at 4°C. The membrane was then processed as above, using Pierce® ECL West Femto Western Blotting Substrate (Thermo Scientific).

2.9 RNA isolation and Northern analysis; transcriptional and translational inhibition

For RNA isolation, 0.5-1x10^8 BF cells and 1-2x10^8 PF cells, were harvested by centrifugation at 1300*g* for 10min, washed in half volume of PBS, and then washed again in 1ml of PBS. The cell pellet was then re-suspended in 600µl Buffer RLT (Qiagen RNeasy kit) plus 6µl β-mercaptoethanol. The RNA was then processed using the Qiagen RNeasy kit as per the manufacturer's instructions, and eluted with sterile RNAse free water. The concentration of RNA was measured using a Nanodrop ND-1000.

To measure the rate of mRNA turnover in PF RNAi 20 and PF 20 OeX cells, these cells were first grown in the presence or absence of tetracycline for 48 hours (for RNAi) or 12h (for OeX). These cells were then treated with 5µg ml^{-1} actinomycin D for 1, 2, 4h, and RNA isolated and processed as described above.

The translational inhibition studies were conducted on WT BF and PF cells treated with 50µg ml^{-1} cycloheximide for 1, 2 and 4h, and RNA isolated and processed as described above. Untreated samples for both the actinomycin D and cycloheximide transcription and translation analyses were also prepared from BF and PF *T. brucei*.

For northern analysis approximately 3µg of RNA was loaded for each sample onto a formaldehyde agarose gel. The gel was covered with [1X] MOPS buffer, and the RNA electrophoresed at 150V for 45min. The RNA was transferred from the gel to a nylon membrane by capillary blotting using [10X] SSC buffer. RNA was cross-linked to the membrane using a CL-1000 ultraviolet crosslinker (UVP), and then prehybridised in hybridisation buffer for more than 1h. The blots were then hybridised at 68°C with 2µl of the relevant Riboprobe (0.5µl for actin and tubulin blots) labelled with digoxygenin (Roche) in fresh hybridisation buffer overnight. Stringency washes were at 68°C; first two washes at low stringency ([2X] SSC, 0.1% SDS) for 30-45min, then two washes at high stringency ([0.1X] SSC, 0.1% SDS) for 30-45min. The blots were blocked in 1% block solution in maleic acid buffer for more than 1h, then incubated for 30-45min with anti-Digoxygenin – AP – Fab fragments antibody (1:2500, Roche) in blocking solution. Maleic acid wash buffer was used to wash the blot 3 times for 10min, and then immersed in detection buffer for 2min. Blot detection was by chemilluminescence using CDP-star (1:100 in detection buffer; Roche) as a reaction substrate. This was incubated with the blot for 10-15min at 37°C before imaged using a FujiFilm LAS-3000 Imager. To quantify the level of transcript in each sample, densitometry of the signal was performed using QuantityONE® software (BioRad). Loading was equalized by the concentration of RNA loaded and signal obtained with tubulin.

2.10 RNA Riboprobe preparation

An approximate 600bp region of the target gene for a riboprobe to be made was amplified by PCR using primers from Table 2.1, using the same PCR conditions as described in Section 1.2.1. The PCR products were then cloned into the pGEM T-easy vector as described above in section 1.2.2, and small-scale plasmid preparations as in section 1.2.3 using the Qiagen MiniPrep Kit. These plasmid preparations were then used in a PCR with the commercially available M13 forward and reverse primers that amplify from regions within the pGEM-T easy vector, incorporating T7 and SP6 promoter sites. The PCR products were then purified using a Gel Extraction kit (Qiagen) and eluted with 30µl sdH_20. The purified DNA was then used in a transcription reaction with 1µg template, 2µl of a digoxygenin labelled (UTP) NTP mix (Roche), 1µl 0.1M DTT, 1µl RNase OUT (Roche), 2µl [10X] transcription buffer (Roche), 2µl SP6 or T7 RNA polymerase

depending on the required direction of transcription (20U μl^{-1}, Roche), and RNase-free water to make up the reaction to 20µl. The reaction is then incubated at 37°C for 2h, and 2µl DNaseI (10U μl^{-1}; Roche) added and incubated for a further 15min at 37°C. To stop the reaction, 2µl 200mM EDTA, pH 8 was added. To precipitate RNA, 2.5µl 4M LiCl and 75µl of cold absolute ethanol was added, and left overnight at -20°C. The following day, the sample was spun at 20,000*g* for 1h at 4°C. The pellet was washed in 50µl of cold 70% ethanol, spun at 20,000*g* for 1h at 4°C, and then left to air-dry before resuspended in 50µl RNase-free water and 1µl RNase OUT (Roche).

2.11 RNA Electrophoretic Mobility Shift Assays (EMSA)

Reaction mixtures of 10µl were set up to contain 5µl of recombinant protein and 5µl of digoxygenin labelled (UTP) RNA. Recombinant GST-ZC3H20 or GST protein was diluted to the appropriate concentrations (at a [2X] of required final concentration) using the [2X] EMSA binding buffer in a total of 5µl. The digoxygenin labelled RNA was diluted to 5ng μl^{-1} using RNase-free water, and added to the 5µl of recombinant protein (or 5µl of [2X] EMSA binding buffer as a control), placed on a 37°C heating block and gently agitated every few min for 10min. Each reaction prepared for loading with addition of 1µl of Bluejuice™ Gel Loading buffer (Invitrogen). The entire mixture was loaded onto a 0.8% agarose gel in TAE buffer and electrophoresed at 40V for 3h. The RNA was then transferred to a nylon membrane by capillary blotting, cross-linked, washed in Maleic acid buffer for 30min, and then blocked and processed as usual for Northern blot analysis (see section 2.9).

2.12 Reverse transcriptase PCR (RT-PCR) and Quantitative Real-Time PCR (qPCR)

In both RT-PCR and qPCR experiments, RNA was treated with DNase I by using the DNA-*free* kit™ (Ambion). Template cDNAs for RT-PCR and qPCR were generated from 2µg RNA using random hexamers and oligo$(dT)_{20}$ with Superscript III First-Strand Synthesis Supermix as described by the manufacturer (Invitrogen). Control reactions without reverse transcriptase were used to confirm the absence of contaminating genomic DNA. To amplify interacting mRNA species with TAP

tagged TbZC3H20, RT-PCR was used with gene specific oligonucleotides within the coding regions (Table 2.1). PCR reactions were as described above using Taq-polymerase, except the template used was 1µl TAP TbZ3H20 cDNA -/+RT, or WT genomic DNA or sterile de-ionised water as positive and negative controls. Amplification conditions were as described above (Section 2.1.1).

Quantitative real-time PCR (qPCR) was performed by Dr. James Trotter, as described previously [197] with slight modification. Integrity of the DNaseI treated RNA for q-PCR was confirmed by using an RNA nanochip on a BioAnalyzer (Agilent RNA 6000 Nano Kit, Agilent Technologies), and the protocol was carried out as per the manufacturer's recommended protocol. For qPCR experiments cDNA reactions were diluted 10 fold for all targets except ß-tubulin mRNA and 18S rRNA internal controls which were further diluted 1:50 to obtain similar *C*t values. Each 15µl qPCR contained 2µl of each diluted cDNA (or minus reverse transcriptase control), 2.75µl each of 1.5µM forward and reverse primers, and 7.5µl SYBR GreenER qPCR Super Mix (Invitrogen) in 96 well plates using the ABI Prism 7700 Sequence Detection System (Applied Biosystems). Amplification conditions for qPCR were 50^{o}C for 2min and 95^{o}C for 10min, followed by 40 cycles of 95^{o}C for 15s and 60^{o}C for 1min. Each mRNA species was analyzed in triplicate. Thermal dissociation and agarose gel electrophoresis confirmed PCR generated a single product of the expected size. Data analysis was carried out by using the Pfaffl method, with PCR efficiencies calculated by linear regression with LinRegPCR software [198, 199]. Relative changes for target amplicons were calculated after normalization to ß-tubulin mRNA and 18S rRNA and were expressed as relative mRNA abundance from the respective control cells. Primer sequences for qPCR, designed with Applied Biosystems PRIMER EXPRESS 1.5a software (by Dr. James Trotter), are in Table 2.1.

2.13 Purifying TAP-tagged TbZC3H20 mRNA complexes

Expression of TbZC3H20-TAP in PF cells was induced for 48h with tet, and TAP-tagged complexes were purified from 2l of cells harvested at a density of 1.5x10^{7} cells ml^{-1}. Cells were harvested by centrifugation at 4°C at 1300*g* for 10min, washed in cold PBS with 6mM glucose, and resuspended in 18ml cold IPP150 and 2ml 10% Triton-X100. Cells were lysed by rotation at 4°C for 25min and then centrifuged at 4°C at 10,000*g* for 15min to remove insoluble material.

200µl of IgG Sepahrose beads ("fast-flow", Pharmacia) were washed in IPP150 in an Econo-Pac column (Bio-Rad) at 4°C for 5min, then the cleared cell lysate was added to the washed column and rotated for 2h at 4°C to allow binding. The column was washed three times in 10ml cold IPP150 and once with 10ml cold TEV cleavage buffer. The TAP tag was then cleaved by adding 1ml of TEV cleavage buffer and 100 units of TEV protease (Invitrogen), and incubated the beads for 2h at 16°C. To the TEV eluate recovered from the column, 3 volumes of calmodulin binding buffer (CBB) and 3µl 1M $CaCl_2$ per ml of eluate was added. 200µl calmodulin resin was added to a disposable 5ml column and washed for 5min at 4°C with 5ml CBB. The sample was then transferred to the column containing the washed calmodulin resin and rotated for 1h at 4°C. The column was washed five times with 5ml CBB, and then the TbZC3H20-mRNA complexes eluted with 250µl calmodulin elution buffer. To this recovered eluate, 0.5ml TRI Reagent® (Sigma-Aldrich) was added and incubated at room temperature for 5min. Isolation of RNA was then carried out as per the manufacturer's instructions, and the RNA pellet resuspended in 10µl RNAse-free water. The entire sample was then DNAse treated and reverse-transcribed as described above.

2.14 Microarray analysis

For the microarray samples, trypanosomes were grown in the presence or absence of tet for 12h (PF ZC3H20 OeX), or 24h (BF ZC3H20 OeX) or 48h (PF ZC3H20 RNAi) to a cell density of 1-2 x 10^6 ml^{-1} in 50ml for BF cells or 1-2 x 10^7 ml^{-1} in 10ml for PF cells. RNA was isolated using the RNeasy kit as described above in Section 2.9. RNA concentration was determined using an ND-1000 NanoDrop spectrophotometer. RNA samples were sent to the Oxford Gene Technology (OGT) Limited for microarray analysis. The microarray chip was designed by OGT and Dr. Edward Hendriks. Three 60-mer gene specific probes were synthesised for each gene across the *T. brucei* genome, where each probe was synthesised *in situ* directly onto each microarray chip. The RNA samples were labelled with Cy3 (green) or Cy5 (red), and each microarray set was carried out in triplicate, with a dye-switch for one of the replicates.

2.15 Computing, Statistics and Bioinformatics

All graphs and charts were generated using Microsoft Office Excel and Powerpoint.

Statistics to test significance of a test sample compared to a control sample used at least three independent experimental values for each sample and determined using a two-tailed Student's t-Test, assuming normal distribution.

Densitometry analysis was carried out using Quantity One software (BioRad). The volume Rectangular tool was used to draw areas of the Northern blot for analysis, and the local background subtraction method to obtain the adjusted volume (density) values. For the actinomycin D assay, time point 0h was assigned 100%, and then the volume values of other time point were calculated as a percentage of the 0h time point value. To determine the half-life of mRNA (Chapter 3), a line of best fit was drawn and used to read the time point at which mRNA had decreased to 50%. To test the significance in mRNA half-life between induced and uninduced cells (Chapter 3), a line of best fit was drawn for each replicate to calculate three individual half lives for both cell line, and these values used in a Student's t-test. For all other uses of the Student's t-test, the values from three replicates were used to test the significance between two conditions as described for that experiment in the Chapter text.

Gene sequences from the *T. brucei* genome (strain 927) were obtained from GeneDB (www.genedb.org). Clustal W2 was used to align gene sequences (http://www.ebi.ac.uk/Tools/msa/clustalw2/), and the software program ApE (online accessible freeware) used to analyse gene sequences.

2.16 Reagents and Buffers

2.16.1 Cloning and general buffers

PBS

136.9mM NaCl, 2.5mM KCl, 10.14mM Na_2HPO_4, 1.76mM KH_2PO_4, pH7.4

Autoclaved when used in cell culture and Northern analysis

TAE buffer [50X] stock (1l)

242g Tris Base (Final [1X] 0.04M Tris – Acetate)

57.1ml Glacial Acetic acid

100ml 0.5 M EDTA pH8.0 (Final [1X] 1mM EDTA)

SOC medium (100ml)

2g Tryptone, 0.5g Yeast Extract, 1ml 1M NaCl, 0.25ml 1M KCl, 1ml 1M $MgCl_2$, 1ml 1M $MgSO_4$, 1ml 2M glucose

Filter-sterilise

Lysogeny broth (LB) medium (1l)

10g Tryptone, 5g NaCl, 5g Yeast Extract

Make upto 1l with distilled water and autoclave

Once cooled, ampicillin can be added (100µg ml^{-1} final)

LB agar plates (500ml)

5g Tryptone, 2.5g NaCl, 2.5g Yeast Extract

Make upto 500ml with distilled water, add 6g Microagar, and autoclave.

Once cool enough, ampicillin can be added (100µg ml^{-1} final), and plates poured.

Alkaline lysis – Solution I

25mM Tris HCl pH 8, 50mM glucose, 10mM EDTA pH 8

Alkaline lysis – Solution II

0.2N NaOH, 1% sodium dodecyl sulphate (SDS)

Alkaline lysis – Solution III

5M KOAc pH 4.8

2.16.2 Trypanosome cell culture

SDM-79 medium (PF culture medium) (1l)

25.4g SDM-79 media powder, 2g $NaCO_3$

10ml Penicillin-Streptomycin (Sigma; 10000U ml^{-1} Penicillin, 10mg ml^{-1} Streptomycin)

pH to 7.3 using NaOH solution

150ml foetal calf serum (tet free), 3ml Hemin (2.5mg ml^{-1} Hemin in 50mM NaOH)

Make up to 1l using deionised water and filter sterilise

HMI-9 medium (BF culture medium) (1l)

18g HMI-9 media powder, 3g $NaCO_3$

10ml Penicillin-Streptomycin (Sigma; 10000U ml^{-1} Penicillin, 10mg ml^{-1} Streptomycin)

14µl β-mercaptoethanol, pH to 7.2 using NaOH solution

100ml foetal calf serum (tet free)

Make up to 1l using deionised water and filter sterilise

T. brucei genomic DNA extraction lysis buffer

10mM Tris-HCL, pH8, 5mM EDTA, 0.5% SDS, 200mM NaCl

2.16.3 Recombinant protein expression and *in vitro* binding assays (EMSA)

Binding buffer for homologous recombination [20X]

200mM Tris-HCl, pH 7.4 (10mM final), 1M NaCl (50mM final)

EMSA binding buffer [2X] (40ml)

13.33ml of 300mM Tris pH7 (autoclaved; 100mM final for [2X], 20ml of 600mM NaCl (autoclaved; 300mM final for [2X]), 20mg bovine serum albumin (0.5mg ml^{-1} final for [2X])

Make up to 38mls with s.d.H_2O, and store at 4°C

Made fresh: Add 50µl of 10mg ml^{-1} tRNA to 950µl of above buffer to make [2X] EMSA binding buffer

2.16.4 Immunofluorescence assay reagents

VPBS

136.9mM NaCl, 2.8mM KCl, 16mM Na_2HPO_4, 3mM KH_2PO_4, 45.9mM sucrose, 10mM glucose, pH7.4, then filter-sterilised.

Paraformaldehyde (6%) (10ml)

0.6g paraformaldehyde, 10ml VPBS, 0.2ml 1M NaOH, pH7.4

MOWIOL

6g glycerol, 2.4g Mowiol, 6ml sdH_2O, 12ml 0.2M Tris pH8.5

2.16.5 SDS PAGE/ Western blot analysis solutions

Laemelli buffer [4X]

250mM Tris-HCl pH6.8, 8% SDS, 40% glycerol, 4mg Bromophenol blue (for 100ml final volume), 5% β-mercaptoethanol

Lower gel buffer

1.5M Tris-HCl, pH 8.8, 0.4% SDS

Upper gel buffer

0.5M Tris-HCl, pH 6.8, 0.4% SDS

Lower stacking gel (10% polyacrylamide, final volume 5ml)

1.25ml lower gel buffer, 1.67ml Acrylamide (30% 37.5:1), 2ml sdH_2O

37.5µl 10% APS, 6.25µl TEMED

Upper stacking gel (7.5% polyacrylamide, final volume 1.5ml)

225µl upper gel buffer, 375µl Acrylamide (30% 37.5:1), 900µl sdH_2O

7.5µl 10% APS, 24µl TEMED

Running buffer

25mM Tris-HCl pH8.3 , 192mM glycine, 0.1% SDS

Coomassie Stain

1g/l Coomassie Brilliant Blue R250, 50% methanol, 10% acetic acid, 40% water

Filter solution

Semi-dry Transfer buffer

50mM Tris Base, 40mM glycine, 1% SDS

Ponceau stain

0.4% Ponceau S, 3% trichloroacetic acid

2.16.6 RNA Northern blot analysis buffers

All RNA solutions were autoclaved/filter sterilised once prepared.

MOPS buffer [10X]

0.221M MOPS, 5mM sodium acetate pH7, 10mM EDTA pH8

RNA gel loading buffer (500µl total volume)

150µl formamide, 83µl formaldehyde (37%), 50µl [10X] MOPS, 0.01% Bromophenol blue

100µl glycerol, 117µl sdH_20

Formaldehyde agarose gel preparation

1.2% agarose , 1.1% formaldehyde, [1X] MOPS

SSC (sodium chloride/sodium citrate) buffer [20X]

3M NaCl, 0.3M Tri sodium citrate

Maleic acid buffer

100mM maleic acid, 150mM NaCl, 7.5g NaOH

Adjust to pH7.5 with liquid 5M NaOH

10% Block Solution

10g Blocking Reagent (Roche), 100ml Maleic Acid Buffer

Dissolved carefully in microwave, and then autoclaved. Stored -20°C

Hybridisation buffer (50ml)

10ml 10% Block solution (2% final), 25ml formamide (50% final),

12.5ml [20X] SSC ([5X] SSC final), 1.9ml sdH_20, 100µl 10% SDS (0.02% final)

0.5ml 10% Sarkosyl (0.1% final)

Maleic acid wash buffer

[1X] Maleic acid buffer, 0.3% Tween ^{20}

Detection buffer

100mM Tris HCl pH9.5, 100mM NaCl

2.16.7 TAP-tag protocol solutions

IPP150

10mM Tris-HCl pH 8.0, 150mM NaCl, 0.1% Igepal

TEV cleavage buffer

10mM Tris-HCl, pH 8.0,150mM NaCl, 0.1% Igepal, 0.5mM EDTA, 1mM DTT

Calmodulin binding buffer (CBB)

10mM Tris-HCl, pH 8.0, 150mM NaCl, 0.1% Igepal, 10mM β-mercaptoethanol
1mM magnesium acetate, 1mM imidazole, 2mM calcium chloride

Calmodulin elution buffer (CEB)

10mM Tris-HCl pH 8.0, 150mM NaCl, 0.1% Igepal, 10mM β-mercaptoethanol
1mM magnesium acetate, 1mM imidazole, 2mM EGTA

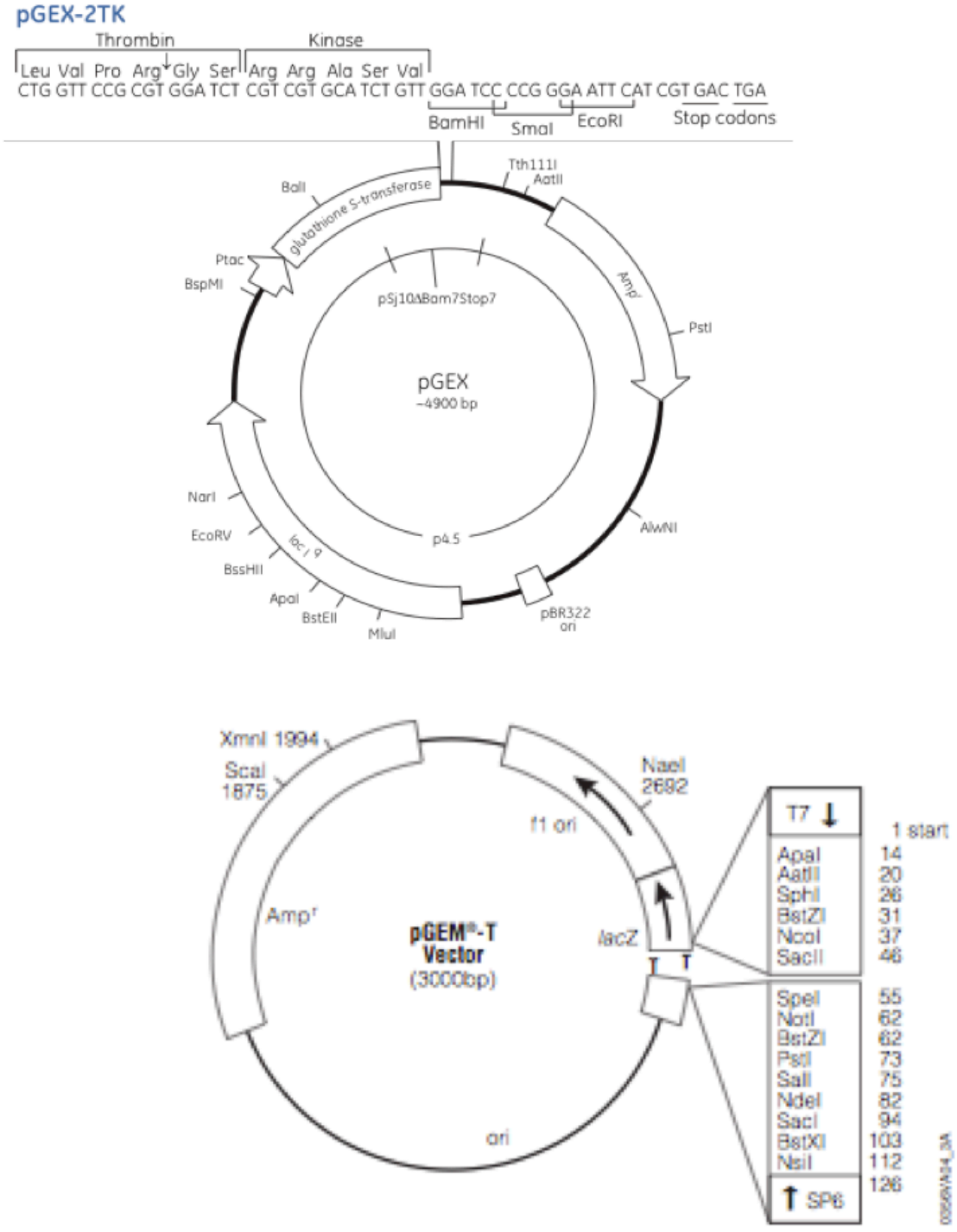
Table 2.1. Oligonucleotides used in this study

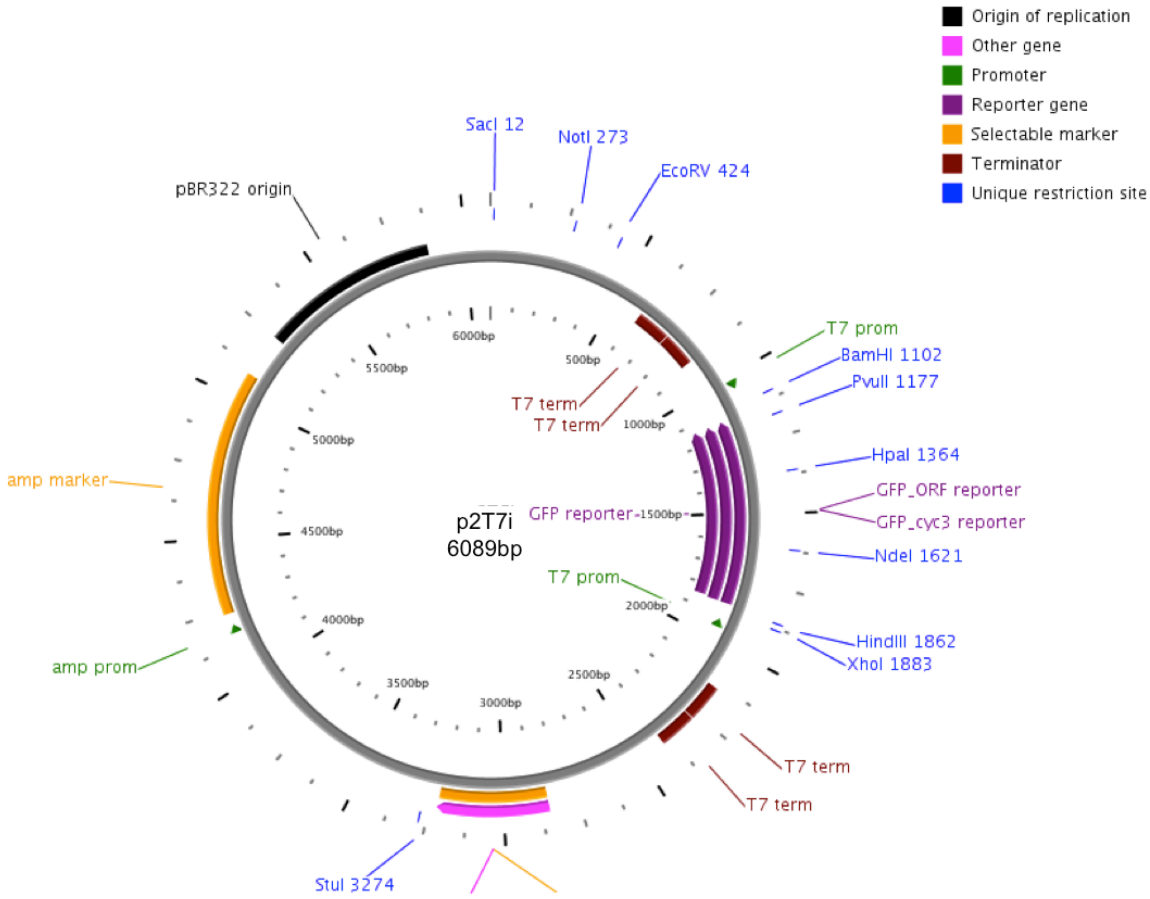
Primer	Sequence	Use
TbZC3H20 BglII R	AGA TCT ATT CCT GCC CCT CCC TTC CCC	pHD451/p2T7i
TbZC3H20 HindIII F	AAG CTT ATG CAG CTC GTA GCC TCG	pHD451/p2T7i
TbZC3H20 BglII F	AGA TCT CAG CTC GTA GCC TCG CCA CTC	pGEX2T
TbZC3H20 EcoR1 R	GAA TTC TTA ATT CCT GCC CCT CCC TTC	pGEX2T
TbZC3H21 HindIII F	AAG CTT ATG AGC CAT CCA CAA TCT C	pHD451/p2T7i
TbZC3H21 BglII R	AGA TCT ATC GCT GAT TCC TCC CGT TGG	pHD451/p2T7i
ZC3H20 CCCH ZFM1	GGCAGGGTACACAGGCCCATCAGGTGCATGC	ZFM1 (C70A)
ZC3H20 CCCH ZFM1	GCATGCACCTGATGGGCCTGTGTACCCTGCCG	ZFM1 (C70A)
ZC3H20 CCCH ZFM2	CGCTACGCGGAGGAGGCCAATTACCTCCACATC	ZFM2 (C178A)
ZC3H20 CCCH ZFM2	GATGTGGAGGTAATTGGCCTCCTCCGCGTAGCG	ZFM2 (C178A)
ZC3H20 Δ111N HindIII	AAG CTT ATG TCG CGC GTT GTG GTT CAC	pHD451 Δ mutant
ZC3H20 Δ206N HindIII	AAG CTT ATG GCG AGG TGT GAT CGG GGC	pHD451 Δ mutant
ZC3H20 Δ148C BglII R	AGA TCT CGG TGC ATC GCA GGC AGC C	pHD451 Δ mutant
ZC3H20 Δ229C BglII R	AGA TCT CTC CAG CAC AAG GCA CGA TG	pHD451 Δ mutant
TbZC3H20 5' UTR F	GCG GCC GCC AGA TGC ATG TGT GTG TTC	pLew13/pLew90
TbZC3H20 5' UTR R	ACG CGT CTC GAG CAA GAA GTG TGG CAG T	pLew13/pLew90
TbZC3H20 3' UTR F	TCT AGA GAT ATC ACA GAC TGC GTT CTG AGC	pLew13/pLew90
TbZC3H20 3' UTR R	AGG CCT GCG GCC GCT GTC TCT TGT CTT ATC AC	pLew13/pLew90
TbZC3H21 5' UTR F	GCG GCC GCC ATG CCA ATT CTG CAC TTA	pLew13/pLew90
TbZC3H21 5' UTR R	ACG CGT CTC GAG GCA ACC AAG TGC AA	pLew13/pLew90
TbZC3H21 3' UTR F	TCT AGA GAT ATC TGG ATG ATG GTA AGG GGT	pLew13/pLew90
TbZC3H21 3' UTR R	AGG CCT GCG GCC GCA CAA ATG AAG CGA TAG	pLew13/pLew90
ZC3H20 3' UTR int R	CTC ACC ACC CTT TCC TTT TC	KO integration
ZC3H20 5' UTR int F	CAC AAA TAC TTA TAG GTG CG	KO integration
ZC3H21 5' UTR int F	GCA TGA AGC CAG CAT ATT TGG	KO integration
ZC3H21 3' UTR int R	CAT GCC CTT TCA CAC GTC AG	KO integration
pLEW13 3' int F	CTT GAC GAG TTC TTC TGA GC	KO integration
pLEW13 5' int R	CAT TCT GTA AGA CTC ATG CTC	KO integration
pLEW90 5' int R	CCT CAT TAA GCA GCT CTA ATG	KO integration
pLEW90 3' int F	GGA ATA GAG TAG ATG CCG AC	KO integration
MCP12 UTR F	GGA TCC TGT CTC ATT AAG TCC CCT TTA C	pGR86/EMSA
MCP12 UTR R	CTC GAG CGT GGC AGT CCA GGC TTG	pGR86/EMSA
TS-like E UTR F	GGA TCC CCA TGT TAT TTC AGC GTG AGG	pGR86/EMSA
TS-like E UTR R	CTC GAG GCA ATA ACC ACA ACA CAT CC	pGR86/EMSA
EP procyclin UTR F	AAG CTT GCG GAT GCA AGC GTG TAA AGC	riboprobe
EP procyclin UTR R	GGA TCC AAA TTC AAA GGA ATG AAA AA	riboprobe
B-tubulin qPCR F	TTC CGC ACC CTG AAA CTG A	qPCR
B-tubulin qPCR R	TGA CGC CGG ACA CAA CAG	qPCR
18S rRNA qPCR F	CGG AAT GGC ACC ACA AGA C	qPCR
18S rRNA qPCR R	TGG TAA AGT TCC CCG TGT TGA	qPCR
TbZC3H20 qPCR F	CGC TTT CAC GGC AGG TAA GT	qPCR
TbZC3H20 qPCR R	AGT TGT CCG AAG GAA AGA ACG TA	qPCR
TbZC3H21 qPCR F	TTG GGT TTC TGG GCG GTA C	qPCR
TbZC3H21 qPCR R	ACG GCA ATG GTG CAG CAT	qPCR
Meta1 BamHI R	GGA TCC CTC CAC GGC CTC AAA CAC	RT-PCR/riboprobe
Meta1 HindIII F	AAG CTT ATG AAA GAG ACT TTA CTC TTG	RT-PCR/riboprobe
HP5.4020 BamH1 R	GGA TCC GAA AGA GAG GGC CGT GGC	RT-PCR/riboprobe
HP5.4020 HindIII F	AAG CTT ATG ATG ATT TCC CGC GC	RT-PCR/riboprobe
TS-like E F	GAA GCT TTT CGT GGG CAC TAT CG	RT-PCR/riboprobe
TS-like E R	GGA TCC CAC GGT CGG TGA GGT CGG TA	RT-PCR/riboprobe
MCP12 F	AAG CTT ATG TCG AAA GAG ACA AAG GC	RT-PCR/riboprobe
MCP12 R	GGA TCC GGC ACG CCA CCC CTT CAC C	RT-PCR/riboprobe
SA C F	AAG CTT TGA AAC CAC CTG CAC TGG G	RT-PCR/riboprobe
SA C R	AGA TCT CGA GTT TCA ATG ACG CGC AG	RT-PCR/riboprobe
PAG4 F	TGG GAC GTC GGG ACA AAA CT	RT-PCR/riboprobe
PAG4 R	ACC GAA CCC TCC AAT CAC CA	RT-PCR/riboprobe
PHAP F	GCG CAA ATG CTG CTA AGG CT	RT-PCR/riboprobe
PHAP R	AGC GAC ATC AGC GAG AAC CC	RT-PCR/riboprobe
CAP15 F	CGG AAG CAA AAC ATG GAC TT	RT-PCR/riboprobe
CAP15 R	TCC GAT TCT TGT TCC ACT CA	RT-PCR/riboprobe

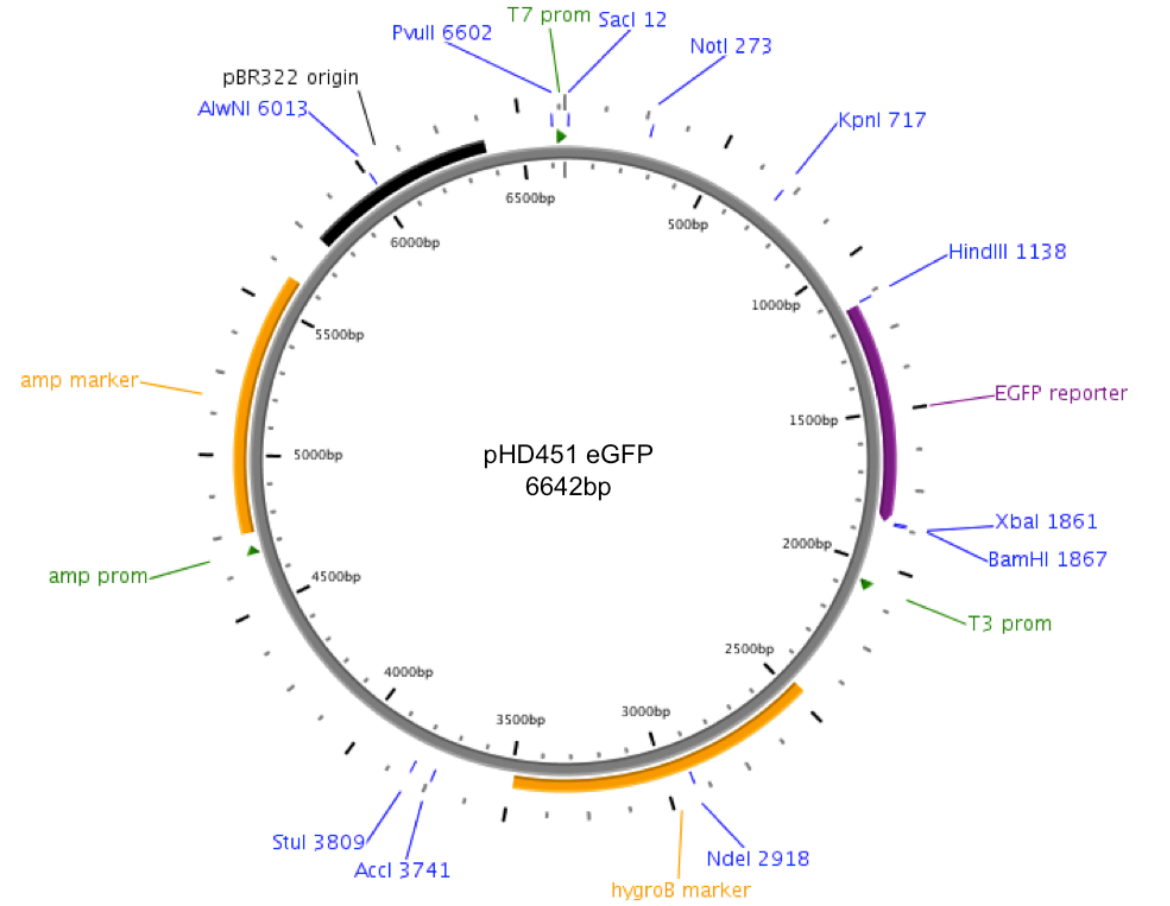
PDI-BS2 F	GCT CTT GCG CTC GCC ACC ATG C	RT-PCR/riboprobe
PDI-BS2 R	CCC CCA AAG GCA ACG CGA G	RT-PCR/riboprobe
TbCLH F	GAG CTG ACG GAG GAA CTG AC	RT-PCR/riboprobe
TbCLH R	TCA AAG CAC TTG TCA GCC AC	RT-PCR/riboprobe
Procyclin F	TCG TTC CCT TTA TCT GCT CG	RT-PCR
Procyclin R	CGG AAG TGC AAC AGA TTT CA	RT-PCR
PAD2 F	ATG AGC GCA CCC GTC GAC AAC G	RT-PCR/riboprobe
PAD2 R	GCT ACG AGC GCT CCC TCC AAG G	RT-PCR/riboprobe
SCAS F	ATG ACC TGT AAC ACG GAC CG	RT-PCR/riboprobe
SCAS R	GCG GTC GAG GAG CAG TGC CAG	RT-PCR/riboprobe
TbTS F	CGT GGG CTT TGA GAA AGA AG	RT-PCR/riboprobe
TbTS R	TTC CTG CAA CAG TGA AGT CG	RT-PCR/riboprobe
Tb α-tubulin R	GGA TCC GTA CTC CTC CAC ATC CTC C	RT-PCR/riboprobe
Tb α-tubulin F	AAG CTT ATG CGT GAG GCT ATC TGC A	RT-PCR/riboprobe
Tb actin R	GGA TCC AAA GCA TTT GCT GTG TAC G	RT-PCR/riboprobe
Tb actin F	AAG CTT ATG TCG GAC GAG GAA CAA AC	RT-PCR/riboprobe
Luciferase F	GAA ATG TCC GTT CGG TTG GC	Riboprobe
Luciferase R	CCC CCA GAA GCA ATT TCG TG	Riboprobe
GRESAG4 F	AAG CTT CGC TGA ACT GCT GAC CCT GA	Riboprobe
GRESAG4 R	GGA TCC CGC TGA ACT GCT GAC CCT GA	Riboprobe
AAT1 F	TCG GTG CGA CGG TTT CCT AT	Riboprobe
AAT1 R	AAG AGG CCA GCC AGC AAC AC	Riboprobe
GT1E F	ATT ATG CTT GCC GCG ATG CT	Riboprobe
GT1E R	CTT ATC CTG GTC GCC GGT TG	Riboprobe
Tb927.8.510 F	TCG GGT CCT CTG CGG ATA AA	Riboprobe
Tb927.8.510 R	TCG GCA TCA GCA CCA TGT TT	Riboprobe
HSP70LP F	GTC GAG CGC TTA TTT GCA GAG G	Riboprobe
HSP70LP R	ACG TGC GGT AGC AGG GGT AA	Riboprobe
Calflagin F	GGT TTG ACA CGA ATG GGA CT	Riboprobe
Calflagin R	TAG TGA CAG CCC AGC ATG AG	Riboprobe

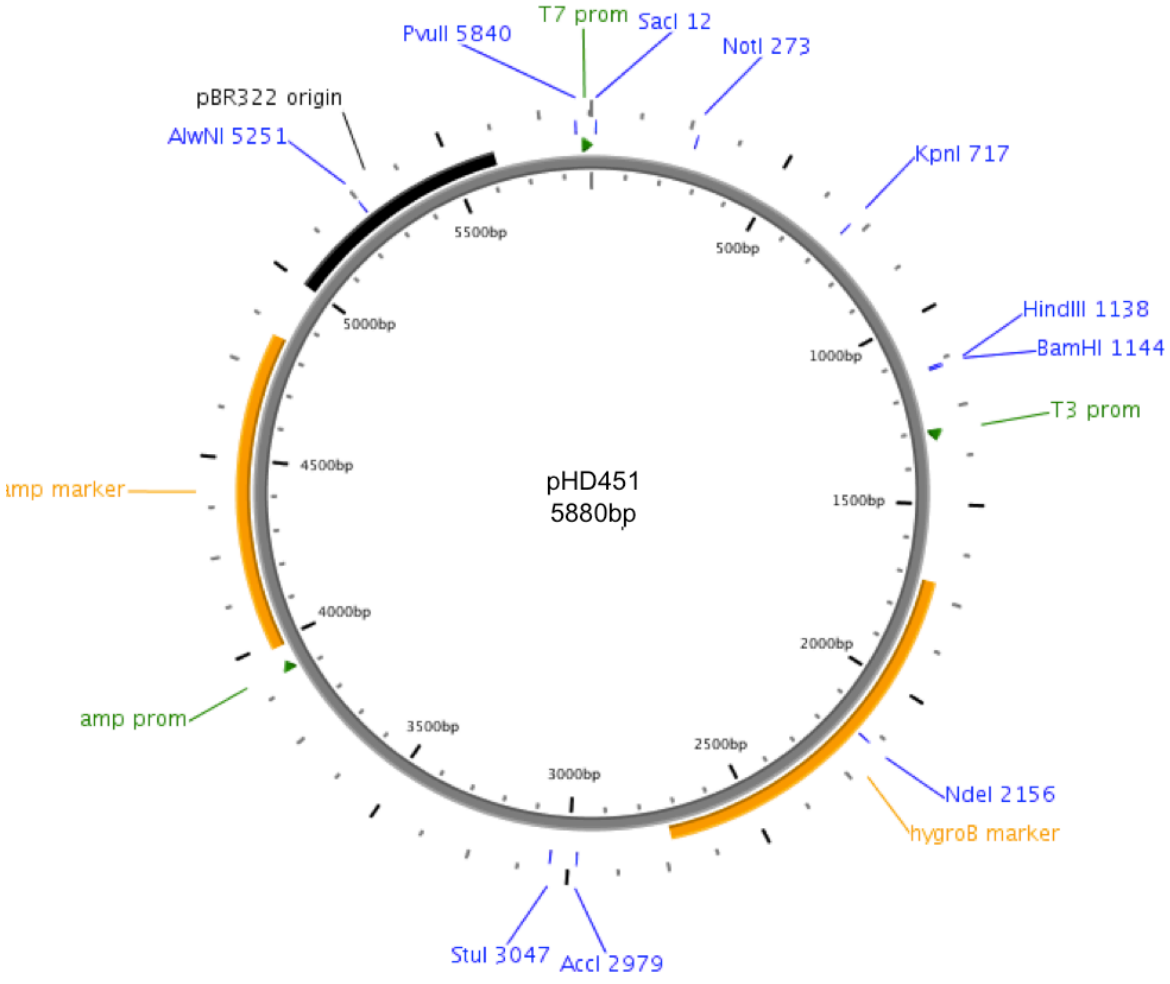
Figure 2.1 Plasmid maps of constructs used in this study

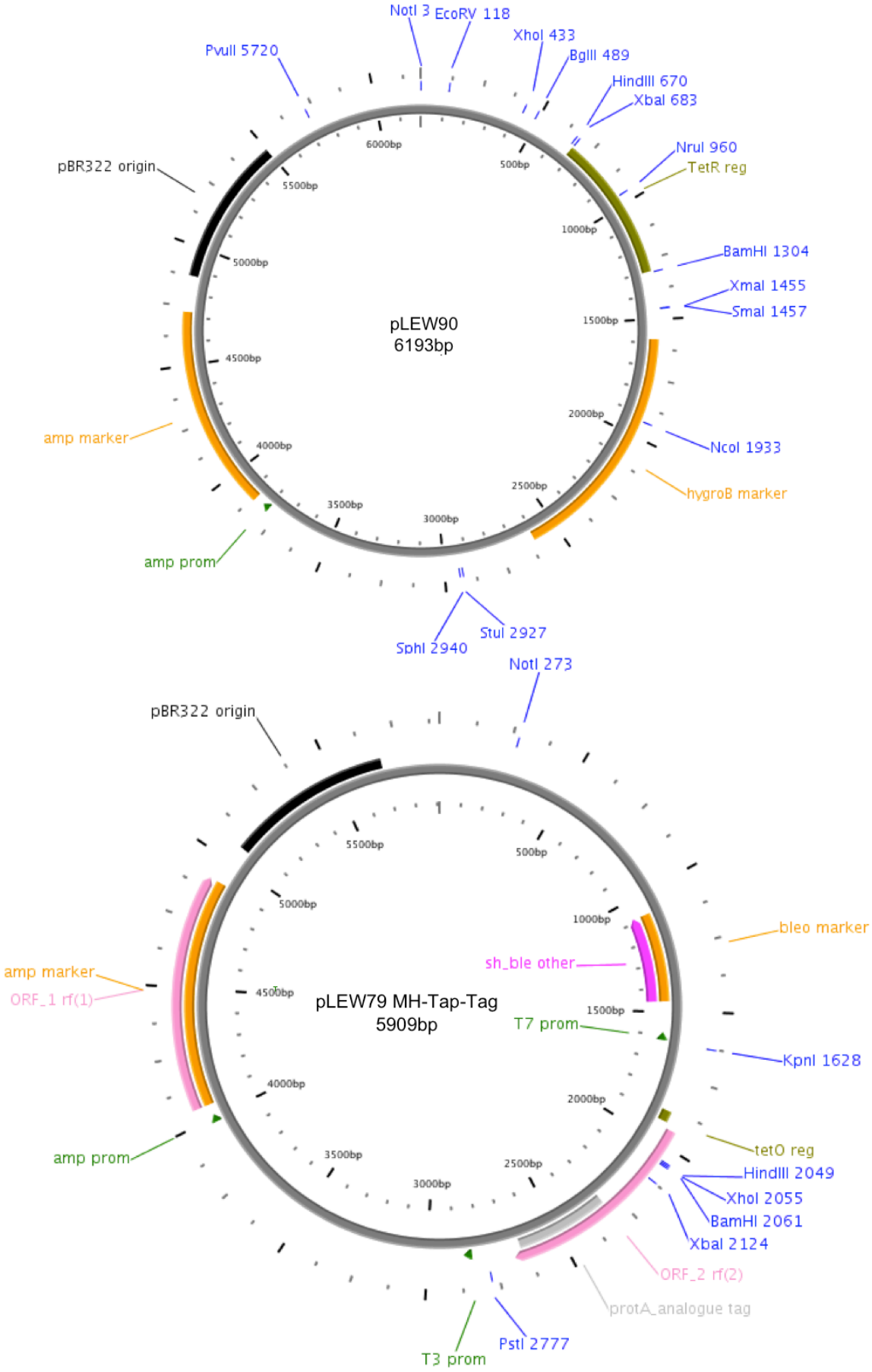
Non-commercially bought plasmids are created using Plasmapper




Origin of replication
Other gene
Promoter
Reporter gene
Selectable marker
Terminator
Unique restriction site
SacI 12
NotI 273
EcoRV 424
pBR322 origin
T7 prom
BamHI 1102
PvuII 1177
T7 term
T7 term
HpaI 1364
GFP_ORF reporter
GFP_cyc3 reporter
amp marker
p2T7i
6089bp
GFP reporter
NdeI 1621
T7 prom
HindIII 1862
XhoI 1883
amp prom
T7 term
T7 term
StuI 3274
pBR322 origin
NotI 477
ClaI 557
EcoRV 592
XhoI 907
amp marker
amp prom
pLEW13
9290bp
T7 RNA
polymerase
StuI 6498
HpaI 2950
TetR reg
XbaI 5605
KpnI 3720
XmaI 4141
NcoI 4944
SmaI 4143
Neomycin
marker
PvuII 4618


T7 prom
SacI 12
PvuII 6602
NotI 273
pBR322 origin
AlwNI 6013
KpnI 717
HindIII 1138
EGFP reporter
amp marker
pHD451 eGFP
6642bp
XbaI 1861
BamHI 1867
amp prom
T3 prom
StuI 3809
AccI 3741
NdeI 2918
hygroB marker


T7 prom
SacI 12
PvuII 5840
NotI 273
pBR322 origin
AlwNI 5251
KpnI 717
HindIII 1138
BamHI 1144
T3 prom
amp marker
pHD451
5880bp
amp prom
NdeI 2156
hygroB marker
StuI 3047
AccI 2979


NotI 3
EcoRV 118
XhoI 433
BglII 489
HindIII 670
XbaI 683
NruI 960
TetR reg
BamHI 1304
XmaI 1455
SmaI 1457
NcoI 1933
hygroB marker
StuI 2927
SphI 2940
amp prom
amp marker
pBR322 origin
PvuII 5720
pLEW90
6193bp
NotI 273
bleo marker
KpnI 1628
tetO reg
HindIII 2049
XhoI 2055
BamHI 2061
XbaI 2124
ORF_2 rf(2)
protA_analogue tag
PstI 2777
T3 prom
T7 prom
sh_ble other
ORF_1 rf(1)
pLEW79 MH-Tap-Tag
5909bp

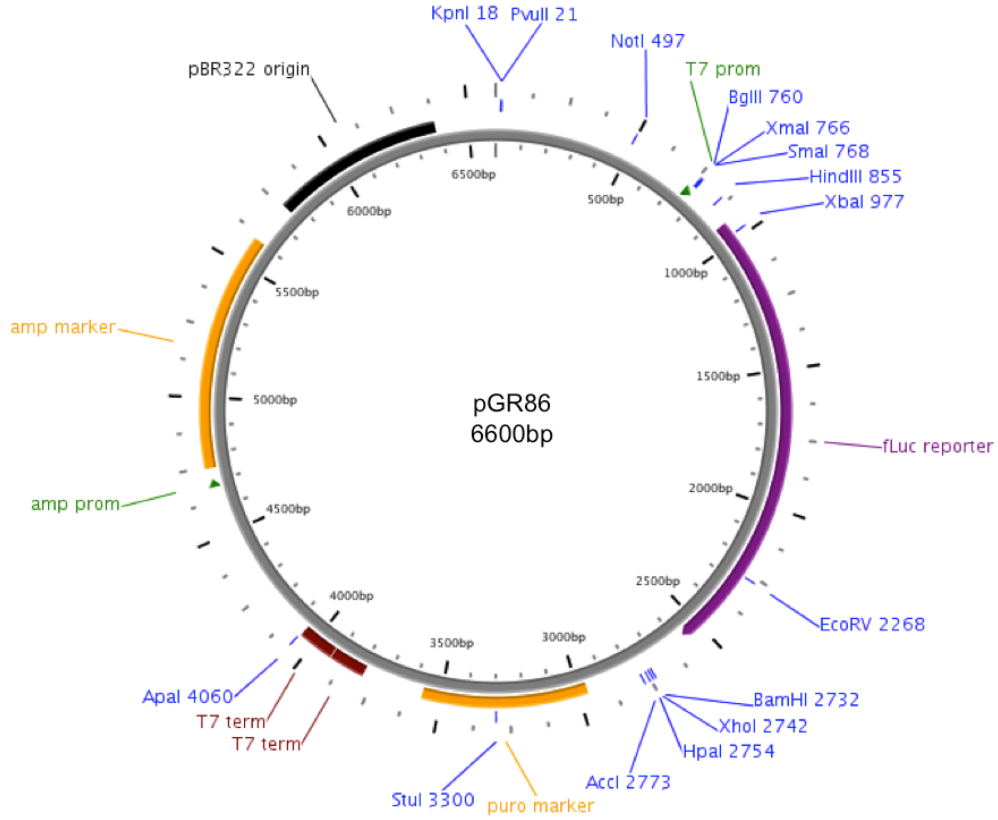


Table 2.2 List of plasmids used in this study

Name of construct	*Cloned by*
pGEM ZC3H20	Dr. E. Hendriks
pGEM ZC3H21	Dr. E. Hendriks
pHD451 ZC3H20	Dr. E. Hendriks
pHD451 ZC3H21	Dr. E. Hendriks
pGEX2TK ZC3H20	Dr. E. Hendriks
pHD451 ZC3H20 - eGFP	A. S. Ling
pHD451 ZC3H21 - eGFP	A. S. Ling
p2T7i ZC3H20	Dr. E. Hendriks
p2T7i ZC3H21	Dr. E. Hendriks
pHD451 ZC3H20 ZFM1	A. S. Ling
pHD451 ZC3H20 ZFM2	A. S. Ling
pHD451 ZC3H20 ZFM1+2	A. S. Ling
pHD451 ZC3H20 Q333A	A. S. Ling
pHD451 ZC3H20 Δ229C	A. S. Ling
pHD451 ZC3H20 Δ148C	A. S. Ling
pHD451 ZC3H20 Δ111N	A. S. Ling
pHD451 ZC3H20 Δ206N	A. S. Ling
pLEW13 TbZC3H20-KO1	Dr. J. Trotter
pLEW90 TbZC3H20-KO2	Dr. J. Trotter
pLEW79 - TAP - TbZC3H20 - MH	A. S. Ling
pLEW79 - TAP - TbZC3H36 - MH	Dr. J. Trotter
pGR86 – MCP12 3'UTR	A. S. Ling
pGR86 – TS-like E 3'UTR	A. S. Ling

CHAPTER 3. ZC3H20 regulates life cycle enriched genes via mRNA stability in procyclic form *T. brucei*

3.1 Introduction

3.1.1 TbZC3H20 is a CCCH zinc finger protein specific to Trypanosomes

The well-characterised CCCH zinc finger (ZC3H) protein tristetrapoline (TTP), and TTP-related ZC3H proteins, contain two conventional ZC3H motifs (both $CX_8CX_5CX_3H$), and have been shown as RBPs to post-transcriptionally regulate gene expression via mRNA stability. However, the vast majority of trypanosome ZC3H proteins defined by the presence of conventional motifs have just one CCCH finger, compared to more than two-thirds of Arabidopsis and rice ZC3H proteins which have at least two [177]. There are just six out of the 48 ZC3H proteins in the *T. brucei* genome that have two conventional ZC3H motifs [177]. Out of these six *T. brucei* ZC3Hs, three have both motifs of the type $CX_7CX_5CX_3H$, two ZC3Hs have one motif $CX_7CX_5CX_3H$ and the other $CX_8CX_5CX_3H$, and one ZC3H has both motifs of the type $CX_7CX_5CX_3H$ but also contains two ubiquitination interacting domains [177]. Two of the three ZC3Hs with two $CX_7CX_5CX_3H$ motifs are adjacent to each other on chromosome 7. These are known as ZC3H20 and ZC3H21, and have a high degree of sequence identity at their N-terminus (Fig. 3.1A and 3.1B). TbZC3H20 does not have an orthologue in the related kinetoplastid *Leishmania major*, unlike the majority of the other *T. brucei* ZC3Hs [177], and therefore represents a potentially interesting RBP containing two ZC3H motifs that is specific to the *Trypanosoma*. As part of an extensive study of ZC3H proteins in the Hendriks' group, TbZC3H20 was chosen for further study as a potential regulator of gene expression in *T. brucei*.

3.1.2 TbZC3H20 can bind RNA *in vitro*

As a putative RBP, the ability of ZC3H20 to bind RNA was assessed *in vitro* (by Dr. James Trotter). Therefore, recombinant ZC3H20 fused to glutathione-S-transferase (GST) was produced in *E. coli* and used in an RNA homopolymer binding assay. GST alone and GST fused to another established RBP were additionally heterologously expressed in *E. coli* to be used as negative and positive controls respectively. These proteins were purified using GST-affinity chromatography and SDS-PAGE used to verify the predicted sizes of the proteins; GST at 26kDa, GST-ZC3H20 at 70kDa and GST-U2AF35 at 55kDa (Fig. 3.1C).

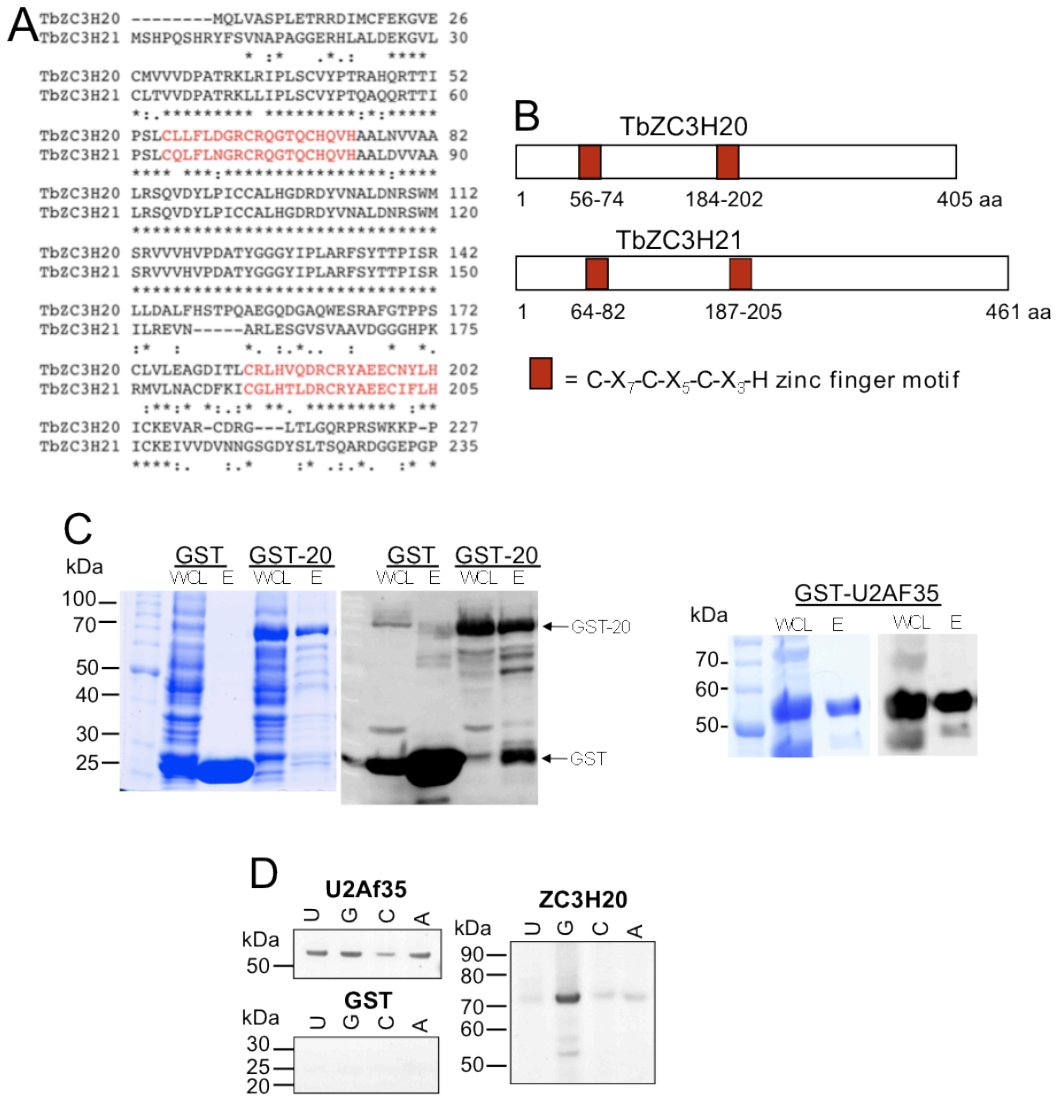


Figure 3.1. ZC3H20 and ZC3H21 as *T. brucei* RNA-binding ZC3H proteins

A. Sequence alignment of TbZC3H20 and TbZC3H21 N-terminus using Clustal W2 (http://www.ebi.ac.uk/Tools/msa/clustalw2/). Red residues indicate both CCCH zinc finger residues.
B. Schematic representation of TbZC3H20 and TbZC3H21 proteins
C. Coomassie (left panel) and Western blot (right panel) of E. coli BL21 whole cell lysates (WCL) induced for recombinant GST or GST-TbZC3H20 (GST-20) or GST-U2AF35 expression and the elution fraction (E) from GST affinity purification. Western blot used an anti-GST antibody to specifically detect GST at ~26kDa, GST-20 at ~70kDa and GST-U2AF35 at ~55kDa. A cleavage GST product is present in the GST-20 samples.
D. Coomassie stain of recombinant GST-TbZC3H20 (ZC3H20) bound to homopolymeric RNA (Poly U, Poly G, Poly C or Poly A). A GST and GST-U2AF35 were used as negative and positive controls respectively. Data by Dr. James Trotter

These proteins were allowed to bind to either poly U, A, C or G linked sepharose beads, and bound protein was identified by SDS-PAGE and Coomassie blue staining (Fig. 3.1D, data by Dr. James Trotter). The GST alone did not bind to any of the RNA homopolymers, whereas the RBP U2AF35 positive control showed

binding to all of them, demonstrating the robustness of the assay. GST-ZC3H20 bound homopolymeric RNA, with a preference for poly-G, and confirms that this *T. brucei* ZC3H is capable of binding RNA in vitro.

3.1.3 Expression of Z3H20 between the life cycle stages

To investigate the expression profile of ZC3H20 between bloodstream form (BF) and procyclic form (PF) *T. brucei*, Northern analysis was used to measure the level of mRNA. Figure 3.2A shows that the level of ZC3H20 is relatively equal between BF and PF cells, thus showing no obvious developmental regulation of ZC3H20 at the mRNA level. To detect the level of protein, GST- tagged recombinant ZC3H20 was heterologously expressed in *E. coli*, and used to raise an antibody in rabbits and mice. However, several attempts were unsuccessful in producing a specific antibody that could be used to detect ZC3H20 from *T. brucei* whole cell lysates. Therefore, a double anti-peptide antibody protocol was tried which involved generating two antigens (from two peptide sequences from ZC3H20, Fig. 3.2B) that were then used to immunise rabbits to generate an antibody to response (Eurogentec). The antibody antiserum purified against Peptide 2 (Fig. 3.2B) by affinity chromatography (done by Eurogentec) proved to be useful in Western blot analysis, but a high concentration of this antibody was needed. This antibody was used to detect the level of ZC3H20 protein between BF and PF *T. brucei*. Western analysis showed that the antibody revealed a protein of the correct predicted size (44kDa) in PF cells, but that this was below the level of detection in BF cells (Fig. 3.2C). The Western blot also shows a non-specific reacting band at 50kDa, which was present in the pre-immune serum, and acts as a loading control. Western analysis was also used with the ZC3H20 antibody to detect GST-tagged recombinant ZC3H20 from *E. coli* whole cell lysates and from a GST affinity chromatography elution. This showed that the antibody had affinity for a recombinant protein of the correct predicted size of 70kDa (ZC3H20 = 44kDa, and GST= 26kDa), which is not present in the pre-immune serum (Fig. 3.2D).

In conclusion, this indicates that ZC3H20 protein is enriched in the PF life cycle stage, and could be regulated at the post-translational level.

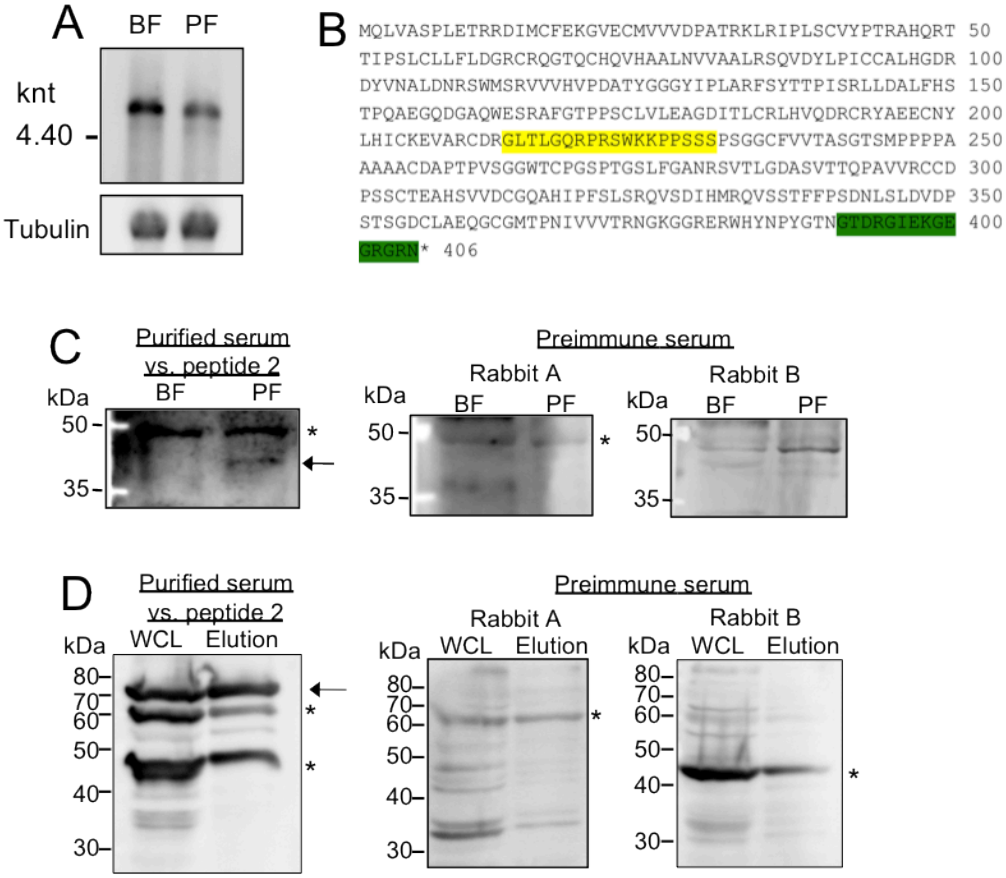


Figure 3.2. Expression of ZC3H20 in BF and PF T. brucei, and generation of an anti-ZC3H20 antibody

A. Northern blot analysis of endogenous ZC3H20 RNA levels in BF and PF *T. brucei*. Tubulin is used as a loading control.
B. Peptide sequences from coding region of TbZC3H20 used as antigens for antibody generation in rabbits. The full protein sequence of ZC3H20 is shown with amino acid number indicated on the right hand side. Peptide 1 is highlighted in yellow and Peptide 2 is highlighted in green.
C. Western blot analysis of BF and PF whole cell lysates using the rabbit serum purified against Peptide 2 of TbZC3H20 and the rabbit preimmune serum. An arrow indicates the endogenous TbZC3H20 protein band (~44kDa). An asterisk indicates a non-specific reacting band at 50kDa, which was present in the pre-immune serum, and acts as a loading control. The equivalent of $2x10^6$ cells is loaded in each lane.
D. Western blot analysis of *E. coli* BL21 whole cell lysates (WCL) induced for recombinant GST-TbZC3H20 protein expression, using the rabbit serum purified against Peptide 2 of TbZC3H20 and the rabbit preimmune serum. An arrow indicates the recombinant GST-TbZC3H20 protein band (~70kDa). Asterisks indicate non-specific reacting bands present in the pre-immune serum.

3.2 Investigation if ZC3H20 and ZC3H21 are essential for growth in procyclic form *T. brucei*

Given the apparent enrichment of ZC3H20 protein in PF *T. brucei*, it was of interest to assess whether it is essential for growth in this life form. The high

degree of homology at the CCCH domains between ZC3H20 and ZC3H21 (Fig. 3.1A and 3.1B) suggested an additional investigation into ZC3H21 as a similar member of the *T. brucei* ZC3H proteins that could also be essential for growth.

3.2.1 Down-regulation of ZC3H20 or 21 by RNA interference (RNAi) causes a growth defect in PF *T. brucei*

Down-regulation by RNAi is a useful tool to determine whether a gene is essential for survival and cellular development. RNAi can also be used to investigate whether down-regulation of a gene causes a loss-of-function phenotype. Thus, a head-to-head promoter RNAi system available in *T. brucei*, was used to down-regulate ZC3H20 or ZC3H21 in PF cells. The vector used, p2T7i [185], was stably transfected into PF 29-13 cells engineered to express T7 polymerase and the tetracycline (tet) repressor, thus double-stranded RNA corresponding to the full open reading frame of 20 or 21 could be expressed in a tet-dependent manner. Down-regulation of ZC3H20 or ZC3H21 was verified by quantitative PCR, carried out by Dr. James Trotter of the Hendriks group. Complementary DNA (cDNA) prepared from cells induced with tet for 48h was compared to cells grown in the absence of tet, and confirmed downregulation of ZC3H20 or ZC3H21 (Fig. 3.3A). Actin and β-tubulin were used as standards, and each product was normalised to 18S rRNA. This analysis showed that tet induction of PF RNAi 20 cells caused a 10-fold decrease in the level of ZC3H20 mRNA whilst the mRNA levels of actin or β-tubulin were unaffected. Induction of ZC3H20 RNAi also caused a significant change in the mRNA levels of ZC3H21, which were decreased by 5-fold. Conversely, tet induction of PF 21 RNAi cells caused a 5-fold decrease in the level of ZC3H21 mRNA, but also caused a 2-fold decrease in the level of ZC3H20 mRNA. RNAi down-regulation of ZC3H21 did not greatly affect the mRNA levels of actin and β-tubulin. It is possible that the double-stranded RNA expressed from p2T7i RNAi system is targeting both ZC3H20 and ZC3H21 via regions of sequence identity, and thus is not specific for one or the other. RNAi down-regulation of ZC3H20 was also confirmed by Western analysis using the anti-ZC3H20 peptide antibody (Fig. 3.3B), and revealed that protein levels of ZC3H20 were undetectable after 48h of tet induction in the PF 20 RNAi cell line.

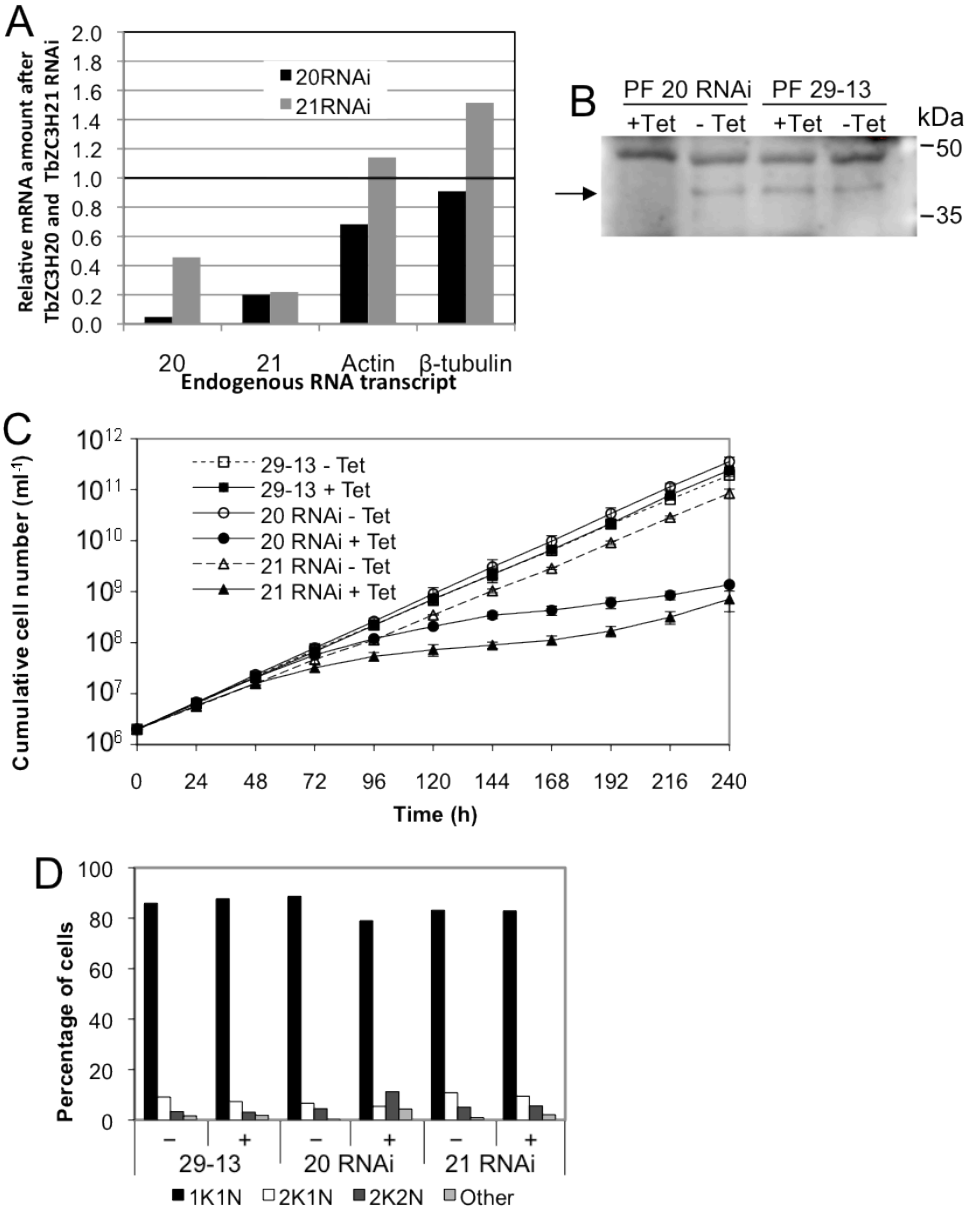


Figure 3.3. RNAi down-regulation of ZC3H20 and ZC3H21 in PF *T. brucei*

A. Quantitative real-time PCR of mRNA from procyclic form *T. brucei* after 72h of RNAi downregulation of TbZC3H20 (20 RNAi) or 48h of RNAi downregulation of TbZC3H21 (21 RNAi). Graph shows relative mRNA amount compared to 18S mRNA expression level. 20 = ZC3H20, 21 = ZC3H21. Actin and tubulin are used as controls. Data from Dr. James Trotter

B. Western blot of protein from whole cell lysate of PF *T. brucei* induced for 48h of RNAi downregulation of ZC3H20 (PF 20 RNAi +Tet). Protein is detected with the affinity-purified polyclonal anti-peptide antibody to ZC3H20. PF29-13 is the procyclic parental cell line

C. Growth curve showing effect of RNAi downregulation of TbZC3H20 and TbZC3H21 in PF cells.
Addition of tetracycline (+ Tet) results in the induction of RNAi. Plotted data are mean values from three independent experiments and error bars show standard deviation.

D. Cell cycle analysis of RNAi downregulation of TbZC3H20 and TbZC3H21 in PF cells. Cells were grown in the presence (+) or absence (-) of tet for 96h. Over 200 cells were counted for each population.

Induction of RNAi down-regulation of TbZC3H20 or 21 caused a growth defect after 72-96h (Fig. 3.3C). Growth started to recover after 192h and the cultures resumed expansion, which has been reported by studies of RNAi in trypanosomes [200]. This suggests that ZC3H20 and ZC3H21 are essential for growth in PF *T. brucei*.

Cell cycle analysis of PF 20/21 RNAi cells was carried out to identify if there are any cell cycle defects as a results of down-regulating these transcripts i.e. an unusual proportion of cells for each karyotype (Fig 3.3D). Trypanosomes possess two genomic units, the nucleus and the kinetoplast, which is the mitochondrial genome. The cell cycle of trypanosomes shows the same nuclear events of that in a normal eukaryotic cells cycle i.e. G1, S, G2 and M phases. However, the segregation of the kinetoplast occurs before nuclear mitosis. As described in Chapter 1 (Section 1.2.2), the order and timing of cell cycle events allows the identification of the cell cycle position of an individual trypanosome [55]. A normal cell population consists of around 80-90% of cells with the karyotype of one kinetoplast and one nucleus (1K1N), 5-10% are 2K1N and 5-10% are 2K2N [56]. There does not appear to be a substantial increase or decrease of any karyotype within the PF 20 RNAi or PF 21 RNAi induced populations, and therefore suggests that RNAi of TbZC2H20 or TbZC3H21 does not result in a cell cycle defect.

Light microscopy of the cells also showed that there were no obvious defect in cell morphology in the RNAi induced cells (data not shown). In conclusion, down-regulation of ZC3H20 or 21 does not cause a phenotypic effect in PF cells, but does cause a growth defect suggesting that both may be essential genes in PF *T. brucei*.

3.2.2 ZC3H20 and ZC3H21 are essential genes in PF *T. brucei*

The RNAi growth data (Fig. 3.3C) suggests that either TbZC3H20 or TbZC3H21 or both of them together (as both are down-regulated) could be essential for growth and survival of procyclic *T. brucei*. To determine if either individual gene is essential in procyclic form cells, the generation of null mutants for each of these genes was attempted. Two different vectors were used to knock-out both alleles of the diploid *T. brucei* i.e. pLEW13 to replace the first allele, and pLEW90 to replace the second allele, as used by [188] (Fig. 3.4A). The 3' end of the 5' UTR and the 5' end of the 3' UTR of TbZC3H20 or 21 were cloned into both constructs (Fig. 3.4A).

Each construct was transfected individually into procyclic 427 wild type cells to show that they could integrate correctly. Primers were designed for PCRs on genomic DNA isolated from each cell line to show correct integration of the construct to replace the allele of interest (Fig. 3.4B).

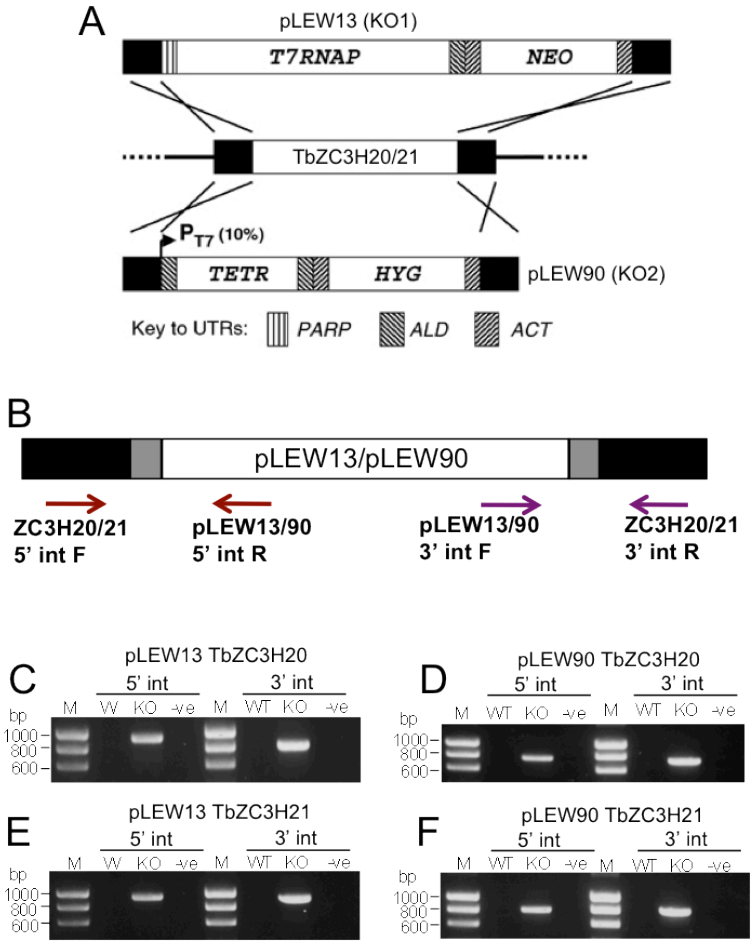


Figure 3.4. Creating ZC3H20 and ZC3H21 null mutants in PF *T. brucei*

A. Constructs and targeting strategy for the replacement of *ZC3H20 and ZC3H21* endogenous alleles, thus creating ZC3H20 and ZC3H21 null mutants in PF *T. brucei.* The black boxes depict regions of 5' and 3' UTRs of ZC3H20 or ZCH21 cloned into pLEW13 and pLEW90 that are homologous with the endogenous copies. P_{T7}(10%) indicates a mutant T7 promoter with 10% activity [188]. Constructs created by Dr. James Trotter.
B. Primer design for PCR to verify correct integration of pLEW13 and pLEW90 into genomic DNA. Red arrows show primers for 5' integration and purple arrows for 3' integration. The 5' and 3' UTR primers bind to a specific region within the endogenous 5' or 3' UTRs of TbZC3H20/21 respectively. The pLEW13/90 5' int R and 3'int F primers bind to a specific region within the 5' and 3' regions of the pLEW13/pLEW90 construct respectively.
C-F. PCRs to verify integration of pLEW13 or pLEW90 constructs individually into WT PF *T. brucei*. C- pLEW13 TbZC3H20 integration into TbZC3H20 locus; D- pLEW90 TbZC3H20 integration into TbZC3H20 locus; E- pLEW13 TbZC3H21 integration into TbZC3H21 locus; F- pLEW90 TbZC3H20 integration into TbZC3H21 locus
M = marker, WT = procyclic wildtype genomic DNA, KO = procyclic (single) knockout genomic DNA, -ve = relevant plasmid DNA, 5' int = 5' integration, 3' int = 3' integration

Each set of primers has one primer that binds to the endogenous UTR of TbZC3H20/21 and one primer that binds to a specific region within pLEW13 or pLEW90, therefore a PCR product was only produced when there is correct integration at the 5' UTR or 3' UTR (Fig. 3.4C-F). Wild type genomic DNA and the relevant plasmid DNA were used as negative controls. Note that this is showing integration and replacement of one allele i.e. they are single knockouts (one allele knocked out), not null mutants (both alleles knocked out). The PCR products amplified from the genomic DNA of procyclic cells transfected with each construct were the expected sizes, and so confirmed each construct could integrate correctly individually (and create a single knockout).

Subsequently, the procyclic pLEW13 TbZC3H20/21 cell lines were transfected with the relevant pLEW90 construct. This transfection was attempted four times for each gene, but none of these generated *bona fide* null mutants. These data, in combination with the RNAi data, strongly suggests that both genes individually are essential for the survival of procyclic *T. brucei*.

3.3 Investigation of the mRNA targets of ZC3H20 in PF *T. brucei*

The RNAi analysis and inability to generate a null mutant, points to the likelihood that ZC3H20 (and ZC3H21) is essential in PF *T. brucei*. Apart from a growth defect when ZC3H20 is down-regulated, there is no morphological phenotype or cell cycle defect that provides a clue to the type of mRNA target(s) that ZC3H20 could be regulating. As an alternative and broader approach, microarray analysis can be used to determine what mRNA species are affected on a genome-wide scale. Consequently, total RNA can be compared between induced and uninduced PF 20 RNAi cells and the information obtained can be analysed to isolate potential mRNAs that may be regulated by ZC3H20.

3.3.1 Microarray analysis identifies a small number of genes with an altered mRNA abundance when ZC3H20 is depleted in PF *T. brucei*

To determine genes with an altered mRNA abundance as a result of ZC3H20 down-regulation, PF 20 RNAi cells were grown in the presence or absence of tet for 48h and total RNA isolated. At this time point of induction, there is no growth defect (Fig. 3.3C) and the level of ZC3H20 is effectively depleted (Fig. 3.3A,B). Microarray analysis was completed on 3 biological replicates, with one that

included a dye-switch. Each array used three unique probes (where possible) for each of the 9344 putative coding sequences in the *T. brucei* genome, and the fold change in mRNA levels for each probe for each array was calculated. Genes that showed more than 2-fold increase/decrease in mRNA levels for at least one probe in all three arrays were scrutinised for further investigation (Table 3.1). The microarray analysis identified six different gene classes (procyclin associated genes (PAGs) and amino acid transporter (AAT) are grouped as one gene each) that had increased mRNA levels and 6 different gene classes that had decreased mRNA levels (Table 3.1). This shows that a total of 12 different classes out of the entire *T. brucei* genome with an altered mRNA level at a 2-fold threshold when ZC3H20 is down-regulated in PF cells. This limited transcriptome response has been reported previously, where a given life stage appears transcriptionally inflexible when a specific gene perturbation or environmental stress is exposed to the parasite, compared to the transcriptome changes that occur during differentiation from one life stage to the next [39]. This small set of 12 classes (18 genes) was therefore investigated further as potential mRNA targets of ZC3H20 regulation.

Table 3.1. Summary of the microarray analysis from PF TbZC3H20 RNAi cells

Genes with altered levels of RNA >2-fold, with up regulated (top section of table) or down regulated (bottom section of table) as a result of RNAi mediated down regulation of TbZC3H20 in PF cells. Signal fold change (+ = up regulated, - = down regulated) for each of the three arrays conducted are shown for each of the gene specific probes on the array. Probes that are not >2-fold across all three arrays are shown in italics.

Number	**Probe**	**Array**			**Product**
		1	2	3	
Tb927.8.480	1	+13.4	+2.1	+2.7	Phosphatidic acid phosphatase (PHAP)
	2	+10.2	+2.1	+2.5	
	3	+8.3	+2.5	+2.7	
Tb927.8.510	1	+10.3	+2.0	+2.0	Hypothetical protein (orphan) (HP8.510)
	2	+6.0	+1.1	+0.6	
	3	*+4.0*	*+1.0*	*+1.5*	
Tb09.160.3090	1	+4.6	+2.1	+3.1	Heat shock protein, HSP70-like protein (HSP70LP)
	2	*+5.1*	*+1.6*	*+2.5*	
	3	*+4.3*	*+1.8*	*+2.1*	
Tb10.6k15.0050/	1	+13.7	+2.6	+3.5	Procyclin-associated gene 5
	2	+9.2	+2.2	+4.0	
	3	+9.6	+2.3	+4.0	
0060/	1	+11.6	+2.7	+3.3	Procyclin-associated gene 2
	2	+8.9	+2.6	+3.8	
	3	+9.3	+3.0	+4.1	

0070/	1	+10.9	+2.4	+3.9	Procyclin-associated gene 4
	2	+8.8	+1.8	+2.4	
	3	*+10.2*	*+1.9*	*+2.2*	
3540	1	+4.9	+2.1	+3.1	Procyclin-associated gene 1
	2	*+6.4*	*+1.9*	*+2.3*	
	3	*+6.8*	*+1.9*	*+2.1*	
Tb10.6k15.2030	1	+6.5	+2.2	+2.8	Glucose transporter 1E (GT1E)
	2	*+2.3*	*+0.6*	*+0.9*	
Tb11.01.7590/	1	+6.3	+2.2	+2.7	Amino acid transporter (AAT)
	2	+6.8	+2.7	+3.7	
	3	*+6.7*	*+1.7*	*+2.1*	
7600	1	+8.6	+3.1	+3.5	Amino acid transporter
	1(2)	+9.0	+3.1	+3.8	
	2	+6.1	+2.6	+2.9	
	3	+9.0	+2.2	+2.7	
	4	*+9.6*	*+1.9*	*+2.4*	

Tb927.5.2160/	1	-3.1	-6.9	-7.4	Hypothetical protein, conserved (META 1)
	2	-4.1	-7.5	-8.5	
2170/	1	-3.1	-6.8	-8.1	
2260	1	-3.7	-9.5	-10.9	
Tb927.5.4020	1	-2.9	-5.8	-3.7	Hypothetical protein (orphan) (HP5.4020)
	2	-3.3	-6	-4.3	
	3	-2.9	-6.8	-3.8	
Tb927.5.440	1	-2.1	-4.4	-3.1	Hypothetical protein, conserved Trans-sialidase (TS-like E)
	2	*-1.8*	*-2.9*	*-2.1*	
	3	*-1.4*	*-4*	*-3.1*	
Tb927.8.7340	1	-2.1	-2.6	-2.3	Trans-sialidase, neuraminidase (SA C)
	2	*-1.9*	*-2.8*	*-2.2*	
	3	*-1.8*	*-2.8*	*-2.6*	
Tb10.389.0690	1	-3.1	-3.2	-2.2	Mitochondrial carrier protein (MCP12)
	2	-2.6	-4.3	-2.5	
	3	-2.7	-3.7	-2.5	
Tb11.02.3740	1	-2.4	-5.8	-4.2	Receptor-type adenylate cyclase (GRESAG 4)
	2	-2.3	-5	-4.1	
	3	*-0.7*	*-4*	*-4.7*	

3.3.2 Inhibition of protein synthesis determines if an mRNA species is stabilised or destabilised in PF *T. brucei*

Post-transcriptional regulation in trypanosomes is considered to involve RBPs that recognise and bind elements in the mRNA 3'UTR, which then results in destabilisation of the target mRNA via turnover, or stabilisation of the mRNA resulting in increased translation, or the presence of the RBP directly affects translational efficiency (Chapter 1.4 and 1.5). To assess if the mRNA abundance

of the PF ZC3H20 RNAi microarray candidates is altered by a protein factor, PF parasites were incubated for up to 4h in the presence or absence of cycloheximide (a translational inhibitor). Total RNA was isolated from wild-type PF cells incubated with cycloheximide for 1h, 2h and 4h, and in the absence of cycloheximide for 0h and 4h to show steady-state levels. The levels of mRNA were examined using Northern analysis with a specific probe to each of the genes up-regulated (Fig. 3.5A top panel) and to genes down-regulated (Fig. 3.5A bottom panel) in the PF 20 RNAi microarray analysis (Table 3.1). The mRNA level of actin after cycloheximide treatment was used as controls (Fig. 3.5A). After the addition of cycloheximide, any proteins that are responsible for stabilising or destabilising mRNA are stopped from being synthesised *de novo*, and thus existing protein will be turned over. Subsequently the levels of the target mRNAs decrease or increase, respectively.

The mRNA levels of AAT, heat-shock protein 70-like protein (HSP70LP), META1 and receptor-type adenlylate cyclase (GRESAG4) did not alter greatly after cycloheximide treatment. The mRNA levels of glucose transporter 1E (GT1E) and hypothetical protein Tb927.8.510 (HP8.510) decreased after 4h of cycloheximide treatment, and the mRNA levels of hypothetical protein Tb927.5.4020 (HP5.4020) were clearly increased. However, these data do not correlate with the PF 20 RNAi microarray data, which shows that down-regulation of ZC3H20 causes an increase in GT1E and HP8.510 mRNA abundance, and a decrease in HP5.4020 mRNA abundance. The level of *trans*-sialidase C (SA C) mRNA appeared to decrease in the 4h sample compared to the untreated 4h sample, but showed some inconsistency with the 0h untreated sample, thus protein factors may or may not be involved in regulating the abundance of this transcript.

Phosphatidic acid phosphatase (PHAP) and PAG4 were up-regulated in the PF 20 RNAi microarrays, and the cycloheximide pattern was consistent with this, showing a clear increase in mRNA level after 4h of treatment (Fig. 3.5A top panel). This suggests that these transcripts are normally destabilised by a protein factor within the PF cell. Additionally, *trans*-sialidase like protein E (TS-like E) and mitochondrial carrier protein 12 (MCP12) mRNA levels were decreased after 4h of cycloheximide treatment (Fig. 3.5A, bottom panel) suggesting that a protein factor may be responsible for stabilising these transcripts in the PF cell. This pattern is also consistent with their destabilisation when ZC3H20 is down-regulated in the microarray.

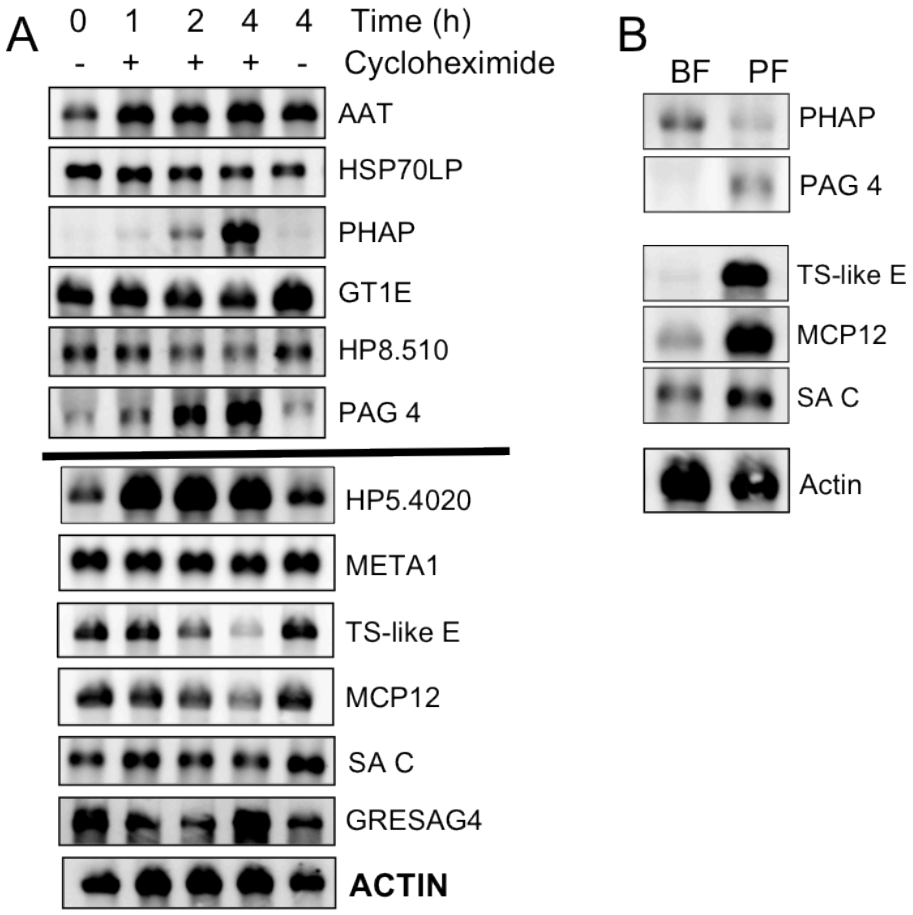


Figure 3.5. Effect of a translational inhibitor on mRNA abundance of genes from PF ZC3H20 RNAi microarray

A. Northern blot analysis of total RNA isolated from PF cells treated with cycloheximide for 1, 2 and 4h. RNA was also isolated from PF cells at time point 0h and 4h without the addition of cycloheximide. RNA riboprobes to each gene were used to detect specific mRNA transcripts. Genes shown above the black line are up-regulated in the microarray, and genes below the line are down-regulated.
B. Northern blot analysis of endogenous PHAP, PAG4, TS-like E, MCP12 and SA C RNA levels in BF and PF *T. brucei*. Actin is used as a loading control.

After microarray and cycloheximide analysis, the only genes that show their mRNA abundance is possibly altered by a protein factor and correlate with the PF 20 RNAi microarrays are PHAP, PAG4, TS-like E, MCP12, and possibly SA C. Recently, microarray analysis have been used to study changes in mRNA levels across the whole *T. brucei* genome during the differentiation from bloodstream to procyclic form, and interestingly, TS-like E and MCP12 genes are identified as PF enriched mRNAs [58]. Therefore, to determine if all five of the potential ZC3H20 mRNA targets are developmentally regulated, RNA was isolated from BF and PF

cells and probed for the mRNA level of each gene between the life stages (Fig. 3.5B). Actin was used as a control and does not show life stage-specific transcript enrichment. The analysis showed that TS-like E and MCP12 are PF enriched transcripts, agreeing with previously published data. SA C and PAG4 showed a slight PF enrichment, and PHAP showed a slight BF enrichment. These probably do not show enough of a difference between the life-cycle stages to be classified as developmentally regulated and may be the reason why other whole genome microarrays have not identified them as such.

In conclusion, down-regulation of ZC3H20 in PF cells alters the mRNA abundance of PHAP, PAG4, SA C, TS-like E and MCP12, and these transcripts are destabilised or stabilised by a protein factor in PF cells. This suggests that ZC3H20 is responsible for regulating their mRNA stability, and in particular, the developmentally regulated TS-like E and MCP12 may be specifically stabilised by ZC3H20 in PF *T. brucei*.

3.3.3 ZC3H20 is capable of binding TS-like E, MCP12 and PHAP mRNA *in vivo*

A subset of genes fit the criteria that their mRNA abundance could be regulated via destabilisation or stabilisation by a protein factor (Fig. 3.5A) and this correlates with their up or down-regulation when ZC3H20 is depleted in PF cells (Table 3.1). As an RBP, it is necessary to determine that ZC3H20 is capable of binding these mRNA targets. Co-immunoprecipitation experiments using the anti-ZC3H20 peptide antibody proved unsuccessful. Therefore, a tandem affinity purification (TAP) tagging approach was employed, an effective method previously used in trypanosomes [189]. PF 29-13 cells were stably transfected with the TAP-20 construct (modified to allow expression of ZC3H20), and induced with tet for 2 days to express TAP-tagged ZC3H20 protein, which was purified from cells using IgG-coated beads (against the Protein A of the tag), and then calmodulin beads (against the Calmodulin Binding Protein domain of the tag). Western analysis using an anti-His antibody (to 6xHis tag at N-terminus of ZC3H20/36) was used to show the progression of the TAP-tagged ZC3H20 (~68kDa) or Z3H36 (~ 55kDa) through the affinity purification and the isolation of the final TAP-cleaved ZC3H20 (~51kDa) and ZC3H36 (~ 39kDa) (Fig. 3.6A).

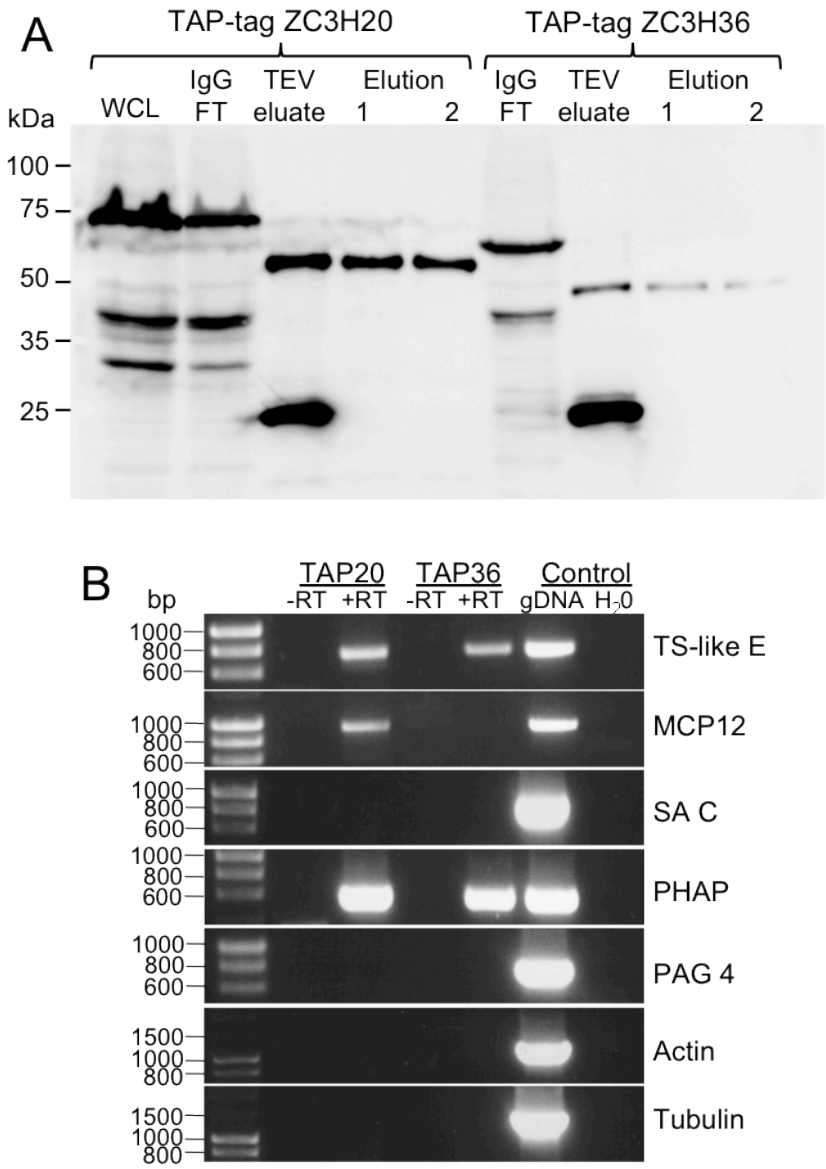


Figure 3.6. ZC3H20 TAP-tag analysis in PF *T. brucei* and RT-PCR of bound mRNA targets

A. Western blot analysis of TAP tag ZC3H20 and ZC3H36 purification, using an anti-His antibody (to 6xHis tag at C-terminus of ZC3H20/36). The TAP-Tag is ~ 23.2 kda (uncleaved) and after TEV cleavage, the portion of Tag cleaved off is ~ 16 kda, with ~ 7.2 kda remaining fused to protein of interest. WCL = whole cell lysate, IgG-FT = IgG flow through, TEV eluate = TEV protease eluate
B. RT-PCR analysis on cDNA reverse-transcribed (+RT) from RNA isolated from TAP tagged ZC3H20 and ZC3H36 purification. Minus reverse transcription (-RT) control is shown for DNA contamination from the TAP purification. Genomic DNA (gDNA) is used as a positive control, and water (H_2O) is used as a non-template negative control.

RNA that co-precipitated with the TAP-20 was isolated, DNase-treated (to remove contaminating genomic DNA), reverse-transcribed to cDNA, and then subjected to PCR (RT-PCR) using primers specific to each of the mRNA targets

(Fig. 3.6). The entire TAP-tagging approach was repeated to express TAP-tagged ZC3H36 protein, another member of the *T. brucei* ZC3H family and isolate bound RNA for RT-PCR as a control for TAP-20 specific binding. Actin and tubulin were used as non-specific negative controls, and the TAP RT-PCR results show that neither of these transcripts were bound by TAP-20 or TAP-36 (Fig. 3.6B). Amplification products for SA C and PAG4 mRNA were not visible from the TAP-20 (or TAP-36) RT-PCR, suggesting that these transcripts are not bound by ZC3H20 in the cell. RT-PCR using primers specific for MCP12 produced a product of the correct predicted size (as shown by the genomic DNA positive control) only from the TAP-20 co-precipitated RNA, suggesting that this mRNA can be bound by ZC3H20. Similarly, RT-PCR identified products of the correct size for TS-like E and PHAP were co-precipitated with TAP-20 and TAP-36 showing that TS-like E and PHAP can be bound by ZC3H20 and ZC3H36. TS-like E and PHAP mRNAs could have general binding specificity by ZC3Hs thus explaining the presence of a product in the TAP-36 RT-PCR. Reverse transcriptase minus (RT-) RNA samples from TAP-20 and TAP-36 did not produce PCR amplification products, ruling out genomic DNA contamination for all targets tested. In conclusion, this analysis shows that PHAP, TS-like E and MCP12 mRNAs are capable of being bound by ZC3H20 *in vivo*.

3.3.4 Down-regulation of ZC3H20 causes an increased decay rate of the developmentally regulated TS-like E and MCP12 mRNA transcripts

Having shown that down-regulation of ZC3H20 alters the abundance and can bind PHAP, TS-like E and MCP12 mRNAs, Northern analyses were performed to determine if the half life of these transcripts is influenced when ZC3H20 is depleted in PF cells. PF 20 RNAi cells were grown in the absence or presence of tet for 48h as for the microarray, where there is evident down-regulation of ZC3H20 and no obvious morphological or growth defect in these cells. After 48h of tet induction, cells were treated with the transcriptional inhibitor actinomycin D for 0, 1, 2 or 4h, to allow the turnover of RNA to be determined with or without ZC3H20 depletion. After actinomycin D treatment at each time point, total RNA was isolated and the level of PHAP, TS-like E and MCP12 mRNAs observed by Northern analysis (Fig. 3.7).

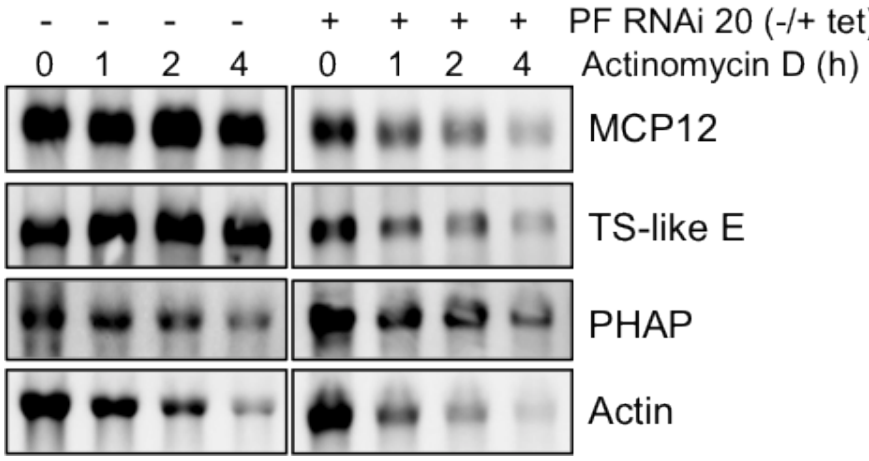


Figure 3.7. RNA abundance after treatment of PF *T. brucei* with a transcriptional inhibitor and induced for ZC3H20 RNAi down-regulation

Northern blot analysis of total RNA isolated from PF 20 RNAi cells grown in the presence or absence of tet for 48h and then treated with actinomycin D over 4h. RNA riboprobes to each gene were used to detect specific mRNA transcripts. The blots shown that are probed for MCP12 and TS-like E when ZC3H20 is down-regulated, have been exposed for a longer period of time than for the uninduced samples, as the initial level of RNA is lower. This is done so that the turnover rate from starting levels can be observed.

Densitometry was used to measure the mRNA levels at each time point and the levels were then calculated as a percentage of the time point 0h, which was expressed as 100%, for –Tet and +Tet PF 20 RNAi samples. These are plotted on a logarithmic graph to show the mRNA half-life (T1/2) after actinomycin D addition (Fig. 3.8). The decay rate of the control mRNA actin was not significantly affected when ZC3H20 was down-regulated in PF cells compared to uninduced cells (54 vs. 66 min) (Figs. 3.7 and 3.8). The microarray and cycloheximide analysis suggested that PHAP could be destabilised by ZC3H20, and so the actinomycin D assay would expect to show an increased stability and half -life when ZC3H20 is depleted. However, the decay rate of PHAP mRNA when ZC3H20 is depleted (150min) was not significantly affected compared to uninduced cells (110min) (Figs. 3.7 and 3.8). This suggests that ZC3H20 does not specifically down-regulate PHAP by mRNA destabilisation. In contrast, the half-life of both MCP12 and TS-like E mRNA in uninduced cells is greater than 240min, but when ZC3H20 was down-regulated, the half-life significantly decreased to 114min and 144min, respectively (Figs. 3.7 and 3.8). This shows that the MCP12 and TS-like E mRNAs are turned over/degraded more rapidly in the absence of ZC3H20, and indicates that ZC3H20 is responsible for stabilising both these transcripts in the PF cell.

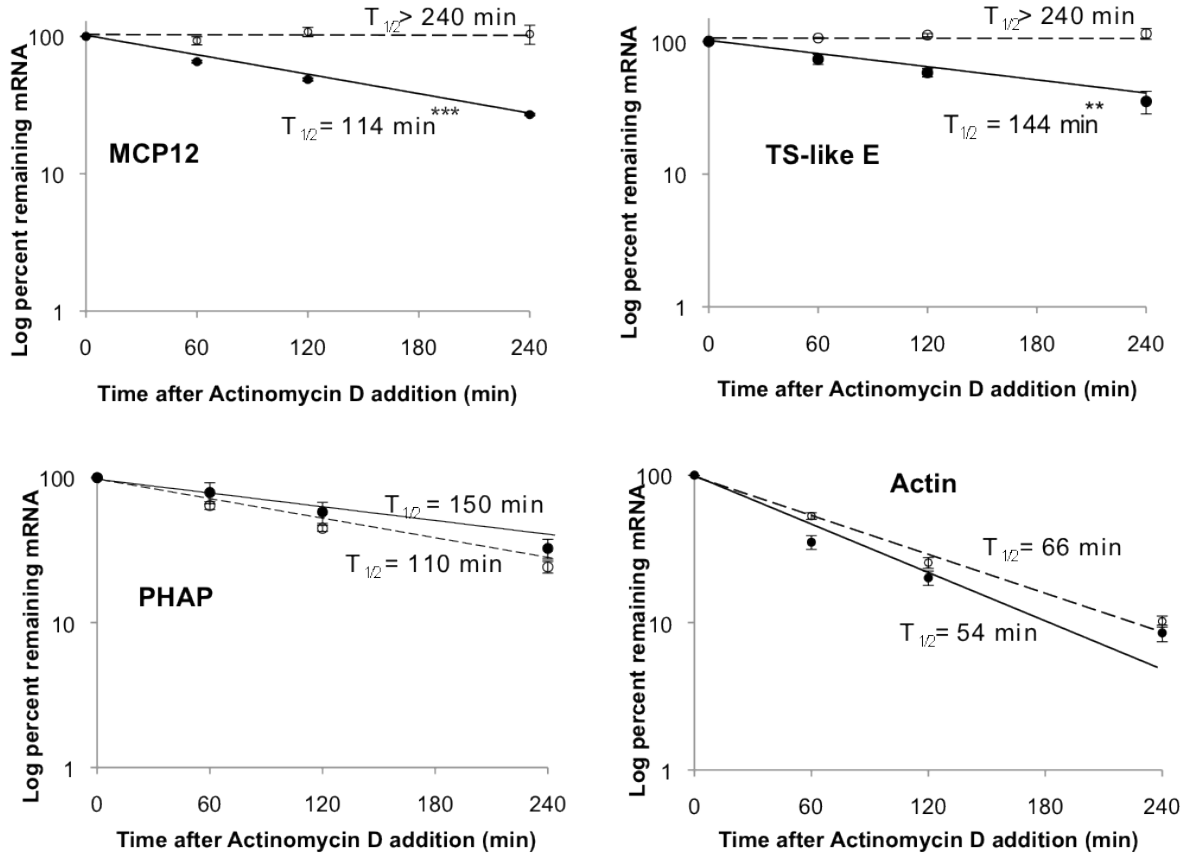


Figure 3.8. Densitometry analysis to determine RNA decay rate after ZC3H20 RNAi down-regulation in PF *T. brucei*

Densitometry analysis of actinomycin D experiment as shown in Fig. 3.7 to determine the half-life of MCP12, TS-like E, PHAP and actin mRNA levels when RNAi of ZC3H20 is induced (filled circles, solid line) or uninduced (open circles, dashed line). Plotted data are mean values from three independent experiments, and error bars show standard error. A Student's t-test was used to determine the significance in the RNA half-life ($T_{1/2}$) when ZC3H20 is down-regulated in PF cells, as described in Chapter 2.15. ** = $p<0.02$, *** = $p<0.001$

After the initial microarray analysis that originally identified 12 genes with a more than 2-fold change in mRNA abundance after ZC3H20 down-regulation, these were then subjected to a translation inhibition assay to determine regulation by a trans-acting factor, *in vivo* ZC3H20 binding assay and an actinomycin D decay rate assay. These criteria subsequently isolated two PF enriched genes, MCP12 and TS-like E that could be regulated by ZC3H20 via mRNA stability in PF *T. brucei*.

3.4 Regulation of MCP12 and TS-like E mRNA via their 3' UTR

ZC3H proteins are shown to regulate mRNA stability through directly binding elements in the 3'UTR of their targets [201]. Therefore, the ability of ZC3H20 to directly bind the 3' UTR of MCP12 and TS-like E must be verified, and whether the 3' UTRs of these transcripts are sufficient to allow regulation by ZC3H20.

3.4.1 ZC3H20 can directly bind the 3'UTR of MCP12 and TS-like E mRNA *in vitro*

The TAP RT-PCR (Section 3.3.3) showed that ZC3H20 is capable of binding MCP12 and TS-like E *in vivo*, but it is unknown if this is a direct or indirect (possibly via another protein factor) RNA-protein interaction. Therefore, an RNA electrophoretic mobility shift assay (EMSA) was used to determine if ZC3H20 can directly bind the 3' UTRs of MCP12 and TS-like E. Recombinant GST-ZC3H20 was produced and isolated from *E. coli*, as performed in Section 3.1.2. Digoxygenin labelled RNA was reverse-transcribed from the 3'UTRs of MCP12 and TS-like E and used in an *in vitro* binding reaction with increasing concentrations (0, 100, 250 and 500nM) of recombinant GST-TbZC3H20. Both labelled RNAs were also incubated with 500nM of GST alone. Each reaction was subjected to agarose gel electrophoresis, transferred to a nylon membrane and analysed by chemiluminesence using a substrate to the digoxygenin label incorporated in the target mRNAs. In the absence of GST-TbZC3H20 (0nM) or in the presence of GST tag alone, the MCP12 and TS-like E 3'UTR RNA displays a single band at the bottom of the gel, showing that the mobility of the RNA is not affected (Fig. 3.9). The shift pattern of the GST control is the same as for the control with no GST-TbZC3H20, verifying that the presence of GST protein does not confer binding to either MCP12 or TS-like E 3' UTR RNA. A different shift pattern is displayed in the presence of increasing concentrations of GST-TbZC3H20 protein for both MCP12 and TS-like E target RNAs. A second band is seen further up the gel indicating that the mobility of the RNA has been affected (Fig. 3.9, asterisk). This shows that the MCP12 and TS-like E 3'UTR RNAs are in an RNA-protein complex with TbZC3H20. The band is shifted even further up the gel as increasing concentrations of TbZC3H20 are used (100-500nM), thus affecting the mobility of the target RNAs more dramatically with increased protein-RNA binding. This shows therefore that TbZC3H20 is capable of directly binding to the 3'UTRs of MCP12 and TS-like E.

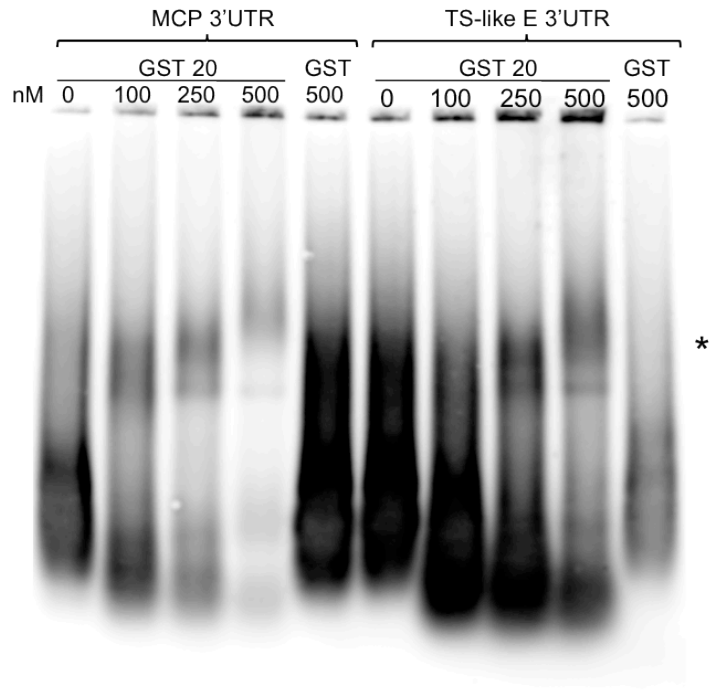
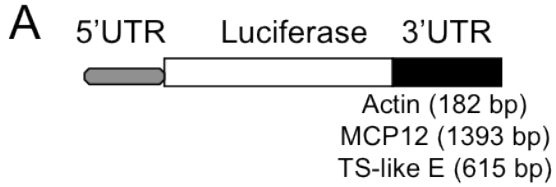


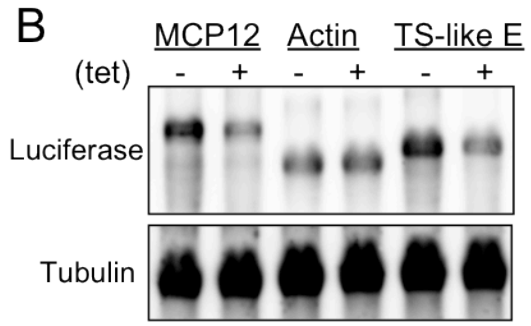
Figure 3.9. RNA EMSA to show direct binding of recombinant GST-ZC3H20 to TbMCP12 and TS-like E 3' UTR RNA

RNA electrophoretic mobility assay of GST-TbZC3H20 to target MCP12 (left side samples) or TS-like E (right side samples) 3'UTR RNAs. Target RNAs are digoxygenin labelled 3'UTR of MCP12 (1393nt) or TS-like E (615nt). For each reaction, 25ng of RNA was incubated with 0, 100, 250, 500nM of GST-TbZC3H20 (GST-20), or with 500nM of GST alone (GST) as a negative control. Asterisk (*) indicates the position of the electrophoretic mobility shifted RNA.

3.4.2 The 3'UTR of MCP12 and TS-like E is sufficient to regulate a reporter gene in a ZC3H20 dependent manner

As discussed in the Introduction chapter (Section 1.4.2), post-transcriptional mechanisms use sequences within the 3' UTR of mRNAs to regulate their abundance. Therefore to determine whether elements in the 3'UTRs of MCP and TS-like E mRNA regulate their abundance in a ZC3H20 dependent manner, a luciferase reporter assay was employed (Fig 3.10A). This allowed the expression of the coding region of the luciferase gene, but under the control of the fused 3'UTR of MCP12 or TS-like E. This system was stably integrated into the PF 20 RNAi cell line, which was then grown in the absence or presence of tet to induce RNAi of ZC3H20. A luciferase reporter gene with the 3'UTR of actin was used as a control.





C

	MCP12	Actin	TS-like E
RNAi 20 -	100	100	100
RNAi 20 +	55 ± 1.2	110 ± 2.9	44 ± 5.3
Difference	45 ± 1.2	10 ± 2.9	56 ± 5.3
Significance	p < 0.001		p < 0.001

Figure 3.10. Luciferase reporter assay to show regulation of TbMCP12 and TS-like E mRNA via the 3'UTR

A. Schematic of the construct used for the luciferase reporter assay. The 5'UTR (and intergenic region) of actin is upstream of the entire open reading frame of luciferase, and then the 3' UTRs of actin, MCP12 and TS-like E were cloned downstream the luciferase gene.
B. A representative northern blot showing the mRNA abundance of the luciferase reporter mRNA with MCP12, actin or TS-like E 3'UTRS in the presence (+) or absence (-) of tet for induction of ZC3H20 down-regulation in PF cells.
C. Average percentage level of mRNA from northern blots seen in B., using densitomtery analysis (from 3 biological replicates). The level of mRNA in the uninduced PF 20 RNAi cell line was expressed as 100%, and the induced samples expressed as a percentage of the uninduced mRNA level. The mean difference (± standard error) in MCP12 and TS-like E levels was then compared to the difference in actin levels and subjected to a Student T-test and both found to be significant at $P<0.001$.

After 48h of RNAi induction of ZC3H20, RNA was isolated from the cells, and the level of luciferase RNA was determined by Northern analysis for each cell line (Fig. 3.10B). The luciferase-actin 3'UTR RNA levels did not change after ZC3H20 depletion, but there is a noticeable decrease in the abundance of the luciferase-MCP12 and luciferase-TS-like E 3'UTR RNA levels after RNAi induction. Northern blots from 3 independent biological replicates were subjected to densitometry to calculate the percentage change in mRNA level when ZC3H20 is down-regulated. The levels were then calculated as a percentage of uninduced PF 20 RNAi reporter

cells, which was expressed as 100%, and the decrease in the MCP12 and TS-like E 3'UTR reporter mRNAs to 55% and 44% of uninduced cells respectively, was significantly different compared to the actin control.

In conclusion, ZC3H20 is able to bind directly to the mRNA 3' UTR of the developmentally regulated genes MCP12 and TS-like E. Additionally, the 3' UTRs of these transcripts are shown to be sufficient to cause ZC3H20-dependent down-regulation of a reporter gene in PF cells. Thus it seems highly likely that ZC3H20 binds elements in the 3' UTR of TS-like E and MCP12, and regulates their mRNA abundance via stabilisation.

3.5 Discussion of Chapter 3

The CCCH zinc finger protein TbZC3H20 is PF-enriched, and RNAi analysis and the inability to create null mutants indicate that ZC3H20 is essential in PF cells for growth. Another similar ZC3H in the genome, TbZC3H21, is inadvertently targeted by ZC3H20 RNAi but the inability to create null mutants for this gene shows it is also essential in PF cells. In the absence of any phenotypic effect on PF cells, microarray analysis produced a small number of genes that had altered mRNA levels from RNAi down-regulation of ZC3H20. A translational inhibitor assay, TAP tag RT-PCR assay, and a transcriptional inhibitor assay were used in combination to isolate genes that fit the criteria of being directly regulated by ZC3H20. This panel of assays in combination with the microarray, represent a relatively simple and effective method to filter thousands of mRNA candidates, to yield small subset of regulated transcripts. Specifically, this method selects for genes that are regulated by mRNA stability, which is the hypothesised function of TbZC3H20 as a tandem CCCH zinc finger protein.

The RNA abundance of 12 genes were increased or decreased greater than 2-fold after down-regulation of ZC3H20 in PF cells, but just two of these indicated that their mRNA stability was regulated in a ZC3H20-dependent manner. These genes were identified as MCP12 and TS-like E, both highly PF-enriched transcripts. Interestingly, the data show that ZC3H20 stabilises these mRNA targets in the PF cell. This is a novel mechanism for this family of ZC3H proteins, as to date, they have only been reported to regulate mRNA stability via destabilisation of their targets. The well-studied tandem ZC3H protein TTP and

other related ZC3Hs specifically destabilise their mRNA targets [167] and the mammalian Zc3h12a is an RNAse and regulates mRNA decay [202]. Despite no reports of mRNA stabilisation by ZC3Hs, other families of RNA-binding proteins have been shown to regulate mRNA targets by stabilisation. The extensively studied mammalian RRM proteins HuR and AUF1, stabilise a range of ARE-containing mRNAs [134]. Transient transfection studies show that over-expression of HuR protects target mRNAs from degradation and that down-regulation of this protein causes increased decay of these mRNAs, consistent with its stabilising role [203]. To date, PUF proteins are normally associated with mediating mRNA degradation, but in *T. brucei*, TbPUF9 has been shown to stabilise specific target mRNAs by over-expression and RNAi analysis [139]. Unlike TTP, which has been shown to recruit mRNA decay enzymes as a mechanism to degrade target mRNAs [168], the mechanism for RBP-mediated mRNA stabilisation has not been defined. A mechanism could be postulated to involve the poly (A) binding protein, which binds to the 3' poly (A) tail and acts to protect mRNA from deadenylation, and PABP1 in *T. brucei* has demonstrated protection and stabilisation of mRNA in trypanosome extracts [104]. Thus, an RBP could bind specific mRNAs through elements in the 3'UTR and additionally associate with PABP or translational machinery to promote stabilisation of the transcript. Alternatively, the ZC3H protein Nab2 recognises polyadenosine RNA with high affinity, which is suggested to bind via a different mechanism to the previously characterised RRM-containing PABP [157], and potentially provides another route for ZC3H-mediated stabilisation.

Classically, ZC3H proteins bind specific sequence elements in the 3'UTR of target mRNAs, thus resulting in mRNA destabilisation. The AU-rich element (ARE) is a well characterised sequence present in the 3'UTR of many mRNAs and is responsible for mRNA destabilisation by the ARE-binding ZC3H TTP and TTP-related proteins [134]. However, AREs have been shown to promote stabilisation of a target mRNA by the RRM proteins HuR and AUF1 [134]. Depending on the dispersion and context of the AUUUA pentamer, AREs are grouped into three basic classes, Class I, Class II or Class III AREs [134]. In the 3' UTRs of MCP12 and TS-like E, there were no elements that fit into the any of the classes. Class I AREs are usually one or more of the AUUUA pentamers dispersed within a U-rich context. The 3' UTR of TS-like E possesses several of these AUUUA pentamers, with three of these pentamers fairly close with a high number of uridines (9/14ntds)

in between each pentamer (Fig. 3.11A, green elements). This could be an example of a Class I ARE. The 3' UTR of MCP12 has a couple of these AUUUA pentamers, but are spaced far apart (Fig 3.11B, green element). Class II elements have at least 2 overlapping UUAUUUA(U/A)(U/A) nonamers, but none of these sequences are present in the 3' UTR of MCP12 or TS-like. A less well-defined motif is the Class III ARE, which consists of a U-rich region that is absent from the AUUUA pentamer [134]. This type of motif is clearly not present in the 3'UTR of TS-like E, but there does appear to be large stretches of U-rich regions on the 3'UTR of MCP-12 (Fig. 3.11B, red).

The U-rich Class III ARE of the *c-jun* proto-oncogene mRNA is surrounded by an overall AU-richness, but does contain a GU-rich sequence with four copies of a GUUUG motif [204]. A recent study has identified a consensus sequence UGUUUGUUUGU, termed a GU-rich element (GRE) that is enriched in the 3' UTR short-lived transcripts in primary T cells, confers instability of the transcript and mediates binding of CUG-binding protein-1 which may promote mRNA decay [205]. GRE-like elements are present in the 3'UTR of TS-like E and MCP12 (Fig. 3.11A and B, blue), but there is no common consensus sequence between these two transcripts. Interestingly, a G-rich element, which comprises of two contiguous CGGGG pentamers, has been identified in the 3' UTR of the developmentally regulated *T. cruzi* SMUG mRNAs that confers stabilisation of the transcript in a specific life cycle stage of the parasite. This type of element is not present in the 3'UTRs of MCP12 or TS-like E mRNAs, but with the presence of GRE-like elements that are fairly "G-heavy" these could be sequences to consider as stabilisation elements. The RNA-homopolymer assay (Fig. 3.1D) shows that recombinant TbZC3H20 has a preference for binding poly-G compared to poly-A/C/U in vitro, and this could provide clues about the types of elements for which ZC3H20 has an affinity.

Figure 3.11. 3' UTR regions of TbTS-like E and TbMCP12 mRNA

Black type indicates the intergenic region between TbMCP12 and TS-like E and the genes down stream (sequences in bold black type). AUUUA pentamer sequences are highlighted in green. The octamer UAUUUUUU element previously discovered in trypanosome life cycle stage regulated transcripts is highlighted in yellow. U rich sequences devoid of the AUUUA pentamer are highlighted in red. GU rich sequences are highlighted in blue.

A. TbTS-like E (Tb927.5.440)

TGATGACACACTGGATGTAAGGAAATGAGGUCUAUAAUCCAUGUUAUUUCAGCGUGAGGAGGAUAAUACGAGC
AGACAUGAAUUUCAUUUAAUAACUUUAAUGGUAGACUCAAGACGGUAAAUUUAAGCGAGUAUGUUUCAACGAU
UUUAUUUUUACAAAUAGGAUGUCAACUAUAACAUAUCAGGUGCUACCGGUUUUCUUCUGAUGUUAAUGACAUC
AGUAGACUGCUUCCGGCACUCUGAGAGCACGGUUAUAUUUUUUUUUUCUCUUUAUCACAUGAUCUAAGGUGGU
UCUGUUGUAUGUGAGACACGAUACAUAUAAUUUUCUUUUUUUGUUCCAACCCCUUUUUUUUGUUCCUGAGCGU
UACGUGAGUGGUAUGAGGUCAGUAGCAUUAUGGUGUAAUAGUUUUAUUUCAUGCCAUGCUCUAUUUACCGUGA
CAUCAUACACUCGGCAUAAAAUAUAUUUAUCUUUAUUUAUCUAUAUAUAUUUAUGCAUAGUCUAUGUUAGUGCU
CGUGUUGUUUUGUUCAACUUGUGACCUGUUGCAUCUUUGUUACUCCUAAUUACUGUUUUAUACAAUGUUUUCC
CCUUGUUUAUAUAUUUGUACGUAUUUGUACGUAUAAAAAAAAUGAAUGUGGAUGUGUUGUGGUUAUUGCAUUU
CAGGCUUAGUGUGUCGUUGAAACUAGUAGUAAAGGU**ATGGGCGCAAGATTGCGTCACTCCTAC**

B. TbMCP12 (Tb927.10.12840/Tb10.389.0690)

TGAAGGGGTGGCGTGCCGCCAAGCTTCAGGCAAAGCAGTAGUGUCUCAUUAAGUCCCCUUUACUUAUUGUAAU
AGUGUGAAUAAAUCACUGCGUCACGUUAUGUUAGAAACAUGAAGCGGCGACAUGUAUGAGUGUCUGUGUGUGU
AUGUUCUGAUUUCCUUUUUUUUUCUAAGUACUGGAGGAGCGAAUAAGUGAAGGGGACAAUCUGUACGAGAUGU
UGCCGUUUUUGGCAGCUUUUUUUUUUUGCUUCGUUUUUUUUUACUGUUGUUUUUCGAAAUCGAUUACUUUGUG
UUCGAAUAUCCUCACACGACGAGACAAGAGCUGAUGAUAACUCCGCUUUUUAGUAAUGCCUUGUGUGUGUGUG
UGUGUGUGUGUGUGUACUGGGCUUUGAAGAUGAAAAAGAGACAAAGCGACAAGAGACCAAAUUGUGGUUCAGC
UGUGACUCUUCUGACACUUUCUUUUGUUUUGUACUUGAUCGCUUAUCUUUUUUUUUUUUGGAGAGUUUCUUCC
UCUGUUUUUCUCACUUUGACUUCAUAUAUACGUAUAUAUAUAUAUGUGUGUGUGUUUGUGUGUACGUGUUUAAAC
ACCAUGAUAAUGGUUCCGCUCCUGGUAACUUUUCAACUUAACGCUCGGACGGGGGAGGGGGAAAUUUGAGGUU
AUGUGAUGAAUACGGGUGGAUGAGAUACGAAAAGAUUAUUUACAUGGGCGUCAUUUUUUUUUUCUCCUAAUCU
UAUCUUUUUUUAAAUUCAUUUUAUUCUUUUUUUUUUUCAGGGAGGGGAUGAGGUGAUGUGCCCAUUUGUGAAC
GAAUUAAUUUAACUAUAGAAGGUAUAGGAUCAGGAGCGUACGGAGACGGGAAAGAAGAGUUGCCGCAAACCUU
CUUGCAUCCACGAUCUGAAAAAGAAAAAAAACUGUAAAAAAAAAAAAAGGAAAAUGUGGUGAAGACAACGGAAU
AAAUAAACCAACUACAAAGGAAAUUAUAUACGAGGCAACUCUCUACAUAUGAUCACUUUUCAGUGGAAUAACA
AAAAAAGAGAAGUGAAGGGGCGUUUAAUAGGAAGGAAUAAGCGAAUGUGUGUGUGUAAAGGCGAAGAGUGGUU
GUUGUUGUAUUGUUGUCCUCUCCCUUUCUUGUUUCUUUUUCUUUAGUUAUCGGUAGGCUAAUUGAGCGCUCAU
AUGUAUAUGCUAAUUGUUACAUAGAUUGUAAUGGUGAAAAAUAAGCACAUGGUUUGUUUAACACAAUUUCUUA
UAUCUUUUUUUAUCUUCUUUUUUUUUUAAAAAAAAAACAUACAACGACAUUACUGGUGAGUUAAGCCAUGAAAU
CAUGUGCUUCCGGUUAGGAGAUAAAGAGAGGAUGCUAGUUGGUGGAGUUCCCGCACCUUUGCUUUGGGUGUAG
AAACCUGCCGUUAUUUCCUUUAGUCAUUUCAAGCCUGGACUGCCACGUUAUUAAUUUCUUUAUCUUGUAGUGC
UUUCCGCUAUCCUCAUUCUCUUUUUUAUUCAUCCAUGAGGUGUAAAUGAGCGCAGUGGAGCUUGUUGCACUCC
CGAGUCGUAAUGGGGGAAGACCAUUAACAGUGCAUCUUAGCUGGGGAAUUGCAGAGAGCGAC**ATGGAAAGCAT**
ACAGGCGCTCCACG

Finally, previous studies of the developmentally-regulated mitochondrial COX genes in *T. brucei* identified a core sequence of the 26mer instability element from EP procyclin (UAUUUUUU) that is present in one-third of PF-enriched genes [136]. The core sequence (and EP procyclin 26mer) is identified as an element that promotes mRNA destabilisation in BF *T.brucei*, thus causing an apparent enrichment in the PF life cycle stage [125, 136]. Both MCP12 and TS-like E are developmentally regulated PF-enriched genes, and this core element is present in

the 3' UTR of TS-like E but is not found in the 3'UTR of MCP12 (Fig. 3.11A, yellow). The absence of the element in MCP12 is not surprising as it is a destabilisation element, and MCP12 is stabilised by ZC3H20. Its presence in TS-like E could mean that it is responsible for destabilisation by other *trans*-acting factors in BF cells. However, an important point to note is that just the presence of an element does not necessarily constitute evidence that it is a functional RNA-destabilising/stabilising element, as suggested by studies on the ARE AUUUA motifs [206]. Thus, even though various putative elements are present in the 3'UTR of TS-like E and MCP12, there is no identified sequence element common between these two, suggesting there could be a completely novel element required for stabilisation by ZC3H20. Oligomer search tools or RNA fold prediction programs are not reliable tools to identify common elements between such a limited set of targets. Extensive 3'UTR mapping of MCP12 and TS-like E would be required to identify regulatory *cis*-elements, which could include sequence elements or secondary structures.

TbMCP12 is a member of the *T. brucei* mitochondrial carrier protein (MCP) family, and is part of a group of structurally conserved proteins that permits the transport of metabolites across the inner membrane of the mitochondrion. There are 24 MCPs identified in *T. brucei* that have been localised to the mitochondrion in PF cells, but out of these, just MCP11 and MCP12 are differentially expressed at the mRNA level, showing enrichment in the PF life cycle stage [207]. MCP12 is suggested to have a putative role in exchanging malate for 2-oxogluarate (an oxoglutarate carrier) and malate for an inorganic compound (a dicarboxylate carrier), which are usually two different carriers in yeast and human cells [207]. Only MCP12 out of the putative *T. brucei* MCPs shows the greatest homology with these two carriers, and given the importance of malate to be transported in or out in the mitochondrion in PF *T. brucei,* suggests a crucial role for MCP12 [207].

TbTS-like E encodes a *trans*-sialidase like protein (type E) that is part of a family of sialidase and *trans*-sialidase enzymes that are responsible for regulating the sialic acid content on the GPI-anchor of the procyclins on the surface of PF *T. brucei* [208]. Trypanosomes are unable to synthesise sialic acid, and so they use the *trans*-sialidase enzyme to transfer sialic acids from the surface on glyconjugates in the tsetse bloodmeal or midgut to the GPI-anchor of procyclin [209]. Surface sialic acids have been suggested to provide protection for the

parasite from the digestive and trypanocidal fly midgut, as depleting the cell surface from sialic acids diminishes survival in the tsetse intestine [210].

This chapter shows that ZC3H20 is responsible for regulating the expression of TS-like E and MCP12 via mRNA stabilisation. The data suggests that ZC3H20 is capable of binding to the 3'UTR and promoting stabilisation of the TS-like E and MCP12 mRNAs. Both the TS-like E and TbMCP12 are developmentally regulated and each mRNA is clearly enriched in the PF life cycle stage. This is unsurprising considering their putative functions that are essential for energy metabolism and survival in the fly midgut. The expression of ZC3H20 itself appears to be PF-enriched at the level of protein and is essential for growth in PF cells. Thus, ZC3H20 is an essential protein that stabilises at least two PF-enriched genes (MCP12 and TS-like E) that are crucial for adaptation and survival in the tsetse fly.

CHAPTER 4. Bloodstream form enriched endocytic molecules are down-regulated by ZC3H20 in procyclic form *T. brucei*

4.1 Introduction

TbZC3H20 regulates two PF enriched genes, MCP12 and TS-like E via mRNA stabilisation in PF *T. brucei* (Chapter 3.3, 3.4). Using RNAi and knockout analysis, ZC3H20 is shown as essential for growth of PF trypanosomes (Chapter 3.2), reinforcing the importance of its role in regulation of gene expression in the cell. The stabilisation of MCP12 and TS-like E is predicted to be necessary to meet the energy needs and surface coat composition of the PF parasite. In addition to up-regulation of life-cycle stage enriched transcripts, the destabilisation of transcripts enriched from the opposite life cycle stage is just as relevant. There are genes that require tight regulation between the life cycle stages to prevent detrimental effects upon the cell for example, the glycosomal phosphoglycerate kinase C is only expressed in BF and the cytosolic phosphoglycerate kinase B is only expressed in PF, and expression of PGKB is toxic in BF *T. brucei* [211]. However, where there are plenty of examples of an upregulated gene that is expendable in the opposite life cycle stage, some genes that are developmentally down-regulated are still necessary for survival in that life form. One example of this is the endocytic pathway, where the endocytic rate is approximately 10-fold slower in the PF parasite than the bloodstream form [26]. As discussed in Chapter 1 (section 1.2.1), endocytosis in trypanosomes is clathrin-mediated, and even though clathrin expression is low compared to BF cells, clathrin is still essential for growth and trafficking in PF *T. brucei* [36]. As described in Chapter 1 (section 1.2.1) studies of clathrin and other endocytic molecules enable a more detailed understanding of the trafficking system in trypanosomes, but the regulatory mechanisms required for the endocytic pathways remain to be elucidated. In higher eukaryotes and yeast, clathrin interacts with a network of protein partners required for clathrin-coated vesicle formation, in particular, adaptor proteins (APs) involved in the recruitment of cargo [212]. Therefore at the molecular level, regulation of adaptors through phosphorylation and ubiquitination might influence these interactions and consequently control endocytosis [213]. The adaptor AP-2 is considered the major clathrin-assembly protein responsible for clathrin assembly [213]. After extensive searches of the *T. brucei* genome, there does not appear to be a homologue for AP-2, [31] thus making the identification of clathrin regulators more challenging. Even so, the dramatic changes in the developmental expression level of clathrin in *T. brucei* suggests there must be regulation at the mRNA transcript level, and there

have been no such factors for clathrin regulation reported in trypanosomes or any other eukaryotic system.

In a contrasting approach to using RNAi down-regulation, ectopic over-expression of ZC3H proteins in trypanosomes is proven to be a useful tool to analyse their role within the cell by producing tractable biological phenotypes [181, 182]. We found that over-expression of ZC3H20 in PF *T. brucei* caused an enlarged flagellar pocket, referred to as BigEye. The flagellar pocket is the site for all endocytosis and exocytosis in *T. brucei*, and the BigEye phenotype has been reported when molecules of the endocytic pathway (including clathrin) are down-regulated, causing a endocytic defect. We show that BigEye cells from over-expression of ZC3H20 are defective for endocytosis. ZC3H20 is likely to be affecting clathrin-mediated endocytosis rather than perturbing flagellar pocket biogenesis or mitochondrial maintenance, which would cause flagellar pocket enlargement. Using microarray analysis, the effect of ZC3H20 over-expression on mRNA abundance was investigated to identify genes associated with the endocytic pathway that may be regulated by ZC3H20 in PF cells. Indeed, various molecules associated with the endocytic pathway, which are usually BF-enriched transcripts, were down-regulated upon ZC3H20 over-expression in PF *T. brucei*. Consequently, these potential mRNA targets were studied in more detail, using the same approach as described in Chapter 3, to investigate if ZC3H20 regulates genes involved in the endocytic pathway via mRNA stability in PF trypanosomes.

4.2 Investigation of the phenotypic effect of over-expression of TbZC3H20 and TbZC3H21 in procyclic form *T. brucei*

4.2.1 Over-expression of TbZC3H20 and TbZC3H21 in procyclic form *T. brucei* causes a growth and morphological defect.

To over-express an ectopic copy of TbZC3H20, the full coding region was cloned into the construct pHD451, which also allowed the addition of a TY1 tag to the C-terminus of ZC3H20 [186]. This modified construct was stably transfected into PF 449 procyclic form cells (see Chapter 2) and allowed the inducible over-expression of ectopic ZC3H20 by addition of tet. As described in Chapter 3 (Section 3.1.1), TbZC3H20 shares a high degree of sequence similarity with another *T. brucei* ZC3H with two conventional zinc finger motifs, TbZC3H21, which

like ZC3H20, causes a growth defect in PF cells when RNAi of ZC3H21 is induced. Therefore, over-expression of ZC3H21 in PF was also investigated to determine the effect of a similar CCCH zinc finger protein. Subsequently, the coding region of ZC3H21 was cloned into the construct pHD451 and stably transfected into PF 449 cells, as done for ZC3H20.

Inducible over-expression of ZC3H20 and ZC3H21 in PF cells was verified by isolating total protein from cells grown in the presence (+tet) or absence (-tet) of tetracycline for 24h. Western analysis using an antibody, BB2, to the TY1 tag at the C-terminus of the expressed ZC3H proteins, showed that there was expression of protein of the expected sizes by the induced ZC3H20 (~45kDa) and 21 (~51kDa) in PF cells (Fig. 4.1A).

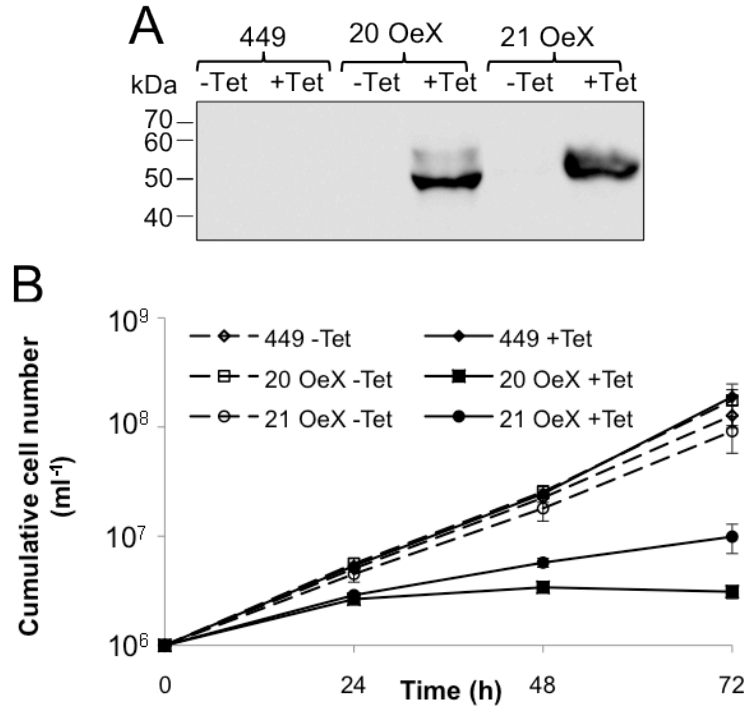


Figure 4.1. Effect on growth from over-expression of ZC3H20 and ZC3H21 in PF *T. brucei*

A. Western blot of protein from whole cell lysate of PF *T. brucei* induced to over-express TbZC3H20 (~45kDa with TY1 tag) and TbZC3H21 (~51kDa with TY1 tag). Cells were grown in the absence or presence of tet (-tet or +tet) for 24h. Protein is detected with an anti-TY1 tag antibody, BB2.
B. Growth curve showing the effect of tet induced (+) or uninduced (-) over-expression of ZC3H20 and ZC3H21 over 72h in PF cells. 449 is the parental cell line and shows no effect on growth in the presence of tet. Plotted data are mean values from three independent experiments, and error bars show standard deviation.
449 = PF449 parental cells, 20 OeX = PF449 TbZC3H20 over-expression cells, 21 OeX = PF449 TbZC2H21 over-expression cells

The effect of ZC3H20/21 over-expression on the growth of PF cells was then analysed. PF 20 OeX (TbZC3H20 over-expression) and PF 21 OeX (TbZC3H21 over-expression) cells were grown in the presence or absence of tet for 72h, and their growth recorded (Fig. 4.1B). The parental cell line, PF449 cells were also grown under the same conditions as a control. Induced over-expression of ZC3H20 and ZC3H21 (+tet) in PF cells resulted in a severe growth defect after 24h, compared to the parental cell line control and the uninduced PF 20/21 OeX cells. By 72h, cells over-expressing TbZC3H20 had ceased growth (Fig. 4.1B).

A morphological change was also apparent within the induced cell population. Fig. 4.2A shows the morphology of a normal PF trypanosome with a kinetoplast (mitochondial genome) and nucleus stained with DAPI. Over-expression of TbZC3H20 after 24h results in the formation of a large vacuolar structure at the posterior end of the cell, close to the kinetoplast (Fig. 4.2B). This phenotype has been named “BigEye” in reference to previous studies reporting a similar phentoype [36]. Over-expression of TbZC3H21 results in a round morphology after 48h of induction (Fig. 4.2C).

The BigEye and round phenotypes were quantified in the induced and uninduced populations (Fig. 4.2D). After 24h of induction, 50% of the induced PF 20 OeX cell population displayed the BigEye phenotype. This proportion then decreased to 20% over the next 48h concurrently with the increase of round cells. The round phenotype observed by over-expression of TbZC3H21 is apparent after 48h of induction, which is displayed by 15% of the cell population (Fig. 4.2D).

Both phenotypes are clearly identifiable compared to the normal morphology of a procyclic trypanosome, and were completely inducible, thus providing a tractable phenotype to explore further.

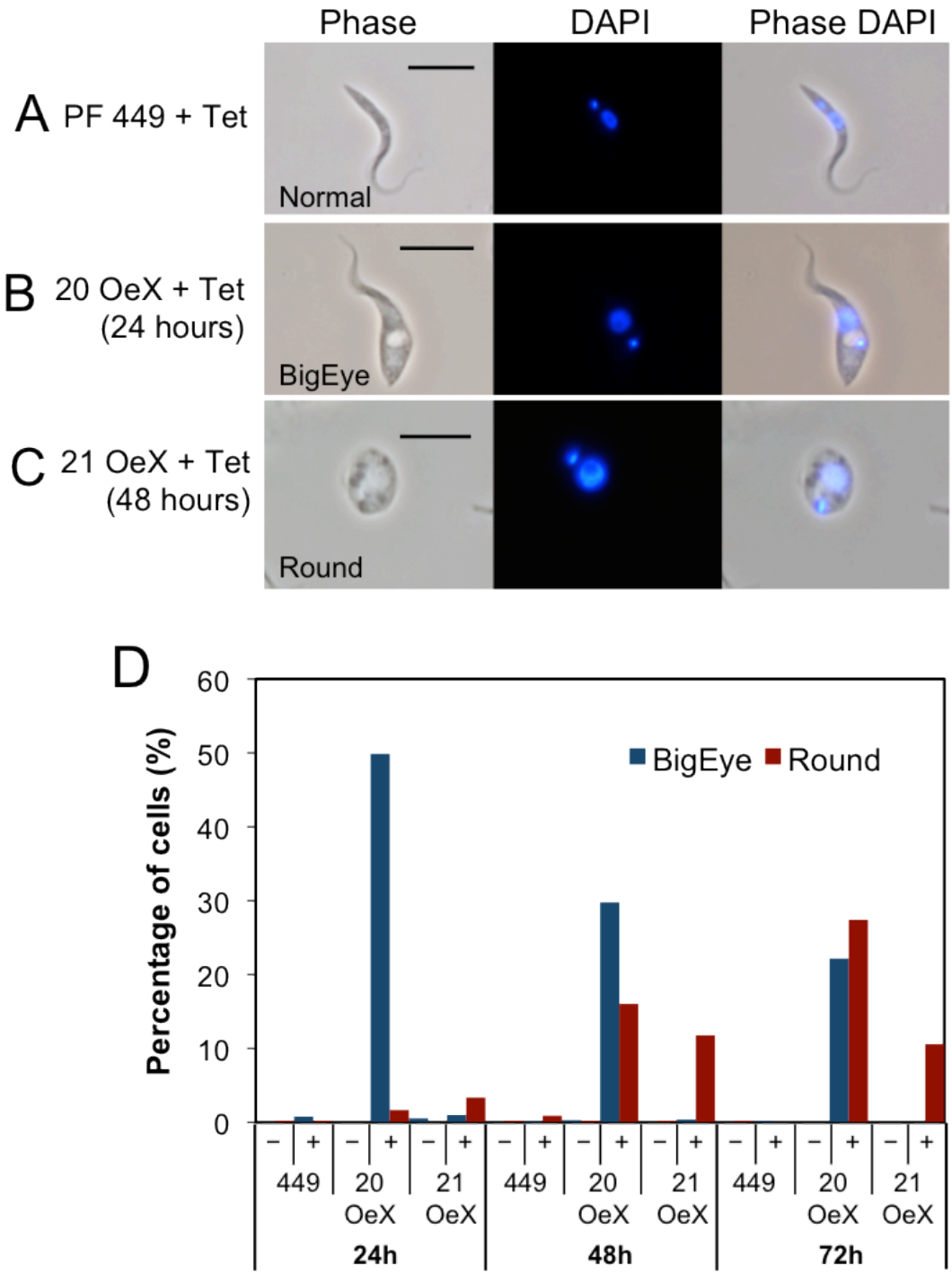


Figure 4.2. Phentoypes caused by over-expression of ZC3H20 or ZC3H21 in PF *T. brucei*

A, B, C. Phenotypes of PF *T. brucei* induced to over-express TbZC3H20 and TbZC3H21. + Tet = addition of tet. DAPI stains the kinetoplast and nucleus. Scale bar = 10µm
D. Quantification of phenotypes observed after overexpression of TbZC3H20 and TbZC3H21 in PF *T. brucei*. Over 200 cells were counted for each population. Cells were grown in absence (-) or presence (+) of tet for 72h. Means are plotted on the chart for two independent replicates.
449 = PF449 parental cells, 20 OeX = PF 449 TbZC3H20 overexpression cells, 21 OeX = PF449 TbZC2H21 overexpression cells.

4.2.2 Over-expression of ZC3H20/21 in PF *T. brucei* correlates to the phenotype observed

Over-expression of a protein above endogenous levels allows its localisation within the cell to be easily determined. Due to the unavailability of an anti-TbZC3H21 antibody and that the anti-TbZC3H20 antibody (as shown in Western blot analysis in Section 3.1.3) is not sensitive or specific enough for immmunofluoresence, the pHD451 construct was modified to allow expression of either protein with an N-terminal GFP tag. The full coding region of ZC3H20 or ZC3H21 was cloned into the pD451 GFP construct and then stably transected into PF449 cells. The trypanosomatid histone acetyltransferase gene, HAT2, localises to the nucleus, and addition of a GFP tag does not affect this localisation [214]. Therefore the coding region of HAT2 cloned into the pHD451 GFP construct can be used as a control for the expression system (a generous gift from David Horn, London School of Hygiene and Tropical Medicine), and was stably transfected into PF449 cells along with the pHD451 GFP ZC3H20/21 constructs.

The over-expression of GFP tagged HAT2, ZC3H20 and ZC3H21 was induced by the addition of tet for 24h (HAT2 and ZC3H20) and 48h (ZC3H21), and cells were then prepared for microsopy to determine expression by fluoresence of GFP. GFP-HAT2 over-expression showed localisation of the protein to the nucleus, verifying that the GFP tag does not interfere with the localisation of this protein (Fig. 4.3A, top panel). GFP-ZC3H20 over-expression caused the BigEye phenotype and over-expression of GFP-ZC3H21 resulted in the cells displaying the round phenotype (Fig. 4.3A, middle and bottom panels). This shows that over-expression of the GFP tagged ZC3Hs produces the same phenotype as over-expression of the TY1-tagged proteins (Fig. 4.2B,C). The GFP signal is seen across the main body of the cell for ZC3H20 or 21 over-expression, showing that neither protein is localised to a specific part of the cell, but expressed throughout the cell cytoplasm.

The presence of the GFP fluorescence as shown in Fig. 3A, also verifies the protein expression at an individual cell level, and so cells can be scored on their expression of the GFP tagged ZC3H20/21 and their corresponding morphology. Therefore for each phenotype displayed within a population, their expression of GFP-ZC3H20/21 was quantified (Fig. 4.3B). This determined that while only 20-30% of cells with a normal morphology expressed ZC3H20 or 21 when induced

with tet, all cells displaying the BigEye or round phenotype showed expression of the respective ZC3H. This correlates over-expression of ZC3H20 or ZC3H21 with the resulting phenotype displayed.

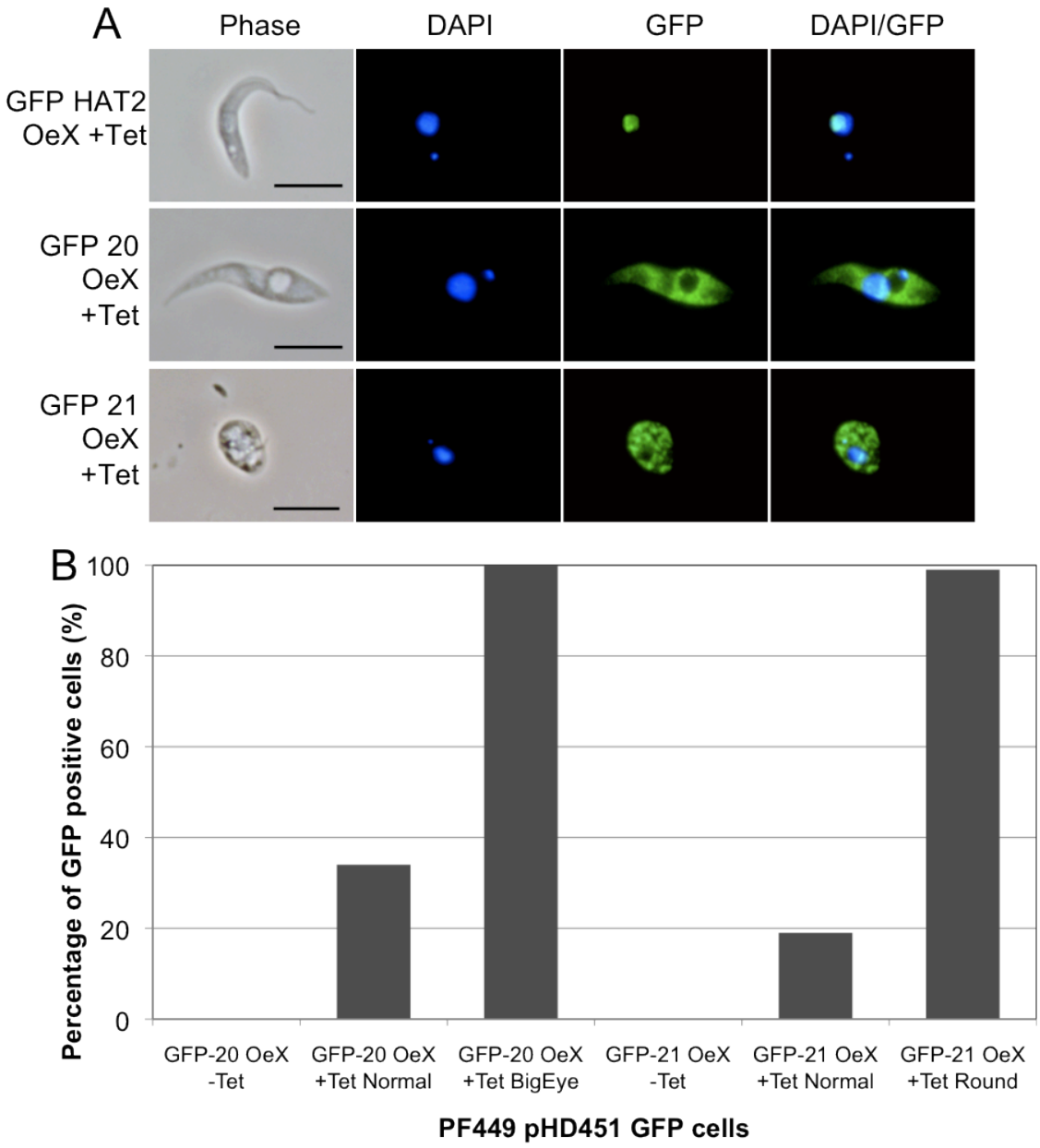


Figure 4.3. GFP-tagged over-expression of ZC3H20 and ZC3H21 in PF *T. brucei*

A. GFP auto-fluorescence of PF *T. brucei* induced to over-express GFP tagged HAT2, -ZC3H20 and -ZC3H21. + Tet = addition of tetracycline. DAPI stains the kinetoplast and nucleus. Scale bar = 10µm.
B. Quantification of GFP positive cells for each phenotype observed after overexpression of GFP tagged - ZC3H20 and -ZC3H21 in PF *T. brucei*. Over 200 cells were counted for each population. Cells were grown in absence (-) or presence (+) of tet for 24h (20 OeX) or 48h (21 OeX).
GFP-20 OeX = PF449 GFP-TbZC3H20 overexpression cells, GFP-21 OeX = PF449 GFP-TbZC2H21 overexpression cells.

4.2.3 Both CCCH zinc finger motifs of ZC3H20 are necessary to cause the BigEye phenotype from ZC3H20 over-expression in PF *T. brucei*

ZC3H20 contains two CCCH zinc finger motifs, which are predicted RNA binding motifs, and shown to be necessary for the function of TbZFP3 and other similar CCCH zinc finger proteins [173, 181]. To determine if neither, one or both of the putative CCCH motifs within ZC3H20 are necessary to cause the BigEye phenotype, deletion mutants and CCCH zinc finger site-directed mutant constructs were created for over-expression in PF (Fig. 4.4).

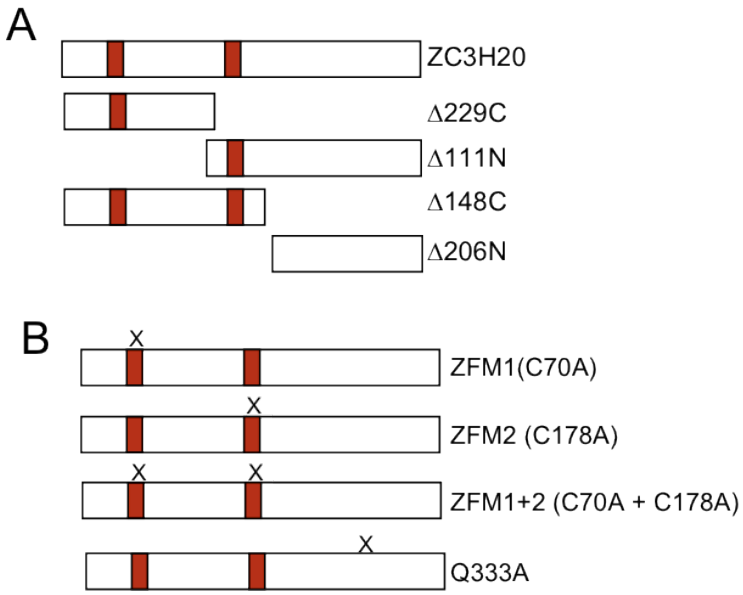


Figure 4.4. Schematic of the ZC3H20 deletion and point mutants

A. Schematic of ZC3H20 deletion mutants, cloned into pHD451 (Chapter 2.1)
Δ111N/Δ206N = Deletion of 111/206 aa from N-terminus of ZC3H20.
Δ229C/Δ148C = Deletion of 229/148 aa from C-terminus of ZC3H20
B. Schematic of ZC3H20 zinc finger motif (ZFM) mutants, and one random point mutant (Q333A). The third critical cysteine residue within the relevant CCCH motif is substituted with an alanine. Created using site-directed mutagenesis cloned in pHD451 (Chapter 2.1). Red boxes indicate position of CCCH zinc finger motifs, and X denotes the position of the site-directed mutagenesis

Inducible over-expression of each deletion mutant and site-directed mutant in PF cells was verified by isolating total protein from cells grown in the presence (+) or absence (-) of tet for 24h. Western analysis using an antibody, BB2, to the TY1 tag added to the C-terminus to the expressed mutant ZC3H proteins, showed that there was expression of protein of the expected sizes (ZC3H20 and ZFM mutants, 45kDa; Δ229C, 20.6kDa; Δ111N, 32.2kDa; Δ148C, 29.2kDa; Δ206N, 21.7kDa) by the induced PF ZC3H20 mutant cells (Fig. 4.5A,B). These PF ZC3H20 mutant cells were then grown in the presence (+) or absence (not shown) of tet to determine the effect on cell growth over 72h (Fig. 4.5C). This analysis showed that

over-expression of ZC3H20 with a random point mutation (Q333A) was the only cell line that showed a growth defect comparable to over-expression of the wild-type ZC3H20.

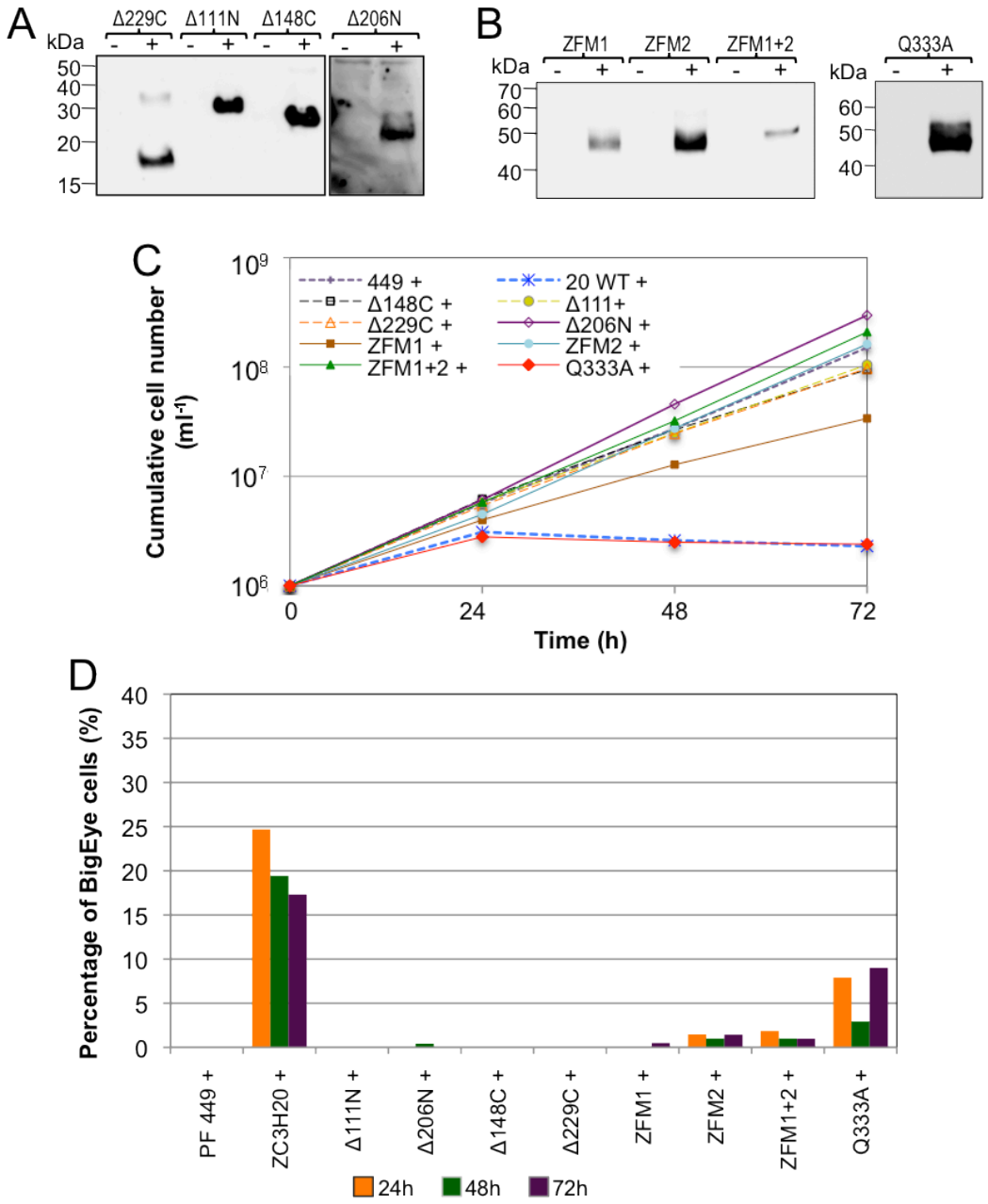


Figure 4.5. Expression of ZC3H20 deletion and point mutants in PF *T. brucei*

A, B. Western blot of protein isolated from PF 20 OeX deletion mutants (A) and site-directed zinc finger motif (ZFM) mutants (B) in the absence (-) or presence (+) of tet after 24h, using an anti-TY1 tag antibody. Expected sizes: Δ229C, 20.6kDa; Δ111N, 32.2kDa; Δ148C, 29.2kDa; Δ206N, 21.7kDa.
C. Growth curve showing the effect of tet induced (+) over-expression of ZC3H20 site-directed mutants and deletion mutant in PF cells. 449 is the parental cell line and shows no effect on growth in the presence of tet.
D. Quantification of BigEye phenotype observed after overexpression of TbZC3H20 site-directed mutants and deletion mutant in PF cells. Cells were grown in presence (+) of tet for 72h. PF449 is the parental cell line.

These cells were quantified for an enlarged flagellar pocket, and over-expression of the ZC3H20 Q333A mutant did cause 9% of PF cells to display the BigEye phenotype (Fig. 4.5D). Over-expression of any other ZC3H20 deletion mutant or zinc finger site-directed mutant in PF cells did not cause a growth defect and caused an enlarged flagellar pocket in less than 2% of cells (Fig. 4.5C and 4.5D). This shows that both zinc fingers are required for ZC3H20 to cause the BigEye phenotype, but also that they are not sufficient i.e. the CCCH motifs cannot act alone and the entire protein coding region is necessary.

4.2.4 Over-expression of TbZC3H20 causes an enlargement of the flagellar pocket

The round phenotype has been reported by studies of RNAi down-regulation of a flagellar pocket protein, BILBO1 or the ADP ribosylation factor ARF in bloodstream form [29, 215] and RNAi of clathrin or tryptophanyl-tRNA synthetase in procyclic form [36, 216]. This round morphology is also adopted when cells endocytose trypanosome lytic factor (TLF) causing them to swell and eventually lyse [217]. As over-expression of TbZC3H21 causes a growth defect and cells to display this round morphology and die, it is a common phenotype that is most probably due to a number of upstream factors. Consequently, it is difficult to characterise this genetic perturbation any further, and so it was decided not to pursue the investigation of TbZC3H21 over-expression in PF *T. brucei* at this point.

However the BigEye phenotype has been reported by studies that show this large vacuolar structure is an enlargement of the flagellar pocket [36, 218]. The flagellar pocket of *T. brucei* is the site for all endocytosis and exocytosis and is located adjacent to the kinetoplast [219]. To determine if the BigEye phenotype displayed by TbZC3H20 over-expression is an enlarged flagellar pocket, a FITC-Tomato Lectin assay was used (Fig. 4.6A). Tomato lectin (*Lycopersicon esculentum*) is used to probe the structure of the flagellar pocket and early endosomal system [220]. The parental cells (PF449) show the FITC-Tomato lectin localised to a discrete position very close to the kinetoplast (Fig. 4.6A top panel, white arrow), which is the correct location for the flagellar pocket and early endosomal system. The induced PF 20 OeX BigEye cells show staining around the vacuolar structure and intense staining adjacent to the kinetoplast (Fig. 4.6A, bottom panel). This suggests that the vacuolar structure is the flagellar pocket.

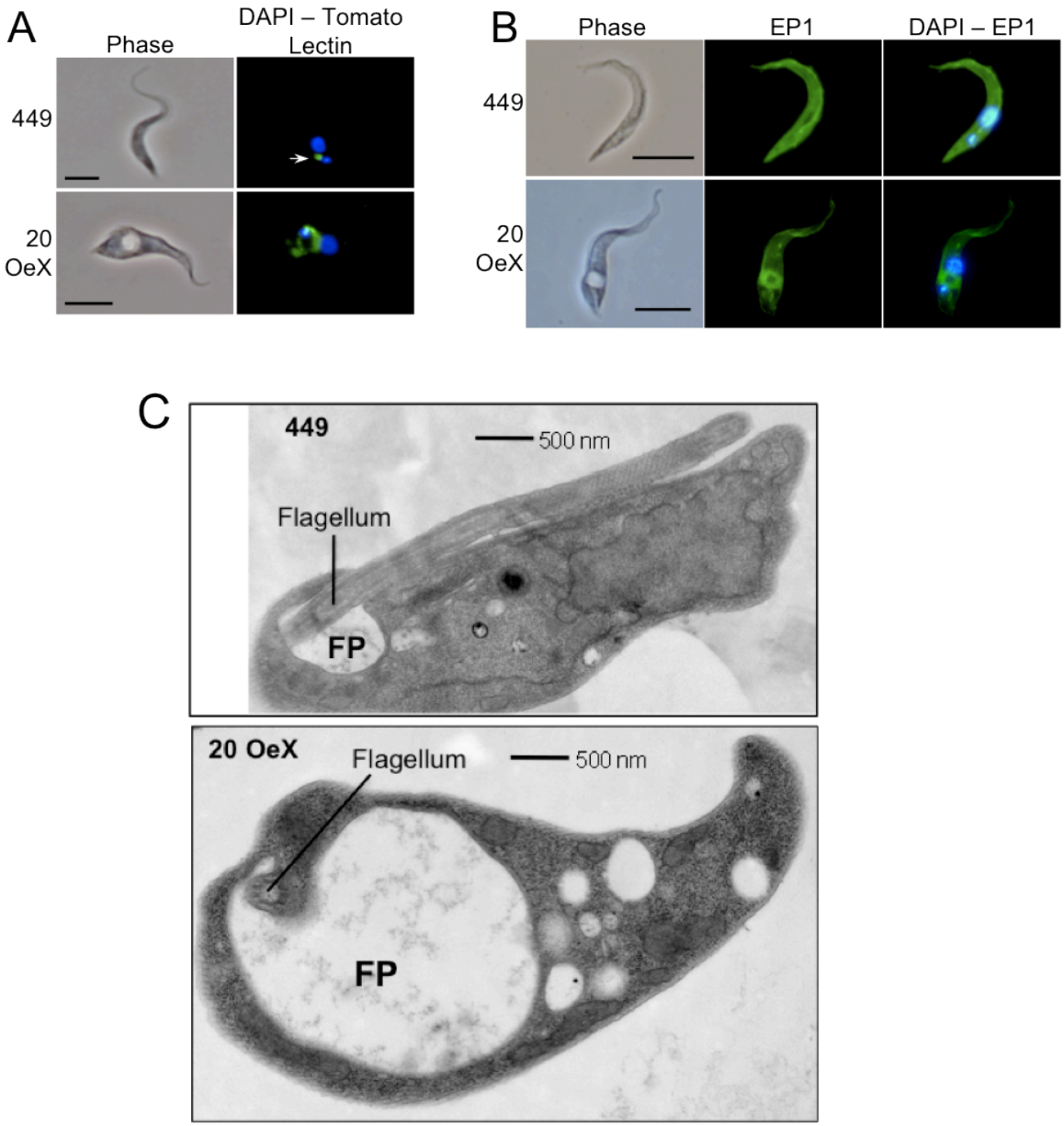


Figure 4.6. Immunofluorescence and electron microscopy to identify the flagellar pocket upon ZC3H20 over-expression in PF *T. brucei*

A. Immunofluorescence FITC-Tomato Lectin assay on PF cells cells induced to over-express TbZC3H20. 449 cells and 20 OeX were induced with tet for 24h.. White arrow shows tight localisation of FITC-Tomato lectin signal. DAPI – Tomato Lectin panel are merged images of DAPI and FITC-Tomato lectin images taken separately. Scale bar = 10µm

B. EP procyclin immunofluorescence assay on PF cells induced to over-express TbZC3H20. 449 cells and 20 OeX were induced with tet for 24h. Microscope slides were probed with goat anti-EP procyclin antibody and anti-goat Oregon Green secondary antibody. DAPI – EP panel are merged images of DAPI and EP images taken separately. Scale bar = 10µm

C. Transmission electron microscopy of PF cells induced to over-express TbZC3H20. 20 OeX cells were induced with tet for 24h. FP= flagellar pocket. Experiment performed in collaboration with Dr. Raffa Carzaniga.

The surface coat of *T. brucei* consists of glycosylphosphatidylinositol (GPI)-anchored proteins i.e. VSG in bloodstream form and procyclin in procyclic form. These are trafficked to the flagellar pocket for release at the surface, and then recycled back through the flagellar pocket to membrane-bound structures in the cytoplasm of the cell [26]. An immunofluorescence assay was carried out on procyclic cells to stain the EP procyclin coat using an anti-procyclin antibody (Fig. 4.6B). The parental (449) cells (Fig. 4.6B top panel) show an even distribution of procyclin staining across the surface of the cells. However, induced PF 20 OeX BigEye cells show a more intense staining around the enlarged vacuole structure (Fig. 6B bottom panel). This polarised localisation of procyclin indicates the flagellar pocket membrane from where procyclin should be trafficked out to and back in from the surface membrane.

To verify that the BigEye phenotype shown by over-expressing TbZC3H20 in procyclic cells is due to an enlarged flagellar pocket, transmission electron microscopy images of these cells were acquired (Fig. 4.6C). The structure of the flagellar pocket is characterised by the presence of electron-dense material in the lumen on the pocket, as well as the presence of the base of the flagellum extending out of the pocket. The induced PF 20 OeX BigEye cell has a massively enlarged flagellar pocket (Fig. 4.6C, bottom panel) and is clearly larger than that compared to the normal PF cell (Fig. 4.6C, top panel). The BigEye phenotype from over-expressing TbZC3H20 in PF is therefore due to flagellar pocket enlargement. Another point to note is the presence of a number of vesicles within the cytoplasm. This has been reported previously when the endocytic molecule clathrin is down-regulated in PF cells, resulting in the rounding up of cells and accumulation of transport intermediates within the cytoplasm [36]. It is possible that a similar situation is occurring in these BigEye cells where the trafficking of molecules is halted, leading to a build up of excess membrane.

In conclusion, over-expression of ZC3H20 or ZC3H21 in PF *T. brucei* causes a growth defect and major morphological defects. Over-expression of ZC3H21 causes a round cell phenotype that could be due to a range of upstream events, resulting in rounding up and dying cells. Therefore, investigation into this phenotype was not pursued. Over-expression of ZC3H20 causes a gross enlargement of the flagellar pocket, which is a highly polarised site for all endocytosis and exocytosis. This phenotype is referred to as BigEye, and has

been reported when the clathrin heavy chain (TbCLH), actin, RAB5 or RAB11 are down-regulated in bloodstream form *T.brucei* [36, 215, 221, 222]. All of these molecules are shown to be necessary for receptor-mediated endocytosis in the bloodstream form parasite. Therefore, this suggests that ZC3H20 over-expression in PF cells may be affecting the regulation of the endocytic pathway and causes a phenotype that is associated with down-regulation of endocytic molecules.

4.2.2 TbZC3H20 over-expression causes an endocytic defect in procyclic form *T. brucei*

All studies to date that show trypanosomes displaying the BigEye phenotype have also demonstrated that these cells have a defect in endocytosis [36, 215, 218, 221-223]. Most of these endocytosis assays are shown in bloodstream trypanosomes, but this is a challenging experiment to carry out in procyclic trypanosomes that have a lower basal rate of endocytosis [36]. In order to assess the ability TbZC3H20 OeX cells to carry out internalisation, the fixable fluorescent lipophilic membrane dye FM4-64X was used to determine their endocytic activity (Fig. 4.7A). Live induced and non-induced PF cells were incubated with the fluorophore at 27°C (normal growing temperature for PF cells) to allow uptake into internal membrane compartments. The cells can then be fixed and viewed by microscopy. Normal PF cells show intense staining around the kinetoplast and between the kinetoplast and nucleus, which indicates normal endocytic activity i.e. uptake into endocytic compartments (Fig. 4.7A, top panel). This staining was also observed in TbZC3H20 OeX cells that were not induced with tetracycline, or that were induced but not displaying the BigEye phenotype (Fig. 4.7A, both middle panels), and these cells are considered as showing no defect in endocytosis. However, the induced PF 20 OeX BigEye cells only show localisation of FM4-64X around the flagellar pocket (Fig. 4.7A, bottom panel). This indicates that these cells are unable to endocytose the dye into intracellular compartments and instead remains in the flagellar pocket membrane, thus showing an endocytic defect.

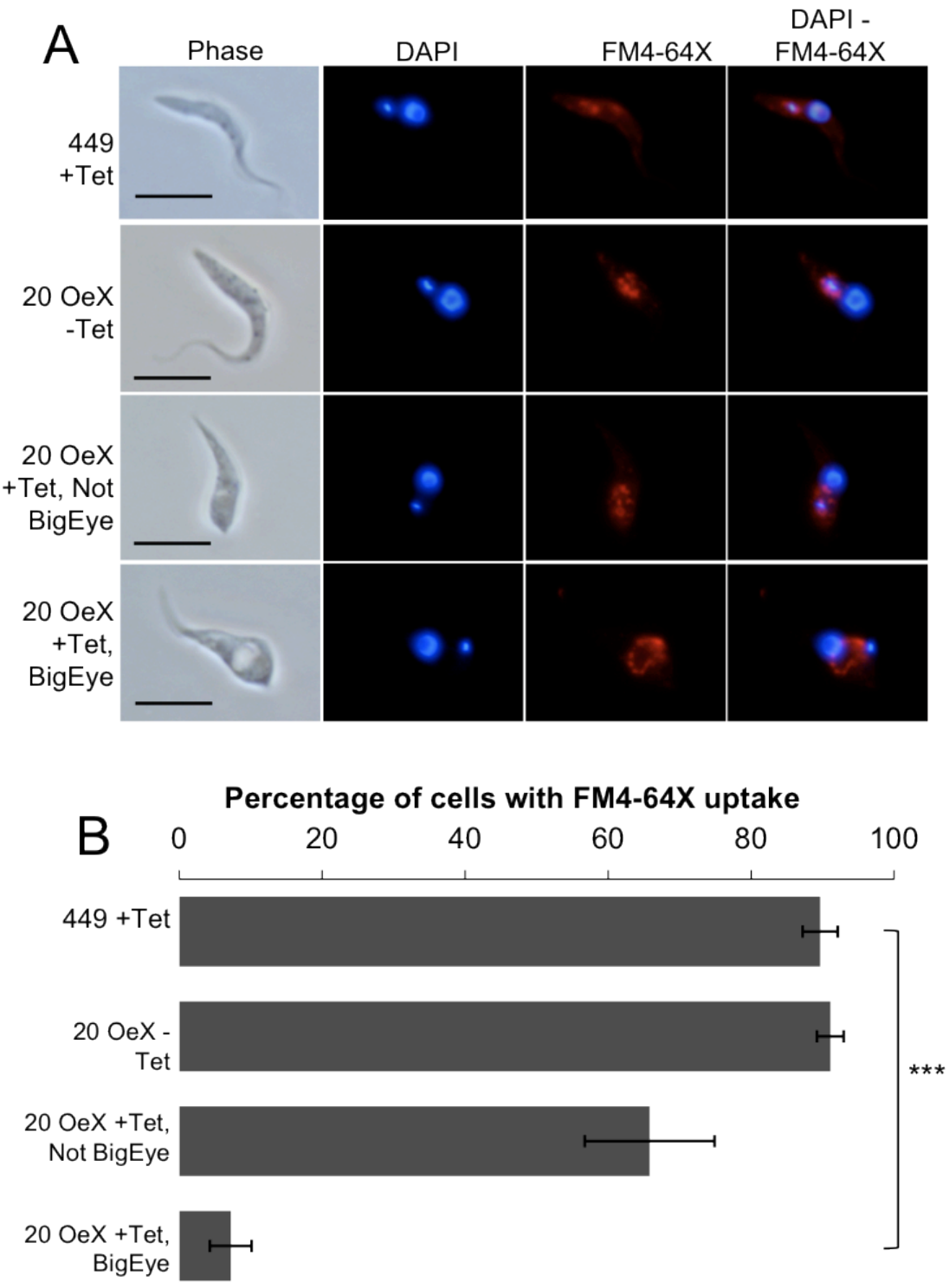


Figure 4.7. Endocytosis assay in PF *T. brucei* to determine endocytic activity when ZC3H20 is over-expressed

A. Immunofluorescence assay for uptake of the lipophilic membrane dye FM4-64X to measure endoyctic activity of PF cells induced to over-express TbZC3H20. 449 cells and 20 OeX were induced with tet for 24h. Cells were incubate with FM4-64X for 15min at 27°C, then fixed in 4% paraformaldehyde. DAPI – FM4-64X panel are merged images of DAPI and FM4-64X images taken separately. Scale bar = 10μm

B. Quantification of uptake into intracellular compartments of the lipophilic membrane dye FM4-64X. Over 200 cells were counted for each population and experiment. Means of three independent experiments are plotted with error bars showing standard error. *** = significant where $p < 0.001$ using a Student's t-test.

Each population was quantified for the percentage of cells that carried out uptake of FM4-64X effectively (Fig. 4.7B). Uptake was defined as correct endocytosis of the dye into intracellular compartments e.g. endosomes (as Fig. 4.7A, top and middle panels). A defect in endocytosis i.e. no uptake, is defined as no uptake of the dye at all (just background staining) or staining of the flagellar pocket membrane (as Fig. 4.7A, bottom panel). This analysis showed that the parental and non-induced populations have around 90% of the cells with normal uptake. This decreases to 66% in induced PF 20 OeX cells not displaying BigEye, but dramatically drops to 7% of induced PF 20 OeX BigEye cells showing uptake of FM4-64X. A Student's t-test was carried out on these data to determine if the percentage of uptake was statistically significant compared to the parental PF449 cells. This concluded that the percentage of non-induced and induced PF 20 OeX not BigEye cells showing normal uptake is not statistically significant. However, the decrease in the percentage of cells showing uptake amongst the induced PF 20 OeX BigEye populations is statistically significant at $p<0.001$.

In conclusion, over-expression of TbZC3H20 in PF trypanosomes results in cells displaying the BigEye phenotype with an enlarged flagellar pocket, and these cells are defective in endocytosis.

4.3 Investigation into the cause of flagellar pocket enlargement by ZC3H20 over-expression in PF *T. brucei*

The enlarged flagellar pocket and endocytosis defect seen from ZC3H20 over-expression could be a result of perturbing the regulation and/or expression of a number of factors required for normal endocytic function. Firstly, biogenesis and maintenance of the flagellar pocket itself is essential for endocytosis, as it is the site for all molecules to enter and exit the cell. A flagellar pocket cytoskeletal protein, BILBO1 has been characterised as a component of the flagellar pocket collar, which provides a bridge between the flagellar pocket, pellicular and flagellum membranes [29]. RNAi of BILBO1 of procyclic cells does not produce the BigEye phenotype, but prevents flagellar pocket biogenesis and causes an endocytic defect [29]. This shows that the integrity of the cytoskeleton is important for maintenance of the flagellar pocket and consequently endocytic function. Thus, it may be that ZC3H20 over-expression in PF cells affects the cytoskeleton and biogenesis of the flagellar pocket causing it to become enlarged and resulting in an

endocytosis defect. The cytoskeleton of *T. brucei* is provided by microtubules arranged as a sub-pellicular corset, cross-linked to each other and to the plasma membrane [224]. Sub-pellicular microtubules are located along the entire plasma membrane, except for the flagellar pocket membrane, thus polarising membrane trafficking to this site [225]. Microtubules consist of α- and β-tubulin. There are no RNAi down-regulation studies of β-tubulin in *T. brucei*, but RNAi of α-tubulin in procyclic cells does not cause an enlarged flagellar pocket [226]. Thus it seems unlikely that ZC3H20 over-expression affects cytoskeleton integrity, which would affect flagellar pocket biogenesis and consequently endocytosis.

In contrast to affecting flagellar pocket maintenance that would cause an endocytic defect, an alternative is that inhibiting the endocytic pathway would result in an enlarged flagellar pocket. Current models consider endocytosis to be receptor-mediated and clathrin-dependent in trypanosomes [227]. Down-regulation of the clathrin heavy chain (TbCLH) via RNAi in BF *T. brucei* causes the BigEye phenotype and an endocytic defect [36]. Additionally, studies have shown that RNAi down-regulation of the RAB GTPases RAB5 and RAB11, responsible for early endosome entry and recycling, in bloodstream parasites causes an enlarged flagellar pocket [218, 221]. In bloodstream parasites, RNAi of RAB5 causes a decrease in clathrin protein expression, and blocks receptor- mediated and fluid phase endocytosis, and RNAi of RAB11 blocks recycling. In PF parasites, these studies have shown that RNAi of TbCLH, RAB5 or RAB11 do not show a BigEye phenotype, but all cause a block in endocytosis [36, 218, 221]. It is likely that the loss of the ability for uptake of molecules consequently results in the gross enlargement of the flagellar pocket as a result of an imbalance of membrane transport [36, 215]. ZC3H20 over-expression clearly results in an endocytic defect, and the imbalance of membrane transport could be such that it causes an enlarged flagellar pocket to be seen, even in a procyclic trypanosome.

Finally, a single dynamin-like protein in *T. brucei*, TbDLP that is required for mitochondrial biogenesis has been shown to be involved in endocytosis [223, 228]. Dynamin-like proteins (DLPs) are large GTPases and generally function in the division of mitochondria and chloroplasts. The *T. brucei* mitochondrion divides only during cytokinesis, so mitochondrial fission must be coordinated with the cell cycle [229]. Two studies have shown that RNAi down-regulation of TbDLP causes the mitochondrial membrane to collapse [223, 228], and when RNAi of TbDLP is

combined with expression of the proapopototic Bax protein, this also blocks mitochondrial fission [223]. In addition to causing a cell cycle defect, Chanez et al., [223] also showed that RNAi of TbDLP in PF cells, resulted in the BigEye phenotype and a block in endocytosis. Classical dynamins are involved in the scission of clathrin-coated pits in the secretory pathway, as well as a wide range of vesicles. However, Chanez et al. [223] showed that endocytosis in *T. brucei* can be mediated by a DLP and suggest an interchangeable function between DLPs and classical dynamins. Interestingly, although all other studies have only shown the BigEye phenotype from down-regulation of endocytic molecules in bloodstream parasites, this study shows the enlarged flagellar pocket morphology from RNAi down-regulation of TbDLP or TbCLH in procyclic parasites.

By using endocytic and immunofluorescence markers, the effect of over-expression of ZC3H20 on the mitochondrial maintenance and endocytosis can be investigated. Thus, the ZC3H20 over-expression phenotype was characterised further to determine the cause of the enlarged flagellar pocket and an endocytosis defect.

4.3.1 TbZC3H20 has no involvement with mitochondrial maintenance in PF *T. brucei*

Down-regulation of TbDLP in PF *T. brucei* has been reported to cause an enlarged flagellar pocket and a block in endocytosis [223]. However, this study, in agreement with another study, also showed that these RNAi TbDLP cells display a collapsed mitochondrion [223, 228]. To investigate if TbZC3H20 has any involvement with mitochondrial integrity, a MitoTracker™ assay was used (like in both studies mentioned) to stain the mitochondrial membrane of induced cells. Fig. 4.8A (top panel) shows the continuous matrix-like pattern of mitochondrial staining of a normal procyclic form cell, and this pattern of staining does not appear to be disrupted in BigEye cells (Fig. 4.8A, bottom panel). Therefore over-expression TbZC3H20 in procyclic cells does not result in a collapsed mitochondrion that is seen when TbDLP is downregulated. The study by Chanez et al., [223] also showed an increase in cells of the karyotype 2K2N (2 kinetoplast, 2 nucleus), where the kinetoplast and nucleus have replicated but the cell has not completed cytokinesis. This suggested that inhibition of mitochondrial fission triggered a cell cycle block at the G2/M phase. To verify that over-expression of TbZC3H20 does

not lead to a block in cytokinesis, karyotype analysis was done on these cells (Fig. 4.8B). As discussed in Chapter 3 (Section 4.2.1) the percentage of 2K2N cells in a normal population is 5-10% (Fig. 3.8B, 449 cells). To this end, cells induced to over-express TbZC3H20 over 72h do not show an increase of 2K2N cells which would be indicative of a cell cycle block.

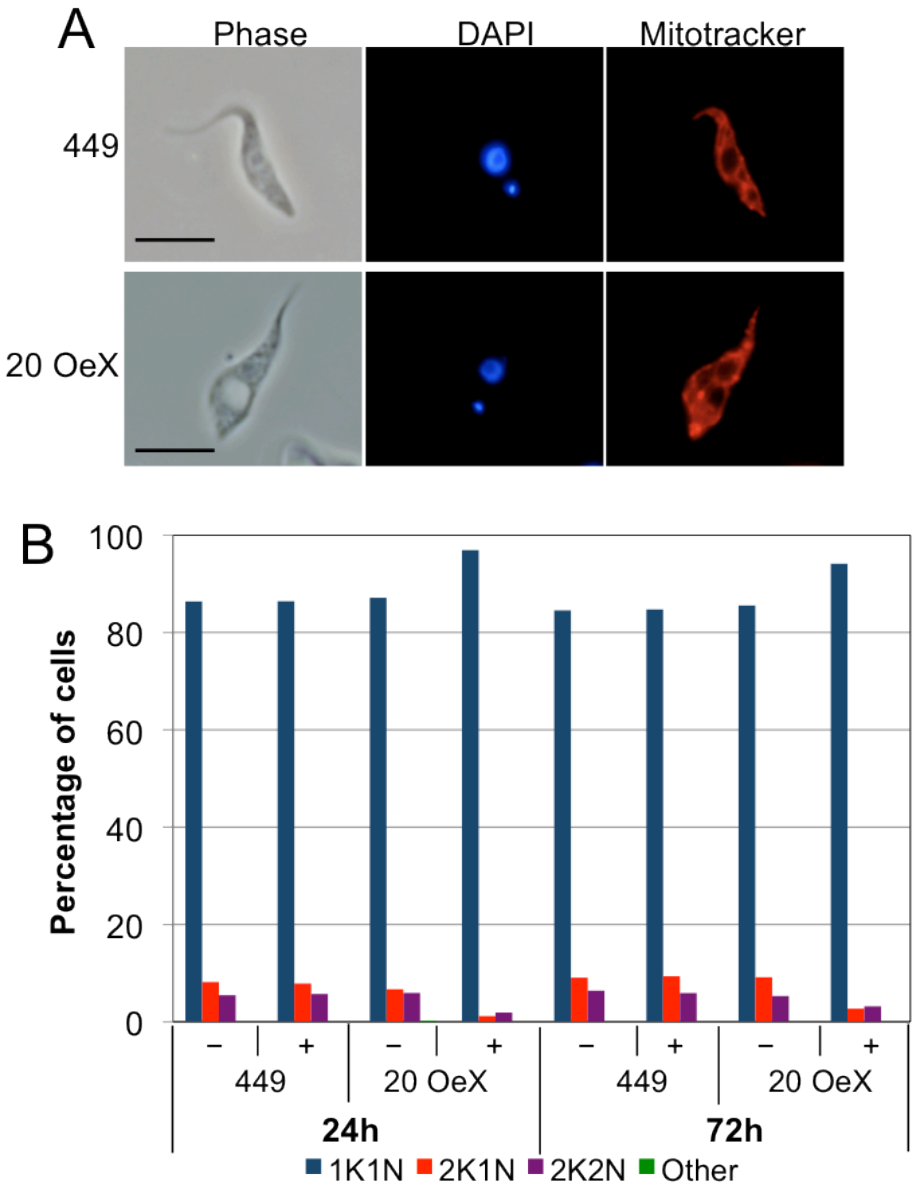


Figure 4.8. Immunofluorescence microscopy of the mitochondrial structure upon ZC3H20 over-expression in PF *T. brucei*

A. Immunofluorescence MitoTracker™ assay to detect mitochondrion of PF cells induced to over-express TbZC3H20. Mitotracker CMXRos™ detects mitochondrial membrane-potential activity and stains the single continuous mitochondrial membrane. 449 cells and 20 OeX were induced with tet for 24h. Cells were incubated with Mitotracker™ for 15min at 27°C then fixed with 3% paraformaldehyde. Scale bar = 10µm
B. Karyotype analysis of PF cells induced to over-express TbZC3H20. Over 200 cells counted for each population. Cells were grown in absence (-) or presence (+) of tet for 72h. K = kinetoplast, N = nucleus
449 = PF449 parental cells, 20 OeX = PF 449 TbZC3H20 overexpression cells.

Down-regulation of TbDLP causes a block in endocytosis, cytokinesis and mitochondrial fission [223], but over-expression of TbZC3H20 results in neither a block in cytokinesis or collapse of the mitochondrion. The dynamin-like protein itself is suggested to mediate *T. brucei* endocytosis through the scission of clathrin-coated pits [223]. This study additionally carried out RNAi down-regulation of TbCLH in PF cells, which caused an enlarged flagellar pocket in 25% of cells, and they were endocytosis deficient. However, PF 20 OeX cells did not show a 2K2N cell cycle block, suggesting that this feature seen by TbDLP ablation is not caused by the endocytosis-associated defects. In conclusion, our data suggest that TbZC3H20 does not have any direct involvement in the function associated with TbDLP.

4.3.2 Investigation of TbZC3H20 involvement with clathrin-mediated endocytosis in PF *T. brucei*

Endocytosis and exocytosis are complex pathways that are not well understood in *T. brucei*, particularly in PF cells, which have a slower endocytosis rate than BF cells [26]. However, current studies suggest that endocytosis is clathrin-dependent in trypanosomes [36, 38, 227] and that clathrin is required in the trafficking of proteins to the flagellar pocket of procyclic *T. brucei* [38]. Clathrin expression is essential in trypanosomes, and as discussed above, down-regulation of clathrin in PF cells results in an endocytic defect, with varying reports of the BigEye phenotype. Down-regulation of clathrin in PF cells also causes an increased level of protein expression of CRAM (a receptor in the flagellar pocket membrane of procyclic *T. brucei*) [36, 38]. Hung et al. [38] also showed TbCLH RNAi prevented the trafficking of CRAM from the ER to the flagellar pocket membrane, but trafficking of the procyclic form surface coat protein, EP procyclin was not compromised. In agreement, trafficking of EP procyclin to the surface is not prevented in PF cells over-expressing TbZC3H20, as shown by an immunofluorescence assay using an anti-EP procyclin antibody (Fig. 4.6B, bottom panel).

In the TbCLH [36] and CRAM [38] studies it was shown that after TbCLH RNAi induction in BF and PF form cells, the integrity of the endoplasmic reticulum (ER) is retained and the localisation of the lysosome is not disrupted. To

investigate if over-expression of TbZC3H20 in PF cells affects these two organelles, immunofluorescence assays were carried out to determine if they were disrupted. An anti-ER antibody to the *T. brucei* homologue of the mammalian BiP was used to stain the ER (Fig. 4.9A). The discrete staining pattern of the ER was retained in induced PF 20 OeX BigEye (Fig. 4.9A bottom panel) compared to parental PF449 cells (Fig. 4.9A top panel).

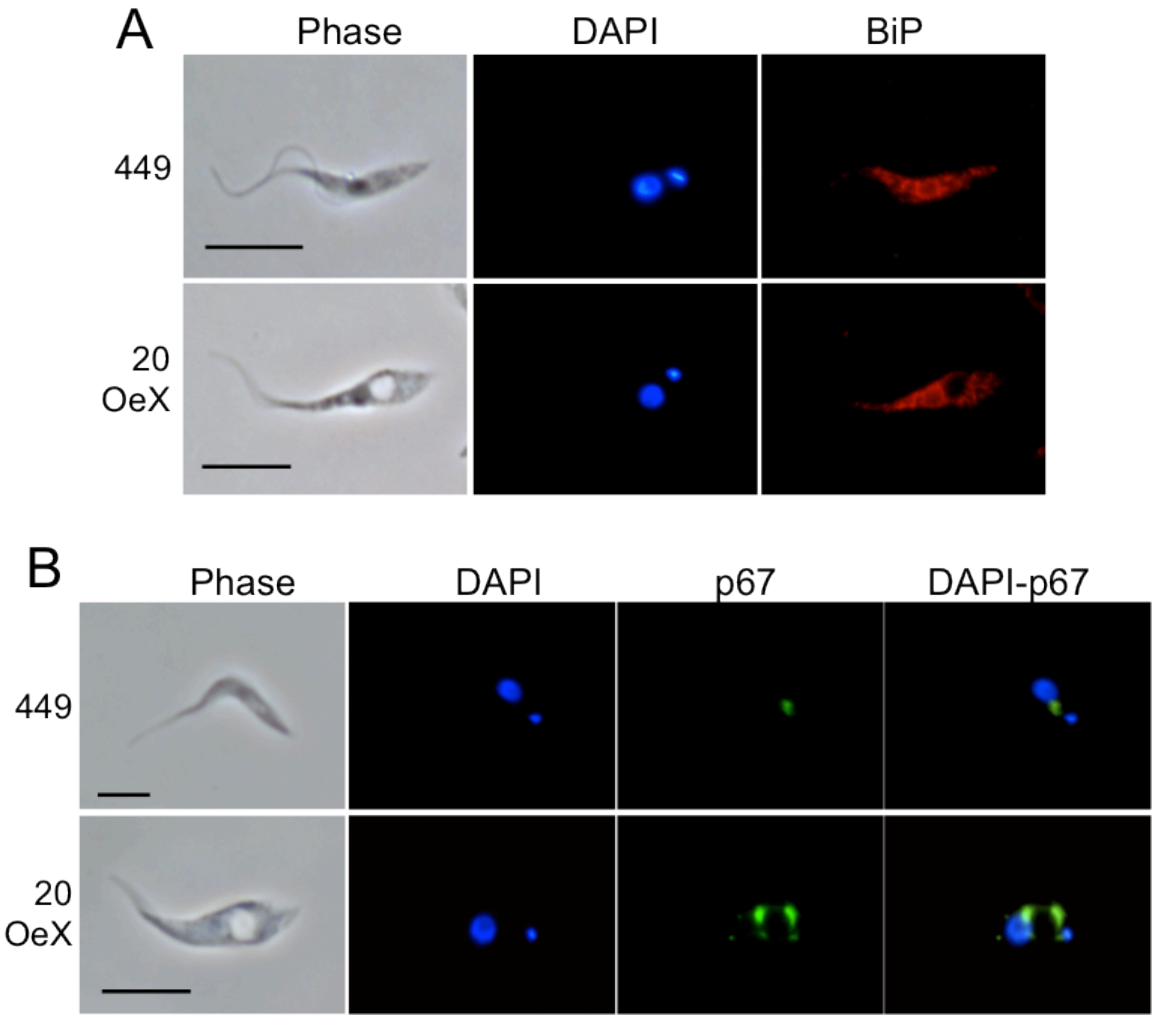


Figure 4.9. Immunofluorescence microscopy to probe the ER and lysosome structure upon ZC3H20 over-expression in PF *T. brucei*

A. Immunofluorescence assay for probing the ER in PF cells induced to over-express TbZC3H20. Cells were fixed with paraformaldehyde, then probed with rabbit anti-BiP antibody and anti-rabbit Texas Red secondary. Scale bar = 10μm
B. Immunofluorescence assay for probing the lysosome in PF cells induced to over-express TbZC3H20. Cells were fixed with paraformaldehyde, then probed with mouse anti-p67 antibody and goat anti-mouse Oregon Green secondary. Scale bar = 10μm
449 cells and 20 OeX were induced with tet for 24h

Secondly, an antibody to p67, a LAMP-like membrane protein of the lysosome was used to stain the lysosome (Fig. 4.9B). The p67 staining in the parental PF cells localises to a discrete spot in between the nucleus and kinetoplast (Fig. 4.9B, top panel). The p67 staining is more dispersed in PF ZC3H20 OeX BigEye cells than shown in normal PF cells, but there is general localisation in the expected area (Fig. 4.9B, bottom panel). This could be due to the physical obstruction imposed on organelles due to the enlarged flagellar pocket, as the nucleus itself is very close to the flagellar pocket unlike in normal cells.

In conclusion, over-expression of TbZC3H20 in PF cells does not affect the integrity of the ER and the lysosome is not disrupted, thus agreeing with the observations shown by the TbCLH and CRAM studies. This suggests that TbZC3H20 may be involved in the regulation of clathrin, and consequently clathrin-mediated endocytosis.

The over-expression of ZC3H20 may affect the expression of clathrin or any other endocytosis-associated molecules, which could cause the BigEye phenotype. This was investigated using microarray analysis to compare total mRNA from induced versus uninduced PF 20 OeX cells. To minimise secondary effects on the levels of non-specific mRNAs as a result of the cell dying, ZC3H20 over-expression was induced for the shortest time possible at which protein could be detected but without the manifestation of the BigEye phenotype. Thus, PF 20 OeX cells were grown in the absence or presence of tet for 12h and total mRNA isolated from these cultures for the microarray. The microarray analysis was performed on three biological replicates. The same microarray setup was used as the RNAi of ZC3H20 in PF cells (Chapter 3.3) and the fold change in mRNA levels for each probe for each array was calculated. Genes that showed more than 2-fold up/down-regulation in mRNA levels for at least one probe in all three arrays were scrutinised for further investigation (Table 4.1, Table 4.2). Regarding mRNAs that were upregulated when ZC3H20 is overexpressed, there were only 4 transcripts that had increased levels above a 2-fold threshold (Table 4.1). However, neither of these genes have an associated putative function/role within the cell that would be unlikely to cause the BigEye phenotype when upregulated.

Table 4.1 Summary of the PF ZC3H20 over-expression microarray analysis to show genes with up-regulated levels of RNA

Showing genes with up-regulated levels of RNA >2-fold, as a result of over-expression of TbZC3H20 in PF T. brucei. Signal fold change (+ = up regulated,) for each of the three arrays conducted are shown for each of the probes on the array for that specific gene. Probes that are not >2 fold across all three arrays are shown in italics.

Number	Probe	Array			Product
		1	2	3	
Tb11.01.0760	1	+2.8	+3.4	+5.6	cation transporter, putative
	2	+3.1	+3.7	+5.5	
	3	+1.0	*+1.3*	*+1.5*	
Tb927.7.5930	1	+2.2	+2.5	+6.6	hypothetical protein, conserved, TbPAD1
	2	+2.0	+2.8	+7.2	
	3	*+1.0*	*+1.3*	*+4.4*	
	4	*+0.8*	*+1.2*	*+2.0*	
	5	*+1.7*	*+1.5*	*+6.7*	
Tb09.160.4460	1	+2.8	+3.5	+33.9	TFIIF-stimulated CTD phosphatase, putative
	2	+3.8	+4.7	+38.9	
	3	+2.9	+3.5	+27.9	
	4	+3.4	+3.7	+26.4	
Tb927.7.4390	1	+2.1	+3.0	+2.1	threonine synthase, putative
	2	*+1.3*	*+1.5*	*+1.7*	
	3	*+1.2*	*+1.7*	*+2.4*	
Tb927.7.2660	1	+15.7	+17.4	+39.3	ZC3H20, hypothetical protein, conserved (from ectopic expression)
	2	+5.7	+6.0	+59.5	
	3	+5.8	+6.5	+31.6	

In contrast, there are 15 genes that were down regulated more than 2-fold when ZC3H20 is over-expressed (Table 4.2). The table does not show all transcripts that were sorted using this threshold, as transcripts that produced a low signal in all three microarrays for each probe were excluded and discounted from further analysis. Of the 15 genes that remained (as shown in Table 4.2) there appears to be five genes that have a putative function that could be associated with endocytosis or flagellar pocket integrity within the cell (highlighted bold Table 4.2). These genes are the 17kDa flagellar calcium-binding protein, calflagin 17, the 44kDa flagellar calcium-binding protein, calflagin 44, (which will be grouped together and referred to as Calflagins), the microtubule-associated protein 15 (CAP15), phosphatidic acid phosphatase (PHAP), and protein disulphide isomerase bloodstream-specific precursor 2 (PDI-BS2). Considering that over-expression of TbZC3H20 causes a phenotype that results in an endocytosis defect, investigation into these mRNA transcripts that are downregulated and may affect endocytosis, were pursued further.

Table 4.2. Summary of the PF ZC3H20 over-expression microarray analysis to show genes with down-regulated levels of RNA

Showing genes with down-regulated levels of RNA >2-fold, as a result of over-expression of TbZC3H20 in PF *T. brucei*. Signal fold change (- = down-regulated,) for each of the three arrays conducted are shown for each of the probes on the array for that specific gene. Probes that are not >2 fold across all three arrays are shown in italics.

Number	Probe	Array			Product
		1	2	3	
Tb927.8.5470	1	-2.5	-4.7	-9.1	**flagellar calcium-binding protein,17**
	2	-2.7	-4.8	-8.2	**kDa calflagin,17 kDa calcimedin**
	3	*-1.8*	*-8.1*	*F*	
Tb927.8.5460	1	-2.2	-8.0	-11.5	**flagellar calcium-binding protein,44**
	2	-2.3	-8.1	-11.9	**kDa calflagin,44 kDa calcimedin**
	3	*-1.9*	*-6.5*	*-9.1*	
Tb10.70.1370	1	-2.7	-8.5	-12.3	fructose-bisphosphate aldolase,
	2	-2.3	-6.6	-8.7	glycosomal
	3	-3.3	-7.6	-10.5	
Tb927.3.4500	1	-2.0	-3.2	-4.2	fumarate hydratase, putative
	2	-2.2	-3.8	-5.1	
	3	*-1.8*	*-3.8*	*-5.2*	
Tb927.1.3830	1	-2.9	-3.9	-5.5	glucose-6-phosphate isomerase,
	2	-2.2	-4.6	-6.1	glycosomal
	3	-2.7	-4.3	-6.2	
Tb11.01.3805	1	-2.5	-6.4	-8.3	**microtubule-associated**
	2	-2.2	-5.8	-8.3	**protein,corset-associated protein 15**
	3	-2.4	-6.3	8.3	**(CAP15)**
Tb927.8.480	1	-3.3	-7.7	-9.7	**phosphatidic acid phosphatase**
	2	-3.2	-6.7	-8.3	**protein, putative (PHAP)**
	3	-3.0	-6.2	-7.7	
Tb10.6k15.0040/	1	-2.7	-2.8	-3.8	procyclin-associated gene 1 (PAG1)
	2	-3.1	-3.4	-4.6	protein
	3	-3.3	-3.3	-4.5	
	4	-2.2	-2.1	-3.0	
Tb10.6k15.3540	1	-2.7	-2.5	-3.9	
	2	-2.7	-2.2	-3.3	
	3	-2.5	-2.5	-3.4	
Tb10.70.1310	1	-2.2	-2.8	-3.3	
	2	*-1.0*	*-2.3*	*-2.7*	
	3	*-1.8*	*-2.6*	*-2.9*	
Tb10.6k15.0060/	1	-3.7	-4.5	-6.3	Procyclin-associated gene 2 (PAG2)
	2	-3.1	-3.5	-5.0	protein
	3	-3.0	-3.6	-4.9	
Tb10.70.1300	1	-2.9	-3.2	-6.3	
	2	*-1.9*	*-3.9*	*-3.9*	
	3	*-1.0*	*-2.7*	*-5.1*	
Tb10.6k15.0070/	1	-4.1	-4.2	-6.5	procyclin-associated gene 4 (PAG4)
	2	-2.7	*-4.6*	-6.2	protein
	3	*-1.7*	*-4.1*	*-5.9*	
Tb11.01.6220	1	-3.9	-4.2	-7.9	
	2	-5.3	-4.9	-5.6	
	3	*-1.2*	*-1.5*	*-9.0*	

Tb10.6k15.0050	1 2 3	-3.7 -3.1 -3.3	-4.5 -3.4 -3.5	-7.0 -5.8 -6.2	procyclin-associated gene 5 (PAG5) protein
Tb10.6k15.2290 (Tb927.10.8230)	1 *2* *3*	-2.2 *-1.9* *-1.9*	-3.0 *-2.6* *-3.6*	-3.8 *-3.4* *-3.6*	**protein disulfide isomerase, bloodstream-specific protein 2 precursor (PDI-BS2)**
Tb10.406.0290	1 *2* *3*	-2.2 *-0.9* *-1.4*	-5.3 *-2.3* *-2.8*	-7.2 *-2.9* *-5.8*	protein tyrosine phosphatase, putative
Tb10.61.2680	1 *2* *3*	-2.0 *-1.7* *-1.9*	-5.3 *-6.9* *-5.3*	-8.2 *-7.5* *-8.2*	pyruvate kinase 1
Tb927.5.470	1 *2* *3*	-2.1 *-1.7* *-1.4*	-3.3 *-4.5* *-3.5*	-4.5 *-6.7* *-4.9*	transporter, putative

Other transcripts that could disrupt endocytosis and/or cause the BigEye phenotype if down-regulated were looked at in the microarray. Although clathrin was not down-regulated at the 2-fold threshold in the microarray, the TbCLH RNA level was decreased at least 1.7-fold across all three arrays for at least one probe when ZC3H20 was over-expressed in PF cells (Table 4.3).

Table 4.3. Summary of the PF ZC3H20 over-expression microarray analysis to show change in RNA level of genes that encode molecules of the endocytic pathway

Signal fold change (+ = up-regulated, - = down-regulated) for each of the three arrays conducted are shown for each of the probes on the array for that specific gene.

Number	Probe	Array			Product
		1	2	3	
Tb10.70.0830	1 2 3	-1.7 -1.1 -1.0	-4.4 -4.7 -3.4	-4.5 -5.3 -6.3	Clathrin heavy chain (TbCLH)
Tb927.3.4720	1 2 3	+1.2 +1.2 +1.7	-2.4 -5.1 -2.0	-1.9 -2.4 -1.5	Dynamin-like protein (TbDLP)
Tb927.10.12960	1 2 3	+1.5 +1.6 +1.4	-2.2 -2.4 -1.8	-1.7 -1.6 -1.4	small GTPase, ras-related protein rab-5 (RAB5A)
Tb11.02.2160	1 2 3	+1.5 +1.4 +1.4	-1.8 -2.4 -2.4	-1.6 -1.9 -1.4	small GTP-binding protein Rab5b, putative (RAB5B)
Tb09.211.2330	1 2 3	-2.1 -2.0 -1.9	-2.7 -2.4 -2.6	+1.7 +1.6 +1.5	GTP-binding protein, putative small GTPase, putative (RAB7)
Tb927.8.4330	1 2 3	+1.2 +1.4 +1.3	-2.6 -2.8 -2.6	-1.8 -1.9 -2.0	small GTP-binding protein Rab11 (RAB11)
Tb09.211.0620	1 2 3	+3.4 +2.2 +3.2	-1.2 -1.4 -1.1	-1.2 -1.1 -1.1	cysteine-rich, acidic integral membrane protein precursor (CRAM)

Studies of CRAM have shown that upon down-regulation of TbCLH in PF cells, this causes an increase in the level of CRAM protein [38]. Thus, the RNA level of CRAM was analysed from the microarray data which showed that in one array there was at least a 2.2-fold increase, and not much change in RNA level in the other two arrays (Table 4.3). As described in section 3.2, down-regulation of RAB5 and RAB11 cause an endocytic defect in PF cells, and down-regulation of TbDLP in PF causes an endocytic defect and the BigEye phenotype. Therefore TbDLP, RAB5a, RAB5b, RAB11 and RAB7 (localises to late endosomes) were investigated, and the microarray data shows that the RNA levels were inconsistent across all three arrays when ZC3H20 was over-expressed (Table 4.3). Consequently, q-PCR was used to determine that the levels of clathrin are decreased upon ZC3H20 over-expression, and to investigate the inconclusive results for the change in RNA abundance of CRAM, TbDLP and the RABs (Fig. 4.10, data by Dr. James Trotter).

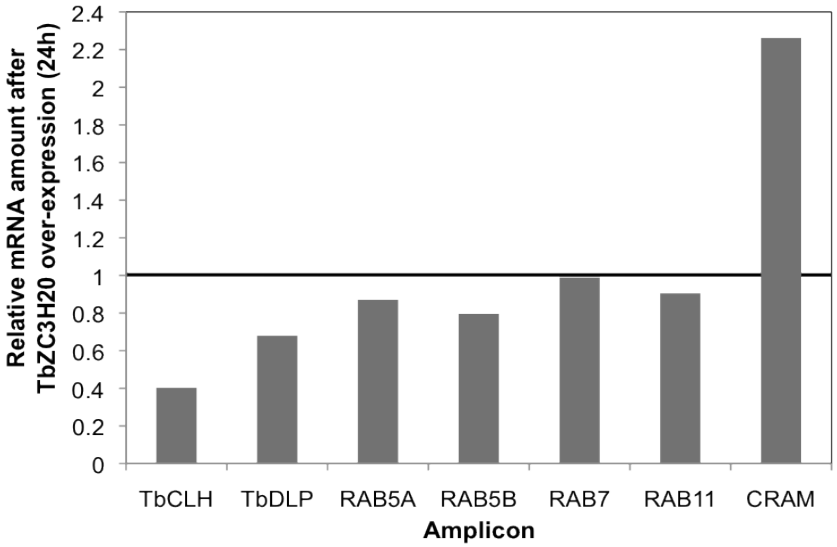


Figure 4.10. Quantitative real-time PCR of mRNA from PF *T. brucei* after ZC3H20 over-expression.

ZC3H20 over-expression was induced for 24h. Graph shows relative mRNA amount compared to 18S mRNA expression level. The black line at 1 shows the level of no change in mRNA. Data by Dr. James Trotter.

This shows that the RNA level of clathrin is decreased 2.5-fold upon ZC3H20 over-expression, and that the level of CRAM mRNA is increased more than 2-fold (Fig. 4.10). This confirms with the microarray, an overall down-regulation of clathrin upon ZC3H20 over-expression, and that the level of CRAM is

increased, in agreement with previous studies, upon clathrin down-regulation [38]. The q-PCR also shows that the RNA levels of the RAB5A, RAB5B, RAB7 or RAB11, does not change considerably (Fig. 4.10), suggesting that these are not affected upon ZC3H20 over-expression. The RNA level of TbDLP was decreased 1.5-fold (Fig. 4.10), but this is not a dramatic change, and in combination with the data shown in section 4.3.1 above, this maybe a secondary effect from affecting endocytosis, as ZC3H20 over-expression does not affect mitochondrial integrity. Thus, as clathrin is shown to be down-regulated when ZC3H20 is over-expressed in PF cells, and due to its close association with the endocytic pathway, it was decided to include this gene in further investigations too.

To verify the decrease in mRNA levels of clathrin, calflagin, CAP15, PHAP and PDI-BS2 when ZC3H20 is over-expressed in PF, total RNA was isolated from PF cells that had been induced or uninduced for ZC3H20 over-expression for 12h. Samples of RNA were examined using Northern analysis with a specific probe to each of the candidate genes and actin and tubulin were used as controls (Fig. 4.11).

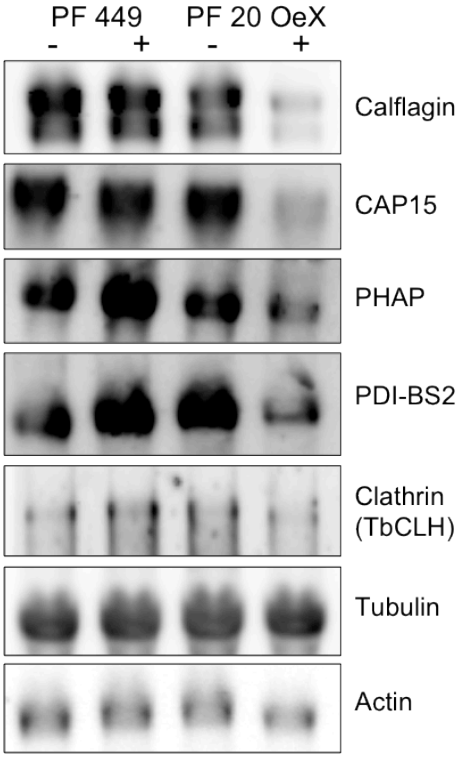


Figure 4.11. Northern analysis of genes down-regulated in microarray when ZC3H20 is over-expressed in PF *T. brucei*

Northern blot analysis to verify decrease in mRNA levels of genes with a putative endocytosis-associated function when ZC3H20 is overexpressed in PF *T. brucei*. Total RNA was isolated from PF449 and PF 20 OeX cells after grown in the absence (-) or presence (+) of tet for 12h.

The northern analysis shows that the mRNA levels of tubulin was not affected, further verifying that ZC3H20 is not directly affecting the cytoskeleton which may compromise flagellar pocket integrity. The mRNA level of actin also does not change when ZC3H20 is over-expressed (Fig. 4.11). This is an important observation to make, as actin is intimately associated with the endocytic system in BF trypanosomes, and RNAi down-regulation of actin in PF cells causes a cell growth defect, the BigEye phenotype and a block in endocytosis [222]. However, actin is not essential in PF cells, is distributed throughout the cell, and RNAi down-regulation in these cells did not affect the flagellar pocket but distorted the Golgi, suggesting an alternative functional requirement between BF and PF parasites [222]. As ZC3H20 over-expression in PF trypanosomes does not affect the mRNA level of actin, this agrees with the report that actin is not involved with endocytosis in PF cells, and thus, can be used as a control. The Northern analysis additionally confirmed that the mRNA level of each candidate gene was decreased when ZC3H20 over-expression was induced in PF *T. brucei* (Fig. 4.11 – CAP15, calflagin, PHAP, PDI-BS2, clathrin). These selected genes that have a putative endocytosis-associated function could thus be investigated further as mRNA targets regulated by ZC3H20.

4.4 Investigation into the regulation of mRNA targets that cause the ZC3H20 over-expression phenotype

4.4.1 The endocytosis-associated mRNAs are destabilised by protein factors and are capable of being bound by ZC3H20 in PF *T. brucei*

As described previously for the PF RNAi 20 analysis (Chapter 3.3.2), a cycloheximide assay was used to assess if the mRNA abundance of the PF ZC3H20 over-expression microarray candidates is altered by a protein factor and PF parasites were incubated for up to 4h in the presence or absence of cyclohexamide. The levels of mRNA were examined using Northern analysis, and tubulin and actin were used as controls (Fig. 4.12). Cycloheximide treatment of PF cells causes a decrease in the mRNA level of Calflagin (Fig. 4.12A), which suggests that this transcript is normally stabilised by a protein factor within the PF cell. This does not correlate with the PF 20 OeX data, which shows that over-

expression of ZC3H20 causes destabilisation of this transcript. Therefore, as it seems likely that ZC3H20 does not directly influence the regulation of this transcript within the cell, the calflagin genes were not investigated further. In contrast, the cycloheximide treatment of PF cells results in an obvious increase in mRNA levels of CAP15, PHAP and PDI-BS2 and a slight increase in the mRNA level of clathrin over 4h (Fig. 4.12A). This suggests that these transcripts are normally destabilised by a protein factor within PF cells, and correlates with the microarray data that they are destabilised when ZC3H20 is over-expressed.

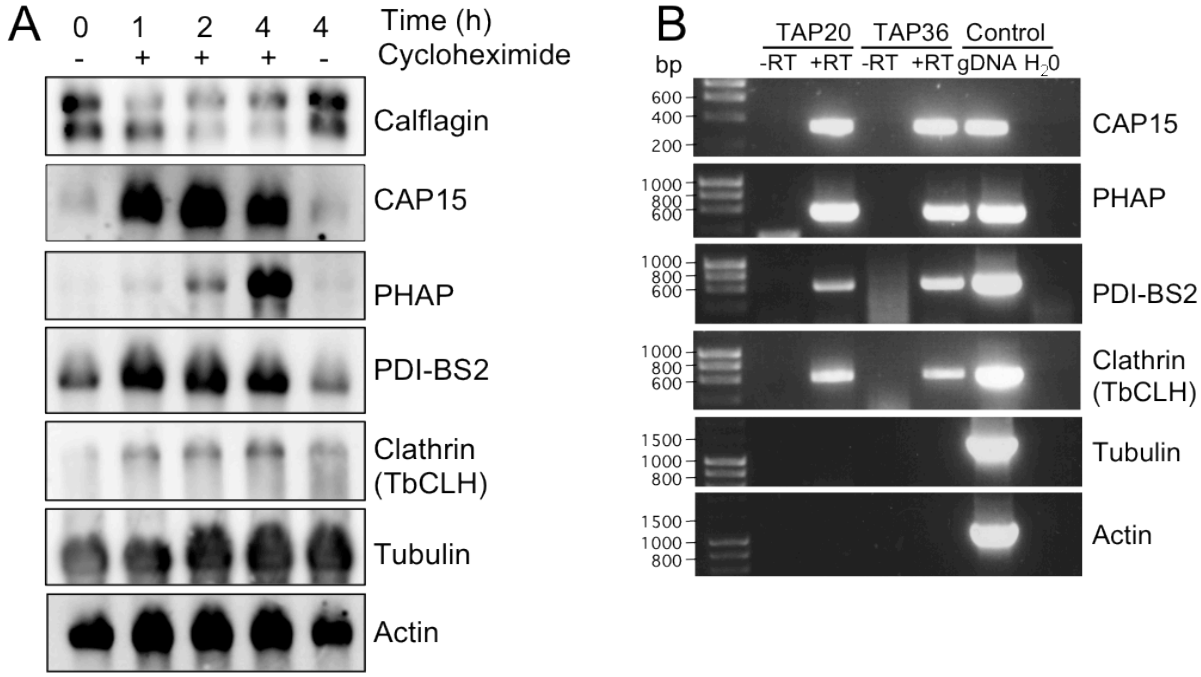


Figure 4.12. Translational inhibitor assay and ZC3H20 TAP-tag RT-PCR for candidate genes from PF ZC3H20 over-expression microarray

A. Northern blot analysis of total RNA isolated from PF cells treated with cycloheximide for 1, 2 and 4h. RNA was also isolated from PF cells at time point 0h and 4h without the addition of cycloheximide. RNA riboprobes to each gene were used to detect specific mRNA transcripts.
B. RT-PCR analysis on cDNA reverse-transcribed (+RT) from RNA isolated from TAP tagged ZC3H20 and ZC3H36 purification. Minus reverse transcription (-RT) control is shown for DNA contamination from the TAP purification. Genomic DNA (gDNA) is used as a positive control, and water (H_2O) is used as a non-template negative control

As the cyclohexmide assay shows that CAP15, PHAP, PDI-BS2 and clathrin are influenced by protein factors, these were then tested for their ability to be bound by ZC3H20. As described in Chapter 3 (Section 3.3.3), TAP-tagged ZC3H20 was expressed in PF cells and used in a tandem affinity purification method to isolate all mRNAs capable of being bound by ZC3H20. The mRNAs

were transcribed to cDNA, and then RT-PCR used to specifically amplify potentially bound mRNA targets of ZC3H20 i.e. tested for the presence of CAP15, PHAP, PDI-BS2 and clathrin (Fig. 4.12B). As mentioned in Chapter 3 (Section 3.3.3), the TAP method was carried out with ZC3H36, another CCCH zinc finger protein to show if there is specific ZC3H20 or general ZC3H RNA binding, and RT-PCR was carried out on tubulin and actin mRNAs as negative controls. RT-PCR of each candidate gene (Fig. 4.12B) produced a positive product from both TAP-ZC3H20 and TAP-ZC3H36, which indicates that they are capable of being bound by ZC3H20 and most likely show a general binding specificity by other ZC3H RNA binding proteins.

In conclusion, the cycloheximide assay shows that CAP15, PHAP, PDI-BS2 and clathrin could be regulated by a protein factor via destablisation, and correlates with the microarray data that they are down-regulated when ZC3H20 is over-expressed. They are also capable of being bound by ZC3H20, suggesting that ZC3H20 could be responsible for regulating these transcripts via mRNA destabilisation within the cell.

4.4.2 Over-expression of ZC3H20 causes an increased turnover of the PDI-BS2 mRNA transcript

As shown so far that over-expression of ZC3H20 causes a decrease in the mRNA level of CAP15, PHAP, PDI-BS2 and clathrin, and that these transcripts can be bound by ZC3H20, Northern analysis was performed to determine if the half life of these transcripts is influenced when ZC3H20 is over-expressed in PF cells. PF 20 OeX cells were grown in the absence or presence tet for 12h as for the microarray, where there is over-expression of ZC3H20 protein detected and no obvious morphological or growth defect is evident in these cells. After 12h of ZC3H20 over-expression in PF *T. brucei,* cells were treated with the transcriptional inhibitor actinomycin D for 0, 1, 2 or 4h, to allow the turnover of RNA to be determined with or without ZC3H20 over-expression. Therefore, after actinomycin D treatment at each time point, total RNA was isolated and the level of CAP15, PHAP, PDI-BS2 and clathrin mRNAs observed by Northern analysis (Fig. 4.13).

Densitometry was used to measure the mRNA levels at each time point and the levels were then calculated as a percentage of the time point 0h, which was

expressed as 100%, for –Tet and +Tet PF 20 OeX samples. These are plotted on a bar chart to show the decay of mRNA after actinomycin D addition (Fig. 4.14).

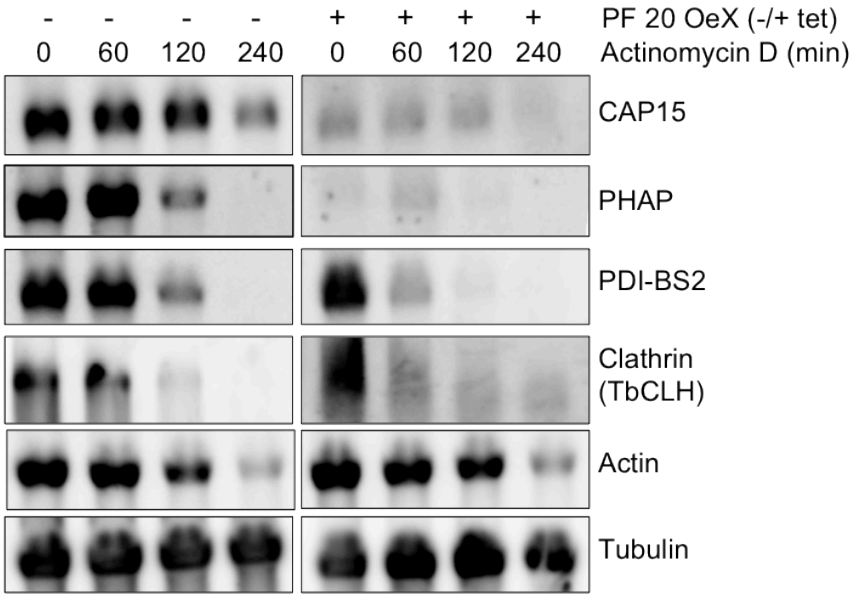


Figure 4.13. RNA abundance after treatment of PF *T. brucei* with a transcriptional inhibitor and induced for ZC3H20 over-expression

Northern blot analysis of total RNA isolated from PF 20 OeX cells grown in the presence or absence of tet for 12h and then treated with actinomycin D over 240min. RNA riboprobes to each gene were used to detect specific mRNA transcripts. The blots shown that are probed for CAP15, PHAP, PDI-BS2 and Clathrin when ZC3H20 is overexpressed, have been exposed for a longer period of time than for the uninduced samples, as the initial level of RNA is lower. This is done so that the turnover rate from starting levels can be observed.

The level of the control mRNA tubulin was not affected after actinomycin D treatment when ZC3H20 is overexpressed in PF cells compared to uninduced cells (Fig. 4.13, tubulin). The decay of CAP15 mRNA over 120mins when ZC2H20 is over-expressed is comparable to the mRNA decay of uninduced cells (Fig. 4.13 and 4.14, CAP15), therefore showing that ZC3H20 over-expression does not result in greater destabilisation of CAP15 mRNA that is responsible for its down-regulation.

The levels of PHAP and clathrin mRNAs are barely detectable when ZC3H20 is overexpressed (Fig. 4.13, PHAP, clathrin). However, densitometry analysis was attempted to determine if the mRNA turnover in the induced cells was affected, and this showed that PHAP mRNA decay does not change (Fig. 4.14, PHAP). This analysis shows that the TbCLH mRNA appears to decay faster when ZC3H20 is overexpressed, as after 60min, 27% of mRNA has decayed, compared

with 63% of TbCLH mRNA decay in uninduced cells (Fig. 4.13 and 4.14, clathrin). However, this mRNA is relatively large thus prone to degradation, and the Northern blot and densitometry analysis could be prone to inconsistencies, therefore it is difficult to make any definitive conclusions about its decay rate.

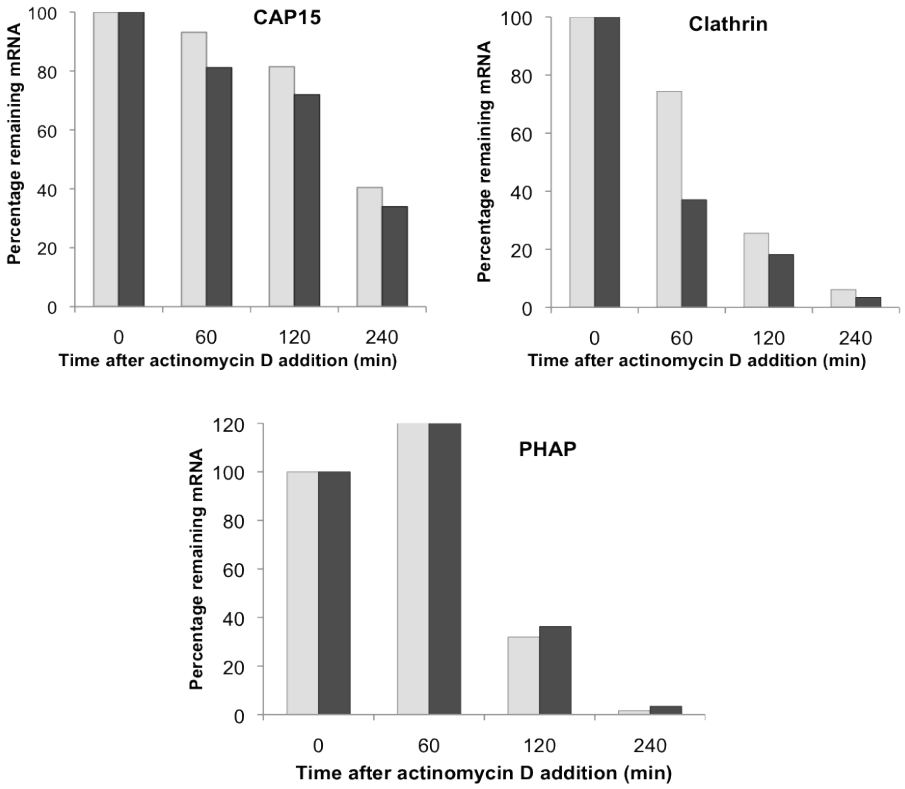


Figure 4.14. Densitometry analysis to show turnover of CAP15, PHAP and clathrin RNA in PF ZC3H20 OeX *T. brucei*

Densitometry analysis of transcriptional inhibitor assay as shown from Fig. 4.13 to analyse the decay of CAP15, PHAP and clathrin mRNA levels in the presence (dark grey) and absence (light grey) of ZC3H20 over-expression.

It appears that the PDI-BS2 mRNA is turned over much quicker when ZC3H20 is over-expressed in PF cells. The northern blot shows that from initial levels the mRNA level of PDI-BS2 decreases around 2h in normal PF cells (Fig. 4.13, PDI BS2 panel, -Tet, time 0h and 2h). In contrast, when ZC3H20 is over-expressed, the mRNA level of PDI-BS2 decreases at 1h relative to initial levels (Fig. 4.13, PDI-BS2 panel, +Tet, time 0h and 1h). To verify that PDI-BS2 has an increased decay rate when ZC3H20 is overexpressed, the analysis was carried out in triplicate and densitometry used to measure the mRNA levels at each time point. Actin was analysed in the same way, and used as a control. When ZC3H20 is

overexpressed in PF cells, the decay of actin mRNA after 60min, 120 min and 240min is comparable with mRNA levels in normal uninduced cells (Fig. 4.15, actin).

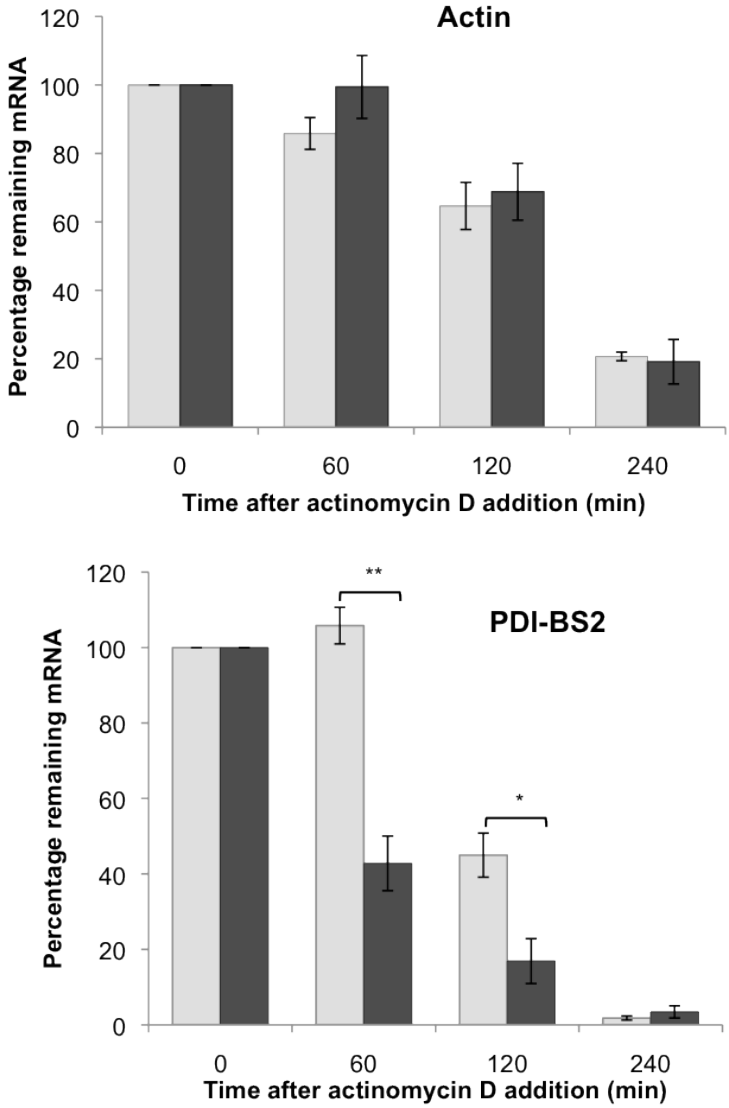


Figure 4.15. Densitometry analysis to show turnover of PDI-BS2 RNA in PF ZC3H20 OeX *T. brucei*

Densitometry analysis of transcriptional inhibitor assay as shown in Fig. 4.13 to determine the decay of Actin and PDI-BS2 mRNA levels in the presence (dark grey) and absence (light grey) of ZC3H20 over-expression. Plotted data are mean values from three independent experiments, and error bars show standard error. A Student's t-test was used to determine the significance of mRNA decay when ZC3H20 is over-expressed after each time point compared with uninduced PF cells. ** = $p<0.002$, * = $p<0.05$

A Student's t-test calculated that the difference in actin mRNA levels at each time point is not significant, therefore ZC3H20 over-expression does not increase or decrease the decay of actin. However, after 60mins, 57% of PDI-BS2

mRNA is turned over when ZC3H20 is over-expressed in PF cells, compared with no change after 60min in uninduced cells (Fig. 4.15, PDI-BS2 60min). Statistical analysis calculated that this difference in decay after 60min is significantly increased ($p<0.002$). This analysis also shows that there is a significant decrease ($p<0.05$) in the decay of PDI-BS2 after 120min, as 87% of PDI-BS2 mRNA was turned over when ZC3H20 was over-expressed compared with 55% decay of PDI-BS2 mRNA in uninduced cells (Fig. 4.15, 120min). This indicates that ZC3H20 over-expression causes an increased decay rate of PDI-BS2 mRNA in PF *T. brucei* and suggests that ZC3H20 may be responsible for destabilising PDI-BS2, consequently causing PDI-BS2 down-regulation.

4.4.3 Down-regulation of PDI-BS2 in PF *T. brucei* does not cause the BigEye phenotype

These data so far suggest that ZC3H20 is responsible for regulating PDI-BS2 via mRNA destabilisation in PF *T. brucei*. As over-expression of ZC3H20 causes the BigEye phenotype and also causes down-regulation of PDI-BS2 in PF cells, an investigation was carried out to determine if directly down-regulating PDI-BS2 alone by RNAi would cause an enlarged flagellar pocket. A 400bp region of the PDI-BS2 coding sequence was cloned into the p2T7i vector, and stably transfected into PF29-13 cells, as described for ZC3H20 RNAi in Chapter 3.2.1. PF RNAi BS2 cells were then grown in the presence or absence of tetracycline for 48h, total RNA isolated and then Northern analysis was used to determine inducible down-regulation of the PDI-BS2 transcript (Fig. 4.16A). After 48h of tet induction, the level of PDI-BS2 mRNA is barely detectable, verifying effective RNAi down-regulation. To determine if down-regulation of PDI-BS2 affects cell growth, PF RNAi BS2 cells were grown in the presence or absence of tet for 96h. Induced RNAi down-regulation of PDI-BS2 in PF cells did not affect cell growth, and grew at the same rate as uninduced cells (Fig. 4.16B). Samples of the induced cultures were taken each day and prepared for microscope analysis. PF cells induced for RNAi down-regulation did not appear to have any morphological defects compared to uninduced or parental cell cultures, and most certainly did not display the BigEye phenotype.

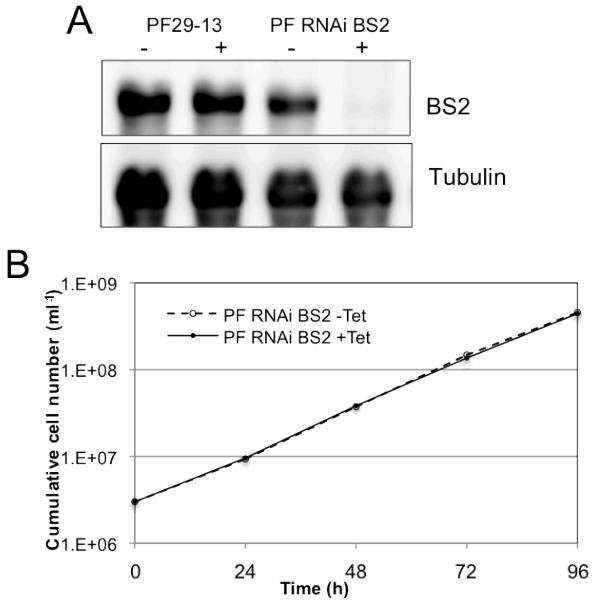


Figure 4.16. RNAi down-regulation of PDI-BS2 in PF *T. brucei*

A. Northern blot analysis of total RNA isolated from cells of tet induced (+) or uninduced (-) RNAi down-regulation of PDI-BS2 for 48h in PF cells
B. Growth curve showing the effect of tet induced (+) or uninduced (-) RNAi downregulation of PDI-BS2 over 96h in PF cells.

In conclusion, these data show that down-regulation of PDI-BS2 does not cause a growth defect and/or the BigEye phenotype. Therefore the BigEye phenotype seen when ZC3H20 is over-expressed in PF cells cannot be attributed to the down-regulation of PDI-BS2 mRNA. The microarray and Northern analysis shown in this section verifies that clathrin is downregulated when ZC3H20 is overexpressed, and in agreement with previous studies, a decrease in clathrin mRNA causes the BigEye phenotype and a defect in endocytosis. These data do not demonstrate that ZC3H20 directly regulates clathrin, and so the BigEye phenotype seen could be as a result of a secondary or indirect effect of ZC3H20 over-expression. However, the analysis shown above does indicate that ZC3H20 could directly regulate and destabilise PDI-BS2 mRNA; a gene that is implicated in the processing and trafficking of proteins in the endocytic pathway.

4.5 Discussion of Chapter 4

Chapter 4 has shown that over-expression of ZC3H20 in PF *T. brucei* causes an enlarged flagellar pocket (Fig. 4.3 and 4.6), which requires both ZC3H motifs of ZC3H20 (Fig. 4.5). The flagellar pocket is the sole site used for all endocytosis and

exocytosis by the trypanosome, and the endocytic activity of PF 20 OeX cells with an enlarged flagellar pocket is compromised. This phenotype (referred to as BigEye) and endocytic defect has been reported when molecules of the endocytic pathway are down-regulated in BF trypanosomes [36, 215, 218, 221, 222], where the endocytic rate is 10-fold higher than in PF cells [31]. One study has reported that down-regulation of a dynamin-like protein, TbDLP, in PF *T. brucei* caused the BigEye phenotype and an endocytic defect [223]. However, ZC3H20 over-expression did not cause a cell cycle block or collapsed mitochondrion, which occurs in TbDLP RNAi BigEye cells, indicating that the PF 20 OeX BigEye and endocytic defect is not as a result of disrupting mitochondrial integrity (Section 4.3.1). Additionally, the microarray and q-PCR analysis showed that the mRNA level of TbDLP was not considerably affected by ZC3H20 over-expression, confirming that ZC3H20 does not have any association with the function of TbDLP that would cause the BigEye phenotype (Section 4.3.2, Table 3.1).

Retaining the structure and integrity of the flagellar pocket is necessary for efficient endocytosis, and as described in Section 4.3, disruption of flagellar pocket biogenesis could cause a defect in endocytosis. The flagellar pocket membrane is closely associated and influenced by the trypanosome cytoskeleton [230], thus an enlarged flagellar pocket could be as a result of cytoskeleton dysregulation and consequently causing an endocytic defect. Microarray and Northern analysis determined that the mRNA level of tubulin, the component of microtubules that constitutes the trypanosome cytoskeleton, was not affected when ZC3H20 was over-expressed. CAP15, which in conjunction with CAP17, is a subpellicular cytoskeleton-associated protein known to stabilise microtubules in *T. brucei* [231], and CAP15 mRNA is down-regulated more than 2-fold when ZC3H20 is over-expressed. However, over-expression of ZC3H20 does not increase the mRNA turnover of CAP15, and thus it seems unlikely that ZC3H20 is directly responsible for the destabilisation of CAP15. These data suggests therefore that ZC3H20 over-expression does not directly affect the flagellar pocket integrity, which would then affect endocytosis.

Endocytosis is considered to be receptor-mediated and clathrin-dependent in trypanosomes, and down-regulation of clathrin causes an endocytic defect and an enlarged flagellar pocket in BF cells [36]. Disrupting the uptake of molecules could cause a gross enlargement of the flagellar pocket as a result of an imbalance

of membrane transport [36, 215]. Thus, ZC3H20 over-expression could perturb the regulation and/or expression of clathrin or any other endocytic molecule that would then block endocytosis and cause the BigEye phenotype in PF cells. Microarray analysis identified a subset of four genes that encode proteins that may have an endocytosis-associated function, and their RNA abundance were decreased more than 2-fold when ZC3H20 is over-expressed in PF cells. In addition to CAP15 as discussed above, one of these targets was the calflagins (17kDa and 24kDa). The calflagins are a family of related flagellar non-calmodulin EF-hand calcium binding proteins that are suggested to be involved in new flagellum formation [232]. Even though they are not associated with the flagellar pocket or endocytosis, and the flagellum itself does not appear to be affected in BigEye cells, the calflagins require trafficking and localisation to the flagellar membrane. Thus dysregulation of components required for the formation of the flagellum could disrupt the biogenesis of the flagellar pocket due to its close proximity and direct association. Northern analysis verified that the calflagin mRNAs were downregulated when ZC3H20 was overexpressed in PF cells, but the cyclohexamide assay suggested that these transcripts were actually stabilised by a protein factor in PF cells, which does not correlate with the microarray data. Thus, the down-regulation of calflagin mRNA from ZC3H20 over-expression is not likely to be due to direct regulation by ZC3H20.

Down-regulation (RNAi) of clathrin in PF cells results in the accumulation of intracellular vesicles, which is suggested to be as a result of transport vesicles unable to fuse with the target membrane [36]. In BigEye PF 20 OeX cells, the electron microscopy images also show that these cells have large cytoplasmic vesicles (Section 4.2.4., Fig. 4.6C). These vesicles are not as significantly accumulated in bloodstream form clathrin RNAi cells, and this highlights different requirements for clathrin between the two life stages i.e. endocytosis in bloodstream and lysosomal trafficking/post-Golgi transport in the procyclic form [36]. It is possible that a similar situation is occurring in these BigEye cells where the trafficking of molecules is halted, leading to a build up of excess membrane. The phosphatidic acid phosphatase protein (PHAP) identified in the microarray was selected due to the findings that acid phosphatase activity is associated with the Golgi membranes and flagellar pocket [233]. The membrane-bound histidine acid phosphatase, TbMBAP1, is reported to be localised to endosomes and the flagellar

pocket, and essential for endocytosis and membrane recycling in *T. brucei* [234]. Therefore there is a precedent for this type of protein to have a role in regulating protein trafficking, and down-regulation of PHAP from ZC3H20 over-expression could have an effect on the endo/exocytosis balance within the cell. The PDI-BS2 identified in the microarray has a similar association with the endocytic pathway. It is one of two phosphate disulphide isomerases that have a putative function as a molecular chaperone, assisting in the folding of ER proteins, as well as possessing disulphide isomerase activity [235]. Interestingly, both are co-localised with the endocytic pathway, rather than the usual resident of PDIs in the ER lumen, [235] suggesting a unique requirement in the processing and trafficking of endocytic proteins. The PDI-BS2 has extensive N-glycosylation, which is specific to processing from the Golgi, suggesting that PDI-BS2 itself must be trafficked from the ER to the Golgi [235]. Thus, mRNA down-regulation of PHAP and/or PDI-BS2 from over-expression of ZC3H20 could affect the balance of trafficked proteins involved in the endocytic pathway, consequently causing an endocytic defect. Northern analysis verified both transcripts are down-regulated when ZC3H20 is overexpressed, that they are destabilised by a protein factor in PF cells and that ZC3H20 is capable of binding both mRNAs. The actinomycin D assay showed that PHAP mRNA turnover was difficult to determine as mRNA levels after ZC3H20 over-expression was barely detectable (at time point 0h of actinomycin D addition), and so no conclusions can be made about the decay of this transcript. However, the decay of PDI-BS2 mRNA was clearly increased when ZC3H20 was over-expressed, and thus suggests that PDI-BS2 is destabilised in a ZC3H20-dependent manner.

PDI-BS2 is bloodstream-stage specific, but there is some discrepancy about the essential nature of the gene in BF *T. brucei*. One study showed that RNAi down-regulation of BS2 does not affect the growth of BF cultures [235]. However, a more recent study has reported that RNAi of PDI-BS2 affects proliferation and morphology of BF parasites, and causes an increase in VSG protein expression [236]. From the data shown in this report, it is clear that RNAi of BS2 in PF cultures does not affect cell proliferation or morphology, suggesting that it is not essential for growth in the PF life cycle stage. Additionally, down-regulation of PDI-BS2 does not cause an enlarged flagellar pocket, demonstrating that the BigEye phenotype is not as a result of ZC3H20 down-regulating PDI-BS2. It is still possible however,

that ZC3H20 is usually responsible for the regulation of this mRNA, as PDI-BS2 is down-regulated in PF *T. brucei* and could be destabilised as a developmentally-regulated gene by ZC3H20.

As discussed in Chapter 3 (Section 3.5), there are a range of AU-rich, U-rich, GU-rich and G-rich elements present in the 3' UTR that confer stability/instability of mRNA targeted by RNA-binding proteins. In addition, a core sequence of the 26mer instability element from EP procyclin (UAUUUUUU) is present in one-third of PF-enriched genes, and identified to promote mRNA destabilisation in BF *T.brucei*, thus causing an apparent enrichment in the PF life cycle stage [125, 136]. An equivalent over-represented element has not been identified in the 3' UTR of bloodstream-enriched transcripts [136]. Regarding the destabilisation of the bloodstream-enriched PDI-BS2 mRNA in procyclic form cells, there does not appear to be any sequence elements in the 3'UTR that resemble an AU-rich motif of any kind (Fig. 4.17).

Figure 4.17. 3' UTR regions of PDI-BS2 mRNA

Black type indicates the intergenic region between PDI-BS2 and the genes down stream (sequences in bold black type). GU-rich element is UGUUUGUUUGU, and elements similar to GRE sequences are highlighted in blue.

PDI-BS2 (Tb10.6k15.2290/Tb927.10.8230)

AGCAATGAAAGTAATGATAGCAATGAGAGCAATGTTGATAAACAAGATCTGTAGCAAGATUAAGAAAACG
UUUGGCCCAGUUUCAAAUCCUUAUCCACUUAGCUAUUUUCGCUUUUCGGCUCCGAUGAUGUGGGCAACAA
UGGUUUGCAAGUUGCCGGAUGGAAGACAAAGUGAAGAACCCCUUAUAUAUGAAUAGAAGGGGUCGUUGGC
GGGGGUGGGUUAUGGGGCUAACGUAAUGCCAGGUAAUAGAGAUGAUAGUGGUAAAAGCGGGGUAUCUUUA
AGAAAUUGAAAUGUCGGAAGGGAGGGGGGGGGGAUAAAUAACGGCGGAGGGUCGGGGGUGCUGCGCGCCU
CUAGAGUCCUACUCGCUGUAGAUAAUAGGUAUAUAAAAAGAUUUGAAAGGGGCGACUGAUAAGAAACUCA
UAUUCAUGCCUUUCUAUGUGGGCUUUGGCUGGUUCCUUGCGUCACCGUUUCUUCAUCUUCAGCUUGAACU
CCUCCUUUUUUGCUUAGGAAGGUUGACAUAUUUUGUGUGCGACAGCGCUCAUUUUUCUACAUAAUAGUGC
GUUUGGGUGGCGUGGACGUUGGAUGGCGUUUUCGUUUCUACGGAUUCACCCCUCCCACAAGCAAUAUACA
GGGCCCCUGUGUUAAGGGGAAGCCGACGAUACUUUACCCAGGAGAUGAAGGAGAUAAGUUGAAUUUACCG
AUUAGUUCGGGGAUGGGAUAAUCCCAAACUCUGUGAAUCGCUGCGCGUCUUGAUGCCUUGUUGAAAGUUU
GAGGCUGGGGGAUAUCCUGCACGAGAGAGCCAGGGGAGAUGCACGCCACCCAGCGUACACAUGCUGCAAC
AAACUCGCGGCUACCCUAUUGGCCAACGAAAAAUGGGAUUAGUUAAUGCUUUUCUUCCAUGACUGGGCUC
UUGCCGAGGCCCGUACACCCCAAACCCACCUUACGGUUGCUUGUCACAAGCACUUCUUGGGGUGCUCACC
ACAUGGGAUGCAUAAAUCGUAAAGGUGCGCACAUUUUGAUCUUUGUAUUAAGUUAGGGAGACUGUUCAAU
GCCACAGACGGAUCUGUUCUGCAAAGGGCGCGCAGUGGUAUAGUCUGAACGCCAAGAAUGCGGUGGGCGG
UGGGGGAGCCCGCUGCACACGGAAAUUAAAGAAGGGUGUACCCUUUCACUGGGGAGCGGAGCAUGGUCUG
AUUGUUUUUAAACUUCUUCGGUUCGUCUGAAGCCAUACGCGUGUGUGUUCGUGGCAAGUUGCACCUCACU
ACCGAUCGGGAAGUGCCUGAACUUGGCGGUGUCUAUCAACAAGCUUCAUGAAGGGGGACACUCUCAACCA
CAUCUAGCGGACGACCUUUUGGCACCA**ATGACCAGCAAAGCAGTTAGTGT**

The consensus sequence UGUUUGUUUGU, termed a GU-rich element (GRE) is enriched in the 3' UTR of short-lived transcripts in primary T cells, confers instability of the transcript and mediates binding of CUG-binding protein-1 [205]. There are some sequences similar to the GRE present in the 3'UTR of PDI-BS2, but the consensus sequence is not evident. Although PDI-BS2 does not contain an identifiable ARE or GRE, it may be that ZC3H20 is binding to a variation of this element or even a completely novel sequence element present within the 3' UTR in order to regulate PDI-BS2 mRNA destabilisation.

As down-regulation of PDI-BS2 does not cause an enlarged flagellar pocket, the BigEye phenotype is likely to be a due to down-regulation of clathrin. These data verify that clathrin mRNA levels are decreased, and published literature definitively shows that RNAi of TbCLH causes the BigEye phenotype. The results shown in section 4.2, determine that ZC3H20 over-expression causes an endocytosis defect, an increase in CRAM mRNA (Fig. 4.10), but the integrity of the ER, mitochondrion and lysosome are maintained, and these data agree with the published studies of clathrin. Clathrin is normally down-regulated in PF cells, but its expression is still essential for PF *T. brucei* growth and survival [36], and the decrease in mRNA levels after ZC3H20 over-expression may be responsible for the severe growth defect in PF cells. TbCLH mRNA was shown by microarray analysis, and confirmed by q-PCR and Northern analysis, to be downregulated when ZC3H20 is overexpressed. Clathrin shown to be destabilised in PF cells by a protein factor, and that it can be bound by ZC3H20 (Section 4.4). Clathrin is developmentally regulated and the TbCLH mRNA level is lower in PF cells compared to BF cells [36]. When ZC3H20 is over-expressed in PF cells, the TbCLH mRNA levels are decreased even further to barely detectable levels, and so accurate calculations of its decay rate could not be made. The TbCLH mRNA appears to be a large transcript, and resolution of the mRNA by Northern blot analysis shows that it may be susceptible to degradation and inconsistencies. It does appear that the half-life of TbCLH is decreased when ZC3H20 is over-expressed (Section 4.2), but this analysis would need to be repeated several times to produce a result with confidence. Thus, at this point, no definitive conclusions made if ZC3H20 over-expression causes a decrease in half-life of clathrin mRNA which could indicate if clathrin is destabilised in a ZC3H20-dependent manner.

Whilst down-regulation of clathrin has been shown to cause the BigEye phenotype in BF *T. brucei*, there is some discrepancy between the phenotypes reported for RNAi of clathrin in PF cells. The TbCLH study [36] and a study of CRAM, a receptor in the flagellar pocket membrane of procyclic *T. brucei* [38], show that RNAi of TbCLH results in a round phenotype in PF cells, but the TbDLP study reports 25% of cells displaying the BigEye phenotype when TbCLH is downregulated [223]. Microarray analysis shows that over-expression of TbZC3H20 causes a 1.7-fold decrease in clathrin mRNA level, (Section 4.4), but the levels of down-regulation may not be as low as those achieved from targeted RNAi. It may be that the modest decrease in clathrin mRNA levels from ZC3H20 over-expression enabled the display the BigEye phenotype. By down-regulating clathrin in procyclic cells by any manner, whether directly by RNAi or perhaps indirectly by over-expressing TbZC3H20, after time, all cells round up and die. Through severely downregulating TbCLH in PF cells (via RNAi), they may not display the BigEye phenotype and instead go straight to rounding up. The level of clathrin down-regulation from ZC3H20 over-expression may also suggest that clathrin is not normally regulated by ZC3H20, and that another RBP, possibly a related ZC3H protein, is responsible for the specific destabilisation of clathrin in PF cells. TbZC3H21 is another CCCH zinc finger protein similar to ZC3H20, and as discussed in Chapter 3, there is possible redundancy between these two proteins. Interestingly, over-expression of ZC3H21 results in cells displaying the round phenotype (Fig. 4.2). Considering over-expression of the ZC3H20 causes BigEye and a defect in endocytosis, the round phenotype from ZC3H21 over-expression may be due to down-regulation of clathrin in PF cells. If ZC3H21 is responsible for specifically regulating clathrin via destabilisation, this may cause a greater decrease in clathrin mRNA, and thus cause the PF cells to round up without display of the BigEye phenotype, as seen from targeted RNAi of TbCLH in other studies.

In comparison to Chapter 3 that concludes with the findings that ZC3H20 stabilises PF-enriched genes in PF cells, this Chapter suggests the role of ZC3H20 in destabilising BF-enriched genes in PF cells. Analysis of the microarray data in Chapter 3, reveals that at a lower threshold of 1.5-fold, there are 21 genes that show an increase in RNA abundance upon RNAi of ZC3H20, and out of these, 9 are BF-enriched transcripts: PDI-BS2 (as shown above as destabilised when

ZC3H20 is over-expressed), 65 kDa invariant surface glycoprotein, glucose transporter 1E (at 2-fold threshold), glucose-6-phosphate isomerase (glycosomal), HSP70-like protein (at 2-fold threshold), glucose transporter 1B, hypothetical *T. brucei* specific protein (Tb927.1.5160) and two hypothetical conserved proteins (Tb927.4.500 and Tb927.8.3730) [58]. This correlates with the suggestion that ZC3H20 destabilises BF-enriched transcripts in PF cells (over-expression of ZC3H20 causes their down-regulation, and down-regulation of ZC3H20 causes their up-regulation).

ZC3H20 over-expression in PF *T. brucei* causes down-regulation of a range of molecules involved in endocytosis; a pathway that is developmentally regulated in trypanosomes. In both PF and BF *T. brucei*, endocytic activity is required for nutrient uptake, but BF trypanosomes are dependent on an increased endocytic rate to recycle the variant surface glycoprotein coat and remove host immune complexes from the surface [23, 25]. However, a recent study shows that endocytic activity is energetically burdensome, and suggests that the rationale behind down-regulating endocytosis in PF trypanosomes is due to energy conservation in the nutrient-poor tsetse midgut [237]. Thus, whilst up-regulation of endocytosis is an obvious mechanism for increasing the endocytic rate to meet the survival needs of a bloodstream parasite, there is a precedent for active down-regulation of endocytosis in the procyclic form parasite to adapt and endure the harsh environment within the insect. In conclusion, these data suggest that TbZC3H20 is involved in the developmental regulation of *T. brucei* trafficking in the PF trypanosome, acting to control the necessary changes in gene expression for cell viability and survival.

CHAPTER 5. ZC3H20 acts as a molecular trigger of differentiation in bloodstream form *T. brucei*

5.1 Introduction

Chapter 3 and 4 show that ZC3H20 controls the mRNA stability of developmentally regulated genes in PF *T. brucei*. Specifically, ZC3H20 stabilises PF enriched genes TbMCP12 and TS-like E, and destabilises BF enriched genes PDI-BS2 and TbCLH in the procyclic life cycle stage. The ZC3H20 protein itself is PF enriched, and is essential for the viability and growth of the PF cell.

Regulation of PF enriched genes has been demonstrated previously for another *T. brucei* ZC3H protein, TbZFP3, which has been identified as an isoform-specific post-transcriptional regulator of procyclin surface coat expression in PF cells [184]. As discussed in the Introduction (Chapter 1.5.1), TbZFP3 and TbZFP2 are implicated in the control of early differentiation events (surface expression of procyclin), and TbZFP1 appears to regulate events later in the differentiation program (kinetoplast repositioning) [182-184]. These ZC3H proteins are the only class of RBPs that have been demonstrated to contribute to controlling the differentiation process in *T. brucei*.

Over the last decade, evidence has been collated to provide a model for signalling pathways that occur upon triggering differentiation. The most recent hypothesis presents a model whereby BF stumpy cells pre-adapted for differentiation, are exposed to a cold shock (20°C) that induces the up-regulation of a thermoregulated surface transporter (PAD) required to detect the physiologically low levels of *cis*-aconitate in the fly midgut, which then intracellularly triggers the differentiation program via a phosphatase cascade [49, 50, 144]. Other investigations into the differentiation pathway include the genome-wide analysis of transcript abundance within each developmental stage and during the differentiation programme [57-59]. Thus, we know the morphological changes that occur (see Introduction Chapter 1.2.2), the changes in the transcriptome during differentiation and the potential environmental signals perceived to trigger differentiation. However, the regulatory molecules required to initiate the switch and control this pathway remain elusive. Previous reports of the involvement of TbZFP1/2/3 in differentiation, suggest the potential for other ZC3Hs in *T. brucei* to control the initiation of differentiation.

The evidence so far demonstrates that ZC3H20 can post-transcriptionally regulate the expression of several developmental genes in PF *T. brucei*. An

undetectable level of ZC3H20 protein in BF cells begs the question as to whether ZC3H20 has a role or not within this life cycle stage. As the gene is essential in PF cells, this also raises the issue if ZC3H20 is required for differentiation from BF to PF or whether its expression level is increased as a result of the BF to PF transformation. Thus, each of these matters can be addressed via RNAi down-regulation and over-expression of ZC3H20 in BF *T. brucei*.

5.2 Investigation into the requirement of ZC3H20 in BF *T. brucei*

As shown in Chapter 3 (3.1.3), ZC3H20 is enriched in PF trypanosomes and responsible for regulating key developmental mRNAs. However, this analysis showed that although ZC3H20 mRNA is present in comparable abundance between BF and PF, ZC3H20 protein is undetectable in BF *T. brucei*. ZC3H20 is essential in PF cells (Chapter 3), however it is not known if ZC3H20 is required for growth in BF *T. brucei*. Thus, in a similar manner to the analysis carried out in PF cells, the essential nature of Z3H20 can be assessed by RNAi down-regulation and attempts to create a null mutant.

5.2.1 Down-regulation of ZC3H20 or ZC3H21 by RNAi does not affect growth in BF *T. brucei*

To investigate if down-regulation of ZC3H20 in BF trypanosomes affects growth, the construct p2T7i, as used in Chapter 3 (3.2.1) for tet inducible RNAi in PF cells, was stably transfected into BF SMB (single marker bloodstream) monomorphic cells (engineered to express T7 polymerase and the tet repressor) [188]. As discussed in Chapter 3 (3.1.1), and shown by RNAi analysis (3.2.2), TbZC3H21 as a similar member of the *T. brucei* CCCH ZFP is also essential for growth in PF *T. brucei*. Thus, the p2T7i ZC3H21 construct used in PF cells was transfected into BF SMB cells to investigate if ZC3H21 down-regulation also affects growth in BF.

To verify inducible RNAi down-regulation of ZC3H20 and ZC3H21, BF 20 RNAi and BF 21 RNAi cells were grown in the presence (+) and absence (-) of tet for 48h, total RNA isolated and the ZC3H20/ZC3H21 mRNA levels assessed by Northern analysis (Fig. 5.1A and 5.1B). The parental cell line, BF SMB was used as a control. This showed that ZC3H20 and ZC3H21 mRNA levels were effectively downregulated when RNAi was induced, and the double-stranded RNA in the

induced BF 20 RNAi cells is also detected (asterisk in Fig. 5.1A). To assess the effect of ZC3H20 or ZC3H21 down-regulation on BF cell growth, BF 20 RNAi and BF 21 RNAi cells were grown in the presence (+) and absence (-) of tet, and growth recorded over 192h (Fig. 5.1C). This analysis reveals that RNAi down-regulation of ZC3H20 or ZC3H21 in BF cells (although not completely down-regulated, Fig. 5.1A,B) does not affect cell growth compared to uninduced or parental cells, and thus ZC3H20 or ZC3H21 may not be essential in this life form.

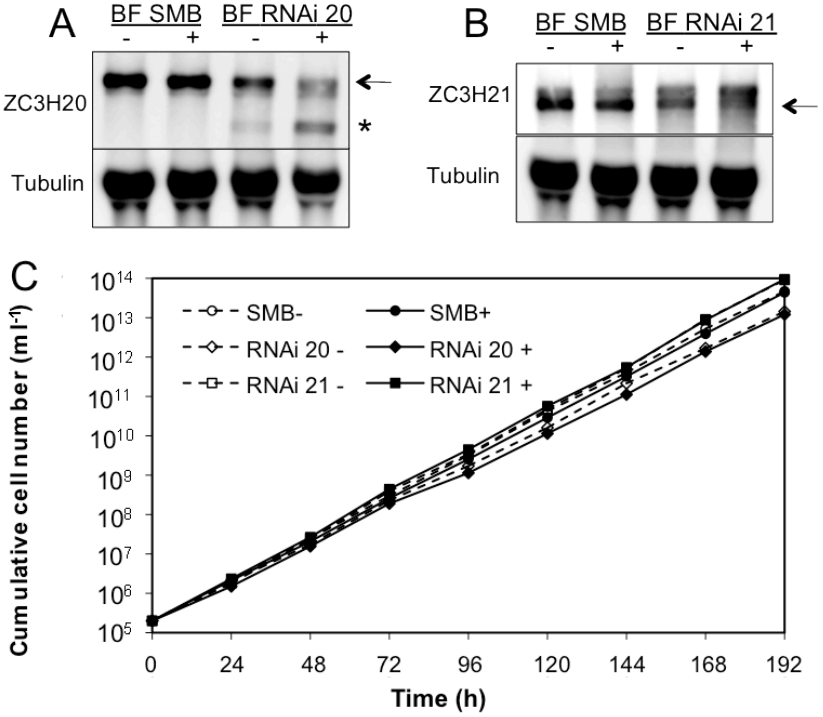


Figure 5.1. RNAi down-regulation of ZC3H20 or ZC3H21 in BF *T. brucei*

A. Northern blot of RNA isolated from BF SMB (parental cell line) and BF RNAi 20 cells in the presence (+) or absence (-) of tet for 48h, and probed with an anti-TbZC3H20 riboprobe. The endogenous ZC3H20 mRNA is indicated with an arrow, and the induced double-stranded RNA for targeting ZC3H20 is indicated with an asterisk (*).
B. Northern blot of RNA isolated from BF SMB and BF RNAi 21 cells in the presence (+) or absence (-) of tet for 48h, and probed with an anti-TbZC3H21 riboprobe. The endogenous ZC3H21 mRNA is indicated with an arrow.
C. Growth curve showing the effect of tet induced (+) or uninduced (-) down-regulation of ZC3H20 (RNAi 20) over 192h in BF cells. SMB is the parental cell line and shows no effect on growth in the presence of tet.

5.2.2 Down-regulation of ZC3H20 or ZC3H21 compromises the ability of BF *T. brucei* to differentiate

The observation that down-regulation of ZC3H20 has no effect in BF cells, correlates to the study of expression between BF and PF life forms, which shows that ZC3H20 protein is enriched in PF but not detectable in BF *T. brucei* (Chapter 3.1.3) and thus, so far the data suggests that ZC3H20 (and ZC3H21) is essential for growth in PF but not in BF. With this in mind, the ability of BF cells to differentiate to PF in the absence (down-regulation) of ZC3H20 or ZC3H21 was investigated. BF 20 RNAi and BF 21 RNAi cells were grown in the presence (+) and absence (-) of tet for 48h (when down-regulation of RNA is detected, Fig. 5.1A and 5.1B), and then induced to differentiate by exposing the cells for 48h to an *in vitro* differentiation trigger of 6mM citrate or *cis*-aconitate and a drop in temperature to 27°C [238]. The cells were then assayed for EP procyclin expression, an early differentiation marker (see Introduction 1.2.2) at 0h, 48h (of RNAi induction), and 72h and 96h (48h after differentiation trigger) (Fig. 5.2).

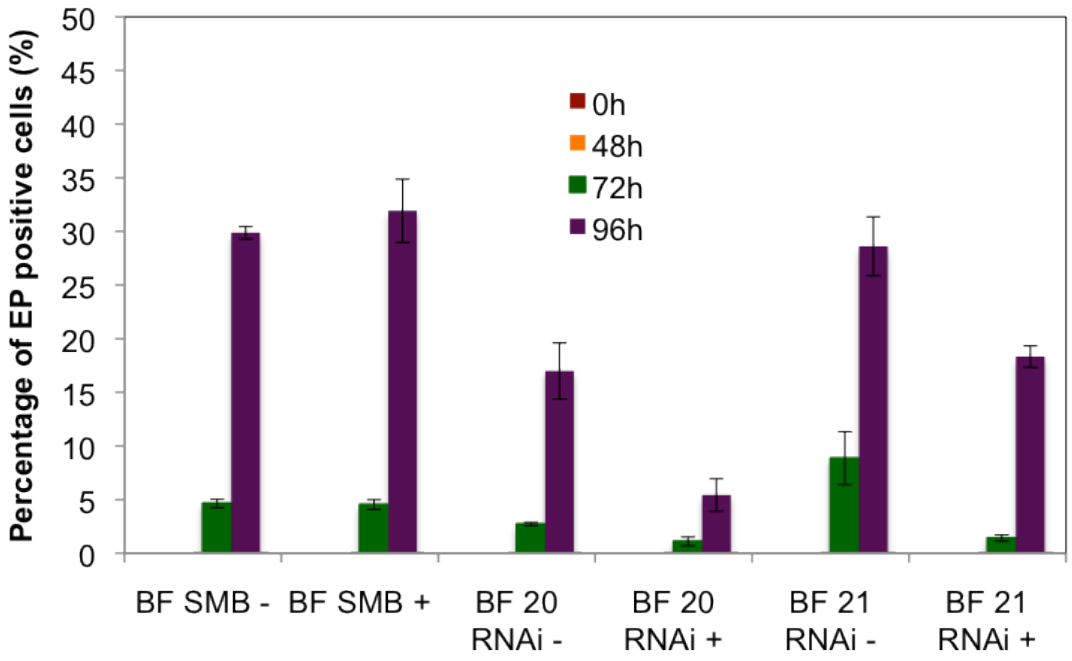


Figure 5.2. Differentiation ability of BF *T. brucei* induced for ZC3H20 or ZC3H21 RNAi down-regulation

Graph to show percentage of EP procyclin positive cells after induction of differentiation in the absence of ZC3H20 or ZC3H21 in BF *T. brucei*. BF SMB, BF 20 RNAi and BF 21 RNAi cells were grown in the presence (+) or absence (-) of tet for 48h and then exposed to 6mM *cis*-aconitate and shifted to 27°C for a further 48h (72h and 96h). Over 200 cells were counted for each experiment. Plotted data are mean values from three independent experiments, and error bars show standard error.

After 96h, 30% of the parental BF SMB cells expressed procyclin at the cell surface showing differentiation to PF (Fig. 5.2). However, when RNAi of ZC3H21 is induced this is reduced to 18% of BF cells, and downregulation of ZC3H20 results in only 5% of the BF population that express procyclin when triggered to differentiate. This equates to a reduction of 83% of the BF population that are not able to differentiate in the absence of ZC3H0 compared to the parental BF cells. In addition, 17% of uninduced BF RNAi 20 cells expressed procyclin, showing a reduction of 43% in their ability to differentiate compared to parental BF cells. This can be explained by the possibility that there may not be tight regulation of the RNAi inducible system, as even if the absence of tet, there appears to be some expression of double stranded RNA targeting ZC3H20, which is detected by the Northern analysis (asterisk in Fig. 5.1C). This leaky expression could down-regulate ZC3H20 enough to cause a small decrease in the proportion of BF cells able to differentiate when given the signal. Consequently, the RNAi system in the BF cells may not provide enough tight regulation, thus causing variability. Despite this, these data still suggest that down-regulation ZC3H20 or ZC3H21 compromises the ability of BF *T. brucei* to differentiate.

5.2.3 ZC3H20 is not an essential gene in BF *T. brucei*

The data shown so far shows that RNAi of ZC3H20 in BF cells has no detrimental effect on cell growth, but compromises the ability of the BF cell to differentiate to PF. This raises two questions: firstly, whether ZC3H20 is essential in this life form i.e. if a BF ZC3H20 null mutant can be created, and secondly, whether the ZC3H20 null mutant is compromised in its ability to differentiate. The use of a null mutant also resolves the problem of incomplete knockdown or leaky expression from RNAi seen in the PF 20 RNAi cell line (Fig. 5.1C and Fig 5.2). Therefore, a knockout strategy was employed, as used in Chapter 3 (3.2.2) for WT PF cells, to replace each endogenous allele of ZC3H20 with a selectable marker in WT BF *T. brucei*. WT 427 BF cells were successfully transfected with each construct, pLEW13 and pLEW90 individually thus creating single knockouts (SKOs). To show correct integration, genomic DNA was isolated from the SKOs, and then PCR was used with a set of primers where one primer binds to the endogenous UTR of TbZC3H20 and the other that binds to a specific region within

pLEW13 or pLEW90 (as demonstrated in Chapter 3, Fig. 3.4B). Each set of primers produced a PCR product of the correct size, showing there was correct integration at the 5' UTR or 3' UTR (as seen in Chapter 3, Fig. 3.4C and 3.4D). One of the SKO clones was then used for transfection with the second construct (in this case a pLEW90 clone was transfected with the pLEW13 construct) to then create a double knockout (DKO). Genomic DNA was isolated from the BF DKO ZC3H20 clones, and then PCR was used to confirm correct integration of both constructs (Fig. 5.3A). Now that both alleles of ZC3H20 had been knocked out, there should be no production of mRNA from this gene. Therefore, total RNA was isolated from the DKO clones, and probed for the existence of ZC3H20 mRNA (Fig. 5.3B), which verified that the BF DKO 20 clones were *bona fide* null mutants. In conclusion, it appears that ZC3H20 is not essential for growth in BF *T. brucei*.

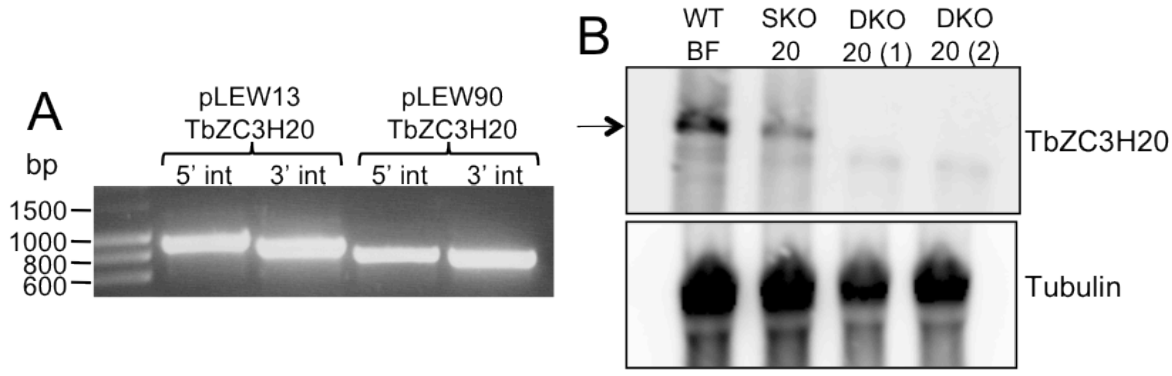


Figure 5.3. Generation of ZC3H20 null mutants in BF *T. brucei*

A. PCR of genomic DNA from BF DKO 20 cells to show correct integration of both pLEW13 and pLEW90 into the TbZC3H20 locus. 5' int = 5' integration, 3'int = 3' integration
B. Northern blot of RNA isolated from WT BF (parental cell line), BF SKO 20 cells (single knockout used for double knock out), and two clones of BF DKO 20 cells, and probed with an anti-TbZC3H20 riboprobe. The endogenous ZC3H20 mRNA is indicated with an arrow, and tubulin is shown as a loading control.

5.2.4 Triggering differentiation in the absence of ZC3H20

When ZC3H20 is down-regulated in BF cells, there is an 83% decrease in the proportion of cells able to differentiate compared to parental BF SMB cells. However, RNAi targeting of ZC3H20 does not result in complete total knockdown (Fig. 5.1A), and residual target/less efficient knockdown in some BF cells could still enable them to differentiate even when ZC3H20 is down-regulated. Therefore, the

BF DKO ZC3H20 cells, where no cell has the ZC3H20 gene, were used to investigate if they could still differentiate in the complete absence of ZC3H20. In addition, the ZC3H20 RNAi system in BF cells was not tightly regulated (i.e. leaky expression in the absence of tet induction), and so the null mutant cell line overcomes this problem.

As discussed in Chapter 3, ZC3H20 is not the only ZC3H protein with two conventional zinc finger motifs encoded in *T. brucei*. Most notably, ZC3H20 shares a high degree sequence homology with TbZC3H21 at the N-terminus regions, which includes the CCCH zinc finger motifs. Thus, it is possible that the presence of similar *T. brucei* ZC3H(s) could compensate for the absence of ZC3H20, and still permits these BF cells to continue through differentiation, i.e. as a result of potential ZC3H redundancy. Therefore, the RNAi ZC3H21 construct (described above) was stably transfected into the BF DKO 20 cell line. To verify that induced RNAi of ZC3H21 caused down-regulation (by addition of tet), total RNA was isolated from each cell line induced/uninduced for 48h, and probed for ZC3H21 mRNA by Northern blot analysis (Figure 5.4A). This showed that ZC3H21 mRNA levels were efficiently downregulated when RNAi was induced.

Consequently, these BF cells and the BF 20 DKO cells were tested for their ability to differentiate in the absence of ZC3H20 and presence or absence of ZC3H21. Thus, BF DKO 20 and BF DKO 20 + RNAi 21 were grown in the presence (+) or absence (-) of tet for 48h at 37°C and then exposed to 6mM *cis*-aconitate and a temperature shift to 27°C to be analysed for their ability to differentiate (Figure 5.4B). After 48h, around 60-70% of WT BF cells differentiate to PF as indicated by EP procyclin expression. Around 40% of BF DKO 20 cells differentiate (a reduction of 30% from WT proportions), which is the same proportion as for the uninduced BF DKO 20 + RNAi 21 cells. However, when RNAi of ZC3H21 is induced in the BF DKO 20 + RNAi 21 cells, only 24% of cells are able to transform to PF (a reduction of 58% from WT proportions). Using a Student's t-test, it was calculated that down-regulation of ZC3H21 in a BF DKO 20 cell line significantly affects their ability to differentiate ($p < 0.025$).

Overall, these data suggest that, in combination with the RNAi data, differentiation from BF to PF is compromised in the absence of ZC3H20 and ZC3H21. By down-regulating ZC3H21 in a BF ZCH320 null mutant cell line, i.e. in

the absence of both ZC3Hs, the ability for the BF cell to differentiate is compromised to a greater level that just the ZC3H20 null mutant alone, suggesting that redundancy exists between the ZC3Hs in the progression of this pathway.

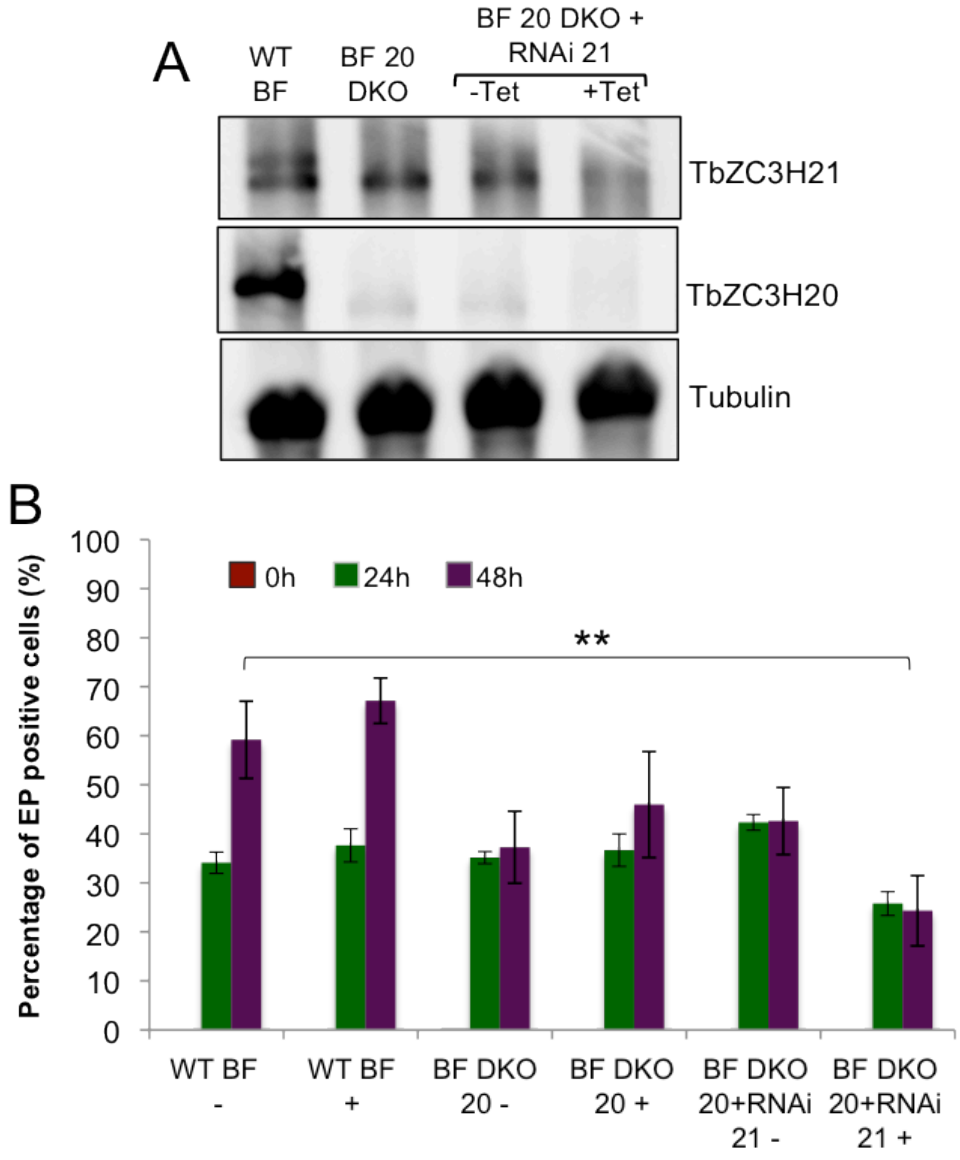


Figure 5.4. Ability of *T. brucei* BF ZC3H20 null mutants to differentiate to PF

A. Northern blot of RNA isolated from WT BF (parental cell line), BF DKO 20 and BF DKO 20 + RNAi 21 cells in the presence (+) or absence (-) of tet. The blots were probed with an anti- TbZC3H21, -TbZC3H20 and -tubulin riboprobe.
B. EP1 positive counts of BF DKO 20 and BF DKO 20 + RNAi 21 over 48h after being triggered to differentiate to PF using 6mM *cis*-aconitate and temperature shift to 27°C. Cells were grown in the presence (+) and absence (-) of tet for 48h prior to being triggered to differentiate. WT BF is the parental cell line. Over 200 cells were counted for each population. Plotted data are mean values from three independent experiments, and error bars show standard error. A Student's T-test was used to compare WT BF – and all other populations at 48h to calculate statistical significance between these counts. ** = $p < 0.025$

5.2.5 Discussion of section 5.2

The data from this section shows two important findings. Firstly, that via RNAi and gene knockout analysis, ZC3H20 and ZC3H21 are not essential genes in BF *T. brucei*. This is in contrast to the finding that both these ZC3Hs are essential in PF cells. These findings are in agreement with the findings in Chapter 3, that ZC3H20 protein is undetectable in BF cells but detectable in PF cells (Chapter 3.1.3). Secondly, down-regulation of ZC3H20 or ZC3H21, or a combination of both, compromises the ability of BF cells to differentiate when triggered by the addition of *cis*-aconitate and a drop in temperature to 27°C. These data therefore suggest that ZC3H20 (and/or ZC3H21) may be involved in the differentiation pathway.

Down-regulation of ZC3H21 in the BF DKO 20 cells does affect their ability to differentiate more than just by DKO of ZC3H20 alone. This indicates that there is redundancy in the system, and there could potentially be other similar ZC3Hs that are able to compensate outside ZC3H20 and ZC3H21 for when these are absent. The ZC3H20 RNAi system used in BF cells, as seen in PF cells (Chapter 3.2.1), could be targeting ZC3H21 due to the region of homology between them, but it could also be targeting other similar ZC3Hs in the *T. brucei* genome. Just 5% of BF cells were able to differentiate in the BF 20 RNAi cell line (a 83% reduction compared to parental cells), and it could be that the RNAi is targeting all potential ZC3Hs that provide redundancy in the differentiation pathway. An alternative explanation, is that the BF DKO 20 (+RNAi 21) cells are still able to differentiate, but due to the coincidence that ZC3H20 is an essential gene in PF cells, the BF DKO 20 cells start to die as they transform into PF cells, and thus a reduction in the proportion of differentiated cells is seen. ZC3H21 is also essential in PF cells (Chapter 3.2.2), and so down-regulation could have an additive detrimental effect on the differentiated PF cell. Whether one or both of these hypotheses is correct cannot be deciphered, but it can be concluded from the data shown that ZC3H20 is not an essential gene BF *T. brucei*, but once triggered to differentiate without ZC3H20, the ability to transform to a PF cell is compromised.

5.3 Cellular effects of TbZC3H20 over-expression in BF *T. brucei*

It appears that ZC3H20 is not essential in the bloodstream life cycle stage, which correlates with the undetectable nature of endogenous ZC3H20 protein. Thus it is possible that ZC3H20 (protein) is down-regulated in BF cells because it is not required in this life cycle stage, or because expression of ZC3H20 in BF *T. brucei* (to PF levels) may be detrimental or disadvantageous to the cell. This has been reported previously for the developmentally regulated PF specific PGKB, which is toxic if expressed in a BF cell [211]. It may also be that, as the data above suggests, ZC3H20 is required during the differentiation from BF to PF, rather than in a normal, proliferating BF cell. To investigate these possibilities, ZC3H20 was over-expressed in BF *T. brucei* to investigate its role within this life cycle stage.

5.3.1 Over-expression of ZC3H20 in BF *T. brucei* causes a growth defect

To over-express an ectopic copy of TbZC3H20, the construct pHD451, as used in section 4.2.1 for tet inducible over-expression in PF cells, was stably transfected into BF SMB (single marker bloodstream) monomorphic cells (see Chapter 2.2). To check the ectopic over-expression of ZC3H20 in the absence and presence of tet, the BF 20 over-expression (BF 20 OeX) cells were induced for 48h and protein isolated. Western analysis was carried out using an antibody to the TY1 tag on the ectopic ZC3H20, and verified that over-expression of ZC3H20 is inducible and detectable (Fig. 5.5A). To assess the effect of ZC3H20 over-expression on growth, cells were grown in the presence (+) or absence (-) of tet for 72h (Fig. 5.5B). The parental cell line (BF SMB) in the presence of tet does not affect cell growth, and BF 20 OeX cells in the absence of tet (BF 20 OeX -) grew similar to the parental BF SMB cells. However, the induced BF 20 OeX cells (BF 20 OeX +) showed a slight growth defect after 24h, and a severe slowing in growth by 48h.

To determine if ZC3H20 over-expression causes a cell cycle defect in BF cells, karyotype analysis was performed on these cells (Fig. 5.5C), as described in Chapter 3.2.1 for PF 20 RNAi cells. This analysis revealed the karyotype profile of induced BF 20 OeX cells was not affected compared to un-induced and parental controls, showing that ZC3H20 over-expression in BF cells does not cause a cell cycle defect. Therefore, over-expression of ZC3H20 in BF cells causes a clear growth defect, and this is not due to a block in cell cycle progression.

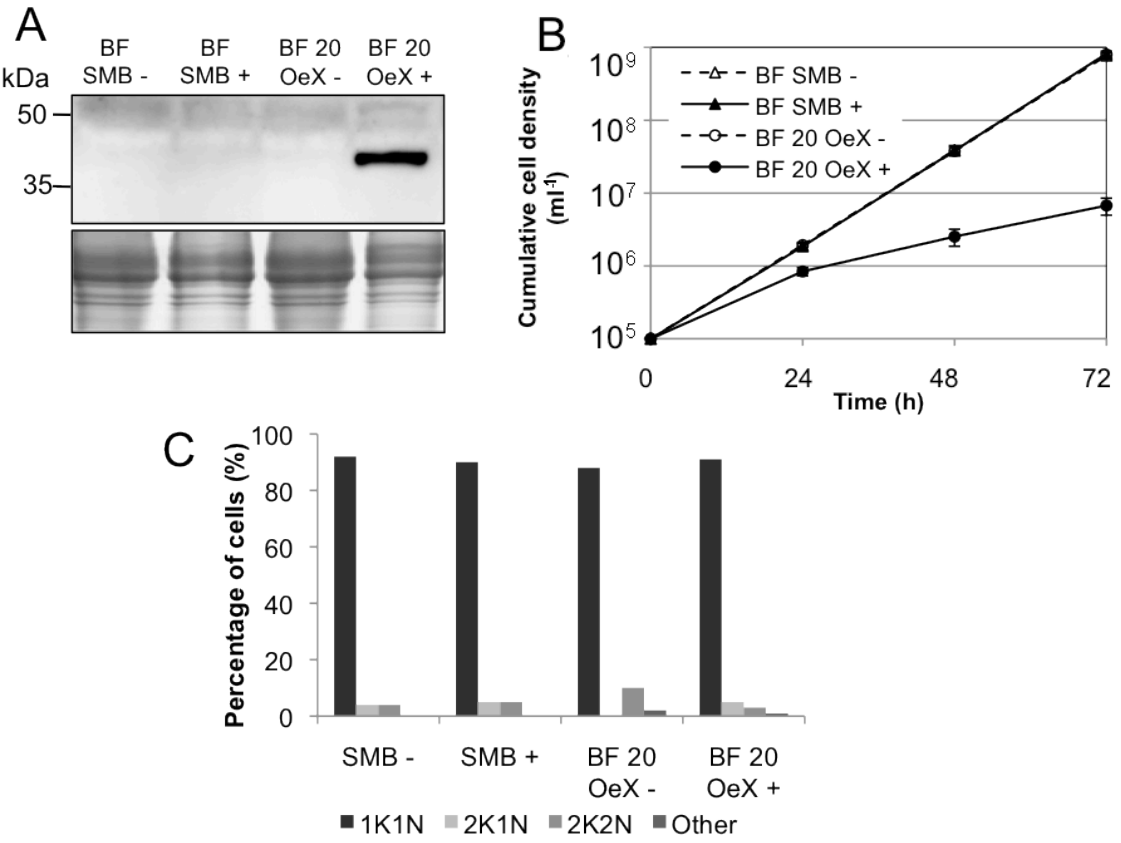


Figure 5.5. Ectopic over-expression of ZC3H20 in BF *T. brucei*

A. Western blot (top panel) of protein isolated from BF 20 OeX cells in the absence (-) or presence (+) of tet after 24h, using an anti-TY1 tag antibody. BF SMB are the parental cell line. The bottom panel shows a Coomassie stain of total protein to show loading of each sample.
B. Growth curve showing the effect of tet induced (+) or uninduced (-) over-expression of ZC3H20 (20 OeX) over 72h in BF cells. SMB is the parental cell line and shows no effect on growth in the presence of tet. Plotted data are mean values from three independent experiments, and error bars show standard deviation.
C. Cell cycle graph of BF cells induced to over-express TbZC3H20. Over 200 cells counted for each population. Cells were grown in absence (-) or presence (+) of tetracycline for 72h. K = kinetoplast, N = nucleus

5.3.2 ZC3H20 over-expression in BF *T. brucei* causes surface expression of procyclin and kinetoplast repositioning

The karyotype analysis did not show any cell cycle defects, but closer inspection of the BF 20 OeX cells via light microscopy revealed a change in morphology for a proportion of cells in the population. These cells did not look as though they were dying, but appeared morphologically like PF cells. Therefore, to investigate if over-expression of ZC3H20 in BF cells causes them to differentiate into PF cells, these cells were stained with an anti-procyclin antibody to the surface

coat of PF cells (Fig. 5.6A). Indeed, it appeared that cells within this population were positive for procyclin expression and this proportion of cells was quantified over 72h (Fig. 5.6B). After 48h, induced over-expression of ZC3H20 in BF cells caused 29% ± 1% (mean±SE) of the cells to express the procyclin coat, suggesting differentiation to PF (Fig. 5.2A field view, Fig. 5.2B).

Gain of the procyclic coat is one of the first programmed events to occur during differentiation from BF to PF (see Introduction 1.2.2). A subsequent differentiation event to occur is kinetoplast repositioning, which is mediated by microtubule outgrowth at the posterior end of the cell [53]. Normally in BF cells, the kinetoplast is located at the very posterior end of the cell, but during differentiation the posterior end grows out by 3μm consequently causing the kinetoplast to reposition equidistance between the posterior end of the cell and its nucleus, the position in a PF cell [8, 13]. Microscope analysis was used to investigate the position of the kinetoplast amongst the BF 20 OeX induced cells. In BF SMB cells, the kinetoplast is located up close to the very posterior end of the cell (BF SMB, Fig. 5.6C). However, amongst the induced BF 20 OeX cell population, a noticeable proportion of cells had repositioned their kinetoplast further away from the posterior end, closer to the nucleus (BF 20 OeX +Tet, Fig. 5.6C). This kinetoplast position is similar to that of a PF cell (PF, Fig. 5.6C).

To quantify this event in procyclin positive BF 20 OeX cells, the length of the kinetoplast from the posterior end of the cell was measured (Fig. 5.6D). As a control, the posterior to kinetoplast distance was measured in normal BF SMBs to compare the expected lengths in a BF cell. Microtubule outgrowth is typically by 3μm [13] and so measurements of posterior to kinetoplast above this dimension are considered to be in the range of that of a PF cell. Within the induced BF 20 OeX cell population that are EP positive after 48h, 16% of these cells have a posterior to kinetoplast distance greater that 3μm, and after 72h 48% of these cells have a distance that would be expected in PF trypanosomes or that are longer than the expected range of a normal BF cell.

Overall, these data show that over-expression of ZC3H20 in BF cells causes the surface expression of procyclin and kinetoplast repositioning events to occur, suggesting that ZC3H20 is triggering BF to PF differentiation.

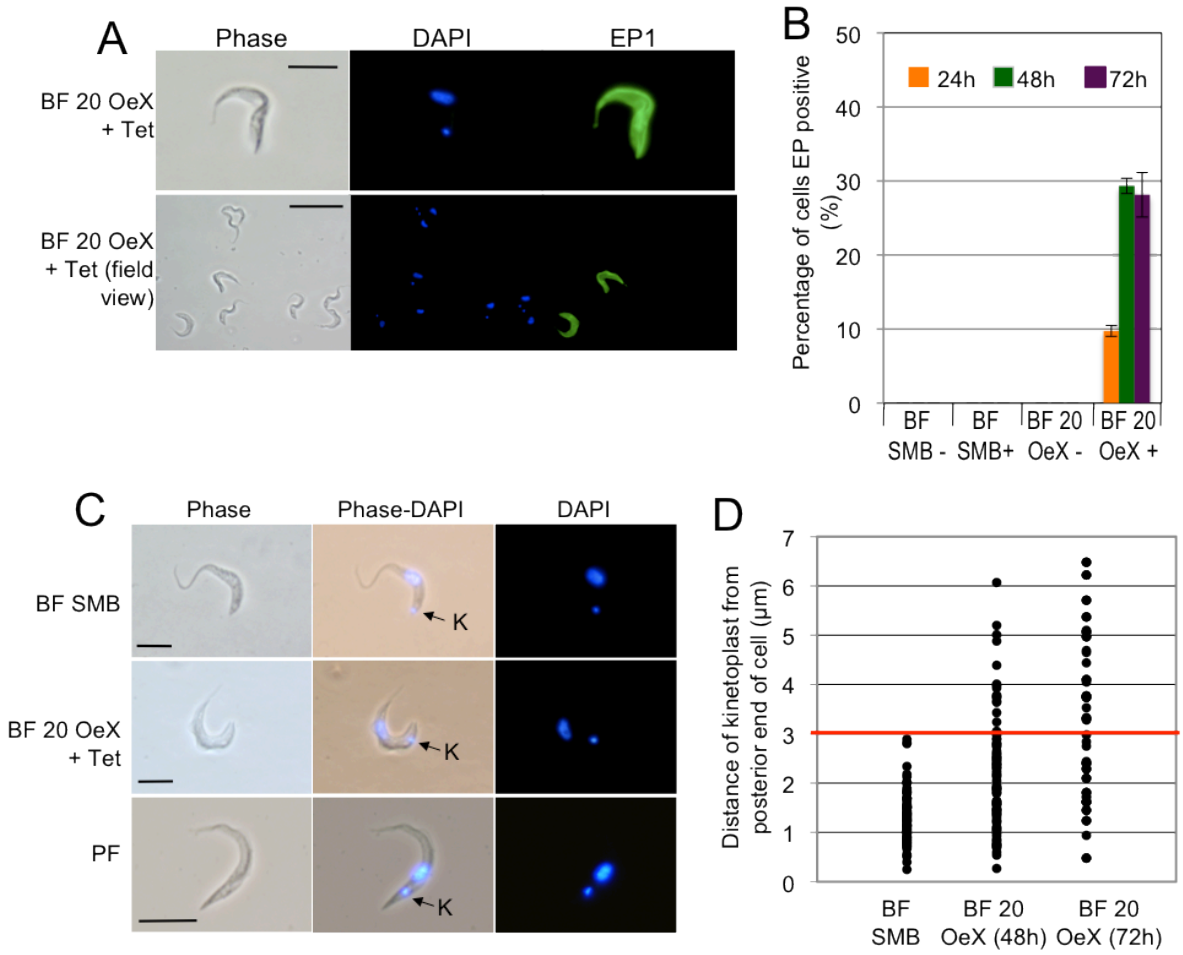


Figure 5.6. Morphological effect of ZC3H20 over-expression in BF *T. brucei*

A. Phase contrast and fluorescent images of BF 20 OeX cells induced with tet for over-expression of ZC3H20 after 48h. The top panel shows a single EP positive cell (scale bar = 10µm), and the bottom panel shows a field view (scale bar = 40µm).
B. Graph to show the percentage of EP positive BF cells after induction with tet (+) or without induction (-) of over-expression of ZC3H20 (20 OeX) over 72h. SMB are the parental cell line grown in the presence or absence of tet. Over 200 cells were counted. Plotted data are mean values from three independent experiments, and error bars show standard error.
C. Phase contrast and fluorescent DAPI images of *T. brucei* cells to show position of kinetoplast (K) in a BF cell induced for over-expression of ZC3H20 (BF 20 OeX +Tet) after 48h. BF SMB and PF shows the position of a kinetoplast in a BF and PF cell, respectively. Scale bar = 10µm.
D. Dot plot to illustrate distance (µm) of kinetoplast to posterior end of each BF 20 OeX cell that is EP1 positive after 48h or 72h of induction. 100 cells were counted. A distance of 0-3µm (below the red line) between kinetoplast and posterior is usually found in bloodstream form trypanosomes, while a distance of 3-7µm (above the red line) is seen in procyclic form trypanosomes.

5.3.3 BF cells triggered to differentiate from ZC3H20 over-expression may be able to re-enter the cell cycle

As mentioned in the Introduction 1.2.2, cell cycle-arrested stumpy cells are pre-adapted for differentiation into PF cells, and consequently, the event of kinetoplast repositioning occurs simultaneously with progression of the cell into its first PF replicative cycle [13, 53]. Stumpy cells are arrested in the G1/G0 phase, and after initiation of differentiation, they synchronously begin S phase after about 6 hours [9]. This proliferative cell cycle re-entry can be assessed visually by noting cells that are in the 2K1N or 2K2N phase whilst expressing EP procyclin. It is suggested that there is a point in the trypanosome cell cycle (probably G0 or G1) in which the cells are receptive to the differentiation signal, and that stumpy cells are homogenously arrested at this receptive window, thus once triggered, differentiate and re-enter the cell cycle synchronously [9, 42]. An asynchronous monomorphic population would have to continue its cell cycle until it got to this receptive window, where these committed cells remain slender in morphology but are functionally equivalent to stumpy forms in terms of their ability to differentiate, a cell state referred to as stumpy* [42, 239]. They then receive the signal to differentiate, or die if they do not continue their cell cycle to receive the signal.

Therefore, within the BF 20 OeX induced population, EP positive cells were assessed for the 2K1N or 2K2N configuration. Figure 5.7 shows a representative cell from the BF 20 OeX population displaying this feature.

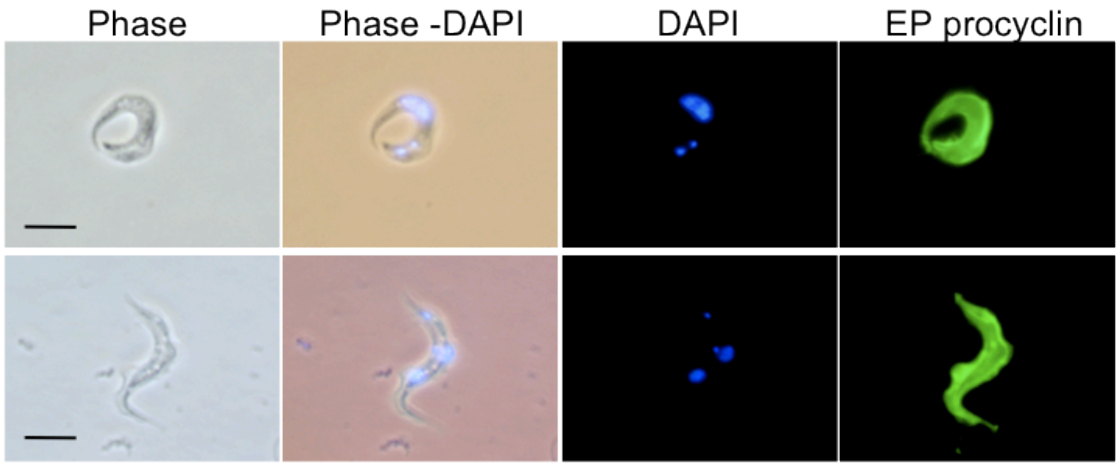


Figure 5.7. Karyotype analysis of EP positive cells after ZC3H20 over-expression in BF *T. brucei*

Phase contrast and fluorescent images of *T. brucei* cells to show karyotype 2K1N (top panel) and 2K2N (bottom panel) present in BF cells induced for over-expression of ZC3H20 after 48h. Both cells are EP procyclin positive. Scale bar = 10μm.

Using the "receptive window" hypothesis, the appearance of BF 20 OeX cells that are EP positive and 2K1N/2K2N suggests that they must have received the signal to differentiate when at the G1/G0 receptive window (as a stumpy* cell), and consequently re-entered the cell cycle. This would imply that BF cells triggered to differentiate from ZC3H20 over-expression are able progress through the pathway and re-enter the cell cycle as a late marker of differentiation.

5.3.4 Both CCCH zinc finger motifs of ZC3H20 are necessary for the function of ZC3H20 in BF *T. brucei*

To determine if neither, one or both of the putative CCCH motifs within ZC3H20 are necessary to cause the differentiation phenotype, the deletion mutants and CCCH zinc finger site-directed mutant constructs used for over-expression in PF (Chapter 4, 4.2.3, Fig 4.4) were transfected into BF SMB cells. Inducible over-expression of each deletion mutant and site-directed mutant in BF cells was verified by isolating total protein from cells grown in the presence (+) or absence (-) of tet for 24h. Western analysis using an antibody, BB2, to the TY1 tag added to the C-terminus to the expressed mutant ZC3H proteins, showed that there was expression of protein of the expected sizes by the induced BF ZC3H20 mutant cells (Fig. 5.8A). These BF ZC3H20 mutant cells were then grown in the presence (+) or absence (not shown) of tet to determine the effect on cell growth over 72h (Fig. 5.8B).

This analysis shows that over-expression of ZC3H20 with a random point mutation (Q333A) was the only cell line that showed a growth defect comparable to over-expression of the "wild-type" ZC3H20. Over-expression of any other ZC3H20 deletion mutant or zinc finger site-directed mutant in BF cells did not cause a growth defect. These cells were also assayed for EP procyclin expression, and over-expression of the ZC3H20 Q333A mutant did cause 10% of BF cells to express procyclin after 48h (Fig. 5.8B). Over-expression of any other ZC3H20 deletion mutant or zinc finger site-directed mutant in BF cells did not cause procyclin expression. This shows that both zinc fingers are required for ZC3H20 to cause the differentiation phenotype, but also that they are not sufficient i.e. the CCCH motifs cannot act alone and the entire protein coding region is necessary.

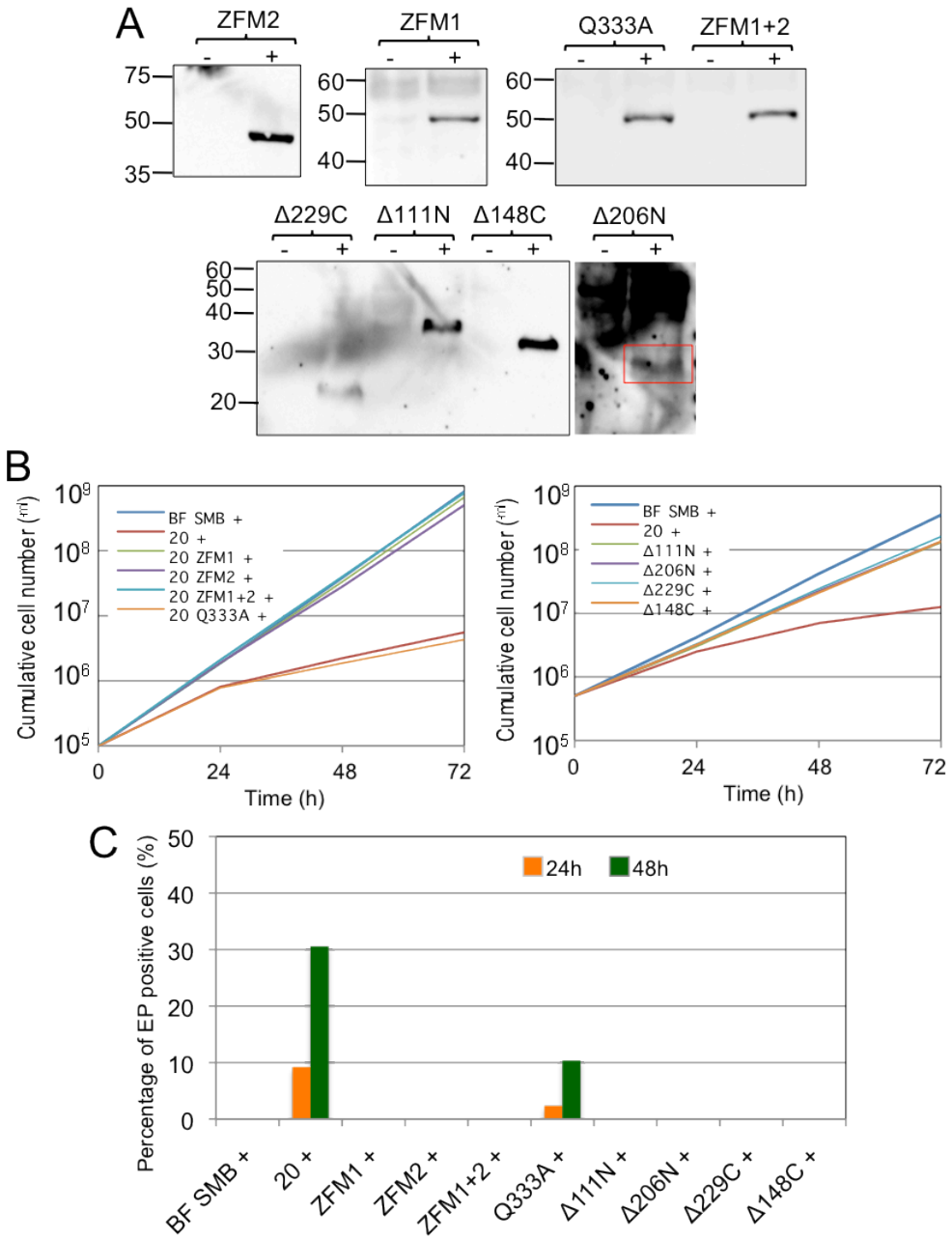


Figure 5.8. Expression of ZC3H20 deletion and point mutants in BF *T. brucei*

A. Western blot of protein isolated from BF 20 OeX site-directed zinc finger motif (ZFM) mutants (top panel) and deletion mutants (bottom panel) in the absence (-) or presence (+) of tet after 24h, using an anti-TY1 tag antibody. The red box indicates the expressed Δ206N mutant on a more exposed blot for identification. Expected sizes: Δ229C, 20.6kDa; Δ111N, 32.2kDa; Δ148C, 29.2kDa; Δ206N, 21.7kDa
B. Growth curve showing the effect of tet induced (+) over-expression of ZC3H20 site-directed mutants (left panel) or deletion mutants (right panel) in BF cells. SMB is the parental cell line and shows no effect on growth in the presence of tet.
C. EP1 positive counts of tet induced (+) over- expression of ZC3H20 site-directed mutants or deletion mutants in BF over 48h. Over 200 cells were counted for each population. ZFM1 = C70A; ZFM2 = C178A; ZFM1+2 = C70A + C178A, of ZC3H20
Δ111N/Δ206N = Deletion of 111/206 aa from N-terminus of ZC3H20
Δ229C/Δ148C = Deletion of 229/148 aa from C-terminus of ZC3H20

5.3.5 Over-expression of the similar ZC3H protein, TbZC3H21 also triggers BF *T. brucei* to differentiate.

As discussed in the PF ZC3H20 RNAi Chapter (3.1.1), ZC3H20 is not the only ZC3H protein with two conventional zinc finger motifs encoded in *T. brucei* genome. Most notably, ZC3H20 shares a high degree sequence homology with TbZC3H21 at the N-terminus regions, which includes the CCCH zinc finger motifs. TbZC3H21 may be able to function similarly to ZC3H20, and so ZC3H21 was investigated for over-expression in BF cells. The full coding region of ZC3H21 was cloned into the over-expression vector pHD451 and transfected into BF SMB cells as described above for ZC3H20. Over-expression of ZC3H21 was induced by addition of tet to BF 21 OeX cells. Growth curves were recorded, and showed that over-expression of ZC3H21 in BF cells causes a growth defect (Fig. 5.9A). These cells were also assayed for EP procyclin expression, and indeed, over-expression of ZC3H21 did cause 10% of BF cells to express procyclin after 48h (Fig. 5.9B). This indicates that ZC3H21 over-expression in BF *T. brucei* can, in addition to ZC3H20, causes cells to differentiate to PF, and suggests that there is functional redundancy in the genome for ZC3Hs, at least between ZC3H20 and ZC3H21.

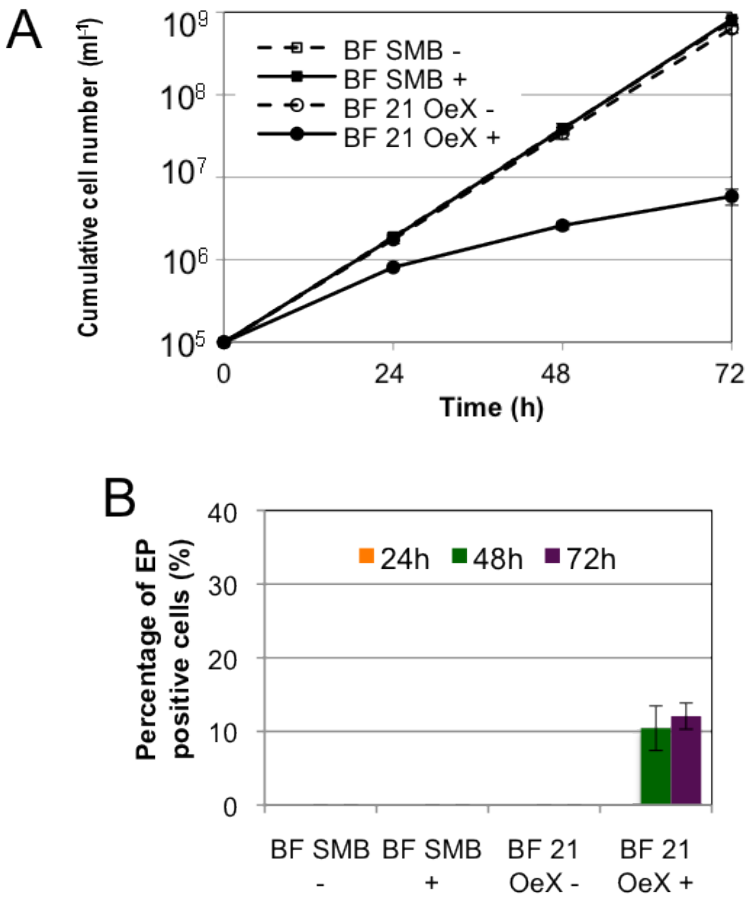


Figure 5.9. Ectopic over-expression of ZC3H21 in BF *T. brucei*

A. Growth curve showing the effect of tet induced (+) or uninduced (-) over-expression of TbZC3H21 in BF cells. SMB is the parental cell line and shows no effect on growth in the presence of tet. Plotted data are mean values from three independent experiments, and error bars show standard deviation.
B. EP1 positive counts of tet induced (+) and uninduced (-) over- expression of TbZC3H21 in BF over 72h. Over 200 cells were counted for each population. Plotted data are mean values from three independent experiments, and error bars show standard error.

5.3.6 Discussion of section 5.3

Over-expression of ZC3H20 causes a significant proportion of BF cells to express procyclin on the cell surface, suggesting that these cells are differentiating to the procyclic insect form. This phenotype is dependent on the presence and functionality of both CCCH zinc finger motifs, and on the integrity of the entire protein. This phenotype can also be caused by over-expression of a similar ZC3H, TbZC3H21, albeit to a lesser extent than ZC3H20. These observations suggest redundancy in the genome for this family of putative RNA-binding proteins.

In a pleomorphic cell population at high density, the bloodstream slender form is triggered to transform into the stumpy form. As discussed in the Introduction chapter (1.2.2), this stumpy form is pre-adapted for differentiation, such that after the signal to differentiate EP procyclin (mRNA) expression occurs after 2h [53]. The peak of EP expression seen by the BF 20 OeX cells however occurs at a much slower rate after 2 days. Importantly however, these are culture adapted monomorphic cell lines derived from continual passage of bloodstream parasites and have lost the ability to generate division-arrested stumpy forms. As a result, these cells divide and differentiate asynchronously, and have slower differentiation kinetics than synchronous stumpy form cells [9]. Analysis of the posterior to kinetoplast distances of BF 20 OeX cells that were procyclin positive showed that these cells were repositioning their kinetoplast as the next programmed differentiation event. The proportion of EP positive BF 20 OeX cells does not increase after 48h, but the number of these cells that have a repositioned kinetoplast continued to increase by 72h, showing the progression of differentiation events within these cells. In conclusion, over-expression of ZC3H20 in BF *T. brucei* causes a significant proportion of cells to differentiate to PF, as shown by surface expression of procyclin and kinetoplast repositioning. This suggests, remarkably, that ZC3H20 is a molecular trigger of differentiation.

The results indicate that BF cells triggered to differentiate by ZC3H20 over-expression may be able to re-enter the cell cycle as one of the late markers of differentiation into a proliferative PF cell. This is of course dependent on the "receptive window" hypothesis regarding the requirement of a BF cell to enter a specific cell cycle phase (G0/G1) before gaining the ability to receive the differentiation signal. However, an important consideration is that Li et al. [240] show that cells are still able to gain EP procyclin in the absence of cell cycle re-entry and progression. Their study demonstrated monomorphic BF cells trapped in either G1 or G2 can still enter and complete the process of differentiation, suggesting that cells do not need to progress through the cell cycle to reach the receptive G0/G1 window for differentiation [240]. If this is the case, the appearance of 2K1N/2K2N EP1 positive cells in the BF 20 OeX population does not necessarily mean that they have re-entered the cell cycle and may have just been able to transform to procyclic form as a 2K1N/2K2N cell when signalled to differentiate. Additionally, Matthews et al. [9] demonstrate that inhibition of S phase does not

disrupt cellular differentiation as the kinetoplast is repositioned and the differentiation marker CAP5.5 (usually after initiation of S-phase) was detected. Therefore, progression through the differentiation pathway can be uncoupled from progression through the cell cycle, showing that they are co-incident processes and not dependent on each other for transformation into the procyclic form [9, 241]. Whether or not the BF 20 OeX cells have truly re-entered the cell cycle, it is still possible to conclude that they have received a signal to differentiate and have successfully transformed morphologically into procyclic cells.

5.4 ZC3H20 as a molecular trigger for differentiation compared to chemical induction and temperature shift *in vitro*

Over-expression of ZC3H20 in BF cells causes 30% to differentiate to PF after 48h (section 5.3.2) in the absence of *cis*-aconitate and shift to 27°C, which are differentiation triggers widely used *in vitro*. A temperature shift from 37°C to 27°C alone is not sufficient to induce differentiation [49]. However addition of 6mM *cis*-aconitate to BF cells at 37°C has been shown to trigger differentiation of both monomorphic and stumpy cells, albeit at different kinetics [241, 242]. Another study has reported that ablation of the protein tyrosine phosphatase TbPTP1B, or inhibiting PTP1B activity using the chemical BZ3, causes 10% of BF monomorphic cells (after 18h) and >70% of stumpy cells (after 6h) to express EP procyclin at 37°C, showing differentiation to PF [243]. Therefore, to understand how ZC3H20 acts as a molecular trigger in the context of what is already reported for inducing differentiation *in vitro*, these environmental triggers were investigated in our cell culture system.

5.4.1 Triggering differentiation in monomorphic BF SMB cells

The effect of *cis*-aconitate and/or temperature shift from 37°C or 27°C to induce differentiation was determined for the parental BF cells (BF SMB) used for over-expression of ZC3H20. These cells were grown in the presence and absence of 6mM *cis*-aconitate with or without a shift to 27°C for 48h, and assayed for EP procyclin expression (Fig. 5.10A). After 48h, addition of *cis*-aconitate alone (at 37°C), or shift in temperature to 27°C alone, only 3% and 4% of BF SMB cells

differentiated, respectively. However, in the presence of both triggers after 48h, 48% of BF SMB cells expressed EP procyclin (Fig. 5.10A). This suggests that both *cis*-aconitate and shift to 27°C are required together to be able to trigger these BF cells to differentiate.

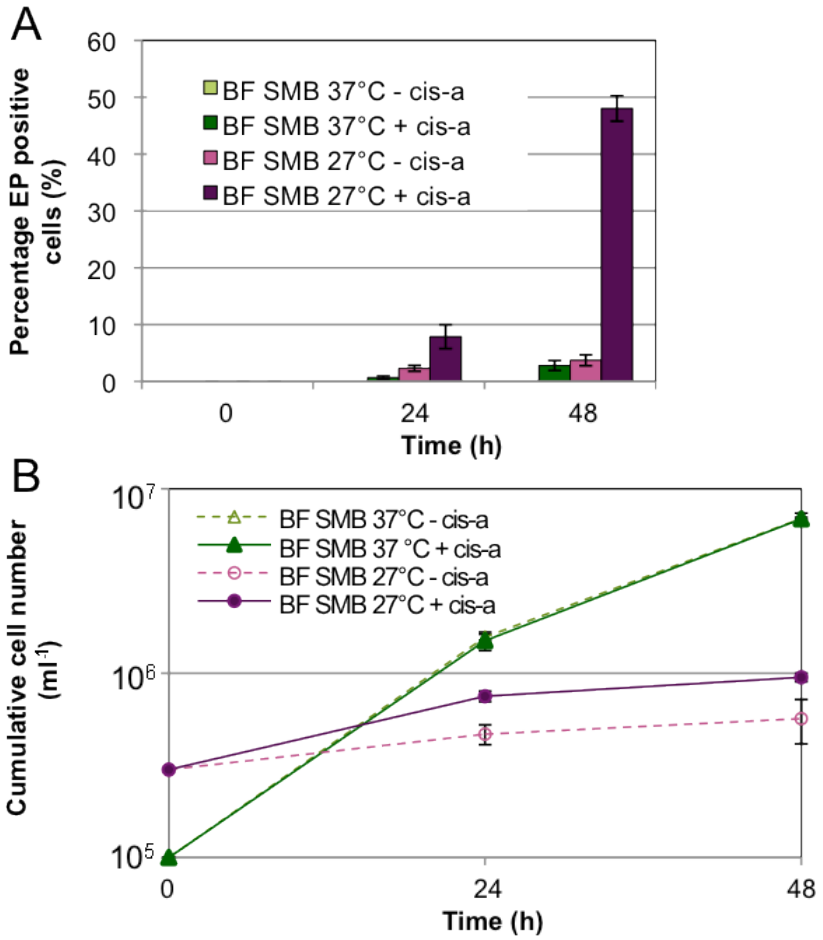


Figure 5.10. Treatment of BF *T. brucei* with *cis*-aconitate and a temperature drop to trigger differentiation to PF

A. Graph to show the percentage of EP positive BF SMB with (+) or without (-) addition of 6mM *cis*-aconitate (cis-a) at 37°C or 27°C over 48h. Over 200 cells were counted. Plotted data are mean values from three independent experiments, and error bars show standard error.
B. Growth curve of BF SMB cells showing the effect with (+) or without (-) addition of 6mM *cis*-aconitate (cis-a) at 37°C or 27°C over 48h. Plotted data are mean values from three independent experiments, and error bars show standard deviation.

A growth curve was also recorded for each cell population (Fig. 5.10B), which showed that cells kept at 37°C continued to grow, but cells shifted to 27°C in the

presence and absence of *cis*-aconitate slowed their growth dramatically after 48h. Thus, slowed growth of these BF cells occurs at 27°C irrespective of whether they are triggered to differentiate or not by *cis*-aconitate, and this agrees with previous reports of monomorphic cells shifted to grow at 27°C [242].

To demonstrate the effect of the TbPTP1B inhibitor BZ3 (3-(3,5-Di-bromo-4-hydroxy-benzoyl)-2-ethyl benzofuran –6-sulfonic acid-(4-(thiazol-2-ylsulfamyl)-phenyl) amide) to induce differentiation, BF SMB cells were grown in the presence and absence of 150μM BZ3 with or without a shift to 27°C for 48h, and assayed for EP procyclin expression (Fig. 5.11A). After 48h, just addition of BZ3 at 37°C only caused 2% of BF SMB cells to express EP procyclin, showing that BZ3 alone cannot trigger differentiation effectively. Again, this analysis showed that exposure of BF SMB cells to a shift in temperature to 27% was not sufficient to trigger differentiation as <1% of cells expressed EP procyclin. In contrast, the presence of BZ3 and a temperature shift to 27°C caused 40% of cells to express EP procyclin, which suggests that both of these are required to induce differentiation in these BF cells.

A growth curve was recorded for each cell population (Fig. 5.11B), which showed that cells exposed to BZ3 even at 37°C slowed their growth after 48h, suggesting this inhibitor may have a detrimental effect on the cells (in the absence of showing differentiation). As shown and discussed above, BF SMB cells shifted to 27°C hardly grew over 48h.

Overall, these data show that addition of *cis*-aconitate or BZ3 to these BF SMB cells at 37°C does not induce differentiation, but in combination with a shift to 27°C, causes nearly half the population to differentiate within 48h.

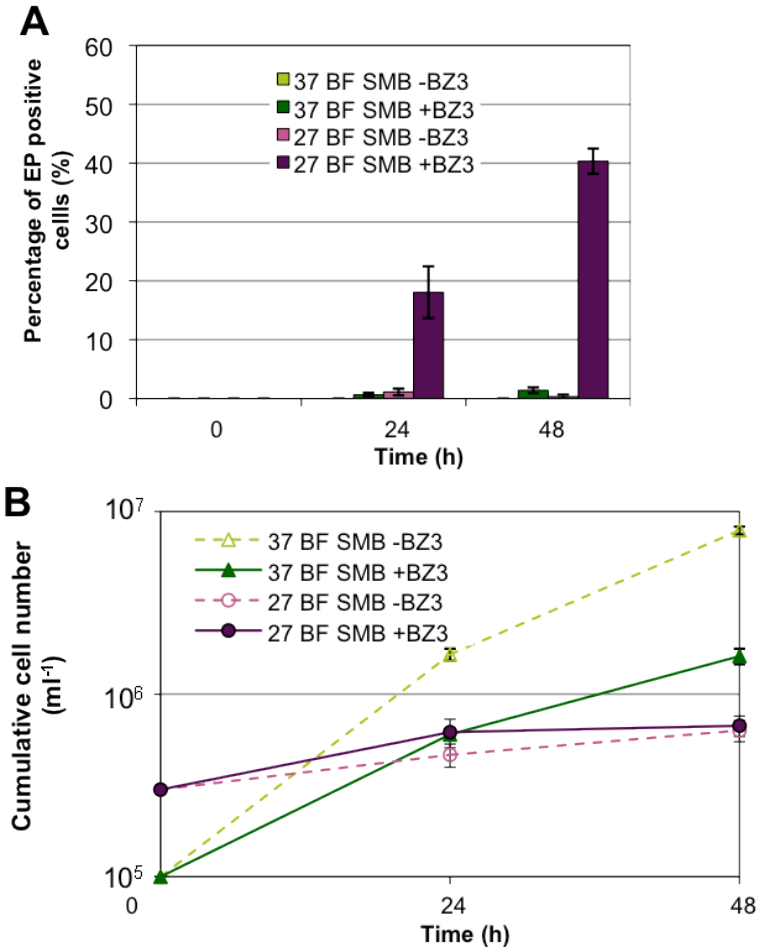


Figure 5.11. Treatment of BF *T. brucei* with TbPT1B inhibitor to trigger differentiation to PF

A. Graph to show the percentage of EP positive BF SMB with (+) or without (-) addition of BZ3 (150μM) at 37°C or 27°C over 48h. Over 200 cells were counted. Plotted data are mean values from three independent experiments, and error bars show standard error. B. Growth curve of BF SMB cells showing the effect with (+) or without (-) addition of BZ3 (150μM) at 37°C or 27°C over 48h. Plotted data are mean values from three independent experiments, and error bars show standard deviation.

5.4.2 ZC3H20 over-expression in combination with a temperature drop to 27°C triggers a greater proportion of BF cells to differentiate than ZC3H20 alone

As shown above, the addition of *cis*-aconitate or BZ3 alone to BF cells at 37°C triggers less than 5% of cells to differentiate, but this increases to nearly half the population if the BF cells are also shifted to 27°C. Over-expression of ZC3H20 alone at 37°C causes a third of the BF SMB cells to differentiate (Fig. 5.6B); already a more effective trigger of differentiation than the two chemical inducers. However, a shift to 27°C in addition to over-expressing ZC3H20 was tested to

determine if a temperature drop causes improved differentiation as seen with the chemical inducers. An experiment was set up that used a starter culture of BF 20 OeX cells at 37°C, at which point tet was added to induce over-expression of ZC3H20. Sample cultures were then taken from this starter culture and moved to 27°C at time 0h, 24h and 48h after tet induction, and the starter culture remained at 37°C for the entire experiment. Expression of EP procyclin was analysed for each sample population 72h to assess their differentiation profiles (Fig. 5.12). Over-expression of ZC3H20 alone at 37°C induced 33% of BF cells to differentiate after 48h, but if these cells were shifted to 27°C after 24h or 48h of ZC3H20 over-expression, a greater proportion of cells were able to differentiate than if they were kept at 37°C. Specifically, BF cells that are induced for over-expression of ZC3H20 at 37°C for 24h and then shifted to 27°C, caused 60% differentiation after 48h. Interestingly, BF 20 OeX cells shifted immediately to 27°C after induction of ZC3H20 over-expression caused dramatic differentiation of 74% 48h compared to the starter culture at 37°C. Thus it appears that temperature shift to 27°C enables a greater proportion of BF cells to differentiate when triggered by over-expression of ZC3H20 than if kept at 37°C.

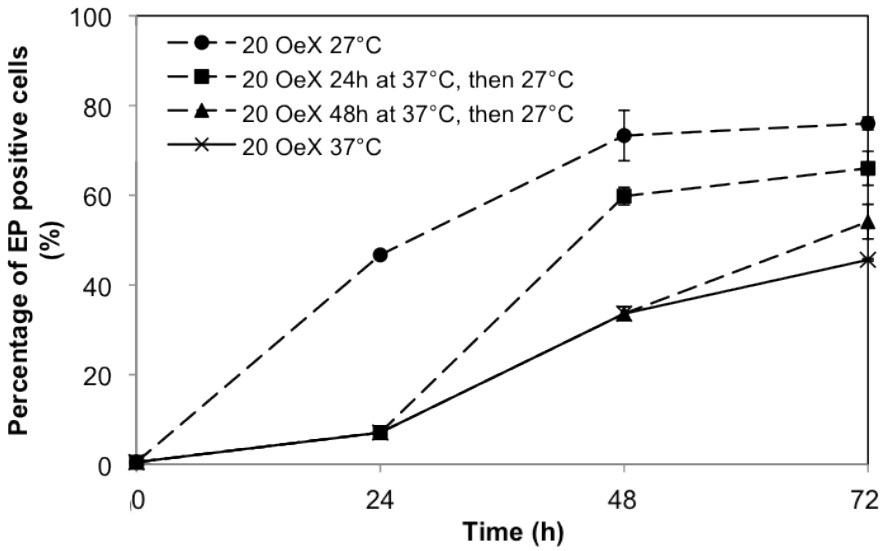


Figure 5.12. Effect of temperature drop in combination with ZC3H20 over-expression of BF *T. brucei* to trigger differentiation

Graph to show the percentage of EP procyclin positive cells after the induction of ZC3H20 over-expression in BF cells and shifting cells from 37°C to 27°C over 72h. Plotted data are mean values from three independent experiments, and error bars show standard error.

5.4.3 Discussion of section 5.4

These data show that exposure of BF SMB cells to the chemical triggers *cis*-aconitate or BZ3 at 37°C, or to a temperature shift to 27°C triggers only very few cells to differentiate after 48h. These low proportions of differentiation are reported for these monomorphic BF cell lines when exposed to these individual triggers [242, 243]. This is in contrast to what is shown for BF stumpy cells where addition of *cis*-aconitate or BZ3 at 37°C causes rapid and efficient differentiation [241, 243]. One study suggests a model whereby at 37°C in the presence of *cis*-aconitate, monomorphic BF cells either undergo 'abortive' transformation (differentiation to a non-dividing PF), or they retain the properties of a dividing BF cell [242]. This same study then shows that shifting monomorphic BF cells to 27°C caused the cells to retain the BF coat and morphology, but they did not divide and eventually died, while a few cells were able to transform after a week [242]. Indeed, the data presented shows that the BF cells were not transforming at 37°C in the presence of *cis*-aconitate, but the growth curve shows they were still continuing to divide normally. Also, if the BF cells were just shifted to 27°C, they did not transform, but just stopped dividing.

When BF SMB cells were exposed to *cis*-aconitate or BZ3, combined with a shift to 27°C, nearly half of the cells were able to differentiate after 48h. This suggests that there is something associated with the drop in temperature that enables more cells to differentiate. Recently, several studies have found that a drop in temperature to 20°C (a cold shock, which is compatible with the temperature of feeding flies at dusk) increases the expression and alters the distribution of surface carboxylate transporters known as PAD proteins, which are then able to transport *cis*-aconitate at physiologically relevant levels into the cell [49, 50]. By using high concentrations of *cis*-aconitate (and most likely with BZ3), this bypasses the need for the hypersensitivity (up-regulation of transporters) induced upon cold shock, and thus at 37 °C stumpy cells (which still express PAD to a lower degree) are able to rapidly differentiate [49, 50]. Monomorphic BF cells are reported to express undetectable levels of PAD at 37°C [50], which correlates with the low differentiation levels in these cells. It is suggested that other transporters may drive signalling on the surface of these cells [50]. There is no report if PAD/other transporters are upregulated in the cell at 27°C, but the increased proportion of cells that are able to differentiate in the presence of both

chemical and temperature shift, when individually they do not do so, could suggest improved transport of *cis*-aconitate/BZ3 into the cell in light of these recent findings.

Over-expression of ZC3H20 in BF cells at 37°C causes a higher proportion of cells to differentiate than *cis*-aconitate exposure at 37°C. This could be explained, as discussed above, that *cis*-aconitate is a chemical trigger that needs to be transported into the cells, but that ZC3H20 is an internal molecular trigger. However, even with a temperature drop to 27°C to allow *cis*-aconitiate to be transported more efficiently, over-expression of ZC3H20 with 27°C shift causes an even greater proportion of cells able to differentiate. As ZC3H20 does not require transport into the cell, the temperature drop must affect a process inside the cell to allow more effective differentiation. This finding demonstrated that shifting monomorphic BF cells to 27°C causes a growth arrest. The growth arrest could be a response to the stress of a 'cold shock', or that exposure of the cells to 27°C triggers an event in the cell, such as that seen for the up-regulation of the PAD transporters, which in combination with the over-expression of ZC3H20 induces differentiation in a high proportion of cells. Either way, an interesting point to note is that only BF stumpy cells are able to route EP procyclin to the surface of the cell, termed surface access control, which restricts EP from surface exposure in proliferating slender cells, even if procyclin is ectopically over-expressed [49]. With evidence that slender BF cells are rapidly killed in the tsetse midgut [244] and that they have this surface access control for procyclin expression, it is implicated that slender cells cannot differentiate. However, monomorphic BF cells can differentiate suggesting that these cells must display stumpy-like characteristics, such as the loss of surface access control. Stumpy cells are cell cycle and growth arrested at high density [245], but monomorphic BF cells continue to proliferate in culture. It could be suggested that the shift to 27°C provides the monomorphic cell with another stumpy characteristic i.e. growth arrest. This could be coincidental as a stress response, or hypothetically, the stumpy-like monomorphic cell is triggered by the temperature drop to prepare for differentiation, and thus responds to ZC3H20 as a molecular trigger.

A recent microarray study shows the changes in gene expression that occur during differentiation of *in vitro* cultured BF to PF, using *cis*-aconitate and temperature shift to 27°C to induce differentiation [59]. This analysis identifies that

ZC3H20 is rapidly upregulated during the first hour of differentiation, and then decreases over the next 24h, increases for another 24h before then slowly decreasing down to PF levels [59]. The study also suggests that the *in vitro* BF "high density" cultures underwent a transition to stumpy-like gene expression during the first 12 hours after triggering differentiation [59]. Thus, ZC3H20 may be required to initiate differentiation. Exposing monomorphic BF cells to a temperature shift that may increase stumpy-like gene expression, in combination with ZC3H20 over-expression, is an effective trigger to induce differentiation to a PF cell.

5.5 Capacity of BF monomorphic cell lines to differentiate

This chapter has shown so far that over-expression of ZC3H20 in BF cells triggers differentiation. After 48h of induction, the peak of EP expression is seen in the population, which is of much slower kinetics than seen by BF stumpy cells, where 90% of cells express EP within 2h upon induction [9]. As well as pre-adapting the cell for differentiation via changes in for example, energy metabolism, transporter expression and surface access control, stumpy cells are growth arrested and stabilised in the G0/G1 phase of the cell cycle [246], thus when triggered, they differentiate synchronously with rapid kinetics. The reduced ability of monomorphic BF cells to differentiate as efficiently and rapidly as stumpy forms is not well understood. One study has reported that reverting a differentiation defective monomorphic cell line to pleomorphism, allowing them to produce stumpy forms, rescued the differentiation defect and restored their capacity to differentiate [42]. This study thus refers to the essential nature of cells to display stumpy characteristics in order to differentiate effectively. As explained above (5.4.3), the fact that monomorphic cells can differentiate but slender cells from a pleomorphic population cannot, suggests that although morphologically slender, monomorphic cells must be capable of displaying stumpy-like characteristic that enable them to differentiate. This acquisition of stumpy-like characteristics required for the capacity to differentiate has been suggested to occur in a transitional state from slender to stumpy forms, referred to as stumpy* [42, 239].

One suggestion as to why monomorphic cells differentiate with slower kinetics is because they are not cell cycle arrested in G1/G0 (like stumpy cells),

they must continue the cell cycle to reach a 'receptive window' in G1/G0 at which the cells are competent to differentiate, consequently causing asynchronous differentiation [9]. Secondly, at high density, proliferating slender forms are triggered to cease growth and differentiate to a stumpy form cell [245]. This is induced by a "stumpy induction factor" released by slender cells which accumulates at high density, but monomorphic cells are not responsive to this factor, and so do not growth arrest to differentiate to stumpy form [247]. Finally, in consideration of these two points raised, the inability to display stumpy characteristics prevents effective differentiation of the monomorphic cell line. Thus, one study has used a chemical cAMP analogue, pCPTcAMP to effectively induce slender-to-stumpy differentiation of monomorphic BF cells, these induced stumpy forms were then able to transform efficiently into procyclic form cells when induced [248].

To investigate if the nature of displaying stumpy characteristics affects the capacity of a monomorphic BF to differentiate when triggered by ZC3H20 over-expression, the requirement of cell cycle position, cell density and a chemical stumpy inducing factor were tested.

5.5.1 Monomorphic BF cells do not require a position in the cell cycle to receive the signal from ZC3H20 to differentiate

Stumpy BF cells are cell cycle arrested in the G1/G0 phase, such that once they received the signal to differentiate, are able to transform and re-enter the cell cycle synchronously. A suggestion behind the asynchronous differentiation of monomorphic BF cells is that they must be at a "receptive window" in the cell cycle (G1/G0) to receive the differentiation signal [9, 42]. Hence, monomorphic cells must continue cell cycling until they reach this "window", then progress from G1 to G0 or acquire competency to differentiate (to stumpy*) before transforming to PF [9, 42], consequently causing asynchronous differentiation.

To test this hypothesis, BF 20 Oex cells were treated with hydroxyurea, a chemical that can be used to synchronise the *T. brucei* cell cycle [249]. Following synchronisation with hydroxyurea, ZC3H20 over-expression can be induced and EP procyclin expression analysis used to determine if a greater proportion of cells differentiate at one time compared to (normal) asynchronous differentiation. Specifically, BF 20 OeX cells were treated in the presence or absence of

hydroxyurea for 6h (Fig. 5.13A). Addition of hydroxyurea caused an enrichment of cells in the S phase (an accumulation of 2K1N cells) compared to untreated cells that showed a normal karyotypic profile (explained in Chapter 3.2.1).

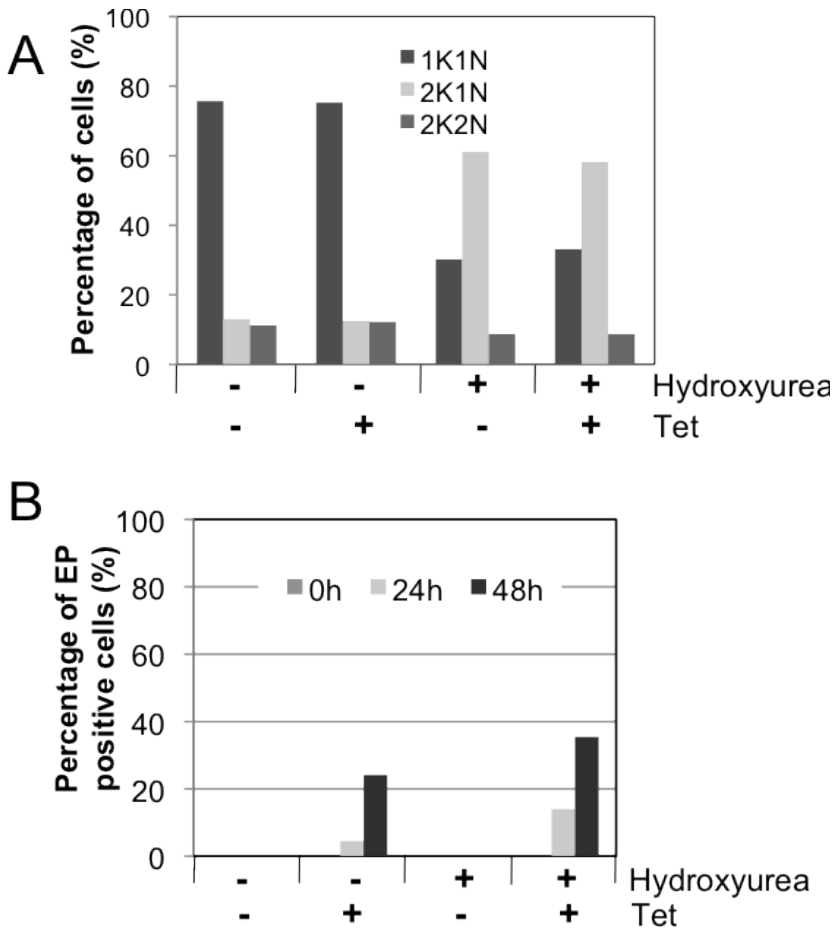


Figure 5.13. Effect of cell cycle synchronisation on the differentiation kinetics of BF *T. brucei* induced for ZC3H20 over-expression

A. Cell cycle analysis of BF 20 OeX cells in the presence (+) or absence (-) of hydroxyurea (10µg ml^{-1}) for 6h, to cause an accumulation of cells in the S phase/2K1N karyotype. The BF 20 OeX cells were then grown in the presence (+) or absence (-) of tet after the 6h pre-incubation with hydroxyurea. Over 200 cells were counted.
B. EP1 procyclin positive counts BF 20 OeX cells grown in the presence (+) or absence (-) of tet over 48h after the 6h pre-incubation with hydroxyurea. Over 200 cells were counted.
C. EP1 procyclin positive counts BF 20 OeX cells grown in the presence of tet over 48h after cells were grown up to a cell density of $1x10^6$ ml^{-1} (log phase growth) or up to a cell density of $4x10^6$ ml^{-1} (stationary phase growth). Over 200 cells were counted.

The hydroxyurea was then washed out to allow progression of the cell cycle once again, and it is assumed that the cells are synchronous for one complete cell cycle (approximately 8h), before returning to asynchrony. Thus, as soon as the

hydroxyurea was washed out, cells were induced or uninduced for ZC3H20 over-expression. Each cell population was assayed for procyclin surface expression to determine the percentage of differentiation over 3 days (Fig. 5.13B).

The BF 20 OeX cells not treated with hydroxyurea i.e. asynchronous, but then induced for ZC3H20 over-expression (BF 20 OeX –HU +Tet) shows 13% of differentiated cells after 24h, and then increases to 33% after 48h. This result is as expected for over-expression of ZC3H20 in BF cells at 37°C (Section 5.3.2). If monomorphic cells continue their cell cycle to a "window" that elicits competence to differentiate, synchronisation should allow them to pass through the window at the same time, and hence see a shift in the differentiated population to one time point i.e. they all differentiate by 24h or 48h. However, the differentiation profile of cell cycle synchronised and induced BF 20 OeX cells was not shown to be different compared to asynchronous and induced BF 20 OeX cells, and the synchronised cells did not differentiate at the same time (Fig. 5.13B). Cells grown in the presence or absence of hydroxyurea, but not induced for ZC2H20 over-expression did not differentiate (Fig. 5.13B). These data therefore suggests that in order to receive the signal from ZC3H20 to differentiate, these cells do not pass through a "receptive window" in the cell cycle to acquire the ability to transform.

5.5.2 Cell density does not affect the ability of monomorphic BF cells to differentiate when triggered by ZC3H20 over-expression

High cell density of pleomorphic *T. brucei* results in growth arrest and triggers slender cells to transform into cell cycle arrested stumpy cells [245]. Trypanosomes possess a cell density sensing mechanism, and it has been shown that at high cell density, there is an accumulation of a factor produced by the slender BF cells, called stumpy induction factor (SIF), which causes then growth arrest and differentiation to a stumpy cell [247]. In contrast, monomorphic cell lines have reduced sensitivity to density sensing, thus do not respond to SIF and do not transform into morphologically stumpy cells [247].

It is possible that due to the nature of isolating monomorphic cell lines from various passages from different laboratories, different cell lines display a range of abilities to differentiate, and may demonstrate a spectrum of forms from extreme monomorphism (i.e. like a true slender cell) to extreme polymorphism, and intermediates between these forms [53, 239]. Consequently, a proportion of cells

within the population may still be responsive to cell density with varying sensitivity, thus shift to a stumpy* cell/obtain stumpy characteristics and then be able to receive the differentiation signal to transform into a procyclic cell. Therefore, varying cell densities were tested for their effect on the proportion of BF cells able to differentiate when induced for ZC3H20 over-expression, with the rationale that more cells may be able to receive the signal to differentiate once grown to a high density. Firstly, BF 20 OeX cells were grown up to two densities: $1x10^6$ ml^{-1}, when the culture is in log phase growth, and $4x10^6$ ml^{-1}, when the culture is entering stationary phase growth. Both cultures were then diluted back to $2x10^5$ ml^{-1} and induced with tet for ZC3H20 over-expression. The cultures were then assayed for EP procyclin expression over 48h (Fig. 5.14).

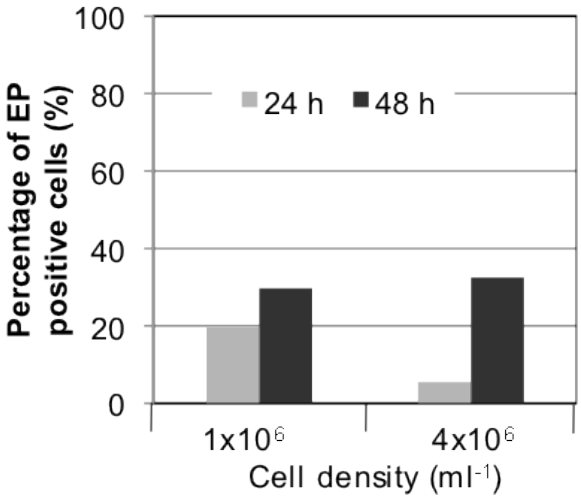


Figure 5.14. Effect of cell density on the differentiation ability of BF *T. brucei* induced for ZC3H20 over-expression

EP1 procyclin positive counts BF 20 OeX cells grown in the presence of tet over 48h after cells were grown up to a cell density of $1x10^6$ ml^{-1} (log phase growth) or up to a cell density of $4x10^6$ ml^{-1} (stationary phase growth). Over 200 cells were counted.

It appears that there is no difference in the differentiation ability of cells grown to high density compared to cells grown to a low/normal density. Therefore, cell density does not affect the capacity of a monomorphic BF cell to differentiate when triggered by ZC3H20.

5.5.3 Inducing stumpy characteristics increases the ability of monomorphic BF cells to differentiate when triggered by ZC3H20 over-expression

Vassella et al. [247] showed that the SIF density sensing mechanism is transduced through signalling the cAMP pathway. The study therefore tested a membrane permeable cAMP agonist derivative, 8-(4-chlorophenylthio)-cAMP (pCPTcAMP) on pleomorphic slender bloodstream trypanosomes. This treatment resulted in cell cycle arrest and induced stumpy cell morphology. Another study used this pCPTcAMP to effectively induce slender-to-stumpy differentiation of monomorphic BF cells [248]. These induced stumpy forms were then able to transform efficiently into procyclic form cells when given *cis*-aconitate and shifted to 27°C. However, a more recent study suggested that it is the hydrolysis products of cAMP analogues i.e. 5'AMP/adensosine analogues, that prevent proliferation of trypanosomes, and that these have a more potent effect on the cell [250]. To investigate if treating monomorphic BF cells to become stumpy-like increases their competency to differentiate when triggered by ZC3H20 over-expression, the membrane-permeable 5'AMP analogue and cAMP analogue were tested on BF 20 OeX cells.

Firstly, BF 20 OeX cells were incubated with 8-pCPT-2'-O-Me-5'-AMP (AMP analogue) or the cAMP analogue at 37°C, and the growth recorded over 48h (Fig. 5.15A). After 24h, both the 5'AMP analogue and cAMP analogue caused cell growth arrest, suggesting that the BF cells were transforming into stumpy-like cells from triggering the cAMP pathway. However, the 5' AMP analogue had a quick and severe effect on cell growth within 24h (Fig. 5.15A) compared to 48h used by Laxman et al [250], and thus was not used in any further analysis.

After 48h, the cAMP treated cells were then induced or uninduced with tet and left at 37°C or shifted to 27°C. Each cell population was assayed for procyclin surface expression over the 3-day experiment (Fig. 5.15B). A control cell population of untreated BF 20 OeX cells was also tested to allow comparison with the cAMP treated cells (Fig. 5.15B). The untreated cAMP control cultures induced for ZC3H20 over-expression at 37°C or 27°C, caused 7% and 34% differentiation, respectively, after 24h (Fig. 5.15B, 72h), as expected from previous data (Fig. 5.12). BF 20 OeX cells that were treated with cAMP for 48h, and then induced with tet at 37°C or 27°C for 24h, caused 36% and 54% differentiation respectively (Fig. 5.15B, 72h). Thus, induced BF 20 OeX cells kept at 37°C treated with cAMP

causes a 5-fold increase in the capability to differentiate compared to untreated cAMP cells induced for ZC3H20 over-expression.

Treatment with cAMP without inducing overexpression of ZC3H20 at 37°C or shift to 27°C, however caused 23% and 68% differentiation, respectively. To determine if cAMP alone causes BF cells to differentiate, or if this is specific to uninduced BF 20 OeX cells, parental BF SMB cells were incubated in the presence of cAMP for 2 days and left at 37°C (Fig. 5.15C). EP procyclin counts showed that just 3% of BF SMB cells treated with cAMP were triggered to differentiate, therefore indicating that the uninduced BF 20 OeX cells may have leaky ectopic expression of ZC3H20 that is enough to trigger differentiation after treatment with cAMP.

Interestingly, BF SMB cells treated with cAMP for 48h, then induced with *cis*-aconitate at 37°C causes 68% of cells to differentiate within 24h, suggesting that the cAMP treatment induces stumpy-characteristics to be able to respond rapidly to the trigger at 37°C. Finally, cold shock (20°C) of stumpy cells induces reversible surface expression of EP procyclin [49]. Treatment of BF monomorphic cells with cAMP for 48h and then exposure to 20°C for 24h, causes 90% of cells to express EP procyclin (Fig. 4.15C). Cold shock of BF monomorphic cells without cAMP treatment does not cause EP procyclin surface expression (Fig. 5.15C).

Overall, this demonstrates that cAMP treatment of monomorphic BF cells induces stumpy-characteristics to provide competency for cells to respond more efficiently and rapidly to the chemical trigger *cis*-aconitate, the environmental temperature shift and to the molecular trigger ZC3H20.

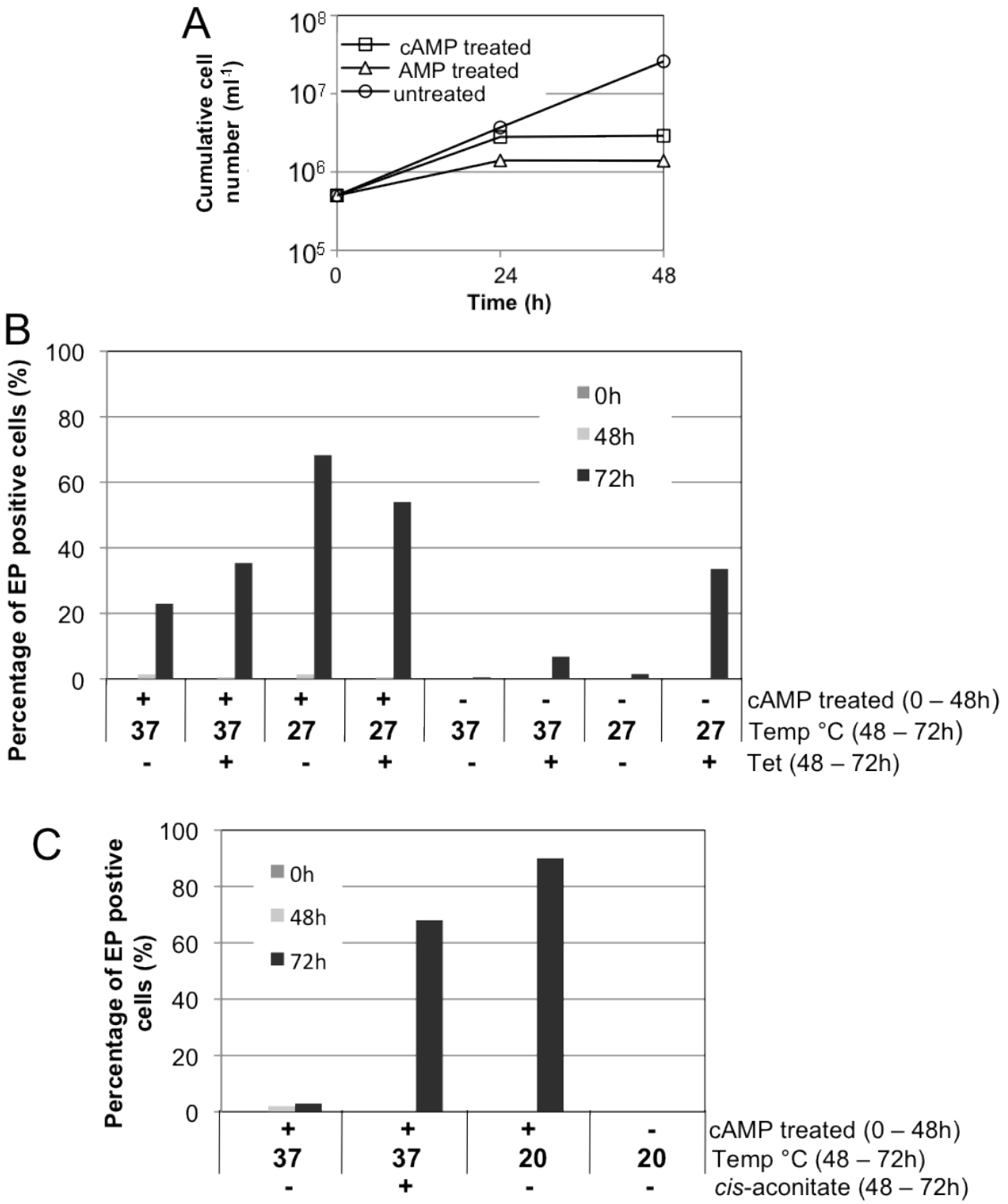


Figure 5.15. Effect of cAMP treatment on the differentiation ability of BF *T. brucei* induced for ZC3H20 over-expression

A. Effect of cAMP (15μM) and 5'AMP (15μM) analogues on cell growth of BF ZC3H20 OeX cells
B. EP procyclin counts of BF ZC3H20 OeX cells after grown in the presence (+) or absence (-) of cAMP (15μM) for 48h (0 – 48h, and then grown in the presence or absence of tet, at 37°C or 27°C, for 24h (48 – 72h). Over 200 cells are counted
C. EP procyclin counts of BF SMB cells after grown in the presence (+) or absence (-) of cAMP (15μM) for 48h (0 – 48h), and then grown in the presence or absence of *cis*-aconitate, at 37°C or 27°C, for 24h (48 – 72h). Over 200 cells are counted.

5.5.4 Discussion of section 5.5

Stumpy form BF cells are growth arrested and stabilised in the G1/G0 phase of the cell cycle [246], thus when triggered, they differentiate synchronously with rapid kinetics. The slow, asynchronous differentiation of BF monomorphic cells is suggested to require these cells to continue cell cycling until they reach a "receptive window" in the cell cycle, then progress from G1 to G0 or acquire competency to differentiate (to stumpy*) before transforming to PF [9, 42]. Contradicting the receptive window hypothesis, Li et al. [240] suggest that BF cells can be in any stage of the cell cycle to receive the signal to differentiate. By down-regulating the expression of proteins from a complex of the 26S proteosome, which are suggested to have a role in degrading certain mitotic cyclins, BF monomorphic cells are arrested in the G1/S and/or G2/M phases of cell cycle [240]. These cells trapped in either G1 or G2 are then able to differentiate once induced by *cis*-aconitate and shift to 27°C, suggesting cell cycle position or progression of the cell cycle is not required for differentiation. Indeed, accumulation in G1 of the cell cycle is not sufficient to elicit competence to differentiate [42]. However, Tasker et al. [42] suggest that cells must pass through a point in the cell cycle to then progress further to a state that allows the acquisition of a stumpy characteristic essential for differentiation i.e. to a stumpy* state. The data above suggests that monomorphic BF cells do not pass through a "receptive window" within the cell cycle to receive the ZC3H20 differentiation signal. However, a possible scenario is that to receive the differentiation signal a BF cell must undergo a transition to a stumpy* state, and although the nature of this transition is unknown, it is suggested to be defined by exit from the cell cycle [239]. Therefore, we hypothesise that it may be necessary to exit the cell cycle to receive the differentiation signal, but in an asynchronous monomorphic BF population, this could be independent of cell cycle position.

Cell-cycle arrested stumpy cells arise from slender BF cells that growth arrest in response to an accumulation of SIF at high density. However monomorphic BF cells do not growth arrest and transform morphologically into stumpy forms at high density, due to a reduced sensitivity to SIF. In agreement, BF 20 OeX cells grown to high density most likely does not induce stumpy-like characteristics, as the data shows high density does not increase their capacity to

respond to the ZC3H20 differentiation trigger. Monomorphic cells are suggested to have a reduced sensitivity to SIF, as monomorphic cells exposed to conditioned medium containing SIF (from high density pleomorphic cultures), caused very little growth arrest [247]. However, if conditioned medium from high-density monomorphic cultures is exposed to a slender BF pleomorphic population, the slender cells growth arrest and differentiate to the stumpy form [247]. This shows that monomorphic BF cells can still produce SIF but are not responsive to it and therefore, importantly, these cells only have reduced sensitivity to density sensing rather than the differentiation process itself [247]. Hence, cell density does not contribute to the ability of a monomorphic culture to differentiate to PF, and our results using ZC3H20 over-expression as a trigger are in line with this observation.

Exposure of a monomorphic cell to a cAMP analogue that induces the expression of stumpy characteristics clearly improves the capacity of cells to differentiate and at faster kinetics when triggered by ZC3H20 over-expression, than in the absence of cAMP treatment. The cAMP analogue causes the BF 20 OeX cells to growth arrest, which is not possible via density sensing, and could allow the transition of the BF cell to a stumpy* state that is capable of receiving the signal to differentiate. The analysis also shows that leaky ectopic expression of ZC3H20 (which is undetectable by western analysis) is enough to cause cAMP treated cells to differentiate. This suggests that once stumpy-induced, just a small level of ZC3H20 is enough to trigger transformation. This consequently implicates the role of ZC3H20 in a normal BF cell, that whilst ZC3H20 protein may be down-regulated/at low levels in a dividing slender cell that is unable to differentiate, a stumpy cell may regulate or respond to ZC3H20 differently. In addition, as discussed earlier (5.4.3) only BF stumpy cells are able to route EP procyclin to the surface of the cell, termed surface access control, which restricts EP from surface exposure in proliferating slender cells, even if procyclin is ectopically over-expressed [49]. Cold shock (20°C) of stumpy cells induces reversible surface expression of EP procyclin [49]. Treatment of BF monomorphic cells with cAMP causes 90% of cells to express EP procyclin in the absence of *cis*-aconitate but untreated BF monomorphic cells does not cause EP procyclin surface expression. This suggests that cAMP treatment of monomorphic cells enables these cells to lose the “surface access control” to then allow procyclin to be expressed on the surface upon cold shock and in the absence of *cis*aconitate.

In conclusion, by providing a monomorphic cell with the capacity to differentiate through the acquisition of stumpy characteristics, ZC3H20 is an effective trigger of differentiation.

5.6 Investigation of the mRNA targets regulated by ZC3H20 as a molecular trigger of differentiation

So far, this chapter has demonstrated that over-expression of ZC3H20 causes BF cells to differentiate to PF, where cells display procyclin surface expression as an early marker of differentiation. This is independent of temperature or exposure to *cis*-aconitate, which are differentiation triggers used *in vitro*, but induction of stumpy-characteristics in addition to ZC3H20 over-expression considerably increases the efficiency of triggered differentiation.

To correlate the cell biology observed with the genes that may be responsible for the phenotype displayed, microarray analysis was used to identify mRNAs that are affected upon ZC3H20 over-expression. After investigating the stability of these transcripts in a ZC3H20-dependent manner, and determining that ZC3H20 is capable of binding these mRNA targets, the analysis can provide clues as to which genes are regulated by ZC3H20 to enable it to act as a differentiation trigger.

5.6.1 Microarray analysis identifies genes involved in differentiation up-regulated when ZC3H20 is over-expressed in BF *T. brucei*

To investigate possible mRNA targets of ZC3H20, microarray analysis was carried out on BF 20 OeX cells to determine the effect on total mRNA levels. Over-expression of ZC3H20 in BF cells was induced (or uninduced) for 24 h at 37°C, and then total RNA isolated for the microarray. The time point of 24 h was used because this was the earliest time point that ZC3H20 protein could be detected. Induction was carried out at 37°C, as temperature reduction to 27°C itself has an effect on BF cells, and it is important to see what mRNAs are affected from ZC3H20 overexpression alone without the added effects from temperature shift. The microarray analysis was performed on three biological replicates. The same microarray setup was used as the RNAi of ZC3H20 in PF cells (see Chapter 3.3.1) and the fold change in mRNA levels for each probe for each array was calculated. Genes that showed more than 2-fold up/down-regulation in mRNA levels for at

least one probe in all three arrays were selected for further investigation (Table 5.1, Table 5.2).

There is just one gene that is down-regulated more than 2 fold when ZC3H20 is over-expressed, which is a putative adenosine transporter (Tb927.2.6220) (Table 5.1). If the threshold is brought down to 1.5 fold, then there are 15 genes that are down-regulated when ZC3H20 is over-expressed (Table 5.1). None of these genes have a putative function associated with the differentiation pathway, but a few genes such as the glycosomal membrane protein (Tb927.8.5460) and CAP15 (Tb11.01.3805), are bloodstream enriched transcripts indicating that these are down-regulated as the BF cell differentiates to PF. Down-regulation of any of these transcripts is unlikely to trigger the cell to differentiate, particularly at 1.5-fold, thus these were not investigated further. Interestingly, PDI-BS2, a gene that is destabilised when ZC3H20 is over-expressed in PF *T. brucei* (Chapter 4.4) is also down-regulated when ZC3H20 is over-expressed in BF (Table 5.1). Due to this correlative regulation of PDI-BS2 by ZC3H20 over-expression, this was investigated further as a target of ZC3H20 over-expression in BF.

Table 5.1 Summary of the BF ZC3H20 over-expression microarray analysis to show genes with down-regulated levels of RNA

Showing genes with down-regulated levels of RNA >1.5-fold, as a result of over-expression of TbZC3H20 in BF *T. brucei*.

Number	Product
Tb927.7.1780	adenine phosphoribosyltransferase, putative
Tb927.2.6220	adenosine transporter 2, putative
Tb927.4.3980	chaperone protein DNAJ, putative
Tb927.6.5270	ESAG3, degenerate
Tb927.8.5460	flagellar calcium-binding protein,44 kDa calflagin,44 kDa calcimedin
Tb09.211.2730	Gim5A protein,glycosomal membrane protein
Tb927.2.1700	hypothetical protein, conserved
Tb927.3.4070	hypothetical protein, conserved
Tb09.160.5290	hypothetical protein, unlikely
Tb927.5.1880	inhibitor of serine peptidase (ISP), putative
Tb11.01.3805	microtubule-associated protein,corset-associated protein 15, CAP15
Tb927.1.700	phosphoglycerate kinase
Tb10.6k15.2290	**protein disulfide isomerase,bloodstream-specific protein 2 precursor, PDI-BS2**
Tb10.61.2680	pyruvate kinase 1
Tb11.57.0012	VSG, pseudogene

Table 5.2. Summary of the BF ZC3H20 over-expression microarray analysis to show genes with up-regulated levels of RNA

Showing genes with up-regulated levels of RNA >2-fold, as a result of over-expression of TbZC3H20 in BF *T. brucei*. Signal fold change (+ = down-regulated,) for each of the three arrays conducted are shown for each of the probes on the array for that specific gene. Probes that are not >2 fold across all three arrays are shown in italics.

Number	Probe	Array			Product
		1	2	3	
Tb927.8.700	1 *2* *3*	+14.5 *+1.8* *+1.4*	+3.5 *+0.6* *+0.6*	+3.5 *+0.5* *+0.6*	Mitochondrial DNA repair and recombination helicase protein TbPIF7
Tb10.6k15.0020	1 *2*	+30.5 +24.4	+2.5 +2.6	+2.5 +2.5	EP1 procyclin
Tb10.6k15.0030	1 *2* *3*	+71.9 +17.3 +22.5	+3.0 +3.2 +3.0	+3.5 +3.1 +2.9	EP2 procylin
Tb927.6.480	1 2	+25.6 +27.3	+2.5 +2.5	+2.5 +2.5	EP3-2 procyclin
Tb927.6.520	1 2	+17.9 +29.8	+2.5 +2.7	+2.5 +2.6	EP3-2 procyclin
Tb927.6.450	1 *2*	+23.6 *+23.4*	+2.6 *+2.4*	+2.7 *+2.5*	EP3-2 procyclin
Tb09.160.5400	1 2 *3*	+11.1 +10.5 *+42.7*	+2.7 +3.3 *+0.3*	+3.1 +3.6 *+0.1*	expression site-associated gene 9 (ESAG9) protein
Tb927.7.4970	1 2 *3*	+8.1 +7.7 *+7.9*	+2.7 +3.6 *+2.3*	+2.9 +4.1 *+2.5*	Glutamine Synthetase (GlnS)
Tb927.6.510	1 2	+41.3 +171.2	+6.6 +6.2	+7.5 +7.9	GPEET2 procyclin
Tb927.5.4020	1 2 3	+11.9 +8.8 +11.0	+3.8 +3.2 +3.1	+2.9 +2.7 +2.9	Hypothetical protein
Tb927.8.510	1 *2* *3*	+12.5 +10.1 *+10.3*	+3.5 +3.8 *+1.9*	+3.0 +3.4 *+3.6*	Hypothetical protein
Tb927.5.2160	1 2	+13.5 +7.8	+2.7 +1.6	+3.6	Hypothetical protein, conserved, META domain (META1)
Tb927.5.2260	1	+20.8	+4.1	+4.8	Hypothetical protein, conserved, META domain (META1)
Tb927.7.5940	1 2 *3*	+17.5 +18.6 +20.5	+3.4 +3.1 +4.6	+3.9 +3.3 +4.5	Hypothetical protein, conserved, PAD2
Tb927.3.2230	1 *2* *3*	+6.5 *+5.4* *+5.4*	+3.1 *+2.3* *+2.0*	+2.9 *+2.0* *+2.3*	Succinyl-CoA synthetase alpha subunit, putative (SCAS)
Tb927.7.6850	1 2 *3*	+8.3 +8.0 *+6.4*	+2.8 +2.8 *+1.8*	+2.5 +2.5 *+1.9*	Trans-sialidase (TS)

There are 16 genes (plus ZC3H20) that show a more than 2-fold increase in RNA abundance when ZC3H20 is overexpressed (Table 5.2). Interestingly, with the exception of hypothetical protein, Tb927.8.510 and TbPIF7, all these genes are

confirmed to be developmentally regulated mRNAs that are normally enriched in PF cells [58] and ESAG9 (Tb09.160.5400) which is upregulated in stumpy forms [58, 251]. It may be that ZC3H20 is responsible for stabilising these mRNAs required for differentiation and establishment into a PF cell. Expression of the procyclins (EP-1, EP-2, EP-3 ad GPEET) is an early marker of differentiation, thus considered important for further study. All the EP procyclin and the GPEET2 procyclin genes were grouped together under the association of the procyclin surface coat, and will be referred to as procyclin from this point. With a similar expression profile during differentiation are the META1 proteins [59]. These are down-regulated when ZC3H20 is down-regulated in PF forms (Chapter 3.3.1), suggesting they stabilised by ZC3H20, thus, are good candidates for further investigation. The PAD proteins (PAD1/6/8) are reported to be upregulated in stumpy forms [57] [58] and PAD2 is upregulated upon cold shock during differentiation to allow transport of *cis*-aconitate [50]. Clearly, these are important molecules involved in the transduction of the differentiation signals, and thus deserved further investigation. Glutamine synthetase and succinyl Co-A synthetase (SCAS) are both required for energy metabolism in PF, and both are upregulated rapidly upon differentiation amongst other functionally related gene [59]. Thus, SCAS was investigated further as one of a group of genes required for energy metabolism that are upregulated upon differentiation. The gene that encodes the trans-sialidase (TbTS) that is responsible for transferring sialic acids from the surface on glyconjugates in the tsetse blood meal or midgut to the GPI-anchor of procyclin [209]. The TS-like E gene that is stabilised by ZC3H20 in PF cells (Chapter 3.3) is putatively functionally related to TbTS, and thus, in addition to being important for the processing of EP procyclin in the differentiating parasite, TbTS deserves to be investigated as a subset of genes (with TS-like E) that may be regulated by ZC3H20. ESAG9 (Tb09.160.5400) is one of a family of ESAG9 genes that are shown to be upregulated in stumpy form cells, encode proteins that are shed into the external milieu and suggested to be involved in interactions with the external environment. In light of this, the gene is unlikely to be necessary for the differentiation capability of the BF, and thus is not a priority to study as a potential target for ZC3H20 regulation. TbPIF7 is from a group of genes that encode kinetoplast helicases, required for kinetoplast minicircle and maxicircle replication [252]. Although this gene is probably important for replication of the

mitochondrial DNA that maybe upregulated for elaboration of the mitochondrion in PF cells, it is unlikely to be involved in the differentiation pathway, and thus was not investigated further. Finally, the mRNA abundance of the hypothetical protein Tb927.8.510 and Tb927.5.4020 were changed when ZC3H20 was downregulated in PF cells (Chapter 3.3). Tb927.5.4020 was down-regulated when ZC3H20 was absent in PF which correlates with Tb927.5.4020 upregulation when ZC3H20 is over-expressed in BF cells. In contrast, Tb927.8.510 was up-regulated after ZC3H20 RNAi in PF cells. Thus, just Tb927.5.4020 was investigated further.

To verify the increase in mRNA levels of procyclin, META1, PAD2, SCAS, TS, and Tb9275.4020, and decrease in the mRNA level of PDI-BS2, when ZC3H20 is over-expressed in BF, total RNA was isolated from BF cells that had been induced or uninduced for ZC3H20 over-expression for 24h. Samples of RNA were examined using Northern analysis with a specific probe to each of the candidate genes and tubulin was used as a control (Fig. 5.16).

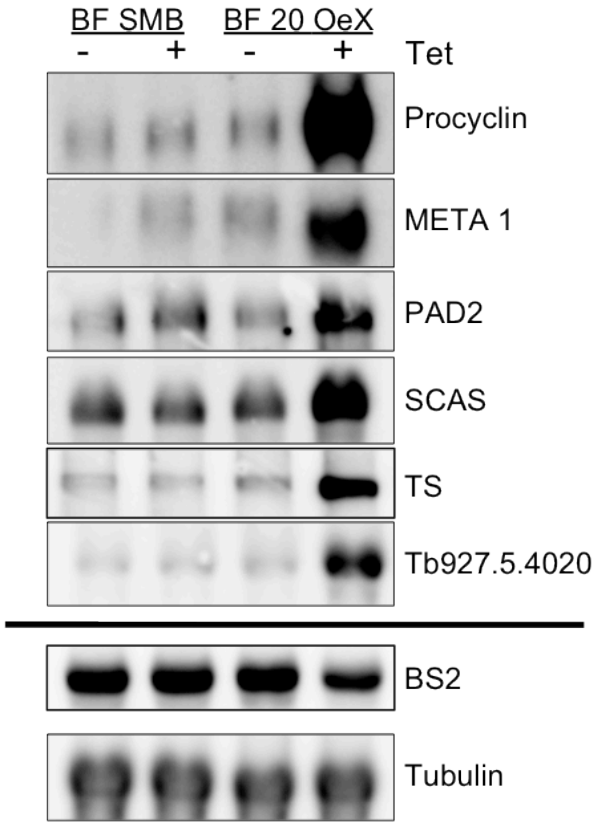


Figure 5.16. Northern analysis to show mRNA abundance when ZC3H20 is over-expressed in BF *T. brucei.*

RNA riboprobes to each gene identified in the microarray were used to detect specific mRNA transcripts. Genes above the black line indicate mRNAs that increased in the microarray and genes below the black line indicate mRNAs that were decreased in the microarray, upon ZC3H20 RNAi down-regulation. Tubulin is used as a loading control.

The Northern analysis confirmed the microarray with a clear increase in the mRNA abundance of the upregulated genes. There is also a decrease in the mRNA abundance of PDI-BS2 mRNA, reflecting the 1.5-fold decrease level shown in the microarray analysis. These selected genes that are involved with the differentiation of BF *T. brucei* could thus be investigated further as mRNA targets regulated by ZC3H20.

5.6.2 ZC3H20 is capable of binding to the upregulated mRNA targets from over-expression in BF *T. brucei*

The genes that are upregulated when ZC3H20 is over-expressed were then tested for their ability to be bound by ZC3H20. As described in Chapter 3.3.3 (PF 20 RNAi), TAP-tagged ZC3H20 was expressed in PF cells and used in a tandem affinity purification method to isolate all mRNAs capable of being bound by ZC3H20. The mRNAs were transcribed to cDNA, and then RT-PCR used to specifically amplify potentially bound mRNA targets of ZC3H20. Therefore, RT-PCR was carried out to test for the presence of procyclin, META1, PAD2, SCAS, TS, and Tb9275.4020 (Fig. 5.16). As shown in Chapter 4.4.1, PDI-BS2 is capable of being bound by ZC3H20, and is shown in Figure 5.16 to provide continuity. As mentioned in Chapter 3.3.3, the TAP method was carried out with ZC3H36, another CCCH zinc finger protein to show if there is specific ZC3H20 or general ZC3H RNA binding, and RT-PCR was carried out on tubulin and actin mRNAs as negative controls. RT-PCR of each candidate gene (Fig. 5.16) produced a positive product from both TAP-ZC3H20 and TAP-ZC3H36, which indicates that they are capable of being bound by ZC3H20 and most likely show a general binding specificity by other ZC3H RNA binding proteins. The exception is Tb927.5.4020, which showed binding specificity by ZC3H20 only.

Thus, ZC3H20 is capable of binding each of these mRNA transcripts that are upregulated during differentiation and ZC3H20 over-expression.

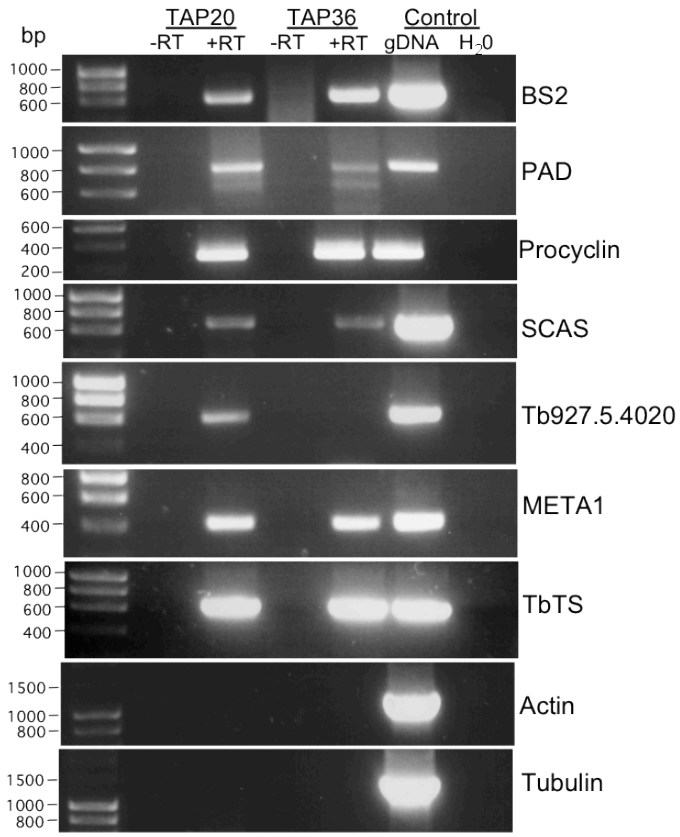


Figure 5.17. RT-PCR of bound mRNA targets from ZC3H20 TAP-tag analysis

RT-PCR analysis on cDNA reverse-transcribed (+RT) from RNA isolated from TAP tagged ZC3H20 and ZC3H36 purification. Minus reverse transcription (-RT) control is shown for DNA contamination from the TAP purification. Genomic DNA (gDNA) is used as a positive control, and water (H_2O) is used as a non-template negative control.

5.6.3 The mRNA targets upregulated during ZC3H20 over-expression are also stabilised when ZC3H20 is over-expressed

Having shown that over-expression of ZC3H20 causes a change in the mRNA level of PDI-BS2, procyclin, META1, PAD2, SCAS, TS, and Tb9275.4020 and that they can be bound by ZC3H20, northern analysis were performed to determine if the half life of these transcripts is influenced when ZC3H20 is overexpressed in BF cells. BF 20 OeX cells were grown in the absence or presence tet for 24h as for the microarray where there is over-expression of ZC3H20 protein detected. After 24h of ZC3H20 over-expression, the cells were grown in the presence of the transcriptional inhibitor actinomycin D for 0, 15, 60 or 120min to allow the turnover of RNA to be determined with or without ZC3H20 over-expression. After each time point, RNA was isolated and the level of RNA for each gene observed by Northern analysis (Fig. 5.18).

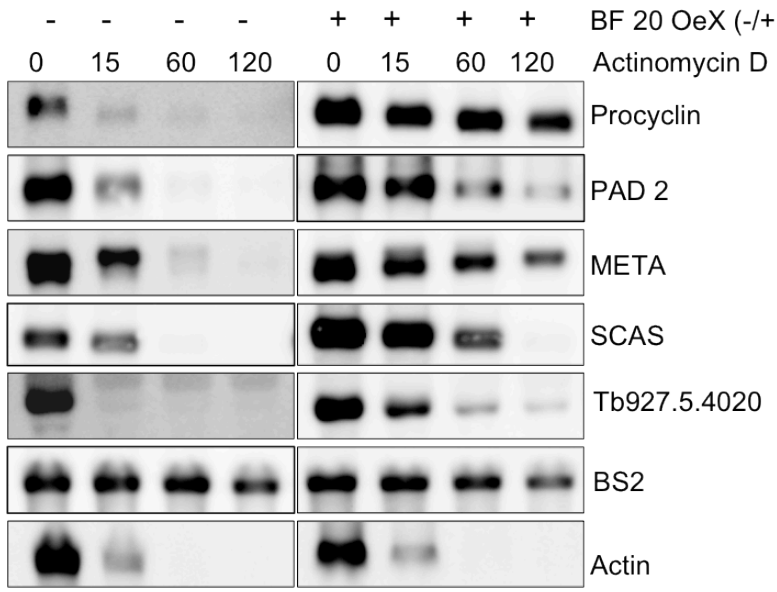


Figure 5.18. RNA abundance after treatment of BF *T. brucei* with a transcriptional inhibitor and induced for ZC3H20 over-expression

Northern blot analysis of total RNA isolated from BF 20 OeX cells grown in the presence or absence of tet for 24h and then treated with actinomycin D over 120min.

Densitometry was used to measure the mRNA levels at each time point and the levels were then calculated as a percentage of the time point 0h, which was expressed as 100%, for –Tet and +Tet PF 20 OeX samples. Each time point is plotted on a bar chart to show the mRNA decay after actinomycin D addition (Fig. 5.19 and 5.20). The decay of the control mRNA, actin, was not affected when ZC3H20 was over-expressed in BF cells compared to uninduced cells (Fig. 5.18 and 5.19). PDI-BS2 is down-regulated upon ZC3H20 over-expression in BF cells, and thus, as seen in PF cells when ZC3H20 is over-expressed, the mRNA turnover is expected to decrease. However, the decay rate of PDI-BS2 upon ZC3H20 over-expression was not affected compared to uninduced BF cells (Fig. 5.18 and 5.120). The turnover of procyclin, PAD2, META, SCAS and Tb927.5.4020 mRNAs were significantly decreased upon ZC3H20 over-expression in BF cells compared to uninduced cells (Fig. 5.18, 5.19, 5.20). Using a Student's t-test, the mRNA decay of each target after 15min was compared between induced and uninduced cells. After 60min of actinomycin D addition, the mRNA levels in uninduced cells were barely detectable (less than 10% remaining mRNA), thus statistical analysis was not used for these samples. However, these data indicate that these mRNA transcripts are stabilised by ZC3H20 in the BF cell.

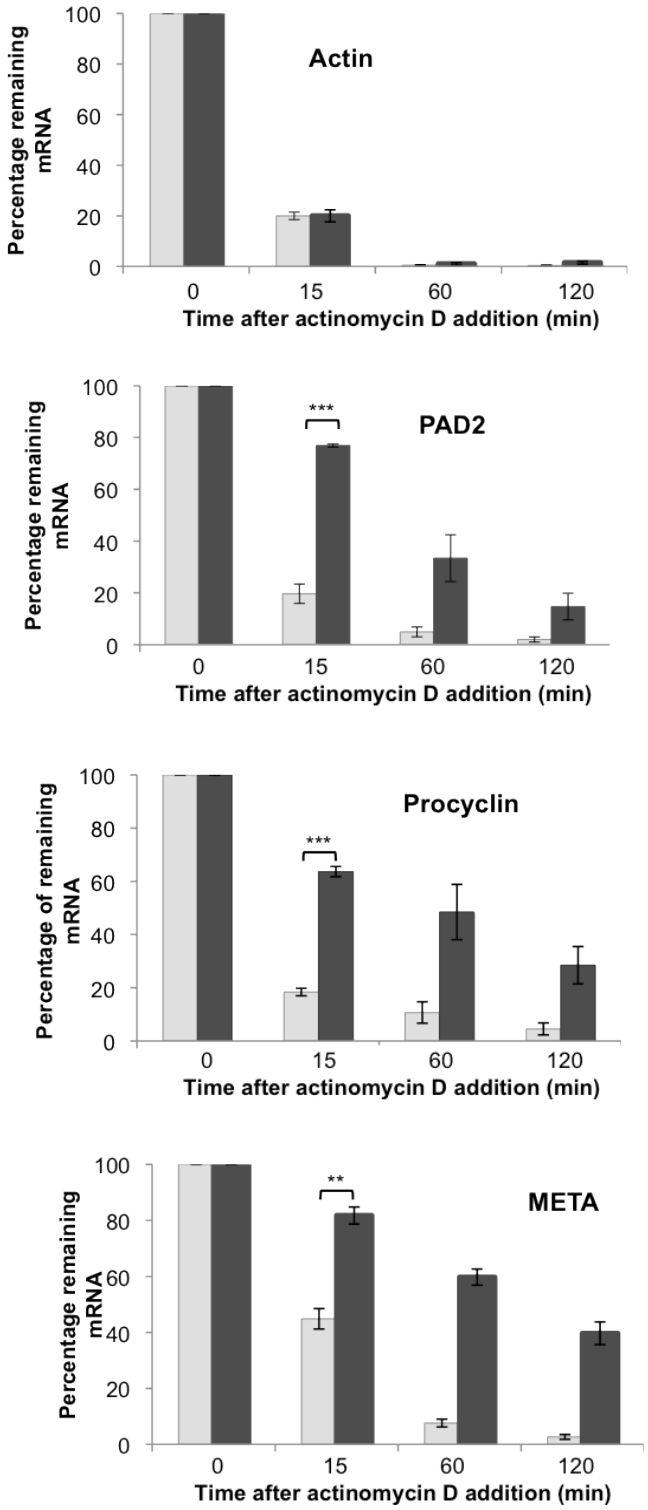


Figure 5.19. Densitometry analysis to show turnover of Actin, PAD2, Procyclin and META RNA in BF ZC3H20 OeX *T. brucei*

Densitometry analysis of actinomycin D experiment as shown in Fig 5.18 to determine the decay of actin, PAD2, procyclin and META mRNA levels when over-expression of ZC3H20 is induced (dark grey) or uninduced (light grey). Plotted data are mean values from three independent experiments, and error bars show standard error. A Student's t-test was used to determine the significance of mRNA decay when ZC3H20 is over-expressed after each time point compared with uninduced PF cells. ***= $p<0.001$,** $p<0.002$

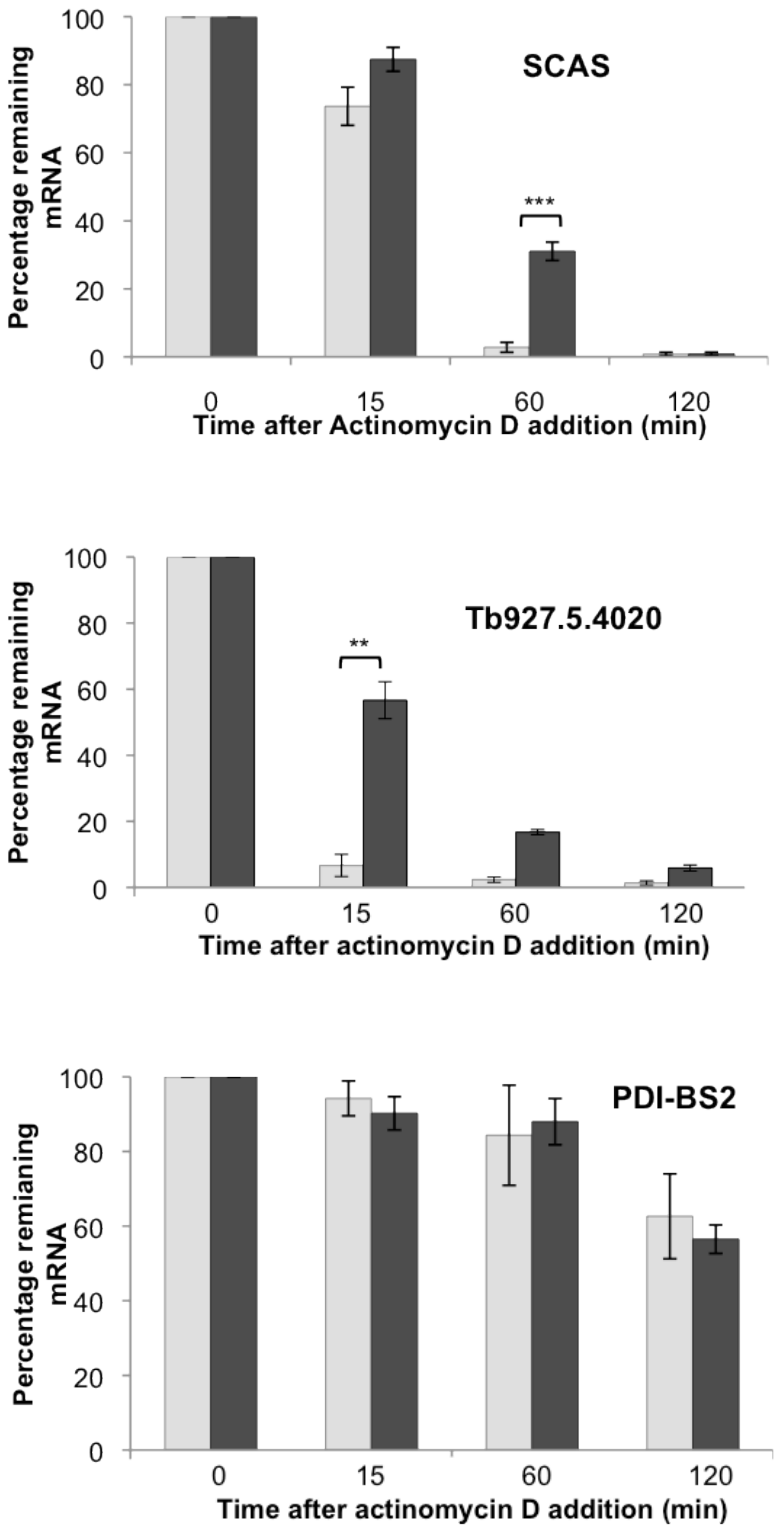


Figure 5.20. Densitometry analysis to show turnover of SCAS, Tb927.5.4020 and PDI-BS2 RNA in BF ZC3H20 OeX *T. brucei*

Densitometry analysis of actinomycin D experiment as shown in Fig. 5.18 to determine the decay of SCAS, Tb927.5.4020 and PDI-BS2 mRNA levels when over-expression of ZC3H20 is induced (dark grey) or uninduced (light grey). Plotted data are mean values from three independent experiments, and error bars show standard error. A Student's t-test was used to determine the significance of mRNA decay decay when ZC3H20 is over-expressed after each time point compared with uninduced PF cells. ***= $p<0.001$,** $p<0.002$

5.6.4 ZC3H20 over-expression increases the abundance of mRNAs that are upregulated in stumpy cells and upon differentiation triggered by cold shock or *cis*-aconitate

From section 5.5 in this chapter, it is clear that induction of stumpy characteristics enables BF monomorphic cells to respond more rapidly and effectively upon over-expression of ZC3H20, a molecular trigger of differentiation. To put this cell biology data into context with the molecular regulation of genes required for the differentiation pathway, each of the mRNA targets upregulated upon ZC3H20 over-expression were probed for their RNA abundance when the cell was exposed to a selection of environmental and chemical conditions. BF 20 OeX cells were grown in the presence or absence of tet for 24h at 37°C, and BF SMB cells grown in the presence or absence of *cis*-aconitate for 24h at 37°C, and then RNA isolated from each cell population. Cold shock (20°C) of stumpy cells induces reversible surface expression of EP procyclin [49]. Cold shock of BF monomorphic cells, treated with cAMP but in the absence of *cis*-aconitate, allowed 90% of cells to express procyclin on the cell's surface, suggesting that they have lost the "surface access control" specific to stumpy vs. slender cells. Thus, BF SMB cells were grown at 20°C for 8h and 20h, and RNA isolated from these cells. BF SMB cells were also treated with cAMP for 48h, and then shifted to 20°C for 24h, or kept at 37°C and grown in the presence and absence of *cis*-aconitate for 24h. RNA was isolated from each of these cell populations and the abundance of each specific transcript determined using Northern analysis (Fig. 5.21). Firstly, this analysis shows that for most genes, the transcript levels do not increase much/at all upon *cis*-aconitate exposure at 37°C compared to cells not exposed to *cis*-aconitate (normal BF levels). As expected, over-expression of ZC3H20 shows a clear increase in the transcript level. Upon cold shock, there is not much difference in the RNA abundance of these genes, although there appears to be a small increase in the RNA abundance of procyclin compared to normal BF levels (Fig. 5.21 SMB 37 –CA vs. SMB 20 20/8h). However, it is important to note that BF SMB cells just cold-shocked do not express procyclin on the cells surface (Fig. 5.14C). Treatment of BF SMB cells with cAMP and then shifted to 20°C causes a huge increase in the mRNA abundance of all upregulated mRNAs, correlating with the 90% of these cells observed expressing procyclin on the cell surface (Fig. 5.14C). Treatment of BF SMB cells with cAMP and exposed to *cis*-aconitate at 37°C unsurprisingly causes a huge increase in the mRNA transcripts, correlating with the

68% of cell differentiation observed (Fig. 5.14C). However, just cAMP treatment of cells caused big increases in mRNA levels of PAD, META1 and Tb927.5.4020, suggesting these transcripts are upregulated upon stumpy induction (cAMP). There is a modest increase of procyclin mRNA level, suggesting that cold shock or *cis*-aconitate in addition to stumpy induction, or even ZC3H20 alone are necessary to up-regulate procyclin to levels required for differentiation (Fig. 5.21). This is a similar situation for SCAS, where the mRNA is only upregulated to high levels upon ZC3H20 over-expression alone, or if a stumpy-induced (cAMP) BF SMB cell is cold-shocked at 20°C (Fig. 5.21). The mRNA level of PDI-BS2 does not change dramatically, except that there is a modest decrease in the level upon cAMP treatment, suggesting this maybe be down-regulated in stumpy cells and remains down-regulated upon differentiation. Finally, the level of endogenous ZC3H20 does not change considerably over all conditions, maybe with a slight overall increase upon cAMP treatment. However, this is expected, as our data suggests that ZC3H20 is regulated at the translational level not at the level of RNA.

In conclusion, this analysis provides a link between the cell biology observed and the molecular regulation of genes when ZC3H20 is over-expressed in BF *T. brucei*. ZC3H20 over-expression causes an increase in mRNA abundance of genes that are upregulated in stumpy form cells, as well as genes that are upregulated upon differentiation, thus confirming the nature of ZC3H20 as a molecular trigger of differentiation.

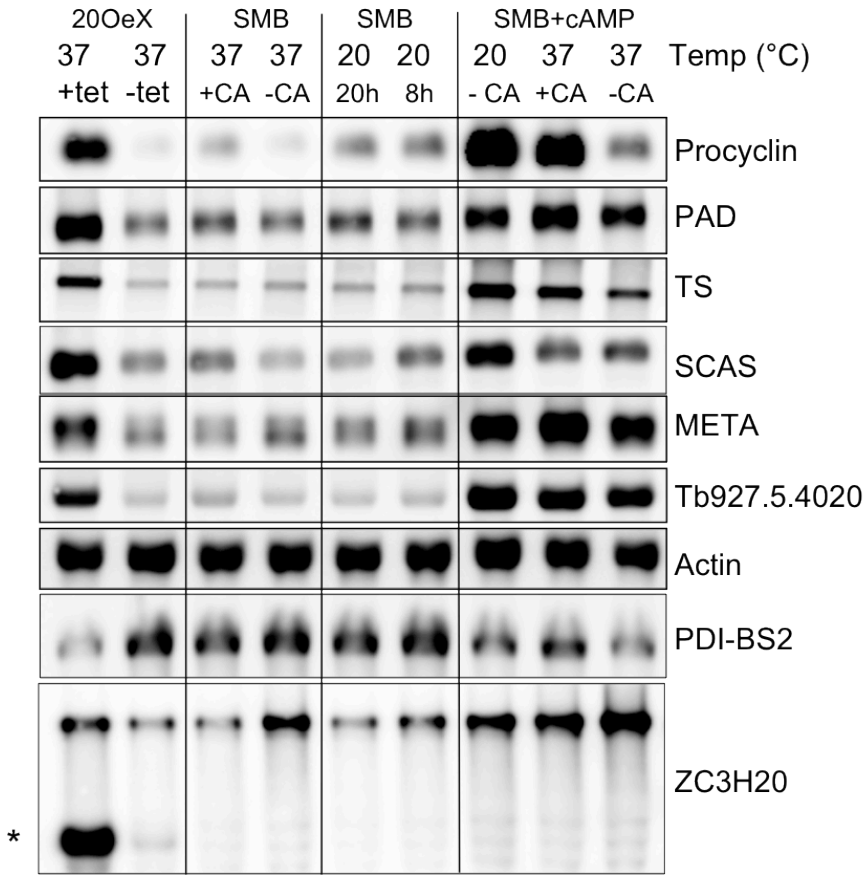


Figure 5.21. Northern analysis of RNA isolated from BF SMB and 20 OeX cells exposed to different conditions.

BF 20 OeX cells are induced (+tet) or uninuced (-tet) for 24h at 37°C. BF SMB cells are grown in the presence (+CA) or absence (-CA) of 6mM *cis*-aconitate for 24h. BF SMB cells are first exposed to cAMP (15μM) for 48h and then shifted to 20°C or left at 37°C with or without *cis*-aconitate, for 24h. The induced ectopic over-expressed of ZC3H20 (RNA) is indicated with an asterisk (*).

5.6.6 Discussion of Section 5.6

Microarray analysis identified 16 genes (plus ZC3H20) that show a more than 2.5 fold up-regulation of their mRNA levels when ZC3H20 is over-expressed in BF *T. brucei*. Unsurprisingly, as over-expression of ZC3H20 acts as a molecular trigger of differentiation, the up-regulation of these genes identified is associated with the differentiation of a BF cell to a PF. The procyclin genes were upregulated correlative with the early marker of differentiation, TS is required for sialidation of the procyclin coat, PAD2 is associated with perceiving the differentiation trigger and SCAS and GlnS are required for the change in energy metabolism upon the differentiated PF cell. The META1 proteins and two hypothetical proteins were also

upregulated, which are PF stage-specific enriched genes, thus suggesting these are required to be upregulated upon initiation of differentiation to a PF cell. Additionally, ESAG9 is upregulated, which is shown usually to be upregulated in stumpy cells, as are the other PAD protein members, suggesting that ZC3H20 over-expression may induce stumpy-specific gene expression. Subsequent analysis showed that ZC3H20 is capable of binding these transcripts *in vivo*, and these mRNAs are stabilised in a ZC3H20-dependent manner (upon ZC3H20 over-expression in BF cells). This suggests that ZC3H20 is responsible for regulating these transcripts via stabilisation in a BF cell (where these genes would normally be down-regulated), and thus upon ZC3H20 expression, triggers the cell to differentiate. Of course, in a PF cell these PF-enriched genes are up-regulated, but these transcripts may be stabilised by other *trans*-acting factors, as upon RNAi down-regulation of ZC3H20 in PF parasites, these genes are not down-regulated (Chapter 3.3, Table 3.1). Normally within the cell, different RBPs have different specificities for mRNA targets that determine specific regulation, but there may also be networks of RBPs that show redundancy that can compensate for the down-regulation of an important *trans*-acting factor, especially if they are responsible for the regulation of developmental genes. Our data suggests this redundancy exists, as a proportion of BF ZC3H20 null mutants (with RNAi down-regulation of ZC3H21) are still able to differentiate upon a *cis*-aconitate trigger and temperature drop (section 5.2.4).

Determining which genes are specifically regulated by ZC3H20 is more challenging, as it is likely that the microarray identified some mRNAs that were up-regulated due to a secondary effect from the cell triggered to differentiate. As seen by the microarray (section 5.6.1) and the cAMP northern blots (Section 5.6.4), genes that are up-regulated upon stumpy/stumpy* induction, whether as reported *in vivo* (ESAG9, PAD1) [50, 251], or from cAMP treatment *in vitro* (PAD, META, Tb927.5.4020, Fig. 5.21), are upregulated upon ZC3H20 over-expression. It may be suggested that ZC3H20 over-expression causes cells to become stumpy or express stumpy-like genes. However, it is more likely that ZC3H20 over-expression, that has triggered cells to differentiate, has indirectly caused cells to express stumpy genes. This has been reported by other studies that have triggered BF cells to differentiate using *cis*-aconitate, but observe a transient expression of stumpy genes in the first few hours of differentiation [59]. However, the simple up-

regulation of a PF specific gene is just as unlikely to trigger differentiation, and thus, ZC3H20 must regulate a subset of genes to enable progression of the differentiation pathway. Other studies have demonstrated this, for example, ectopic over-expression of EP procyclin allows a stumpy cell to express procyclin on the cell surface, but it is insufficient to release cell cycle arrest and commit the cell to differentiate [49].

The microarray analysis also identified that PDI-BS2 mRNA level decreased at a 1.5-fold threshold upon ZC3H20 over-expression, which additionally caused down-regulation of PDI-BS2 in PF cells. As discussed in Chapter 4 (4.5), PDI-BS2 has a putative function as a molecular chaperone, assisting in the folding of ER proteins, and due to its co-localisation with the endocytic pathway, rather than the usual resident of PDIs in the ER lumen, this suggests a unique requirement in the processing and trafficking of endocytic proteins [235]. Consequently, as PDI-BS2 is a BF enriched transcript, it could be possible that this molecular chaperone is involved in the processing of developmentally regulated proteins. This may be important for regulation of the surface coat proteins that are trafficked to the cell surface upon differentiation, and thus represents an interesting target that is down-regulated by ZC3H20 over-expression in BF cells. As shown in Chapter 4, ZC3H20 over-expression causes a 2-fold decrease in PDI-BS2 mRNA level, ZC3H20 is capable of binding PDI-BS2 mRNA (Chapter 4.4.1), and the half-life of PDI-BS2 mRNA is decreased upon ZC3H20 over-expression (Chapter 4.4.2), indicating that ZC3H20 destabilises PDI-BS2 in PF cells. The half-life of PDI-BS2 mRNA does not change however when ZC3H20 is over-expressed in BF cells (section 5.6.5). This could be explained by the difference in ectopic ZC3H20 expression levels observed between BF and PF cells, as a more sensitive Western blot substrate was required to detect the lower protein levels in BF cells compared to PF cells (see Chapter 2 section 2.8). Thus, the down-regulation and destabilisation of PDI-BS2 is more apparent upon ZC3H20 over-expression in PF cells, compared to a lower ZC3H20 over-expression in BF cells.

5.6.7 Chapter 5 conclusions

Combining the cAMP experiment used in section 5.5.3 with Northern analysis of the microarray targets, provided a link between what is observed at the molecular level and the effect seen at the cellular level. To put these results into context, Figure 5.22 describes a model to integrate the analysis from this Chapter with published studies on the differentiation pathway.

Point 1 depicts the state of the proliferative BF slender cell *in vivo*, and **Point 1a** depicts the equivalent proliferative BF monomorphic cell *in vitro*. At **Point 2**, the density sensing mechanism is used by BF slender cells *in vivo*, such that at high density, SIF accumulates and triggers the cells to cease growth and differentiate to a cell cycle arrested BF stumpy cell (**Point 3**) [245]. *In vitro*, our data suggests that monomorphic BF cells may demonstrate a spectrum between these two forms [53]. This is shown by the varying ability of differentiation between WT and SMB cell lines (60%, Fig. 5.4 vs. 30% Fig 5.2 after 48h), and the fact that a proportion of monomorphic BF cells are able to express procyclin on the cell surface from ZC3H20 over-expression, or *cis*-aconitate addition, suggests they must have lost "surface access control", which is a trait specific to stumpy cells and not slender cells [49]. Our data also shows that the monomorphic BF cells are not responsive to SIF, unlike slender cells [247], and do not differentiate to a stumpy form cell upon high cell density, as depicted by **Point 2a** (section 5.5.3). However, treatment of BF SMB cells with a cAMP analogue causes a cell growth arrest and may induce these cells to go through a transition to a stumpy* state (**Point 3a**) (section 5.5.3/.4), which has been used to describe the nature of a monomorphic cell line that has obtained the ability to receive the differentiation signal [42, 239]. At **Point 3**, stumpy cells are arrested in the G1/G0 phase of the cell cycle, which we hypothesise allows a "reset button" for the re-entry of the cell cycle upon transformation to a PF cell (see later). Our data shows that it may not be necessary for BF SMB cells to find a point in the cell cycle that allows them to become stumpy*, and this suggests instead that it may be defined by exit from the cell cycle (section 5.5.1/.4) [239]. As monomorphic BF cells most likely do not exit the cell cycle at G1/G0, they will not receive the hypothesised "reset button".

Point 4 depicts the molecular state of the stumpy or stumpy* cell. The level of META, ESAG9, stumpy-enriched PADs and other stumpy-enriched transcripts are

upregulated upon stumpy/stumpy* induction (section 5.6.5) [58]. Additionally, the "surface access control" is lost in stumpy cells [49], and this could be due to the down-regulation of a molecule(s) involved with the trafficking of surface bound proteins, for example, our data suggests the putative molecule, PDI-BS2, which is down-regulated by ZC3H20 and upon cAMP treatment (Chapter 4.4 and section 5.6). Our data shows that the levels of these stumpy transcripts increase upon ZC3H20 over-expression in a non-stumpy* cell (section 5.6), and as discussed in section 5.6.6, ZC3H20 is probably not directly regulating these stumpy genes, but they are expressed as a result triggering differentiation to a PF cell. **Point 1b** indicates that when ZC3H20 is over-expressed in a BF monomorphic cell (non-stumpy*), this bypasses the stumpy* route. We hypothesise that the non-stumpy* monomorphic cell assumes it must have gone through a stumpy state when triggered to differentiate by ZC3H20 over-expression, as ZC3H20 is normally only expressed when triggered to differentiate (see later), and thus up-regulates/down-regulates the relevant stumpy genes.

Normally within a stumpy/stumpy* cell, negative regulators may bind to procyclin mRNA, PAD2, etc, thus destabilising these transcripts to prevent their expression, and may outcompete any stabilising *trans*-acting factors. This concept has been reported for the regulation of EP procyclin, which contains negative and positive elements within its 3'UTR that affect the mRNA and protein abundance (see Introduction 1.4.2). TbZFP3 is demonstrated to regulate the protein expression of EP procyclin isoforms, and a proposed model suggests that TbZFP3 has to compete with a negative regulator to bind the Loop II region within the 3'UTR [184]. The negative regulator causes poor translation/mRNA destabilisation of EP procyclin, but if TbZFP3 is ectopically over-expressed, the negative regulator is out-competed, and the expression of procyclin increases [184]. A similar situation may happen when ZC3H20 is over-expressed in monomorphic BF cells (**Point 1b**), where excess ZC3H20 it is able to outcompete the negative regulators, and stabilise procyclin, PAD2, etc mRNA expression. This is more effective in BF SMB cells that are stumpy* from cAMP treatment which have the capacity to respond to the trigger of ZC3H20 more effectively compared to normal monomorphic BF SMB cells (from **Point 4b** via cAMP) (section 5.5.3).

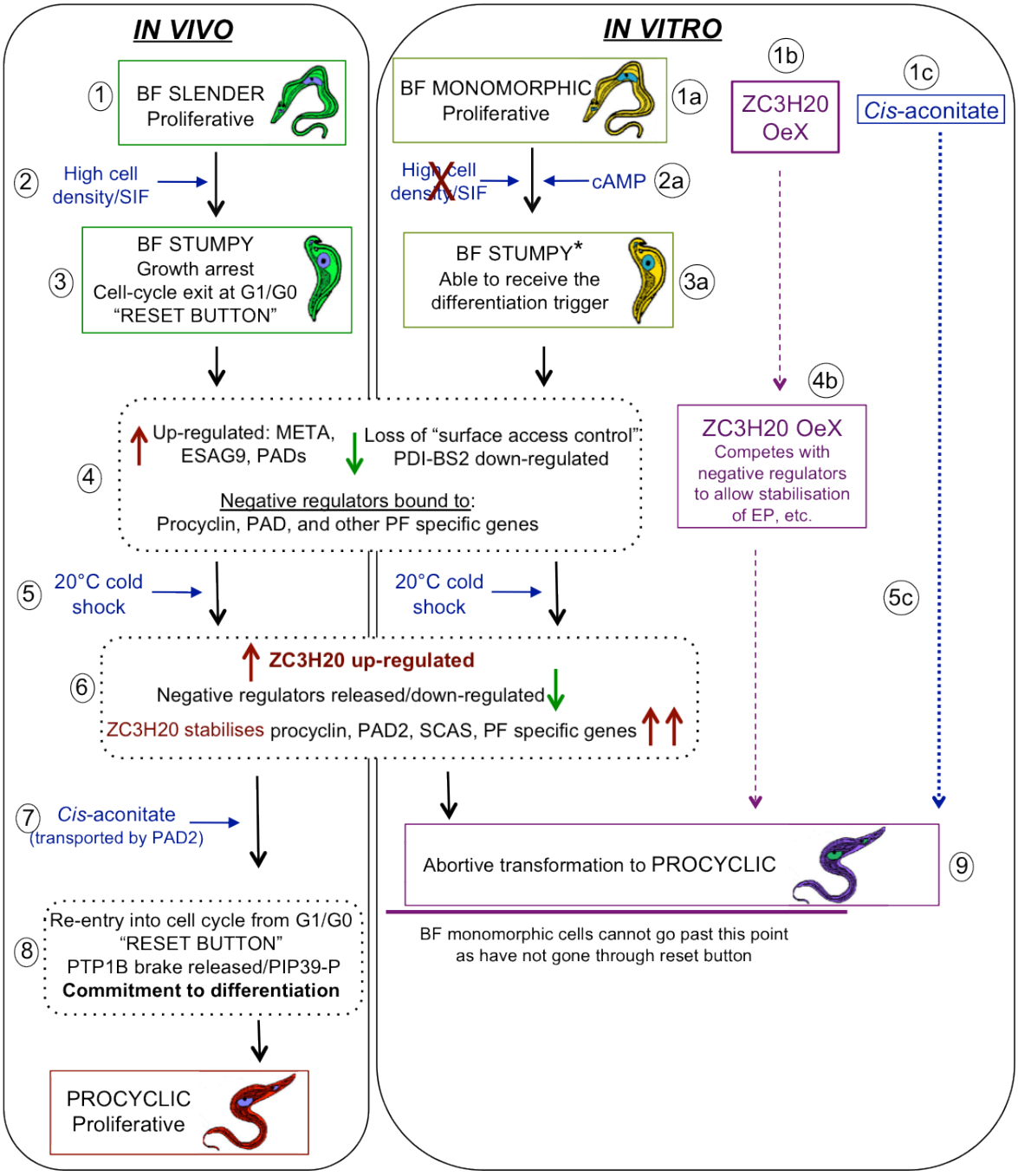


Figure 5.22. Model for involvement of ZC3H20 in regulating *T. brucei* differentiation from BF to PF pathway

This model incorporates published studies and data from Chapter 5, but does not exclude other regulatory proteins or environmental cues that maybe involved in this pathway. Points 1-9 are explained in section 5.6.6.

Point 5 illustrates the exposure of cells to a cold shock (20°C), which causes the up-regulation of procyclin and expression on the cell surface of stumpy cells [49], and up-regulation of the transporter PAD2 [50]. The cold shock at 20°C is

suggested to be a natural condition as the feeding temperature of the tsetse fly is during dusk [49].

Point 6 depicts the molecular state of the cell upon cold shock. Our data show that the ZC3H20 RNA level in BF cells is equivalent (if not slightly higher) to PF cells, but the protein is undetectable in BF cells suggesting it is down-regulated via translational/post-translational mechanisms. The level of ZC3H20 RNA does not change considerably upon cAMP treatment (section 5.6.5), but this is not unexpected, as maybe the level of ZC3H20 protein is actually up-regulated. However, we hypothesise that upon cold shock, ZC3H20 protein is 'released' from down-regulation. The cold shock down-regulates or releases binding of the negative regulators, and thus ZC3H20 is able to bind and stabilise procyclin, PAD2, etc, causing up-regulation and procyclin surface expression in stumpy* cells (section 5.5.3, 5.6.5). At 37°C, stumpy* cells (cAMP treated BF SMB cells) cannot express procyclin mRNA and thus on the surface (section 5.5.3, 5.6.5), as negative regulators are bound at this temperature. Exposure of cells to 27°C must allow the partial release of negative factors, as over-expression of ZC3H20 at this temperature allows more cells to express procyclin than cells at 37°C (section 5.4.2). Treating cells with cAMP to induce stumpy* and then shifting to 27°C, causes rapid differentiation with over-expression of ZC3H20 (section 5.5.3). However, even leaky ectopic expression of Z3H20 is enough to allow cAMP treated cells to express procyclin at 37°C or at 27°C (section 5.5.3). Ectopic ZC3H20 protein is not detectable, but a low level of RNA can be detected (Fig. 5.21) which will not be translationally regulated, and thus in a stumpy* cell, just a low level of unregulated ZC3H20 protein is sufficient to trigger differentiation. This data also indicates that ZC3H20 protein is unlikely to be up-regulated in a stumpy cell to stabilise stumpy genes, as just a relatively small amount of ZC3H20 protein will trigger differentiation, which would be detrimental to a stumpy cell in an *in vivo* situation i.e. the mammalian bloodstream. Of course, we do not know the relative amount of ZC3H20 protein compared to endogenous levels, and so an alternative is that there may be a very fine balance of ZC3H20 in the cell that triggers the cell to differentiate or not.

Point 7 shows that after cold-shock and the up-regulation of PAD2, cells are hypersensitive to low levels of *cis*-aconitate that can be transported in to the cell [50].

Point 8 then depicts that *cis*-aconitate triggers stumpy cells (*in vivo*) to re-enter the cell cycle which have been "reset" at G1/G0, and the glycosomal PIP39 is phosphorylated by releasing the PTP1B brake [144]. The *cis*-aconitate signal is considered necessary for commitment for differentiation [49], and thus the rest of the pathway is followed through to result in a fully differentiated proliferative PF cell. An important point to make is that *in vitro* cultured monomorphic cells in the presence or absence of cAMP will never go through a *bona fide* stumpy stage. Thus they have not been able to go through the "reset button" by exiting the cell cycle at G1/G0, and when triggered to differentiate, even in the presence of *cis*-aconitate, may not re-enter the cell cycle properly from G1/G0 to establish as proliferative procyclic cells (at **Point 9**, Fig. 5.22).

Flooding stumpy, or monomorphic BF SMB cells, or stumpy* (cAMP treated) cells with high levels of *cis*-aconitate, (at **Point 1c** or **Point 5c,** Fig 5.22), bypasses all molecular regulation for triggering the initiation of differentiation, and allows cells to differentiate, although the differentiation efficiency is variable depending on the cell's state. A stumpy cell is better prepared for differentiation than a stumpy* (cAMP) monomorphic cell, and even more so than a non-stumpy* monomorphic cell, and so will differentiate more effectively that either of these cell states when "triggered" by *cis*-aconitate alone. This is a similar situation to when ZC3H20 over-expression in BF SMB cells forces them to up-regulate procyclin, but have not gone through a stumpy* state, thus differentiation is asynchronous and slow (from **point 1b**, Fig. 5.22). In parallel, the presence of *cis*-aconitate, which is normally later on in the pathway, "tricks" a cell into up-regulating PF genes even when the cell has not been properly triggered by cold-shock and ZC3H20 to initiate differentiation. This may also explain the observation that even in the absence of ZC3H20, some BF cells are still able to differentiate when triggered with high levels of *cis*-aconitate (section 5.2.4), as the requirement of ZC3H20 has been bypassed.

In light of this discussion, it seems likely that ZC3H20 over-expression causes the up-regulation and expression of procyclin, a major early differentiation

event, and maybe the regulation of other early differentiation molecules. The stumpy stage is obligatory to prepare and "reset" the BF cell to receive the signal for efficient differentiation, and to complete the pathway, *cis*-aconitate is needed to commit the cell to differentiate to a proliferative PF cell. In conclusion, ZC3H20 acts to stabilise transcripts required in initiation of differentiation, and thus can be considered as a molecular trigger to signal transformation from BF to PF *T. brucei*.

Chapter 6. Final conclusions

6.1 Discussion and conclusion of thesis

This project has characterised the role of TbZC3H20 as a post-transcriptional regulator of gene expression in *T. brucei*. ZC3H20 is an essential gene in the procyclic life form, and is demonstrated to regulate the expression of key developmental genes via mRNA stability. Trypanosomes use post-transcriptional mechanisms as the main point of controlling gene expression, and consequently the role of RNA-binding proteins (RBPs) in this organism are of the upmost importance. Thus, this work displays a significant finding as the first example of a CCCH zinc finger (ZC3H) protein to regulate gene expression via mRNA stability in trypanosomes.

ZC3H20 is shown to stabilise PF-enriched transcripts and destabilise BF-enriched transcripts in the PF life cycle stage. In addition to demonstrating the regulation of developmental genes, ZC3H20 is the first example of a ZC3H to stabilise mRNA in any organism. ZC3H20 is not essential in the bloodstream life stage, but over-expression of ZC3H20 in BF cells causes them to differentiate to PF, revealing ZC3H20 as a molecular trigger of differentiation in *T. brucei.* To date, temperature, chemical and genetic inhibition of phosphatase activity (PTP1B) have been used to trigger differentiation *in vitro*, but this project has discovered the first differentiation trigger of this kind i.e. up-regulation of a post-transcriptional regulator to control the changes in gene expression required for transformation. This is a considerable finding that demonstrates the tight regulation of differential gene expression, during differentiation and within each life cycle stage to adapt to the mammalian bloodstream and insect midgut.

Genes that are stabilised by ZC3H20 fall into two groups, genes that encode proteins directed to the cell surface or proteins that associate with surface proteins of the PF cell (procyclin, PAD, TbTS, TS-like E, META) and genes required for energy metabolism in the PF cell (MCP12, SCAS, Gln S). Genes that are destabilised by ZC3H20 encode proteins involved in the trafficking pathway (clathrin and PDI-BS2), which are down-regulated in the PF cell. Interestingly, there is a biological relationship between proteins directed to the cell surface/flagellar pocket and their dependency on the trafficking system for their transport. This is apparent within the bloodstream form stage, where a high rate of endocytosis is required to recycle the variant surface glycoprotein coat and remove

host immune complexes from the surface [23, 25]. Additionally, during differentiation from BF slender form to stumpy form, the stumpy cells lose “surface access control” which allows procyclin to be routed onto the surface of the cell (in slender cells procyclin remains trapped in the endocytic system) [49]. This latter point is of particular interest concerning the regulation of these molecules by ZC3H20 during differentiation. As discussed in Chapter 5, the up-regulation of procyclin and the down-regulation of PDI-BS2 by ZC3H20 may represent the regulatory relationship at the molecular and biological level to trigger differentiation. There is a more subtle relationship between the trafficking system and the energy needs of the trypanosome, where the BF parasites utilises glucose from the mammalian bloodstream, which must be endocytosed and trafficked to glycosomes. Of course, the PF cell still takes up metabolites from the insect midgut (mainly proline as a carbon source) that must be trafficked to the mitochondrion for ATP synthesis. However, as mentioned in Chapter 4 (section 4.5), there may be a regulatory relationship between endocytosis and trafficking, whereby in the tstete fly midgut when the PF parasite must up-regulate mitochondrial genes for energy metabolism, and endocytic activity must be down-regulated to conserve energy [237]. This demonstrates the fine balance of regulating developmental gene expression that must occur between these sets of molecules, and this project shows how ZC3H20 may be involved with co-ordinating their expression to ensure cell development and survival.

The *T. brucei* ZC3Hs, ZFP1, ZFP2 and ZFP3 have shown to be implicated in the regulation of differentiation events, where ZFP2 and ZFP3 are involved in the early differentiation events (procyclin expression) and ZFP1 is involved in later differentiation events (kinetoplast repositioning) [181-183], thus displaying their role in trypanosome development. Genetic ablation of ZFP1 affects the ability of cells to reposition their kinetoplast during differentiation (a morphological elongation at the posterior end), and specifically during the PF stage, ectopic over-expression of ZFP2 or ZFP3 causes a specific kinetoplast-posterior morphological extension. Additionally, analysis of the interactions of these proteins *in vivo* shows that these three ZFPs are able to form a complex suggesting functional interaction between this family of ZC3Hs in cellular development. ZC3H proteins in *C. elegans* are shown to be key developmental regulators in early embryonic development, and a gradient of PIE-1, POS-1, MEX-1 and MEX5/6 are required to co-ordinate axis

polarisation and germline differentiation [253]. Although their contributions to development only partially overlap, and there is no evidence to show that complexes are formed, it is suggested that a network of developmental RNA regulation in the embryo is provided by each specific ZC3H protein [253]. Overall, in both *T. brucei* and *C. elegans*, we hypothesise that the ZC3H proteins could potentially represent a family of RBPs that regulate gene expression and work as a network of related proteins to control biological development.

The data show that ZC3H0 regulates subsets of genes involved in trafficking, surface proteins and energy metabolism required for development. However, it is possible that ZC3H20 actually only regulates one of these subsets, for example, surface proteins, and the other subsets are regulated by a similar, related ZC3H protein. This is possible considering the high homology between ZC3H20 and ZC3H21. ZC3H21 is also essential in PF *T. brucei* and is able to trigger differentiation upon over-expression in BF cells (not as effectively as ZC3H20), suggesting redundancy in the *T. brucei* genome for these ZC3H proteins. It could be that while ZC3H20 is necessary to regulate a subset of mRNAs associated with cell surface proteins, ZC3H21 is the actual regulator of trafficking proteins (i.e. PDI-BS2 and clathrin in this instance). RNAi down-regulation of ZC3H20 in PF cells (90% reduction) also targets ZC3H21 (Chapter 3.2.1), causing a 2-fold down-regulation of ZC3H21. Although not at the 2-fold threshold level, our microarray analysis showed that PDI-BS2 mRNA is up-regulated 1.7-fold, suggesting it may normally be destabilised by the ZC3H protein. However, this increase in PDI-BS2 mRNA level may be greater if there was complete depletion of ZC3H21. Our data also shows that upon over-expression of ZC3H20 in PF cells, PDI-BS2 is down-regulated more than 2-fold and is destabilised in ZC3H20-dependent manner. As explained above, there is redundancy in the *T. brucei genome*, and due to the excess ectopic ZC3H20 expression, ZC3H20 may be able to bind and regulate the targets of ZC3H21. An additional target in this experiment is clathrin, which is only down-regulated 1.7 fold, and as discussed in Chapter 4, may not be the real target of ZC3H20 i.e. it may actually be the target of ZC3H21. Our data show that over-expression of ZC3H20 in PF cells causes a BigEye phenotype – indicative of clathrin down-regulation in BF and PF cells. The data also show that over-expression of ZC3H21 in PF cells causes a round phenotype –reported from clathrin RNAi down-

regulation specifically in PF cells (amongst other genetic perturbations). As discussed in Chapter 4, a dose-dependent down-regulation of clathrin in PF cells may determine if the BigEye phenotype is displayed (from an incomplete down-regulation of clathrin) or if cells just round up (total knockdown of clathrin). Thus, over-expression of ZC3H21 could cause a greater down-regulation of clathrin and thus a round phenotype, which would suggest a greater specificity for clathrin than ZC3H20. Finally, over-expression of ZC3H20 in BF cells causes a decrease in PDI-BS2 at just 1.5-fold and no apparent change in stability. This could be because the ectopic expression level of ZC3H20 is not as great in BF cells as in PF cells (as discussed in Chapter 5), or because PDI-BS2 is not the specific target of ZC3H20, or a combination of both these scenarios. As suggested, a molecule like PDI-BS2 may be important to surface access control to allow procyclin to be routed to the cell surface upon differentiation, and down-regulation of PDI-BS2 by ZC3H20 is enough to permit this process. However, our data shows that over-expression of ZC3H21 also causes a small percentage of cells to differentiate. In this case, ZC3H21 may specifically destabilise PDI-BS2 mRNA (to remove surface access control), but up-regulation of ZC3H20 mRNA targets (procyclin, PAD2, META, TS, etc) may not be quite as effective.

This difference in recognition vs. specificity between ZC3H20 and ZC3H21 may be achieved through different domains within each protein. A family of RRM-containing proteins in *T. cruzi* all contain the signature RRM motif, but with different auxiliary domains, and a study of these reported that many RNAs that were bound by the TcRBPs *in vitro* were not bound *in vivo* [254]. This suggests the RRM motifs themselves are not the only part of the protein to consider which may modulate the RNA recognition, and that the auxiliary domains of the proteins may be responsible for specific RNA interactions *in vivo* [254]. The C-termini of ZC3H20 and ZC3H21 are not very similar (13% sequence identity in last 200 amino acids), compared to the N-termini (70% identity in the first 200 amino acids, including both ZC3H motifs). Thus, whilst the N-terminus and ZC3H motifs are necessary for recognition of mRNA targets, the C-terminus of either protein may determine the specificity for binding and regulation.

As discussed in Chapter 5 (section 5.6.6), the increase in RNA abundance of PF-enriched genes seen upon ZC3H20 over-expression in BF cells, could be stabilised by other *trans*-acting factors, as upon RNAi down-regulation of ZC3H20

in PF parasites, many of these genes are not down-regulated (Chapter 3.3, Table 3.1). This suggests that either ZC3H20 is not the specific regulator of these genes, or that other RBPs are “compensating” for the absence of ZC3H20 to prevent down-regulation of the PF-enriched genes. Whilst different RBPs have different specificities for mRNA targets that determine specific regulation, there may be networks of RBPs that show redundancy to ensure the correct expression of developmental genes. An example of this may explain why our data shows that a proportion of BF ZC3H20 null mutants are still able to differentiate when triggered by *cis*-aconitate and temperature drop. The RNAi and over-expression analysis of these ZC3H proteins can reveal the relationship, redundancy and possible co-ordination between them as a group of RBPs. Thus, ZC3H20 and ZC3H21 may independently and specifically regulate subsets of key related developmental genes i.e. surface proteins or trafficking proteins, but additionally work as a network, possibly with other similar ZC3Hs and act co-ordinately to control the differentiation program, as is suggested for the *C. elegans* developmental ZC3H proteins explained above.

As described in Chapter 1, the concept that an RBP regulates a specific subset of co-ordinated genes is receiving much attention, and there is increasing evidence of post-transcriptional regulons in a range of eukaryotic systems, including trypanosomes [136, 139]. Transcriptome analysis of trypanosomes at different stages in the differentiation process show that sets of mRNAs that function in particular pathways are often co-regulated and show almost identical patterns of regulation, such as those which encode surface coat proteins, or are involved in specific metabolic pathways [59]. The *T. brucei* RBP, Puf9 has been shown to regulate mRNAs that encode proteins involved in replicative processes of the cell cycle, and analysis of the 3’UTRs showed an over-represented 6-mer sequence required for Puf9 stabilisation, thus demonstrating an example of a post-transcriptional regulon [139]. Whilst the specific sequence elements within the 3’UTR of ZC3H20/21 mRNA targets have not been defined for regulation, our work suggests that these ZC3Hs regulate subsets of key developmental genes, thus strongly supporting the idea of a post-transcriptional regulon.

In addition to the possibility that one RBP will bind and regulate several mRNA targets, it may also be that one mRNA target will be bound by more than one RBP at any one time. This may be as part of a complex of RBPs that interact

with each other via other domains within the protein that also bind the RNA directly or indirectly, or two RBPs may be competing for the same sequence element within a target mRNA to promote negative or positive regulation (as discussed in Chapter 5.6.6). It has already been demonstrated that ZC3Hs are able to recruit the exosome machinery that would enable destabilisation and degradation of the target mRNA [83], but the mechanism of stabilisation is unclear. Thus, whilst we hypothesise that ZC3H20 regulates mRNA targets via stabilisation and ZC3H21 regulates via destabilisation, it is apparent that due to the redundancy they can do both, but that interactions and/or co-operations with other proteins may be necessary to determine the precise mechanism of regulation. It may also be that the target mRNAs themselves have subtle or clear differences in the recognition sequence elements that they contain, and thus ZC3H20 and 21 are able to discriminate between these elements and regulate their stability in the appropriate manner.

In the post-genomics era, the accessibility of genetics information and the tools available to explore gene expression are invaluable and powerful. The eukaryotic organism and pathogenic protozoa presented here, *T. brucei*, possesses the unique feature of post-transcriptional regulation as the main point of controlling gene expression, and as discussed, RBPs represent an extremely important resource to tightly control the regulation of gene expression required in this parasite. Cell survival within a life stage and during differentiation between each stage requires co-ordination between biological processes and events. This study, in combination with other reports, demonstrates the capacity of ZC3H proteins as essential regulators of gene expression, in particular of developmental genes, and the potential of these proteins to operate within a network to regulate interconnected cellular events required for cell survival and development. Of course, *T. brucei* has special relevance as a parasite that causes devastating disease and thus the further study of these ZC3Hs this may provide information about potential virulence factors. However, just as importantly, these will address general aspects of cell and molecular biology that are of interest and applicable to a broad scientific audience.

6.2 Potential further work on TbZC3H20/21

1. Investigate the expression of ZC3H20 during differentiation from BF to PF

The model shown in Chapter 5, suggests that ZC3H20 protein is upregulated in a BF (stumpy) cell upon cold-shock, thus allowing it to bind and stabilise procyclin and other PF-enriched transcripts and thus triggering differentiation to a PF cell. It may be that the up-regulation of ZC3H20 protein is transient to trigger differentiation, as reported by the RNA level [59], but within an asynchronous monomorphic differentiation, this is difficult to determine. Thus, a suggestion would be to determine the level of ZC3H20 protein at each stage from differentiation of a slender BF cell, to a stumpy BF cell, upon cold shock of a stumpy cell and/or then upon *cis*-aconitate addition. Using *in vivo* cell lines, so that slender and stumpy cells can be used, this will be able to map the expression of ZC3H20 and determine at which point in the differentiation pathway that this molecular trigger is able to initiate transformation. This will consequently provide invaluable information about how the differentiation pathway is initiated and regulated at the molecular level, amongst the environmental and chemical cues shown to be involved.

2. Investigate the regulation of TbZC3H20:

Chapter 3 shows that ZC3H20 is likely to be regulated at the translational or post-translational level. Clearly, perturbed expression of ZC3H20 in BF cells (as seen by ectopic over-expression) triggers cells to differentiate, and thus determining the mechanism of ZC3H20 regulation may provide clues to the differentiation signal upstream of ZC3H20. Post-translational modification of ZC3H proteins via phosphorylation have been demonstrated to regulate their stabilising/destabilising action of target mRNAs for example, phosphorylation of TTP via the MAP kinase pathway prevents its destabilising activity and thus the stability of the target mRNA TNFα increases [145]. Ubiquitination may also regulate the stability or localization of RNA binding proteins and the *C. elegans* CCCH proteins (PIE-1, POS-1, MEX-1, MEX-5, MEX-6) are degraded via the binding of a protein ZIF-1 to the CCCH motif and recruiting an E3 ubiquitin ligase [146].

3. Investigate possible ZC3H20-protein interactions

The ZC3H proteins TTP and ZAP have been demonstrated to directly interact with the exosome, suggesting a mechanism for mRNA decay [83, 172]. TbZFP3 has been shown to co-associate with the translation apparatus suggesting a

translation mechanism for regulation of EP procyclin isoforms [184]. Thus, investigation into the possible ZC3H20-protein interactions may provide information into the post-translational regulatory mechanisms behind ZC3H20-dependent mRNA stability.

4. Define the sequence elements and specificity of target mRNAs

The specific sequence elements within the 3'UTR of ZC3H20/21 mRNA targets that enable regulation have not been defined. The concept of a post-transcriptional regulon, whereby a subset of mRNAs containing the same/similar sequence elements in their 3' UTR are regulated in a coordinated fashion, shows great potential to exist in *T. brucei* [138].

As explained above, the *T. brucei* RBP, Puf9 has been shown to regulate cell cycle mRNAs that have an over-represented 6-mer sequence in their 3' UTRs required for Puf9 stabilisation 3'UTRs [139]. Whilst there is no known sequence elements within the 3'UTR of ZC3H20 mRNA targets and no obvious over-representation within a small set of specific mRNAs, there may be novel sequences or secondary structure may play a greater part. Defining and exploring these stability elements will then also elucidate the specificity of ZC3H20-RNA binding, in addition to revealing the potential of post-transcriptional regulons.

REFERENCES

1. WHO. *Human African trypanosomiasis*. 2010 [cited; Available from: http://www.who.int/trypanosomiasis_african/en/.

2. WHO. *Human African trypanosomiasis: number of new cases drops to historically low level in 50 years*. 2010 [cited; Available from: http://www.who.int/neglected_diseases/integrated_media/integrated_media_hat_june_2010/en/index.html.

3. Kioy, D., J. Jannin, and N. Mattock, *Human African trypanosomiasis.* Nat Rev Microbiol, 2004. 2(3): p. 186-7.

4. Stuart, K., et al., *Kinetoplastids: related protozoan pathogens, different diseases.* J Clin Invest, 2008. 118(4): p. 1301-10.

5. Legros, D., et al., *Treatment of human African trypanosomiasis--present situation and needs for research and development.* Lancet Infect Dis, 2002. 2(7): p. 437-40.

6. BBC. *Scientists in sleeping sickness 'breakthrough'*. 2010 [cited; Available from: http://news.bbc.co.uk/1/hi/world/africa/8597774.stm.

7. BBC-World-News. *The deadliest disease*. Survival 2008 [cited; Available from: http://bbcworldnews.survival.tv/documentaries/sleeping_sickness.php.

8. Matthews, K.R., *The developmental cell biology of Trypanosoma brucei.* J Cell Sci, 2005. 118(Pt 2): p. 283-90.

9. Matthews, K.R. and K. Gull, *Evidence for an interplay between cell cycle progression and the initiation of differentiation between life cycle forms of African trypanosomes.* J Cell Biol, 1994. 125(5): p. 1147-56.

10. Sharma, R., et al., *The heart of darkness: growth and form of Trypanosoma brucei in the tsetse fly.* Trends Parasitol, 2009. 25(11): p. 517-24.

11. El-Sayed, N.M., et al., *The African trypanosome genome.* Int J Parasitol, 2000. 30(4): p. 329-45.

12. Jack, R.M., et al., *Indomethacin promotes differentiation of Trypanosoma brucei.* Infect Immun, 1984. 43(1): p. 445-8.

13. **Matthews, K.R., T. Sherwin, and K. Gull, *Mitochondrial genome repositioning during the differentiation of the African trypanosome between life cycle forms is microtubule mediated.* J Cell Sci, 1995. 108 (Pt 6): p. 2231-9.**

14. **Vickerman, K., *Polymorphism and mitochondrial activity in sleeping sickness trypanosomes.* Nature, 1965. 208(5012): p. 762-6.**

15. **van Hellemond, J.J., F.R. Opperdoes, and A.G. Tielens, *The extraordinary mitochondrion and unusual citric acid cycle in Trypanosoma brucei.* Biochem Soc Trans, 2005. 33(Pt 5): p. 967-71.**

16. **Durieux, P.O., et al., *Alterations in Krebs cycle enzyme activities and carbohydrate catabolism in two strains of Trypanosoma brucei during in vitro differentiation of their bloodstream to procyclic stages.* Mol Biochem Parasitol, 1991. 45(1): p. 19-27.**

17. **Lamour, N., et al., *Proline metabolism in procyclic Trypanosoma brucei is down-regulated in the presence of glucose.* J Biol Chem, 2005. 280(12): p. 11902-10.**

18. **Overath, P. and M. Engstler, *Endocytosis, membrane recycling and sorting of GPI-anchored proteins: Trypanosoma brucei as a model system.* Mol Microbiol, 2004. 53(3): p. 735-44.**

19. **Ruepp, S., et al., *Survival of Trypanosoma brucei in the tsetse fly is enhanced by the expression of specific forms of procyclin.* J Cell Biol, 1997. 137(6): p. 1369-79.**

20. **Acosta-Serrano, A., et al., *The surface coat of procyclic Trypanosoma brucei: programmed expression and proteolytic cleavage of procyclin in the tsetse fly.* Proc Natl Acad Sci U S A, 2001. 98(4): p. 1513-8.**

21. **Vassella, E., et al., *Major surface glycoproteins of insect forms of Trypanosoma brucei are not essential for cyclical transmission by tsetse.* PLoS One, 2009. 4(2): p. e4493.**

22. **Pays, E., L. Vanhamme, and D. Perez-Morga, *Antigenic variation in Trypanosoma brucei: facts, challenges and mysteries.* Curr Opin Microbiol, 2004. 7(4): p. 369-74.**

23. **Engstler, M., et al., *Kinetics of endocytosis and recycling of the GPI-anchored variant surface glycoprotein in Trypanosoma brucei.* J Cell Sci, 2004. 117(Pt 7): p. 1105-15.**

24. Dean, S.D. and K.R. Matthews, *Restless gossamers: antibody clearance by hydrodynamic flow forces generated at the surface of motile trypanosome parasites.* Cell Host Microbe, 2007. 2(5): p. 279-81.

25. Engstler, M., et al., *Hydrodynamic flow-mediated protein sorting on the cell surface of trypanosomes.* Cell, 2007. 131(3): p. 505-15.

26. Morgan, G.W., et al., *The kinetoplastida endocytic apparatus. Part I: a dynamic system for nutrition and evasion of host defences.* Trends Parasitol, 2002. 18(11): p. 491-6.

27. Webster, P. and D.G. Russell, *The flagellar pocket of trypanosomatids.* Parasitol Today, 1993. 9(6): p. 201-6.

28. Landfear, S.M. and M. Ignatushchenko, *The flagellum and flagellar pocket of trypanosomatids.* Mol Biochem Parasitol, 2001. 115(1): p. 1-17.

29. Bonhivers, M., et al., *Biogenesis of the Trypanosome Endo-Exocytotic Organelle Is Cytoskeleton Mediated.* PLoS Biol, 2008. 6(5): p. e105.

30. Nichols, B.J. and J. Lippincott-Schwartz, *Endocytosis without clathrin coats.* Trends Cell Biol, 2001. 11(10): p. 406-12.

31. Morgan, G.W., et al., *The endocytic apparatus of the kinetoplastida. Part II: machinery and components of the system.* Trends Parasitol, 2002. 18(12): p. 540-6.

32. Field, M.C. and M. Carrington, *Intracellular membrane transport systems in Trypanosoma brucei.* Traffic, 2004. 5(12): p. 905-13.

33. Schmid, E.M. and H.T. McMahon, *Integrating molecular and network biology to decode endocytosis.* Nature, 2007. 448(7156): p. 883-8.

34. Hinners, I. and S.A. Tooze, *Changing directions: clathrin-mediated transport between the Golgi and endosomes.* J Cell Sci, 2003. 116(Pt 5): p. 763-71.

35. Schmid, S.L., *Clathrin-coated vesicle formation and protein sorting: an integrated process.* Annu Rev Biochem, 1997. 66: p. 511-48.

36. Allen, C.L., D. Goulding, and M.C. Field, *Clathrin-mediated endocytosis is essential in Trypanosoma brucei.* Embo J, 2003. 22(19): p. 4991-5002.

37. Morgan, G.W., et al., *Developmental and morphological regulation of clathrin-mediated endocytosis in Trypanosoma brucei.* J Cell Sci, 2001. 114(Pt 14): p. 2605-15.

38. Hung, C.H., et al., *Clathrin-dependent targeting of receptors to the flagellar pocket of procyclic-form Trypanosoma brucei.* Eukaryot Cell, 2004. 3(4): p. 1004-14.

39. Koumandou, V.L., et al., *The trypanosome transcriptome is remodelled during differentiation but displays limited responsiveness within life stages.* BMC Genomics, 2008. 9: p. 298.

40. Tyler, K.M., et al., *Limitation of Trypanosoma brucei parasitaemia results from density-dependent parasite differentiation and parasite killing by the host immune response.* Proc Biol Sci, 2001. 268(1482): p. 2235-43.

41. Bass, K.E. and C.C. Wang, *The in vitro differentiation of pleomorphic Trypanosoma brucei from bloodstream into procyclic form requires neither intermediary nor short-stumpy stage.* Mol Biochem Parasitol, 1991. 44(2): p. 261-70.

42. Tasker, M., et al., *A novel selection regime for differentiation defects demonstrates an essential role for the stumpy form in the life cycle of the African trypanosome.* Mol Biol Cell, 2000. 11(5): p. 1905-17.

43. MacGregor, P. and K.R. Matthews, *New discoveries in the transmission biology of sleeping sickness parasites: applying the basics.* J Mol Med, 2010. 88(9): p. 865-71.

44. Bienen, E.J., et al., *Mitochondrial development in Trypanosoma brucei brucei transitional bloodstream forms.* Mol Biochem Parasitol, 1991. 45(2): p. 185-92.

45. Nolan, D.P., et al., *Slender and stumpy bloodstream forms of Trypanosoma brucei display a differential response to extracellular acidic and proteolytic stress.* Eur J Biochem, 2000. 267(1): p. 18-27.

46. Ziegelbauer, K., et al., *Synchronous differentiation of Trypanosoma brucei from bloodstream to procyclic forms in vitro.* Eur J Biochem, 1990. 192(2): p. 373-8.

47. Brun, R. and M. Schonenberger, *Stimulating effect of citrate and cis-Aconitate on the transformation of Trypanosoma brucei bloodstream forms to procyclic forms in vitro.* Z Parasitenkd, 1981. 66(1): p. 17-24.

48. **Hunt, M., R. Brun, and P. Kohler, *Studies on compounds promoting the in vitro transformation of Trypanosoma brucei from bloodstream to procyclic forms.* Parasitol Res, 1994. 80(7): p. 600-6.**

49. **Engstler, M. and M. Boshart, *Cold shock and regulation of surface protein trafficking convey sensitization to inducers of stage differentiation in Trypanosoma brucei.* Genes Dev, 2004. 18(22): p. 2798-811.**

50. **Dean, S., et al., *A surface transporter family conveys the trypanosome differentiation signal.* Nature, 2009. 459(7244): p. 213-7.**

51. **Grandgenett, P.M., et al., *A function for a specific zinc metalloprotease of African trypanosomes.* PLoS Pathog, 2007. 3(10): p. 1432-45.**

52. **Vassella, E., et al., *A major surface glycoprotein of trypanosoma brucei is expressed transiently during development and can be regulated post-transcriptionally by glycerol or hypoxia.* Genes Dev, 2000. 14(5): p. 615-26.**

53. **Hendriks, E., et al., *Life-cycle differentiation in Trypanosoma brucei: molecules and mutants.* Biochem Soc Trans, 2000. 28(5): p. 531-6.**

54. **Sherwin, T. and K. Gull, *The cell division cycle of Trypanosoma brucei brucei: timing of event markers and cytoskeletal modulations.* Philos Trans R Soc Lond B Biol Sci, 1989. 323(1218): p. 573-88.**

55. **Woodward, R. and K. Gull, *Timing of nuclear and kinetoplast DNA replication and early morphological events in the cell cycle of Trypanosoma brucei.* J Cell Sci, 1990. 95 (Pt 1): p. 49-57.**

56. **Ploubidou, A., et al., *Evidence for novel cell cycle checkpoints in trypanosomes: kinetoplast segregation and cytokinesis in the absence of mitosis.* J Cell Sci, 1999. 112 (Pt 24): p. 4641-50.**

57. **Kabani, S., et al., *Genome-wide expression profiling of in vivo-derived bloodstream parasite stages and dynamic analysis of mRNA alterations during synchronous differentiation in Trypanosoma brucei.* BMC Genomics, 2009. 10: p. 427.**

58. **Jensen, B.C., et al., *Widespread variation in transcript abundance within and across developmental stages of Trypanosoma brucei.* BMC Genomics, 2009. 10: p. 482.**

59. Queiroz, R., et al., *Transcriptome analysis of differentiating trypanosomes reveals the existence of multiple post-transcriptional regulons.* BMC Genomics, 2009. 10: p. 495.

60. Berriman, M., et al., *The genome of the African trypanosome Trypanosoma brucei.* Science, 2005. 309(5733): p. 416-22.

61. Mair, G., et al., *A new twist in trypanosome RNA metabolism: cis-splicing of pre-mRNA.* RNA, 2000. 6(2): p. 163-9.

62. Jae, N., et al., *Essential role of a trypanosome U4-specific Sm core protein in small nuclear ribonucleoprotein assembly and splicing.* Eukaryot Cell, 2010. 9(3): p. 379-86.

63. Johnson, P.J., J.M. Kooter, and P. Borst, *Inactivation of transcription by UV irradiation of T. brucei provides evidence for a multicistronic transcription unit including a VSG gene.* Cell, 1987. 51(2): p. 273-81.

64. Liang, X.H., et al., *trans and cis splicing in trypanosomatids: mechanism, factors, and regulation.* Eukaryot Cell, 2003. 2(5): p. 830-40.

65. Campbell, D.A., S. Thomas, and N.R. Sturm, *Transcription in kinetoplastid protozoa: why be normal?* Microbes Infect, 2003. 5(13): p. 1231-40.

66. Palenchar, J.B. and V. Bellofatto, *Gene transcription in trypanosomes.* Mol Biochem Parasitol, 2006. 146(2): p. 135-41.

67. Martinez-Calvillo, S., et al., *Gene expression in trypanosomatid parasites.* J Biomed Biotechnol, 2010. 2010: p. 525241.

68. Ivens, A.C., et al., *The genome of the kinetoplastid parasite, Leishmania major.* Science, 2005. 309(5733): p. 436-42.

69. Gilinger, G. and V. Bellofatto, *Trypanosome spliced leader RNA genes contain the first identified RNA polymerase II gene promoter in these organisms.* Nucleic Acids Res, 2001. 29(7): p. 1556-64.

70. Gibson, W., et al., *Structure and sequence variation of the trypanosome spliced leader transcript.* Mol Biochem Parasitol, 2000. 107(2): p. 269-77.

71. Clayton, C.E., *Life without transcriptional control? From fly to man and back again.* Embo J, 2002. 21(8): p. 1881-8.

72. Matthews, K.R., C. Tschudi, and E. Ullu, *A common pyrimidine-rich motif governs trans-splicing and polyadenylation of tubulin polycistronic pre-mRNA in trypanosomes.* Genes Dev, 1994. 8(4): p. 491-501.

73. Benz, C., et al., *Messenger RNA processing sites in Trypanosoma brucei.* Mol Biochem Parasitol, 2005. 143(2): p. 125-34.

74. Ullu, E., K.R. Matthews, and C. Tschudi, *Temporal order of RNA-processing reactions in trypanosomes: rapid trans splicing precedes polyadenylation of newly synthesized tubulin transcripts.* Mol Cell Biol, 1993. 13(1): p. 720-5.

75. Bangs, J.D., et al., *Mass spectrometry of mRNA cap 4 from trypanosomatids reveals two novel nucleosides.* J Biol Chem, 1992. 267(14): p. 9805-15.

76. Meyer, S., C. Temme, and E. Wahle, *Messenger RNA turnover in eukaryotes: pathways and enzymes.* Crit Rev Biochem Mol Biol, 2004. 39(4): p. 197-216.

77. Tucker, M., et al., *The transcription factor associated Ccr4 and Caf1 proteins are components of the major cytoplasmic mRNA deadenylase in Saccharomyces cerevisiae.* Cell, 2001. 104(3): p. 377-86.

78. Korner, C.G. and E. Wahle, *Poly(A) tail shortening by a mammalian poly(A)-specific 3'-exoribonuclease.* J Biol Chem, 1997. 272(16): p. 10448-56.

79. Clayton, C., et al., *Control of mRNA degradation in trypanosomes.* Biochem Soc Trans, 2008. 36(Pt 3): p. 520-1.

80. Schwede, A., et al., *A role for Caf1 in mRNA deadenylation and decay in trypanosomes and human cells.* Nucleic Acids Res, 2008. 36(10): p. 3374-88.

81. Schwede, A., et al., *The role of deadenylation in the degradation of unstable mRNAs in trypanosomes.* Nucleic Acids Res, 2009. 37(16): p. 5511-28.

82. Mitchell, P., et al., *The exosome: a conserved eukaryotic RNA processing complex containing multiple 3'-->5' exoribonucleases.* Cell, 1997. 91(4): p. 457-66.

83. Chen, C.Y., et al., *AU binding proteins recruit the exosome to degrade ARE-containing mRNAs.* Cell, 2001. 107(4): p. 451-64.

84. Estevez, A.M., T. Kempf, and C. Clayton, *The exosome of Trypanosoma brucei.* Embo J, 2001. 20(14): p. 3831-9.

85. **Haile, S., A.M. Estevez, and C. Clayton, *A role for the exosome in the in vivo degradation of unstable mRNAs.* RNA, 2003. 9(12): p. 1491-501.**

86. **Beelman, C.A., et al., *An essential component of the decapping enzyme required for normal rates of mRNA turnover.* Nature, 1996. 382(6592): p. 642-6.**

87. **Dunckley, T. and R. Parker, *The DCP2 protein is required for mRNA decapping in Saccharomyces cerevisiae and contains a functional MutT motif.* Embo J, 1999. 18(19): p. 5411-22.**

88. **Franks, T.M. and J. Lykke-Andersen, *The control of mRNA decapping and P-body formation.* Mol Cell, 2008. 32(5): p. 605-15.**

89. **Larimer, F.W., et al., *Characterization of the XRN1 gene encoding a 5'-->3' exoribonuclease: sequence data and analysis of disparate protein and mRNA levels of gene-disrupted yeast cells.* Gene, 1992. 120(1): p. 51-7.**

90. **LaGrandeur, T.E. and R. Parker, *Isolation and characterization of Dcp1p, the yeast mRNA decapping enzyme.* Embo J, 1998. 17(5): p. 1487-96.**

91. **Milone, J., J. Wilusz, and V. Bellofatto, *Identification of mRNA decapping activities and an ARE-regulated 3' to 5' exonuclease activity in trypanosome extracts.* Nucleic Acids Res, 2002. 30(18): p. 4040-50.**

92. **Kramer, S., et al., *Heat shock causes a decrease in polysomes and the appearance of stress granules in trypanosomes independently of eIF2(alpha) phosphorylation at Thr169.* J Cell Sci, 2008. 121(Pt 18): p. 3002-14.**

93. **Li, C.H., et al., *Roles of a Trypanosoma brucei 5'->3' exoribonuclease homolog in mRNA degradation.* RNA, 2006. 12(12): p. 2171-86.**

94. **Tharun, S. and R. Parker, *Targeting an mRNA for decapping: displacement of translation factors and association of the Lsm1p-7p complex on deadenylated yeast mRNAs.* Mol Cell, 2001. 8(5): p. 1075-83.**

95. **Parker, R. and U. Sheth, *P bodies and the control of mRNA translation and degradation.* Mol Cell, 2007. 25(5): p. 635-46.**

96. **Coller, J. and R. Parker, *General translational repression by activators of mRNA decapping.* Cell, 2005. 122(6): p. 875-86.**

97. Brengues, M., D. Teixeira, and R. Parker, *Movement of eukaryotic mRNAs between polysomes and cytoplasmic processing bodies.* Science, 2005. 310(5747): p. 486-9.

98. Cassola, A., J.G. De Gaudenzi, and A.C. Frasch, *Recruitment of mRNAs to cytoplasmic ribonucleoprotein granules in trypanosomes.* Mol Microbiol, 2007. 65(3): p. 655-70.

99. Kramer, S., et al., *The RNA helicase DHH1 is central to the correct expression of many developmentally regulated mRNAs in trypanosomes.* J Cell Sci, 2010. 123(Pt 5): p. 699-711.

100. Maquat, L.E., W.Y. Tarn, and O. Isken, *The pioneer round of translation: features and functions.* Cell, 2010. 142(3): p. 368-74.

101. Sonenberg, N. and T.E. Dever, *Eukaryotic translation initiation factors and regulators.* Curr Opin Struct Biol, 2003. 13(1): p. 56-63.

102. Caponigro, G. and R. Parker, *Multiple functions for the poly(A)-binding protein in mRNA decapping and deadenylation in yeast.* Genes Dev, 1995. 9(19): p. 2421-32.

103. Clayton, C. and M. Shapira, *Post-transcriptional regulation of gene expression in trypanosomes and leishmanias.* Mol Biochem Parasitol, 2007. 156(2): p. 93-101.

104. Milone, J., J. Wilusz, and V. Bellofatto, *Characterization of deadenylation in trypanosome extracts and its inhibition by poly(A)-binding protein Pab1p.* RNA, 2004. 10(3): p. 448-57.

105. Pays, E., et al., *The VSG expression sites of Trypanosoma brucei: multipurpose tools for the adaptation of the parasite to mammalian hosts.* Mol Biochem Parasitol, 2001. 114(1): p. 1-16.

106. Chaves, I., et al., *Control of variant surface glycoprotein gene-expression sites in Trypanosoma brucei.* Embo J, 1999. 18(17): p. 4846-55.

107. Taylor, J.E. and G. Rudenko, *Switching trypanosome coats: what's in the wardrobe?* Trends Genet, 2006. 22(11): p. 614-20.

108. Liniger, M., et al., *Overlapping sense and antisense transcription units in Trypanosoma brucei.* Mol Microbiol, 2001. 40(4): p. 869-78.

109. Pays, E., et al., *Trypanosoma brucei: constitutive activity of the VSG and procyclin gene promoters.* Embo J, 1990. 9(10): p. 3145-51.

110. Vanhamme, L., et al., *Stimuli of differentiation regulate RNA elongation in the transcription units for the major stage-specific antigens of Trypanosoma brucei.* Nucleic Acids Res, 1995. 23(11): p. 1862-9.

111. Ansorge, I., et al., *Transcription of 'inactive' expression sites in African trypanosomes leads to expression of multiple transferrin receptor RNAs in bloodstream forms.* Mol Biochem Parasitol, 1999. 101(1-2): p. 81-94.

112. Vanhamme, L., et al., *Differential RNA elongation controls the variant surface glycoprotein gene expression sites of Trypanosoma brucei.* Mol Microbiol, 2000. 36(2): p. 328-40.

113. Navarro, M. and K. Gull, *A pol I transcriptional body associated with VSG mono-allelic expression in Trypanosoma brucei.* Nature, 2001. 414(6865): p. 759-63.

114. Landeira, D. and M. Navarro, *Nuclear repositioning of the VSG promoter during developmental silencing in Trypanosoma brucei.* J Cell Biol, 2007. 176(2): p. 133-9.

115. Hughes, K., et al., *A novel ISWI is involved in VSG expression site downregulation in African trypanosomes.* Embo J, 2007. 26(9): p. 2400-10.

116. Figueiredo, L.M., C.J. Janzen, and G.A. Cross, *A histone methyltransferase modulates antigenic variation in African trypanosomes.* PLoS Biol, 2008. 6(7): p. e161.

117. Yang, X., et al., *RAP1 is essential for silencing telomeric variant surface glycoprotein genes in Trypanosoma brucei.* Cell, 2009. 137(1): p. 99-109.

118. Hotz, H.R., et al., *PARP gene expression: control at many levels.* Mol Biochem Parasitol, 1998. 91(1): p. 131-43.

119. Thomashow, L.S., et al., *Tubulin genes are tandemly linked and clustered in the genome of trypanosoma brucei.* Cell, 1983. 32(1): p. 35-43.

120. Lee, J.H., et al., *Spliced leader RNA gene transcription in Trypanosoma brucei requires transcription factor TFIIH.* Eukaryot Cell, 2007. 6(4): p. 641-9.

121. Jager, A.V., et al., *mRNA maturation by two-step trans-splicing/polyadenylation processing in trypanosomes.* Proc Natl Acad Sci U S A, 2007. 104(7): p. 2035-42.

122. Hehl, A., et al., *A conserved stem-loop structure in the 3' untranslated region of procyclin mRNAs regulates expression in Trypanosoma brucei.* Proc Natl Acad Sci U S A, 1994. 91(1): p. 370-4.

123. Furger, A., et al., *Elements in the 3' untranslated region of procyclin mRNA regulate expression in insect forms of Trypanosoma brucei by modulating RNA stability and translation.* Mol Cell Biol, 1997. 17(8): p. 4372-80.

124. Schurch, N., et al., *Contributions of the procyclin 3' untranslated region and coding region to the regulation of expression in bloodstream forms of Trypanosoma brucei.* Mol Biochem Parasitol, 1997. 89(1): p. 109-21.

125. Hotz, H.R., et al., *Mechanisms of developmental regulation in Trypanosoma brucei: a polypyrimidine tract in the 3'-untranslated region of a surface protein mRNA affects RNA abundance and translation.* Nucleic Acids Res, 1997. 25(15): p. 3017-26.

126. Irmer, H. and C. Clayton, *Degradation of the unstable EP1 mRNA in Trypanosoma brucei involves initial destruction of the 3'-untranslated region.* Nucleic Acids Res, 2001. 29(22): p. 4707-15.

127. Gibson, W.C., B.W. Swinkels, and P. Borst, *Post-transcriptional control of the differential expression of phosphoglycerate kinase genes in Trypanosoma brucei.* J Mol Biol, 1988. 201(2): p. 315-25.

128. Colasante, C., et al., *Regulated expression of glycosomal phosphoglycerate kinase in Trypanosoma brucei.* Mol Biochem Parasitol, 2007. 151(2): p. 193-204.

129. Blattner, J. and C.E. Clayton, *The 3'-untranslated regions from the Trypanosoma brucei phosphoglycerate kinase-encoding genes mediate developmental regulation.* Gene, 1995. 162(1): p. 153-6.

130. Quijada, L., et al., *Expression of the human RNA-binding protein HuR in Trypanosoma brucei increases the abundance of mRNAs containing AU-rich regulatory elements.* Nucleic Acids Res, 2002. 30(20): p. 4414-24.

131. Caput, D., et al., *Identification of a common nucleotide sequence in the 3'-untranslated region of mRNA molecules specifying inflammatory mediators.* Proc Natl Acad Sci U S A, 1986. 83(6): p. 1670-4.

132. Bakheet, T., et al., *ARED: human AU-rich element-containing mRNA database reveals an unexpectedly diverse functional repertoire of encoded proteins.* Nucleic Acids Res, 2001. 29(1): p. 246-54.

133. Bakheet, T., B.R. Williams, and K.S. Khabar, *ARED 2.0: an update of AU-rich element mRNA database.* Nucleic Acids Res, 2003. 31(1): p. 421-3.

134. Barreau, C., L. Paillard, and H.B. Osborne, *AU-rich elements and associated factors: are there unifying principles?* Nucleic Acids Res, 2005. 33(22): p. 7138-50.

135. Priest, J.W. and S.L. Hajduk, *Developmental regulation of mitochondrial biogenesis in Trypanosoma brucei.* J Bioenerg Biomembr, 1994. 26(2): p. 179-91.

136. Mayho, M., et al., *Post-transcriptional control of nuclear-encoded cytochrome oxidase subunits in Trypanosoma brucei: evidence for genome-wide conservation of life-cycle stage-specific regulatory elements.* Nucleic Acids Res, 2006. 34(18): p. 5312-24.

137. Keene, J.D., *RNA regulons: coordination of post-transcriptional events.* Nat Rev Genet, 2007. 8(7): p. 533-43.

138. Ouellette, M. and B. Papadopoulou, *Coordinated gene expression by post-transcriptional regulons in African trypanosomes.* J Biol, 2009. 8(11): p. 100.

139. Archer, S.K., et al., *Trypanosoma brucei PUF9 regulates mRNAs for proteins involved in replicative processes over the cell cycle.* PLoS Pathog, 2009. 5(8): p. e1000565.

140. Torri, A.F., K.I. Bertrand, and S.L. Hajduk, *Protein stability regulates the expression of cytochrome c during the developmental cycle of Trypanosoma brucei.* Mol Biochem Parasitol, 1993. 57(2): p. 305-15.

141. Colasante, C., et al., *Characterization and developmentally regulated localization of the mitochondrial carrier protein homologue MCP6 from Trypanosoma brucei.* Eukaryot Cell, 2006. 5(8): p. 1194-205.

142. Jones, A., et al., *Visualisation and analysis of proteomic data from the procyclic form of Trypanosoma brucei.* Proteomics, 2006. 6(1): p. 259-67.

143. Seo, J. and K.J. Lee, *Post-translational modifications and their biological functions: proteomic analysis and systematic approaches.* J Biochem Mol Biol, 2004. 37(1): p. 35-44.

144. **Szoor, B., et al., *A novel phosphatase cascade regulates differentiation in Trypanosoma brucei via a glycosomal signaling pathway.* Genes Dev, 2010. 24(12): p. 1306-16.**

145. **Sandler, H. and G. Stoecklin, *Control of mRNA decay by phosphorylation of tristetraprolin.* Biochem Soc Trans, 2008. 36(Pt 3): p. 491-6.**

146. **DeRenzo, C., K.J. Reese, and G. Seydoux, *Exclusion of germ plasm proteins from somatic lineages by cullin-dependent degradation.* Nature, 2003. 424(6949): p. 685-9.**

147. **Keene, J.D. and P.J. Lager, *Post-transcriptional operons and regulons co-ordinating gene expression.* Chromosome Res, 2005. 13(3): p. 327-37.**

148. **Keene, J.D., *Ribonucleoprotein infrastructure regulating the flow of genetic information between the genome and the proteome.* Proc Natl Acad Sci U S A, 2001. 98(13): p. 7018-24.**

149. **Glisovic, T., et al., *RNA-binding proteins and post-transcriptional gene regulation.* FEBS Lett, 2008. 582(14): p. 1977-86.**

150. **Foldynova-Trantirkova, S., et al., *The Trypanosoma brucei La protein is a candidate poly(U) shield that impacts spliced leader RNA maturation and tRNA intron removal.* Int J Parasitol, 2005. 35(4): p. 359-66.**

151. **Ismaili, N., et al., *Characterization of a SR protein from Trypanosoma brucei with homology to RNA-binding cis-splicing proteins.* Mol Biochem Parasitol, 1999. 102(1): p. 103-15.**

152. **Dallagiovanna, B., et al., *Functional genomic characterization of mRNAs associated with TcPUF6, a pumilio-like protein from Trypanosoma cruzi.* J Biol Chem, 2008. 283(13): p. 8266-73.**

153. **D'Orso, I. and A.C. Frasch, *TcUBP-1, an mRNA destabilizing factor from trypanosomes, homodimerizes and interacts with novel AU-rich element- and Poly(A)-binding proteins forming a ribonucleoprotein complex.* J Biol Chem, 2002. 277(52): p. 50520-8.**

154. **D'Orso, I. and A.C. Frasch, *TcUBP-1, a developmentally regulated U-rich RNA-binding protein involved in selective mRNA destabilization in trypanosomes.* J Biol Chem, 2001. 276(37): p. 34801-9.**

155. **Klug, A. and J.W. Schwabe, *Protein motifs 5. Zinc fingers.* Faseb J, 1995. 9(8): p. 597-604.**

156. **Brown, R.S., *Zinc finger proteins: getting a grip on RNA.* Curr Opin Struct Biol, 2005. 15(1): p. 94-8.**

157. **Kelly, S.M., et al., *Recognition of polyadenosine RNA by zinc finger proteins.* Proc Natl Acad Sci U S A, 2007. 104(30): p. 12306-11.**

158. **De, J., et al., *Identification of four CCCH zinc finger proteins in Xenopus, including a novel vertebrate protein with four zinc fingers and severely restricted expression.* Gene, 1999. 228(1-2): p. 133-45.**

159. **Wang, D., et al., *Genome-wide analysis of CCCH zinc finger family in Arabidopsis and rice.* BMC Genomics, 2008. 9: p. 44.**

160. **Ogura, K., et al., *Translational control of maternal glp-1 mRNA by POS-1 and its interacting protein SPN-4 in Caenorhabditis elegans.* Development, 2003. 130(11): p. 2495-503.**

161. **Ramos, S.B., et al., *The CCCH tandem zinc-finger protein Zfp36l2 is crucial for female fertility and early embryonic development.* Development, 2004. 131(19): p. 4883-93.**

162. **Shimada, M., H. Kawahara, and H. Doi, *Novel family of CCCH-type zinc-finger proteins, MOE-1, -2 and -3, participates in C. elegans oocyte maturation.* Genes Cells, 2002. 7(9): p. 933-47.**

163. **Li, J., D. Jia, and X. Chen, *HUA1, a regulator of stamen and carpel identities in Arabidopsis, codes for a nuclear RNA binding protein.* Plant Cell, 2001. 13(10): p. 2269-81.**

164. **Begemann, G., et al., *muscleblind, a gene required for photoreceptor differentiation in Drosophila, encodes novel nuclear Cys3His-type zinc-finger-containing proteins.* Development, 1997. 124(21): p. 4321-31.**

165. **Tenenhaus, C., et al., *PIE-1 is a bifunctional protein that regulates maternal and zygotic gene expression in the embryonic germ line of Caenorhabditis elegans.* Genes Dev, 2001. 15(8): p. 1031-40.**

166. **Barabino, S.M., M. Ohnacker, and W. Keller, *Distinct roles of two Yth1p domains in 3'-end cleavage and polyadenylation of yeast pre-mRNAs.* Embo J, 2000. 19(14): p. 3778-87.**

167. **Blackshear, P.J., *Tristetraprolin and other CCCH tandem zinc-finger proteins in the regulation of mRNA turnover.* Biochem Soc Trans, 2002. 30(Pt 6): p. 945-52.**

168. **Lykke-Andersen, J. and E. Wagner, *Recruitment and activation of mRNA decay enzymes by two ARE-mediated decay activation domains in the proteins TTP and BRF-1.* Genes Dev, 2005. 19(3): p. 351-61.**

169. **Fenger-Gron, M., et al., *Multiple processing body factors and the ARE binding protein TTP activate mRNA decapping.* Mol Cell, 2005. 20(6): p. 905-15.**

170. **Gao, G., X. Guo, and S.P. Goff, *Inhibition of retroviral RNA production by ZAP, a CCCH-type zinc finger protein.* Science, 2002. 297(5587): p. 1703-6.**

171. **Bick, M.J., et al., *Expression of the zinc-finger antiviral protein inhibits alphavirus replication.* J Virol, 2003. 77(21): p. 11555-62.**

172. **Guo, X., et al., *The zinc-finger antiviral protein recruits the RNA processing exosome to degrade the target mRNA.* Proc Natl Acad Sci U S A, 2007. 104(1): p. 151-6.**

173. **Guo, X., et al., *The zinc finger antiviral protein directly binds to specific viral mRNAs through the CCCH zinc finger motifs.* J Virol, 2004. 78(23): p. 12781-7.**

174. **Hartmann, C. and C. Clayton, *Regulation of a transmembrane protein gene family by the small RNA-binding proteins TbUBP1 and TbUBP2.* Mol Biochem Parasitol, 2008. 157(1): p. 112-5.**

175. **Estevez, A.M., *The RNA-binding protein TbDRBD3 regulates the stability of a specific subset of mRNAs in trypanosomes.* Nucleic Acids Res, 2008. 36(14): p. 4573-86.**

176. **Stern, M.Z., et al., *Multiple roles for polypyrimidine tract binding (PTB) proteins in trypanosome RNA metabolism.* RNA, 2009. 15(4): p. 648-65.**

177. **Kramer, S., N.C. Kimblin, and M. Carrington, *Genome-wide in silico screen for CCCH-type zinc finger proteins of Trypanosoma brucei, Trypanosoma cruzi and Leishmania major.* BMC Genomics, 2010. 11: p. 283.**

178. **Vazquez, M., et al., *Unique features of the Trypanosoma cruzi U2AF35 splicing factor.* Mol Biochem Parasitol, 2003. 128(1): p. 77-81.**

179. **Bercovich, N., M.J. Levin, and M.P. Vazquez, *The FIP-1 like polyadenylation factor in trypanosomes and the structural basis for its interaction with CPSF30.* Biochem Biophys Res Commun, 2009. 380(4): p. 850-5.**

180. **Hendriks, E.F., A. Abdul-Razak, and K.R. Matthews, *tbCPSF30 depletion by RNA interference disrupts polycistronic RNA processing in Trypanosoma brucei.* J Biol Chem, 2003. 278(29): p. 26870-8.**

181. **Paterou, A., et al., *Identification and stage-specific association with the translational apparatus of TbZFP3, a CCCH protein that promotes trypanosome life-cycle development.* J Biol Chem, 2006. 281(51): p. 39002-13.**

182. **Hendriks, E.F., et al., *A novel CCCH protein which modulates differentiation of Trypanosoma brucei to its procyclic form.* Embo J, 2001. 20(23): p. 6700-11.**

183. **Hendriks, E.F. and K.R. Matthews, *Disruption of the developmental programme of Trypanosoma brucei by genetic ablation of TbZFP1, a differentiation-enriched CCCH protein.* Mol Microbiol, 2005. 57(3): p. 706-16.**

184. **Walrad, P., et al., *Differential trypanosome surface coat regulation by a CCCH protein that co-associates with procyclin mRNA cis-elements.* PLoS Pathog, 2009. 5(2): p. e1000317.**

185. **LaCount, D.J., B. Barrett, and J.E. Donelson, *Trypanosoma brucei FLA1 is required for flagellum attachment and cytokinesis.* J Biol Chem, 2002. 277(20): p. 17580-8.**

186. **Biebinger, S., et al., *Vectors for inducible expression of toxic gene products in bloodstream and procyclic Trypanosoma brucei.* Mol Biochem Parasitol, 1997. 85(1): p. 99-112.**

187. **Bastin, P., et al., *A novel epitope tag system to study protein targeting and organelle biogenesis in Trypanosoma brucei.* Mol Biochem Parasitol, 1996. 77(2): p. 235-9.**

188. **Wirtz, E., et al., *A tightly regulated inducible expression system for conditional gene knock-outs and dominant-negative genetics in Trypanosoma brucei.* Mol Biochem Parasitol, 1999. 99(1): p. 89-101.**

189. **Panigrahi, A.K., et al., *Identification of novel components of Trypanosoma brucei editosomes.* Rna, 2003. 9(4): p. 484-92.**

190. **Estevez, A.M., *The RNA-binding protein TbDRBD3 regulates the stability of a specific subset of mRNAs in trypanosomes.* Nucleic Acids Res, 2008.**

191. **Birnboim, H.C. and J. Doly, *A rapid alkaline extraction procedure for screening recombinant plasmid DNA.* Nucleic Acids Res, 1979. 7(6): p. 1513-23.**

192. Brun, R. and Schonenberger, *Cultivation and in vitro cloning or procyclic culture forms of Trypanosoma brucei in a semi-defined medium. Short communication.* Acta Trop, 1979. 36(3): p. 289-92.

193. Hirumi, H. and K. Hirumi, *Continuous cultivation of Trypanosoma brucei blood stream forms in a medium containing a low concentration of serum protein without feeder cell layers.* J Parasitol, 1989. 75(6): p. 985-9.

194. Wirtz, E., et al., *A tightly regulated inducible expression system for conditional gene knock-outs and dominant-negative genetics in Trypanosoma brucei.* Mol Biochem Parasitol, 1999. 99(1): p. 89-101.

195. van den Hoff, M.J., A.F. Moorman, and W.H. Lamers, *Electroporation in 'intracellular' buffer increases cell survival.* Nucleic Acids Res, 1992. 20(11): p. 2902.

196. Rotureau, B., A. Gego, and B. Carme, *Trypanosomatid protozoa: a simplified DNA isolation procedure.* Exp Parasitol, 2005. 111(3): p. 207-9.

197. Carnes, J., et al., *An essential RNase III insertion editing endonuclease in Trypanosoma brucei.* Proc Natl Acad Sci U S A, 2005. 102(46): p. 16614-9.

198. Pfaffl, M.W., *A new mathematical model for relative quantification in real-time RT-PCR.* Nucleic Acids Res, 2001. 29(9): p. e45.

199. Ramakers, C., et al., *Assumption-free analysis of quantitative real-time polymerase chain reaction (PCR) data.* Neurosci Lett, 2003. 339(1): p. 62-6.

200. Motyka, S.A. and P.T. Englund, *RNA interference for analysis of gene function in trypanosomatids.* Curr Opin Microbiol, 2004. 7(4): p. 362-8.

201. Lai, W.S., et al., *Interactions of CCCH zinc finger proteins with mRNA. Binding of tristetraprolin-related zinc finger proteins to Au-rich elements and destabilization of mRNA.* J Biol Chem, 2000. 275(23): p. 17827-37.

202. Matsushita, K., et al., *Zc3h12a is an RNase essential for controlling immune responses by regulating mRNA decay.* Nature, 2009. 458(7242): p. 1185-90.

203. Brennan, C.M. and J.A. Steitz, *HuR and mRNA stability.* Cell Mol Life Sci, 2001. 58(2): p. 266-77.

204. Peng, S.S., C.Y. Chen, and A.B. Shyu, *Functional characterization of a non-AUUUA AU-rich element from the c-jun proto-oncogene mRNA: evidence for a novel class of AU-rich elements.* Mol Cell Biol, 1996. 16(4): p. 1490-9.

205. Vlasova, I.A., et al., *Conserved GU-rich elements mediate mRNA decay by binding to CUG-binding protein 1.* Mol Cell, 2008. 29(2): p. 263-70.

206. Chen, C.Y. and A.B. Shyu, *Selective degradation of early-response-gene mRNAs: functional analyses of sequence features of the AU-rich elements.* Mol Cell Biol, 1994. 14(12): p. 8471-82.

207. Colasante, C., et al., *Mitochondrial carrier family inventory of Trypanosoma brucei brucei: Identification, expression and subcellular localisation.* Mol Biochem Parasitol, 2009. 167(2): p. 104-17.

208. Montagna, G.N., J.E. Donelson, and A.C. Frasch, *Procyclic Trypanosoma brucei expresses separate sialidase and trans-sialidase enzymes on its surface membrane.* J Biol Chem, 2006. 281(45): p. 33949-58.

209. Engstler, M., G. Reuter, and R. Schauer, *The developmentally regulated trans-sialidase from Trypanosoma brucei sialylates the procyclic acidic repetitive protein.* Mol Biochem Parasitol, 1993. 61(1): p. 1-13.

210. Nagamune, K., et al., *Surface sialic acids taken from the host allow trypanosome survival in tsetse fly vectors.* J Exp Med, 2004. 199(10): p. 1445-50.

211. Blattner, J., et al., *Compartmentation of phosphoglycerate kinase in Trypanosoma brucei plays a critical role in parasite energy metabolism.* Proc Natl Acad Sci U S A, 1998. 95(20): p. 11596-600.

212. Kirchhausen, T., *Adaptors for clathrin-mediated traffic.* Annu Rev Cell Dev Biol, 1999. 15: p. 705-32.

213. Maldonado-Baez, L. and B. Wendland, *Endocytic adaptors: recruiters, coordinators and regulators.* Trends Cell Biol, 2006. 16(10): p. 505-13.

214. Kawahara, T., et al., *Two essential MYST-family proteins display distinct roles in histone H4K10 acetylation and telomeric silencing in trypanosomes.* Mol Microbiol, 2008. 69(4): p. 1054-68.

215. Price, H.P., M. Stark, and D.F. Smith, *Trypanosoma brucei ARF1 plays a central role in endocytosis and golgi-lysosome trafficking.* Mol Biol Cell, 2007. 18(3): p. 864-73.

216. Garcia, L.T., et al., *Effects of Trypanosoma brucei tryptophanyl-tRNA synthetases silencing by RNA interference.* Mem Inst Oswaldo Cruz, 2007. 102(6): p. 757-62.

217. Vanhamme, L. and E. Pays, *The trypanosome lytic factor of human serum and the molecular basis of sleeping sickness.* Int J Parasitol, 2004. 34(8): p. 887-98.

218. Hall, B., et al., *Both of the Rab5 subfamily small GTPases of Trypanosoma brucei are essential and required for endocytosis.* Mol Biochem Parasitol, 2004. 138(1): p. 67-77.

219. Field, M.C. and M. Carrington, *The trypanosome flagellar pocket.* Nat Rev Microbiol, 2009. 7(11): p. 775-86.

220. Nolan, D.P., M. Geuskens, and E. Pays, *N-linked glycans containing linear poly-N-acetyllactosamine as sorting signals in endocytosis in Trypanosoma brucei.* Curr Biol, 1999. 9(20): p. 1169-72.

221. Hall, B.S., et al., *Developmental variation in Rab11-dependent trafficking in Trypanosoma brucei.* Eukaryot Cell, 2005. 4(5): p. 971-80.

222. Garcia-Salcedo, J.A., et al., *A differential role for actin during the life cycle of Trypanosoma brucei.* Embo J, 2004. 23(4): p. 780-9.

223. Chanez, A.L., et al., *Ablation of the single dynamin of T. brucei blocks mitochondrial fission and endocytosis and leads to a precise cytokinesis arrest.* J Cell Sci, 2006. 119(Pt 14): p. 2968-74.

224. Gull, K., *The cytoskeleton of trypanosomatid parasites.* Annu Rev Microbiol, 1999. 53: p. 629-55.

225. Gull, K., *Host-parasite interactions and trypanosome morphogenesis: a flagellar pocketful of goodies.* Curr Opin Microbiol, 2003. 6(4): p. 365-70.

226. Shi, H., et al., *Genetic interference in Trypanosoma brucei by heritable and inducible double-stranded RNA.* Rna, 2000. 6(7): p. 1069-76.

227. Field, M.C., et al., *Intracellular trafficking in the trypanosomatids.* Traffic, 2007. 8(6): p. 629-39.

228. Morgan, G.W., D. Goulding, and M.C. Field, *The single dynamin-like protein of Trypanosoma brucei regulates mitochondrial division and is not required for endocytosis.* J Biol Chem, 2004. 279(11): p. 10692-701.

229. McKean, P.G., *Coordination of cell cycle and cytokinesis in Trypanosoma brucei.* Curr Opin Microbiol, 2003. 6(6): p. 600-7.

230. Gadelha, C., et al., *Membrane domains and flagellar pocket boundaries are influenced by the cytoskeleton in African trypanosomes.* Proc Natl Acad Sci U S A, 2009. 106(41): p. 17425-30.

231. Vedrenne, C., et al., *Two related subpellicular cytoskeleton-associated proteins in Trypanosoma brucei stabilize microtubules.* Mol Biol Cell, 2002. 13(3): p. 1058-70.

232. Portman, N. and K. Gull, *The paraflagellar rod of kinetoplastid parasites: from structure to components and function.* Int J Parasitol, 2010. 40(2): p. 135-48.

233. Grab, D.J., et al., *Golgi-associated phosphohydrolases in Trypanosoma brucei brucei.* Mol Biochem Parasitol, 1997. 86(1): p. 127-32.

234. Engstler, M., et al., *The membrane-bound histidine acid phosphatase TbMBAP1 is essential for endocytosis and membrane recycling in Trypanosoma brucei.* J Cell Sci, 2005. 118(Pt 10): p. 2105-18.

235. Rubotham, J., et al., *Characterization of two protein disulfide isomerases from the endocytic pathway of bloodstream forms of Trypanosoma brucei.* J Biol Chem, 2005. 280(11): p. 10410-8.

236. Field, M.C., et al., *Chaperone requirements for biosynthesis of the trypanosome variant surface glycoprotein.* PLoS One, 2010. 5(1): p. e8468.

237. Natesan, S.K., et al., *Evidence that low endocytic activity is not directly responsible for human serum resistance in the insect form of African trypanosomes.* BMC Res Notes, 2010. 3: p. 63.

238. Czichos, J., C. Nonnengaesser, and P. Overath, *Trypanosoma brucei: cis-aconitate and temperature reduction as triggers of synchronous transformation of bloodstream to procyclic trypomastigotes in vitro.* Exp Parasitol, 1986. 62(2): p. 283-91.

239. Matthews, K.R., J.R. Ellis, and A. Paterou, *Molecular regulation of the life cycle of African trypanosomes.* Trends Parasitol, 2004. 20(1): p. 40-7.

240. Li, Y., Z. Li, and C.C. Wang, *Differentiation of Trypanosoma brucei may be stage non-specific and does not require progression of cell cycle.* Mol Microbiol, 2003. 49(1): p. 251-65.

241. Matthews, K.R. and K. Gull, *Commitment to differentiation and cell cycle re-entry are coincident but separable events in the transformation of African trypanosomes from their bloodstream to their insect form.* J Cell Sci, 1997. 110 (Pt 20): p. 2609-18.

242. Overath, P., J. Czichos, and C. Haas, *The effect of citrate/cis-aconitate on oxidative metabolism during transformation of Trypanosoma brucei.* Eur J Biochem, 1986. 160(1): p. 175-82.

243. Szoor, B., et al., *Protein tyrosine phosphatase TbPTP1: A molecular switch controlling life cycle differentiation in trypanosomes.* J Cell Biol, 2006. 175(2): p. 293-303.

244. Turner, C.M., J.D. Barry, and K. Vickerman, *Loss of variable antigen during transformation of Trypanosoma brucei rhodesiense from bloodstream to procyclic forms in the tsetse fly.* Parasitol Res, 1988. 74(6): p. 507-11.

245. Reuner, B., et al., *Cell density triggers slender to stumpy differentiation of Trypanosoma brucei bloodstream forms in culture.* Mol Biochem Parasitol, 1997. 90(1): p. 269-80.

246. Shapiro, S.Z., et al., *Analysis by flow cytometry of DNA synthesis during the life cycle of African trypanosomes.* Acta Trop, 1984. 41(4): p. 313-23.

247. Vassella, E., et al., *Differentiation of African trypanosomes is controlled by a density sensing mechanism which signals cell cycle arrest via the cAMP pathway.* J Cell Sci, 1997. 110 (Pt 21): p. 2661-71.

248. Breidbach, T., E. Ngazoa, and D. Steverding, *Trypanosoma brucei: in vitro slender-to-stumpy differentiation of culture-adapted, monomorphic bloodstream forms.* Exp Parasitol, 2002. 101(4): p. 223-30.

249. Forsythe, G.R., R. McCulloch, and T.C. Hammarton, *Hydroxyurea-induced synchronisation of bloodstream stage Trypanosoma brucei.* Mol Biochem Parasitol, 2009. 164(2): p. 131-6.

250. Laxman, S., et al., *Hydrolysis products of cAMP analogs cause transformation of Trypanosoma brucei from slender to stumpy-like forms.* Proc Natl Acad Sci U S A, 2006. 103(50): p. 19194-9.

251. Barnwell, E.M., et al., *Developmental regulation and extracellular release of a VSG expression-site-associated gene product from Trypanosoma brucei bloodstream forms.* J Cell Sci, 2010. 123(Pt 19): p. 3401-11.

252. Liu, B., et al., *Trypanosomes have six mitochondrial DNA helicases with one controlling kinetoplast maxicircle replication.* Mol Cell, 2009. 35(4): p. 490-501.

253. Pagano, J.M., et al., *Molecular basis of RNA recognition by the embryonic polarity determinant MEX-5.* J Biol Chem, 2007. 282(12): p. 8883-94.

254. De Gaudenzi, J.G., I. D'Orso, and A.C. Frasch, *RNA recognition motif-type RNA-binding proteins in Trypanosoma cruzi form a family involved in the interaction with specific transcripts in vivo.* J Biol Chem, 2003. 278(21): p. 18884-94.